18 August 2006 | $10

Science

AAAS

Volume 313, Issue 5789

COVER

A wildfire consumes ponderosa pine trees in the Santa Catalina Mountains near Tucson, Arizona, in May 2002. This blaze covered 18,300 hectares and was one of dozens of large wildfires during an extreme drought in the western United States. See page 940.

Photo: David Sanders/Arizona Daily Star

DEPARTMENTS

EDITORIAL

NEWS OF THE WEEK

NEWS FOCUS

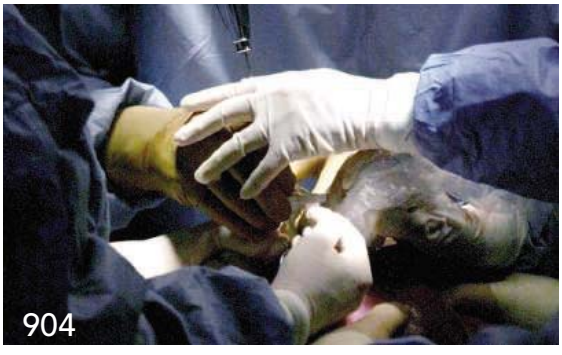
904

LETTERS

BOOKS *ET AL.*

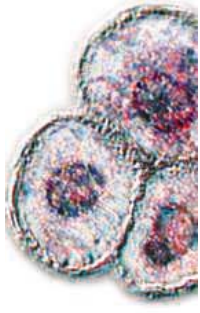
891 & 921

POLICY FORUM

PERSPECTIVES

CONTENTS continued >>

SCIENCE EXPRESS

www.sciencexpress.org

NEUROSCIENCE

PirB Restricts Ocular-Dominance Plasticity in Visual Cortex
J. Syken, T. GrandPre, P. O. Kanold, C. J. Shatz
A molecule that is usually thought of as a hallmark of the immune system interacts with a receptor in the brain to limit the plasticity of the visual system during development.
10.1126/science.1128232

GENETICS

Dok-7 Mutations Underlie a Neuromuscular Junction Synaptopathy
D. Beeson et al.
An inherited muscle disease in which certain muscles are weak is caused by mutations in a protein needed for proper formation of the neuromuscular junction.
10.1126/science.1130837

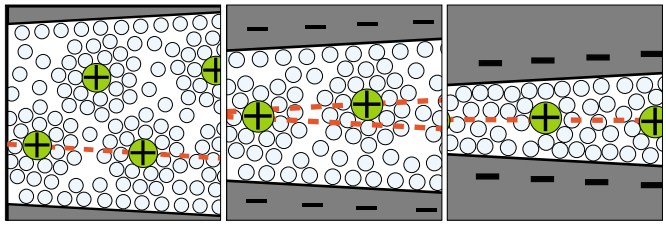

MATERIALS SCIENCE

Anomalous Increase in Carbon Capacitance at Pore Sizes Less Than 1 Nanometer
J. Chmiola, G. Yushin, Y. Gogotsi, C. Portet, P. Simon, P. L. Taberna
Pores comparable in size to solvated anions and cations unexpectedly improve the capacitance in a carbon-based supercapacitor.
>> News story p. 902
10.1126/science.1132195

TECHNICAL COMMENT ABSTRACTS

MICROBIOLOGY

Comment on "Computational Improvements Reveal Great Bacterial Diversity and High Metal Toxicity in Soil" 918
I. Volkov, J. R. Banavar, A. Maritan
full text at www.sciencemag.org/cgi/content/full/313/5789/918a

Response to Comment by Volkov *et al.* on "Computational Improvements Reveal Great Bacterial Diversity and High Metal Toxicity in Soil"
J. Gans, M. Wolinksy, J. Dunbar
full text at www.sciencemag.org/cgi/content/full/313/5789/918b

Comment on "Computational Improvements Reveal Great Bacterial Diversity and High Metal Toxicity in Soil"
J. Bunge, S. S. Epstein, D. G. Peterson
full text at www.sciencemag.org/cgi/content/full/313/5789/918c

Response to Comment by Bunge *et al.* on "Computational Improvements Reveal Great Bacterial Diversity and High Metal Toxicity in Soil"
J. Gans, M. Wolinksy, J. Dunbar
full text at www.sciencemag.org/cgi/content/full/313/5789/918d

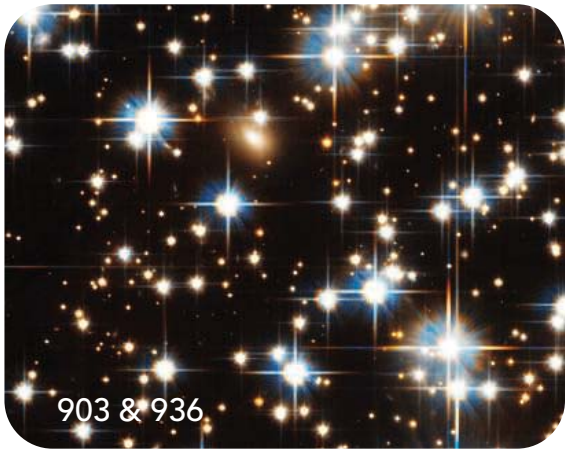

REVIEW

ASTRONOMY

The First Stars in the Universe and Cosmic Reionization 931
R. Barkana

BREVIA

ASTRONOMY

Pinwheels in the Quintuplet Cluster 935
P. Tuthill et al.
The five enigmatic stars in the Quintuplet Cluster in the center of the Milky Way are old, massive binaries with outflowing winds that appear as rotating pinwheels.

RESEARCH ARTICLES

ASTROPHYSICS

Probing the Faintest Stars in a Globular Star Cluster 936
H. B. Richer et al.
Hubble telescope images of a globular star cluster show that the smallest star capable of burning hydrogen is about 0.08 solar masses, consistent with theoretical predictions. *>> News story p. 903*

CLIMATE CHANGE

Warming and Earlier Spring Increase Western U.S. Forest Wildfire Activity 940
A. L. Westerling, H. G. Hidalgo, D. R. Cayan, T. W. Swetnam
Climate change in the western United States has dramatically increased the number of large forest wildfires during the past 35 years. *>> Perspective p. 927*

CELL BIOLOGY

The Molecular Architecture of Axonemes Revealed by Cryoelectron Tomography 944
D. Nicastro et al.
The internal structure of the flagellum reveals how its motor enzyme dynein regulates flagellar movement and thus cellular motility.

CONTENTS continued **>>**

REPORTS

AAAS
ADVANCING SCIENCE, SERVING SOCIETY

SCIENCE (ISSN 0036-8075) is published weekly on Friday, except the last week in December, by the American Association for the Advancement of Science, 1200 New York Avenue, NW, Washington, DC 20005. Periodicals Mail postage (publication No. 484460) paid at Washington, DC, and additional mailing offices. Domestic individual membership and subscription (51 issues): $139 ($74 allocated to subscription). Domestic institutional subscription (51 issues): $650; Foreign postage extra: Mexico, Caribbean (surface mail) $55; other countries (air assist delivery) $85. First class, airmail, student, and emeritus rates on request. Canadian rates with GST available upon request, GST #1254 88122. Publications Mail Agreement Number 1069624. **Printed in the U.S.A.**

Change of address: Allow 4 weeks, giving old and new addresses and 8-digit account number. **Postmaster:** Send change of address to AAAS, P.O. Box 96178, Washington, DC 20090–6178. **Single-copy sales:** $10.00 current issue, $15.00 back issue prepaid includes surface postage; bulk rates on request. The identification code for *Science* is 0036-8075. *Science* is indexed in the *Reader's Guide to Periodical Literature* and in several specialized indexes.

CONTENTS continued **>>**

SCIENCENOW

www.sciencenow.org DAILY NEWS COVERAGE

Who You Calling Fruity?
Belligerent fruit flies reveal clues about the genetics of aggression.

Why Mussels Can Stick to Anything
Amino acid in mussels' glue ensures that they're not slippery when wet.

Wine's Benefit Knows No Color
Some white wine is as good as red for lowering heart attack risk, and here's why.

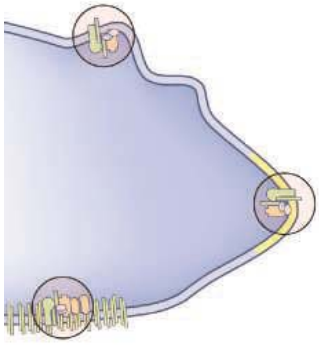

ROS at the leading edge.

SCIENCE'S STKE

www.stke.org SIGNAL TRANSDUCTION KNOWLEDGE ENVIRONMENT

PERSPECTIVE: A RSK(y) Relationship with Promiscuous PKA
M. D. Housley
The often-studied cyclic AMP–dependent protein kinase still has a few tricks up its sleeve.

REVIEW: Localizing NADPH Oxidase-Derived ROS
M. Ushio-Fukai
Subcellular targeting of NADPH oxidase allows reactive oxygen species to stimulate specific signaling processes.

Are you fit for management?

SCIENCE CAREERS

www.sciencecareers.org CAREER RESOURCES FOR SCIENTISTS

US: Tooling Up—Are You "Management Material"?
D. Jensen
Few scientists make it to management, but it is useful to know what hiring managers look for in potential executives.

UK: Testing the Science-Enterprise Market
R. Phillips
Venturefest gives aspiring science entrepreneurs the opportunity to pitch their ideas to an audience of investors.

GRANTSNET: International Grants and Fellowship Index
GrantsNet Staff
Get the latest listing of funding opportunities from Europe, Asia, and the Americas.

SCIENCE PODCAST

Listen to the 18 August *Science* Podcast for stories about the psychological toll of war, the faintest hydrogen-burning stars, challenges in fetal surgery, and more.
www.sciencemag.org/about/podcast.dtl

Separate individual or institutional subscriptions to these products may be required for full-text access.

EDITED BY STELLA HURTLEY AND PHIL SZUROMI

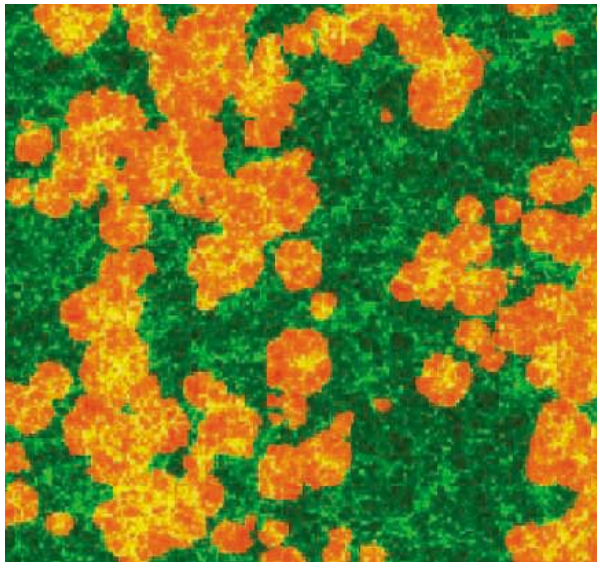

Light and Hydrogen

Soon after the universe formed, it was filled with hydrogen atoms, yet today almost all the diffuse hydrogen between galaxies is ionized. **Barkana** (p. 931) reviews how and when the first stars and black holes lit up and ionized primordial hydrogen gas throughout the universe. Some understanding has come from computer simulations of the change that show the ionization is patchy and happens first in the densest regions of space. However, a full picture must await a new generation of radio telescopes that will map out this key epoch. Stars must exceed a certain size if they are to burn hydrogen through fusion, and **Richer *et al.*** (p. 936; see the news story by **Bhattacharjee**) have identified this fundamental mass limit in a deep census of globular cluster stars in our Milky Way taken with the Hubble Space Telescope. They also see a characteristic change in the color of white dwarfs in the cluster caused by the onset of molecular hydrogen formation in their atmospheres. Both effects had been predicted by theorists, and this experimental confirmation helps improve our understanding of the physics of low-mass stars and white dwarfs.

Assessing Wildfire Activity

Understanding the underlying causes of the increases in wildfire activity in the western United States during the last several decades will impact how to manage the risk that wildfires pose. **Westerling *et al.*** (p. 940, published online 6 July with the Perspective by **Running**; see the cover) compiled a comprehensive time series of large forest wildfires in the western United States for the period from 1970 to 2003, and compared those data with corresponding observations of climate, hydrology, and land surface conditions. Wildfire activity increased suddenly in the mid-1980s. Hydroclimate and fires are closely related, and climate variation has been the primary cause of the increase in fires during the period of their study, although land use changes can also be important. Longer springs and summers that could result as the world warms will continue to lengthen the fire season and continue to cause more large wildfires.

Stimulated Atomic Hopping

The tip of the scanning tunneling microscope can be used to pick up atoms and move them on surfaces, as well as induce motion through electronic excitations produced by the tunneling electrons. **Stroscio *et al.*** (p. 948) assembled short chains of Cu atoms terminated by a Co atom on a Cu(111) surface and analyzed the hopping induced by tunneling electrons of the Co atom between different sites at the end of the chain, which manifested itself as low-frequency "telegraph" noise. Density functional calculations help explain why the tip location that maximizes this hopping is not directly over the Co atom and how the barrier for motion increases with Cu chain length.

An Open Arrangement

The adsorption of organic molecules on close-packed surfaces of transition metals often leads to the formation of complete monolayers, but intermolecular forces such as hydrogen bonding can cause molecules to form ordered structures such as rows that leave areas uncovered. **Pawin *et al.*** (p. 961) report an example where competing interactions create a honeycomb network that has open pores with a diameter of 50 angstroms. The network formed by very low coverage of anthraquinone adsorbed on the Cu(111) surface has openings that are about five molecular diameters. The structure appears to balance hydrogen-bonding contacts, which facilitate the formation of molecular rows, but which compete with intermolecular repulsive forces.

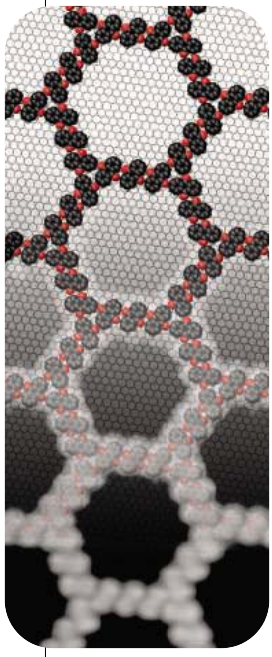

Graphene Sheets on the Double

Single sheets of graphene can display unusual and potentially useful electronic properties, and theoretical work on coupled bilayer systems has indicated that a controllable gap may be induced if there is an asymmetry between the layers, which could be induced either by doping with atoms or application of an external electric field. **Ohta *et al.*** (p. 951) have used angle-resolved photoemission spectroscopy to determine the band structure of graphene bilayers in which asymmetry was induced by doping one sheet with adsorbed potassium atoms. The authors confirm that such control over the energy gap between the valence and conduction bands is possible.

Emulsions on Demand

Surfactants are widely used to stabilize emulsions in products, such as cosmetics, whose constituents would otherwise fail to mix. Many industrial processes, however, have multiple steps that require separating emulsion components after reaction or transport. **Liu *et al.*** (p. 958) show that amidine molecules bearing long hydrophobic tails can be cycled reversibly between surfactant and nonsurfactant forms. Room-temperature treatment of the amidines with an atmosphere of CO_2 produces bicarbonate salts that stabilize aqueous-hydrocarbon emulsions. Bubbling of air through the system at 65°C reverses the reaction and breaks the emulsion. In the absence of CO_2, the amidines act as effective de-emulsifiers of aqueous–crude oil suspensions.

CREDITS (TOP TO BOTTOM): BARKANA *ET AL.*; PAWIN *ET AL.*

Revisiting Vietnam's Psychological Toll

The magnitude of the Vietnam War's psychological toll on U.S. soldiers has been a subject of heated debate since 1988, when two major government-funded studies reported widely divergent rates of posttraumatic stress disorder (PTSD) in Vietnam veterans. Interest in this question has intensified as comparisons are now being made between the Vietnam War and the ongoing conflict in Iraq. **Dohrenwend *et al.*** (p. 978; see Perspective by **McNally**) have reexamined PTSD rates in Vietnam War veterans using improved diagnostic methods and military records (rather than self-reports) to document exposure to war zone stress. Their analysis revealed a lifetime PTSD rate of 18.7%, in between the two previous estimates (of 30.9% and 14.7%). An even stronger dose-response relation seen between war-related stress exposure and PTSD confirms that the war's psychological toll was real and substantial.

Nailing the Axoneme

Cilia and flagella are motile appendages that project from eukaryotic cells that play roles in motility and sensing in a variety of organisms and tissues. **Nicastro *et al.*** (p. 944) present cryoelectron tomography of frozen-hydrated, eukaryotic flagella to reveal structural features of life-like axonemes at ~4 nanometer resolution that are important for axoneme function.

Mixed Bouquets

Flower color in plants is often selected through pollinator preference. Intermediate colors, when they arise in hybrids between two closely related species, are often selected against. **Whibley *et al.*** (p. 963; see the Perspective by **Kramer and Donohue**) investigated the genetic basis of flower color differences between closely related species of snapdragon. By analyzing a hybrid zone involving two color morphs, they identified three loci underlying color variation. Modeling of the genotypic space of color variation was used to map species into this space. The colors of flowers found in the hybrid zone occupied a distinct position in this space, one that is presumably less fit. These findings increase our understanding of adaptation in natural populations and suggest a new way of thinking about transitions between adaptive peaks.

p53 and Tumor Angiogenesis

The tumor suppressor protein, p53, transcriptionally activates genes that control cell cycle arrest, apoptosis, and other cellular processes that help to prevent tumor development. **Teodoro *et al.*** (p. 968) now show that p53 appears to keep tumors in check by activating the gene encoding α(II) collagen prolyl-4-hydroxylase. This enzyme is required for the extracellular release of collagen-derived peptides, such as endostatin and tumstatin, that are potent inhibitors of tumor angiogenesis. The p53 gene is inactivated in many human cancers, presumably leading to reduced production of endogenous antiangiogenic peptides that defend against tumor growth.

Aging and Cancer

Is there a link between organismal aging and cancer? **Pinkston *et al.*** (p. 971) address this question in a worm model of aging and tumor development and find that different signaling pathways implicated in the aging process also control tumorigenesis. Mutant worms with long life spans appear immune to the life-shortening effects of tumors because of enhanced defense mechanisms, including increased apoptosis and decreased cell proliferation within the tumors. Signaling pathways that control longevity may have coevolved with tumor suppressive mechanisms.

CREDIT: ANNABEL WHIBLEY/JOHN INNES CENTRE, NORWICH

Ruth Faden is the Philip Franklin Wagley Professor of Biomedical Ethics and executive director of the Phoebe R. Berman Bioethics Institute at Johns Hopkins University, Baltimore, MD.

The Road to Balanced Oversight

EARLIER THIS YEAR, AN INTERNATIONAL GROUP OF SCIENTISTS AND OTHERS CONVENED AT Hinxton, England (see the related Policy Forum in this issue, p. 921), to address the moral challenges facing collaboration in human embryonic stem cell research that emerge from differences in national laws. Although a focus on embryo research is understandable, it is not the only area of science in which societies differ in values and laws. Scientists throughout the world work under different regulatory regimes governing human subjects, nonhuman animals, pathogens and biohazards, genetic modification of organisms and plants, and access to medical and public health records. In some cases, these differences reflect disagreements about ethically permissible conduct that approach the intensity of debates about the moral status of the embryo.

Whether the issue is research on chimpanzees, the creation of novel organisms, or the destruction of human embryos, scientists need to consider whether it is ethical to travel to other countries to engage in research practices that would not be legally permissible in their home countries. Many scientists may see this as a personal decision that should turn largely on whether they accept or reject the moral premises that underlie their nation's laws. Scientists also need to consider, however, the potential impact of "research tourism" on the public's trust in the scientific community and on the ethics of science itself.

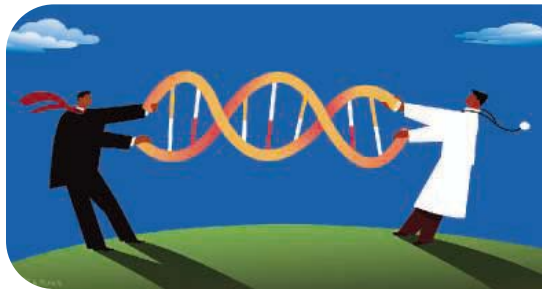

An English stem cell scientist who failed to follow standards set by the United Kingdom's Human Fertilization and Embryology Authority (HFEA) when working outside the United Kingdom would probably be viewed by colleagues as acting unethically. Moreover, such conduct might compromise public trust in the effectiveness of the HFEA to keep embryo research within socially acceptable ethical bounds, and thus might have negative effects on public support for the science itself. Similarly, a U.S. clinical scientist who elected to conduct research in a country whose regulations were more lax than those set by the U.S. Common Rule governing research on human subjects would probably also be viewed by colleagues as acting unethically. In many contexts, this scientist would also be subject to government and institutional penalties.

By contrast, the Hinxton group concluded that scientists living in countries that restrict elements of human embryonic stem cell research should be free to engage in those practices in more permissive countries without legal repercussions. At the same time, however, many in the group recognized the tension that taking this position raises for the ethics of science overall. Scientists should welcome societal oversight of their research, much as all citizens should welcome the benefits of a well-ordered, lawful society more generally. The question is not whether science should be given a special pass when it comes to the reach of national laws. Rather, it is how best to strike a balance between ensuring that science conforms to a society's values and respecting the global context in which science increasingly operates.

Of course, striking this balance is made more complicated when there is substantive moral disagreement not only between societies but also within societies about whether a particular research practice or line of investigation is ethical. The case is complicated still further when, as seems to be true with regard to human embryonic stem cell research, much if not most of the scientific community lines up on one side of the moral issue. These specific conditions of moral disagreement may warrant particular circumspection on the part of lawmakers with regard to extraterritorial jurisdiction. That said, even if there is complete consensus within the global scientific community about the ethics of a particular scientific practice, scientists should not expect societies to defer to their views when it comes to matters of morality. Rather, scientists must continuously make their case to society by appealing to public moral reasons that are accessible to all. This is hard work that requires scientists to leave their laboratories and make themselves available to lawmakers, the public, and the media. At the same time, however, most scientists operate in institutional and professional cultures that rarely reward, and certainly do not prepare, scientists for engaging with the public. Until these structural disincentives to effective interaction between scientists and societies are remedied, we can expect the road to balanced oversight of science to be more complicated than it need be.

Ruth Faden

10.1126/science.1129124

CREDIT: GETTY IMAGES

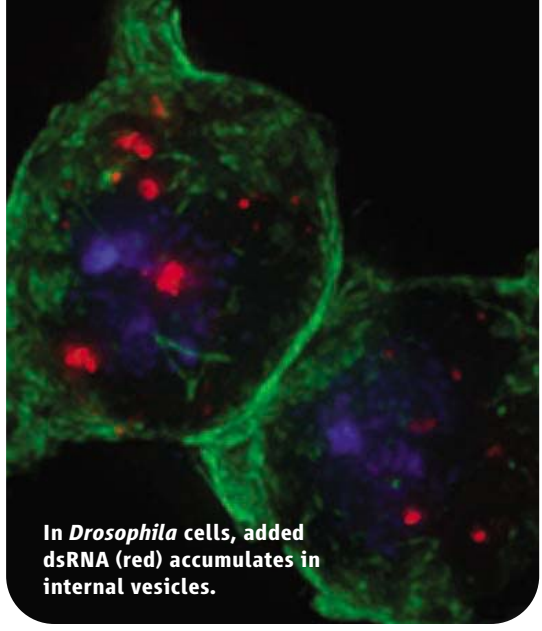

In *Drosophila* cells, added dsRNA (red) accumulates in internal vesicles.

CELL BIOLOGY

RNAin

The uptake of double-stranded RNA (dsRNA) from the medium is the mainstay of many an RNA silencing strategy, but what is the mechanism by which animal cells take up these macromolecules? It has been difficult to address this directly because in some cases, cells seem to take up dsRNA directly from the medium, yet in others there can be cell-to-cell transfer.

Because *Drosophila* cells can take up dsRNA but do not transport it between cells, Saleh *et al.* used *Drosophila* tissue culture cells to characterize the uptake pathway. In a genome-wide screen for participants, components of the receptor-mediated endocytosis pathway were found to predominate. The receptors involved were members of the pattern-recognition receptor family, which is important in innate immunity and antimicrobial defense. Furthermore, similar mechanisms are likely to be widespread in evolution: Knockdown of orthologous endocytic players in nematodes also prevented RNA interference. How incoming dsRNA is diverted from the endocytic pathway so as to avoid degradation in lysosomes remains a mystery. — SMH

Nat. Cell Biol. **8**, 793 (2006).

PHYSICS

One In, One Out

The successful development of optical-based quantum information processing and quantum cryptography will require the ability to store and retrieve known numbers of photons in a medium of choice. Despite significant progress in techniques to store single photons within a cloud of rubidium or cesium atoms, the overall efficiency of the storage and retrieval process in such systems has been limited by low retrieval efficiencies and relatively high noise levels. Laurat *et al.* show that the retrieval efficiency of single excitations stored in an ensemble of cold cesium atoms can be increased by careful optimization of the experimental parameters. The authors found that by increasing the number of photons in each read pulse to approximately 10^7 and increasing the optical depth of the atomic ensemble, they could raise retrieval efficiency to ~50%, with a concurrent order-of-magnitude reduction in two-photon emission events. They argue that such an improvement bodes well for long-distance quantum communication. — ISO

Opt. Express **14**, 6912 (2006).

CHEMISTRY

Relaxing Toward Rotaxanes

Traditional approaches to the chemical synthesis of complex molecular topologies, such as knots and interlocked rings, have focused on reducing kinetic barriers. More recently, an alternative approach has relied on the reversible assembly of comparatively simple building blocks that relax eventually into the desired topological conformation because it is the most favorable thermodynamic arrangement. Northrop *et al.* apply this second strategy to the preparation of [4]pseudorotaxanes, in which a Y-shaped core bears a ring on each of its three axes, and the rings in turn are linked to one another through either one or two central capping groups parallel to the planar core.

The rings in this case are crown ether derivatives attracted to the core axes through hydrogen bonding to cationic ammonium groups. Capping is achieved by reversible imine bond formation between formyl groups appended to the ends of the rings and amine groups on the phenyl cap. The singly capped complex assembled within 2 hours of mixing the components in solution, whereas the doubly capped analog (in which the caps straddled the core) required 8 days to wend through assorted kinetic intermediates. Both complexes were characterized by nuclear magnetic resonance and mass spectrometry. — JSY

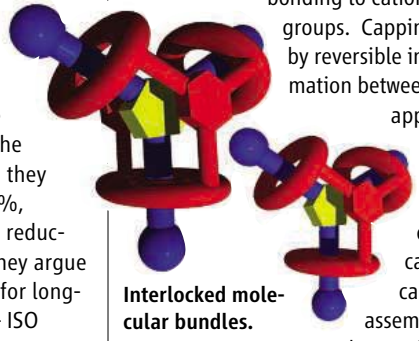

Interlocked molecular bundles.

Org. Lett. **8**, 10.1021/ol061262u (2006).

IMMUNOLOGY

Pattern Formation in Mosquitos

Like the innate immune systems of vertebrates, those of the insect world possess pattern recognition receptors that detect the broad signatures displayed by different classes of pathogens. In contrast, the narrow immune receptor specificity afforded by mechanisms of genetic recombination has been considered a feature unique to adaptive immunity in higher vertebrates. This view has recently undergone some revision, however, with the observation that lower vertebrates and invertebrates are also adept at manufacturing diverse immune receptors. For example, *Drosophila* use alternative splicing of transcripts from an immunoglobulin domain–containing locus—the Down syndrome cell adhesion molecule gene *Dscam*—to generate recognition receptors that assist in the phagocytosis of bacteria.

Dong *et al.* observe that in the mosquito *Anopheles gambiae* (the vector for malaria), the large number of exons in *AgDscam* could yield as many as 31,000 alternatively spliced products, a range similar to that calculated for *Drosophila*. Challenging mosquito cell lines with different pathogens resulted in a varied representation of these exons via alternative splicing and AgDscam molecules with distinct specificities. Evidence for alternative splicing of *AgDscam* was also demonstrated in adult mosquitos, and RNA interference–mediated silencing decreased the resistance of mosquitos to bacterial infection and to oocytes of the

CREDITS (TOP TO BOTTOM): RAUL ANDINO; NORTHROP *ET AL., ORG. LETT.* **8**, 10.1021/OL061262U (2006)

malaria parasite carried in the insect midgut. As in *Drosophila*, the AgDscam forms appeared to enhance phagocytosis of bacteria by hemocytes, although it is likely that the mechanism of Dscam action extends to other modes of immune defense. A further series of experiments revealed that the repertoires of AgDscam molecules could be tailored, in terms of binding affinity, to the infecting pathogens, underscoring the degree to which specificity provided by the Dscam system might help refine pathogen pattern recognition in insects. — SJS

PLoS Biol. **4**, e229 (2006).

MICROBIOLOGY

One of Everything

Recent molecular analyses of marine microbes (see, for example, DeLong *et al.* Reports, 27 January 2006, p. 496) have documented how the environmental pressures of living in the ocean at depths down to several kilometers are reflected in the corresponding genomic complements. Derelle *et al.* provide the genome sequence of *Ostreococcus tauri*, a green alga of extraordinarily small size (about 1 μm in diameter) and remarkably high gene density. This picoeukaryote achieves the feat of packing over 8000 genes into less than 13 Mb by making the average gene just slightly longer than 1.2 kb and reducing the intergene distance to 0.2 kb. Nevertheless, it still contains entire plantlike metabolic pathways, such as the enzymes for C_4 photosynthesis (an evolutionary adaptation to low CO_2 levels) and for storing glucose as one large starch granule within the single chloroplast. Also appearing in only one copy each are the mitochondrion, a Golgi body, and the nuclear pore, which presumably reflect the physical advantages of small intracellular distances and a high surface-to-volume ratio. — GJC

Proc. Natl. Acad. Sci. U.S.A. **103**, 11647 (2006).

MATERIALS SCIENCE

Advantages of Neutrality

Electron beam lithography, often used to pattern the smallest features on semiconducting silicon substrates, can also modify insulating substrates. However, at typical beam energies, the insulating surface builds up negative charge that deflects the beam and so distorts the desired pattern. Several approaches have been developed to overcome this problem, but they require additional sample processing steps or complex gas-handling and vacuum equipment. Joo *et al.* note that at lower energies, electron beams can instead induce positive charging of insulating surfaces; therefore, a critical energy exists for which the surface will remain neutral. For 65-nm-thick poly(methyl methacrylate) films on glass, they determine a critical energy value of 1.3 keV. By tuning the incident beam to this energy, they successfully create features finer than 100 nm on this substrate. A 5-keV beam, in contrast, produces distortions that are clearly evident in scanning electron micrographs. — PDS

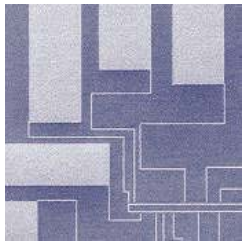

Precisely patterned insulator.

CREDIT: JOO *ET AL.*, *NANO LETT.* **6**, 10.1021/NL061211Q (2006)

Nano Lett. **6**, 10.1021/nl061211q (2006).

Science stke AAAS

www.stke.org

<< Moving PIP_3 About

Phosphatidylinositol-(3,4,5)-phosphate (PIP_3), the product of phosphatidylinositol 3-kinase (PI3K), is important in the establishment of cell polarity. Horiguchi *et al*. provide evidence that PIP_3 is produced not only at the plasma membrane by local activation of PI3K, but also at internal membranes that are then transported as PIP_3-containing vesicles on microtubules to the growing tips of neuronal projections. First, they determined that GAKIN (guanylate kinase–associated kinesin) interacted with PIP_3 binding protein (PIP_3BP); in vitro, GAKIN and PIP_3BP mediated the movement of PIP_3 liposomes on microtubules. In PC12 cells and in cultured hippocampal neurons, tagged GAKIN, tagged PIP_3BP, and a marker for PIP3 were colocalized at the tips of neurites, and in hippocampal cells, these three molecules were most abundant in the longest neurite, the axon. Overexpression of a dominant-negative form of GAKIN (with the kinesin motor domain deleted) in PC12 cells decreased the abundance of PIP_3 at neurite tips. In hippocampal neurons, overexpression of wild-type GAKIN or dominant-negative GAKIN disrupted the formation of the morphologically distinct axon-dendrite structure and produced cells with multiple, highly branched neurites. The authors suggest that PIP_3 produced at internal membranes or PIP_3 produced at the cell body may contribute to cell polarity. – NRG

J. Cell Biol. **174**, 425 (2006).

www.sciencemag.org

Science

1200 New York Avenue, NW
Washington, DC 20005
Editorial: 202-326-6550, FAX 202-289-7562
News: 202-326-6500, FAX 202-371-9227

Bateman House, 82-88 Hills Road
Cambridge, UK CB2 1LQ
+44 (0) 1223 326500, FAX +44 (0) 1223 326501

Subscription Services For change of address, missing issues, new orders and renewals, and payment questions: 866-434-AAAS (2227) or 202-326-6417, FAX 202-842-1065. Mailing addresses: AAAS, P.O. Box 96178, Washington, DC 20090-6178 or AAAS Member Services, 1200 New York Avenue, NW, Washington, DC 20005

Institutional Site Licenses please call 202-326-6755 for any questions or information

Reprints: Author Inquiries 800-635-7181
Commercial Inquiries 803-359-4578
Corrections 202-326-6501

Permissions 202-326-7074, FAX 202-682-0816

Member Benefits Bookstore: AAAS/BarnesandNoble.com bookstore www.aaas.org/bn; Car purchase discount: Subaru VIP Program 202-326-6417; Credit Card: MBNA 800-847-7378; Car Rentals: Hertz 800-654-2200 CDP#343457, Dollar 800-800-4000 #AA1115; AAAS Travels: Betchart Expeditions 800-252-4910; Life Insurance: Seabury & Smith 800-424-9883; Other Benefits: AAAS Member Services 202-326-6417 or www.aaasmember.org.

science_editors@aaas.org	(for general editorial queries)
science_letters@aaas.org	(for queries about letters)
science_reviews@aaas.org	(for returning manuscript reviews)
science_bookrevs@aaas.org	(for book review queries)

Published by the American Association for the Advancement of Science (AAAS), *Science* serves its readers as a forum for the presentation and discussion of important issues related to the advancement of science, including the presentation of minority or conflicting points of view, rather than by publishing only material on which a consensus has been reached. Accordingly, all articles published in *Science*—including editorials, news and comment, and book reviews—are signed and reflect the individual views of the authors and not official points of view adopted by the AAAS or the institutions with which the authors are affiliated.

AAAS was founded in 1848 and incorporated in 1874. Its mission is to advance science and innovation throughout the world for the benefit of all people. The goals of the association are to: foster communication among scientists, engineers and the public; enhance international cooperation in science and its applications; promote the responsible conduct and use of science and technology; foster education in science and technology for everyone; enhance the science and technology workforce and infrastructure; increase public understanding and appreciation of science and technology; and strengthen support for the science and technology enterprise.

Information for Contributors

See pages 102 and 103 of the 6 January 2006 issue or access www.sciencemag.org/feature/contribinfo/home.shtml

RESOURCES

Botanical Bounty

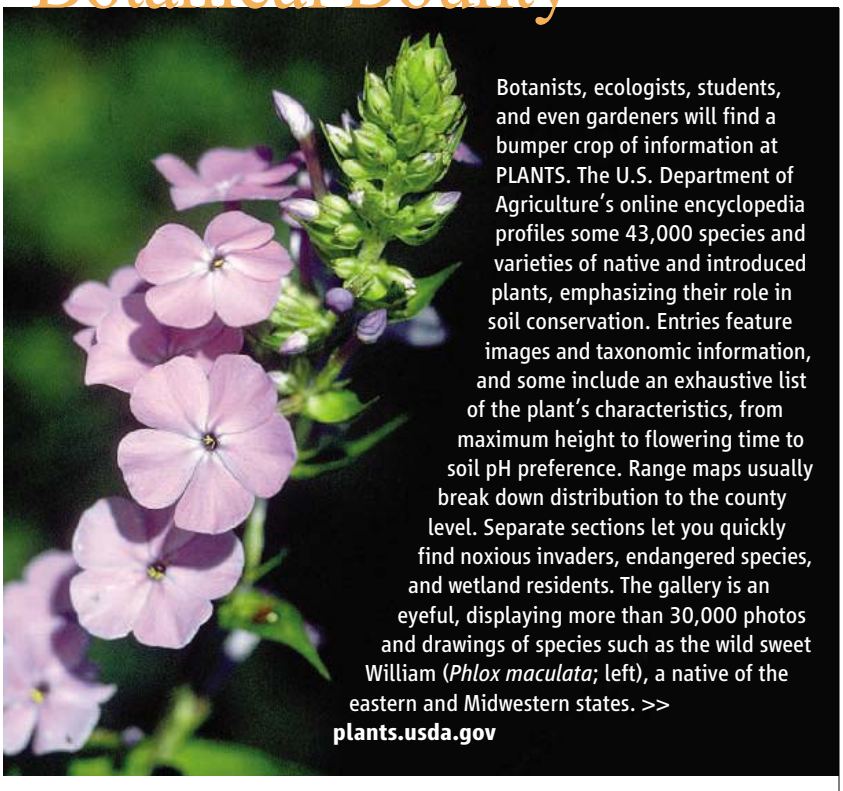

Botanists, ecologists, students, and even gardeners will find a bumper crop of information at PLANTS. The U.S. Department of Agriculture's online encyclopedia profiles some 43,000 species and varieties of native and introduced plants, emphasizing their role in soil conservation. Entries feature images and taxonomic information, and some include an exhaustive list of the plant's characteristics, from maximum height to flowering time to soil pH preference. Range maps usually break down distribution to the county level. Separate sections let you quickly find noxious invaders, endangered species, and wetland residents. The gallery is an eyeful, displaying more than 30,000 photos and drawings of species such as the wild sweet William (*Phlox maculata*; left), a native of the eastern and Midwestern states. >>
plants.usda.gov

WEB LOGS

More Than Skin Deep

For the real scoop on cosmetics and hair care, forget stylists—ask the scientists at The Beauty Brains. On this new blog, a pair of cosmetic chemists weigh product claims, answer reader questions, and highlight research that's germane to the beauty business. Although most of the answers aren't very technical, they usually touch on scientific issues, from the dangers of mixing hair-care products to the harmless mites that inhabit your hair follicles. For example, the question, "Can you fix split ends?" prompts a short discussion of hair structure. No matter what the shampoo ads assert, the site concludes, split ends are unfixable because hair isn't alive and can't heal. >>
thebeautybrains.blogspot.com

EDUCATION

<< When Molds Attack

The fungus *Penicillium marneffei* (left) is a sinister cousin of the molds that make penicillin. On the loose in Southeast Asia, *P. marneffei* invades the skin, eyes, lungs, and other organs, often picking on HIV-infected patients. Doctors and researchers can brush up on pathologic fungi such as *P. marneffei* at Mycology Online, hosted by David Ellis of the University of Adelaide in Australia. After you pore over the descriptions of medically significant fungi, try your hand at the identification quiz. Browse the laboratory methods section to learn how to culture molds from skin swabs or mix a stain that delineates fungal filaments inside tissue. The site also features a gallery and lets you download 500 slides of fungi and their symptoms gathered by the eminent Australian mycologist Geraldine Kaminski. >>
www.mycology.adelaide.edu.au

CREDITS (TOP TO BOTTOM): ROBERT H. MOHLENBROCK/USDA; MARC ZIMMER; DAVID ELLIS; GETTY/VISUALS UNLIMITED

EDUCATION

Lighting Up Life

To learn why biologists are all aglow about a luminous jellyfish molecule called green fluorescent protein (GFP), check out this brief primer from Marc Zimmer of Connecticut College in New London. By allowing scientists to track proteins and cells, GFP has become a lab workhorse. The site, which supplements Zimmer's book on the topic, describes the molecule's structure, introduces the researchers who isolated GFP and pioneered its use, and surveys its applications.

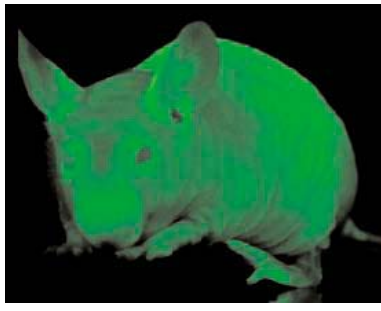

This GFP-making mouse (above) allows researchers to observe interactions between tumors and the surrounding tissue. >>
www.conncoll.edu/ccacad/zimmer/GFP-ww/GFP-1.htm

DATABASE

Powered by Cilia

Fluttering cilia speed a paramecium across a microscope slide, but the hairlike filaments are more than cellular equivalents of outboard motors. New research suggests that cilia detect fluid movement in the kidney, tune in molecular signals that help orchestrate embryonic development, and perform other stationary tasks (*Science*, 14 October 2005, p. 216). The new Cilia Proteome site from Johns Hopkins University in Baltimore, Maryland, is sweeping up data on all proteins found in cilia and basal bodies, the sockets that hold the filaments. You can browse the known human proteins or call up comparable molecules from model organisms such as the mouse and fruit fly. >> www.ciliaproteome.org

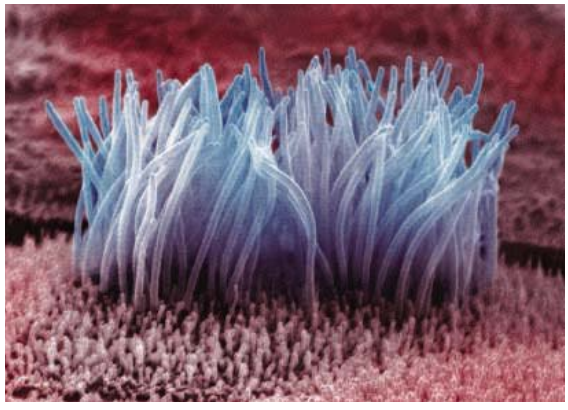

Send site suggestions to >>
netwatch@aaas.org
Archive: www.sciencemag.org/netwatch

For news and research with impact, turn to *Science*

There's only one source for news and research with the greatest impact – *Science*. With over 700,000 weekly print readers, and millions more online, *Science* ranks as one of the most highly read multidisciplinary journals in the world. And for impact, *Science* can't be beat. According to the recently released Thomson ISI Journal Citation Report 2005, *Science* ranked as the No. 1 most-cited multidisciplinary journal with a citation factor of 31. Founded in 1880 by inventor Thomas Edison, and published by the nonprofit AAAS, *Science*'s reputation as the leading source for news, research, and leading edge presentation of content continues to grow. Looking for news and research that will impact the world tomorrow? Then look in *Science*.

www.sciencemag.org

To join AAAS and receive your own personal copy of *Science* every week go to **www.aaas.org/join**

Science
AAAS

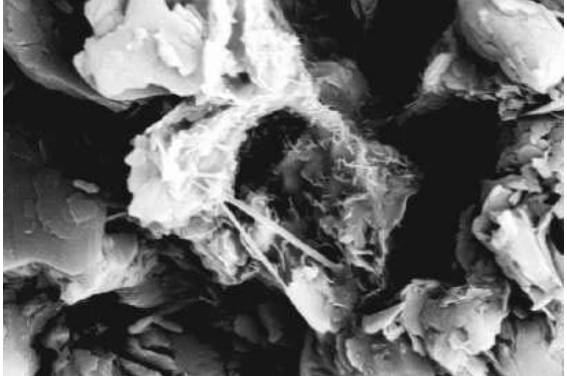

SPELUNKING THROUGH TIME

Clay samples (above) drawn from a set of interconnected caves west of Sydney, Australia, suggest that the caverns may be 340 million years old, making them the most ancient accessible ones anywhere in the world. If the result holds up, the Jenolan Caves would be more than 200 million years older than the current record holder.

Although dating caves can offer insights into geological history, it's also exceedingly difficult to accomplish. In part that's because the materials inside caves, and the stone from which they're made up, often predate the cave itself by millions of years. To date the Jenolan caves, which are a popular tourist destination, geologist Armstrong Osborne of the University of Sydney and his colleagues turned to clay considered a remnant of volcanic ash that helped the caves take shape, they write in the *Australian Journal of Earth Sciences*.

The researchers estimated the age of the clay samples by comparing levels of radioactive potassium, which decays over time, to those of argon gas, which appears as the potassium decays. "The implication … that the caves formed by alteration of volcanic ash" is "entirely possible," says Paul Renne, director of the Berkeley Geochronology Center at the University of California, Berkeley. Still, he's not convinced the clay didn't erode from preexisting rocks, although Osborne insists that's not the case.

Eradicated >>

All out. In a major effort, divers killed this invasive alga before it spread out of control.

There's not much good news about invasive species these days, so biologists were thrilled last month to declare victory in a 6-year, $7 million battle to rid the coastal waters of southern California of an exotic alga. "It's quite an achievement," says ecologist Daniel Simberloff of the University of Tennessee, Knoxville, who was not involved in the effort.

The enemy was *Caulerpa taxifolia*, a tropical species that has run rampant in the Mediterranean Sea, causing problems for commercial fishing, recreational diving, and pleasure boating. After it was discovered in two lagoons near San Diego in 2000, divers repeatedly searched every square meter of the murky waters (*Science*, 22 March 2002, p. 2201). They covered patches of *Caulerpa* with tarps weighted by sandbags and pumped in chlorine.

Quarterly surveys have come up empty-handed since 2002. "We can say with 99.9% confidence that the *Caulerpa* is gone, so we declared success," says Robert Hoffman of the National Marine Fisheries Service in Long Beach. "It feels great," adds team member Lars Anderson of the U.S. Department of Agriculture in Davis, California. "We just hope we never see it again."

MOOD BOOST

A veterinary anesthetic also favored as a rave drug is offering a glimmer of hope for treating depression.

Ketamine, or "Special K" to clubgoers, improved the mood of 12 of the 17 depressed volunteers who received a single injection of it, Carlos Zarate, a psychopharmacologist at the U.S. National Institute of Mental Health in Bethesda, Maryland, and his colleagues report in this month's *Archives of General Psychiatry*. A placebo offered to the same group helped much less. The antidepressant effect lasted up to a week, but most exciting to pharmacologists was that ketamine started working in just 2 hours; typical antidepressants can take up to 2 months to kick in. Because suicidal behaviors are associated with the first days of standard therapy, that difference could prove critical.

The study adds to mounting evidence that the brain's glutamate signaling system, controlled in part by the receptor hit by ketamine, is a specific target for depression therapies, says John Krystal, a psychopharmacologist at Yale University: "The glutamate story as it has emerged is very promising."

Gene Hunt

Police in the German city of Dresden are hunting for a rapist, and they're ready to collect DNA from up to 100,000 men to catch him. German police netted a killer in Cloppenburg in 1998 after 18,000 men were tested, but the Dresden effort could become the largest DNA dragnet ever performed in a criminal investigation.

Dresden police devised the plan after finding identical genetic blueprints from sperm in two rape cases since last September. More than 3000 men so far have submitted to saliva swabs. Participation is voluntary, but the police acknowledge that those who refuse will be scrutinized, according to German media reports.

"I think the strategy is worth it," says Michael Brand, director of the Biotechnology Center at the Technical University in Dresden, even at its maximum cost of $3.5 million. The Dresden police have said publicly that after testing for a match, they will discard DNA from all men who do not have a serious criminal record, as the law requires.

But "even if privacy is protected, to ask for DNA under threat of special scrutiny for those who do not cooperate may be coercive," says Peter Lipton, a philosopher at the University of Cambridge, U.K. "Is this justified?"

CREDITS (TOP TO BOTTOM): A. OSBORNE *ET AL.*, *AUSTRALIAN JOURNAL OF EARTH SCIENCES*, 53 (2006); RACHEL WOODFIELD, MERKEL & ASSOCIATES; INSET: GREIG PETERS; DEA

A puzzling supercapacitor
902

Seeing faint stars
903

U.S. SCIENCE POLICY

Congress Quietly Tries to Craft Bill To Maintain U.S. Lead in Science

In the dog days of August, while most members of Congress are back home campaigning for reelection or on holiday, a small group of staffers is at work in Washington, D.C., on legislation that could influence science spending for years to come. Their goal is to craft a broad bill aimed at bolstering U.S. competitiveness that Congress could pass before the November elections.

They face long odds. The White House has already expressed reservations about some aspects of the legislation, and the congressional calendar is short and already very crowded. Although Senate leaders say they are committed to the goal, House leaders appear less enthusiastic. But a powerful coalition of forces, including business leaders who can bend a member's ear, is keen for Congress to act. "Legislation would show the public that our nation's leaders have a long-range plan of action on U.S. competitiveness," says Susan Traiman of the Business Roundtable, a consortium of 160 CEOs from across U.S. industry.

The legislation draws upon several efforts over the past year examining the status of U.S. science and technology, including the National Academies' *Rising Above the Gathering Storm* report and the National Summit on Competitiveness (*Science*, 21 October 2005, p. 423; 16 December 2005, p. 1752). In February, the Bush Administration proposed starting a 10-year doubling of basic research at the National Science Foundation (NSF), the Department of Energy's (DOE) Office of Science, and the National Institute of Standards and Technology's (NIST) core labs (*Science*, 17 February, p. 929) as part of its 2007 budget request. And the initial funding for what the Administration has dubbed the American Competitiveness Initiative (ACI) is working its way through the legislative process.

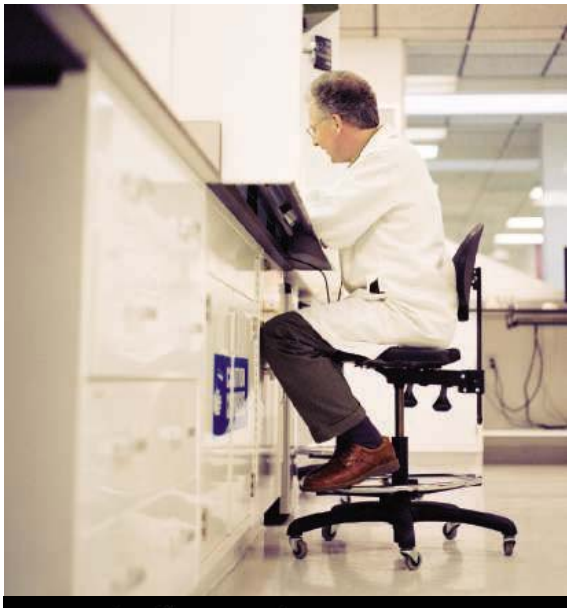

Competing for Attention

Bill Number	Covers	Status
U.S. Senate		
S. 2802	NSF, DOE, NIST, NASA	Adopted 18 May by Commerce committee
S. 2197	NSF, DOE	Adopted 8 March by Energy and Natural Resources committee
S. 2198	Education, NSF, DOE, NASA, NIST	Referred to Health, Education, Labor, Pensions committee
S. 2199	Treasury	Referred to Finance committee
U.S. House of Representatives		
H.R. 5356	NSF, DOE, NIST, NASA	Adopted 7 June by Science committee
H.R. 5358	NSF, DOE	Adopted 7 June by Science committee

Science advocates can't say enough about the importance of ACI. But they believe even more is needed to improve math and science education and enhance U.S. innovation. Taking their cue from *Gathering Storm* and other reports, legislators from both parties introduced a fistful of bills earlier this year that would expand existing research and education activities at several agencies and set up new programs (see table).

Unlike annual appropriations bills, which determine how much each federal agency can spend in a given year, these authorization bills set desired funding levels over several years. Although they don't provide the cash, they can build political support for ongoing spending increases. Notes one university lobbyist: "You want Congress on record and the key committees behind an authorization bill, so that they can bail out appropriators when they hit rough seas."

The goal of the quiet negotiations taking place this summer is a single bill. But the calls for increased spending are a sticking point for a Republican Party whose president, George W. Bush, has repeatedly pledged to reduce the federal deficit and whose congressional leaders hope to campaign this fall on their success in shrinking government. Several of the bills also expand NSF's role in science and math education, a position that clashes with the Administration's plans for the Department of Education to lead efforts to improve math and science education and manage all the ACI's education components.

Presidential science adviser Jack Marburger emphasized those points in hardline letters this spring to the chairs of the committees as they prepared to vote out one of the Senate bills (S. 2802) and two House bills (HR 5356/5358). The Senate measure, Marburger warned Senator Ted Stevens (R–AK) on 17 May, "would undermine and delay" ongoing research at the three agencies, "duplicate or complicate existing education and technology programs," and "compete with private investment" in both areas. The House bills, he told Representative Sherry Boehlert (R–NY) on 5 June, "would diminish the impact" of the requested increases for the three ACI agencies.

Boehlert says he was "quite disappointed" by Marburger's letter, noting the president's declaration in his January State of the Union

CREDITS (PHOTO): HELEN KING/CORBIS

Surgery's tiny frontier 904

Battling the stress of battle 908

Astronomy's four-site saga 910

address that the country "must continue to lead the world in human talent and creativity." Boehlert added, "I thought that we had been working with OSTP on these issues," referring to the White House Office of Science and Technology Policy that Marburger heads.

Three weeks after the House committee passed both bills, überstaffer Karl Rove, new domestic policy chief Karl Zinsmeister, and a score of high-tech industry and academic lobbyists met at the White House to discuss the pending legislation. Although nothing was resolved—some participants say Rove and Marburger scolded them for supporting the bills, whereas others say there was confusion over the various components—the White House told the lobbyists that its Office of Legislative Affairs, led by Candida Wolff, would be taking the lead in trying to craft an acceptable bill, pushing OSTP to the sidelines. In the Senate, lobbyists are heartened by the willingness of Senate Majority Leader Bill Frist (R–TN) to negotiate with the three chairs whose panels must sign off on the legislation—Stevens, Senator Pete Domenici (R–NM), who leads the Energy and National Resources Committee, and Senator Mike Enzi (R–WY), who heads the Health, Education, Labor, and Pensions Committee. Another important player, Senator Lamar Alexander (R–TN), acknowledged when he introduced a trio of bills in January that some of his colleagues "may wince at the price tag" of the legislation. But he cautioned that "maintaining America's brainpower advantage will not come on the cheap."

Although none of the staffers involved would speak on the record, several confirmed that talks are taking place "on a regular basis." They say Frist is determined to cobble together a single bill—with lower authorization levels and fewer new programs than in any of the pending versions—that the Senate could adopt during a 4-week window in September. Prospects in the House are less certain, although Boehlert says, "Hope springs eternal that we'll get an opportunity to go to the floor in September."

Optimists, who hope that all sides will view a competitiveness bill as an asset heading into the November elections, dream of an Administration that accepts a competitiveness bill in return for getting its ACI education programs authorized. Pessimists worry that the House leadership will scuttle the effort by portraying the bills as a vehicle for "wasteful spending" and "a bloated bureaucracy." And although nobody's betting that Congress will act this year, nobody has thrown in the towel. **–JEFFREY MERVIS**

AVIAN INFLUENZA

Panel Confirms Report of Early H5N1 Human Case in China

An international panel of experts has confirmed that China's first human death from H5N1 avian influenza occurred in November 2003, and not 2 years later as Chinese authorities had previously reported. The finding raises as many questions as it settles.

The case was first reported in the 22 June issue of the *New England Journal of Medicine (NEJM)* by Wu-Chun Cao of the State Key Laboratory of Pathogens and Biosecurity, Beijing, and colleagues at institutions mainly affiliated with China's military. In a strange twist, someone claiming to be Cao tried to withdraw the letter, but the magazine had gone to press; Cao later told the editors the request did not come from him (*Science*, 30 June, p. 1855).

To verify the results, China's Ministry of Health retested tissue samples and assembled an international panel of flu experts to review the results with the cooperation of the World Health Organization (WHO). On 8 August, the ministry announced the panel's conclusion: The death of a 24-year-old male in November 2003, from what were then called unknown causes, was actually due to H5N1. The death occurred 3 months before China reported its first H5N1 outbreaks in poultry and 2 years before it reported any human cases. Chinese media reported that Vice Minister of Health Jiang Zuojun said at a 10 August press conference in Beijing that the case indicates the need for researchers "to improve communication and contact with disease prevention organizations."

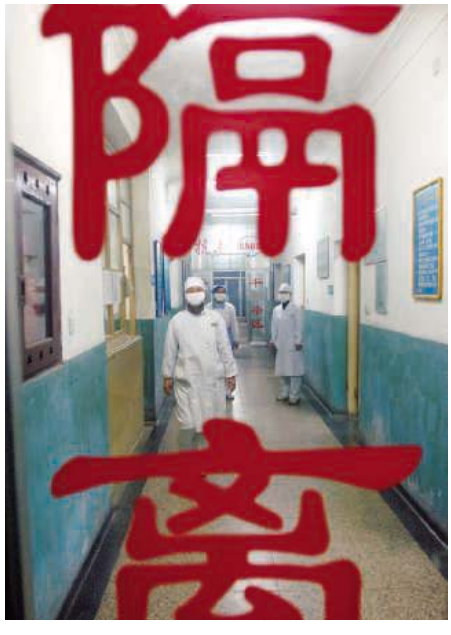

Keep out! The Chinese characters on the door to an isolation ward at a hospital warn people to stay away.

CREDIT: ASSOCIATED PRESS

Flu experts widely believe H5N1 has been circulating in southern China at least since the virus was first identified in Hong Kong in 1997. It has never been clear if it was undetected or if local or national authorities were withholding information from the international community—or whether they were even aware of how serious a threat the virus posed.

Reached by phone, Cao said his team concluded the man died of H5N1 only shortly before submitting their letter to the *NEJM*. He said he is willing to discuss the results with scientists but not reporters. "It's a very sensitive issue," he said, declining to take further questions.

Roy Wadia, a WHO spokesperson in Beijing, says that when two members of a Hong Kong family tested positive for H5N1 after a trip to the mainland's Fujian Province in February 2003, WHO asked Chinese authorities to investigate. Wadia says the agency was told that the H5N1 virus was not present in Fujian. Confirmation that the virus was in circulation earlier than reported "begs the question of whether more aggressive action might have made a difference in the (near worldwide) spread of this virus," he says. **–DENNIS NORMILE**

ASTRONOMY

Judge Slaps Hawaii Over Mauna Kea Telescopes

A Hawaii state judge has found fault with the process of approving new telescopes at the world's largest astronomical observatory. A 3 August ruling by Third Circuit Court Judge Glenn Hara could affect the pace of development atop the 4200-meter Mauna Kea, a mountain with special significance to native Hawaiians.

The case involves a 2004 permit issued to the University of Hawaii's Institute for Astronomy (IFA) to house a quartet of 1.8-meter telescopes that would have worked in conjunction with the twin 10-meter Keck telescopes on the summit to hunt for planets outside the solar system. The $70 million Outrigger interferometry project, which NASA canceled in February because of a tight budget after spending $20 million on the telescopes and domes, would have operated in a protected area that requires a special permit from the state's Board of Land and Natural Resources (BLNR). But Hara said the board should not have approved Outrigger in the absence of a "comprehensive management plan" for the summit, which already hosts 13 telescopes. "The resource that needs to be conserved, protected, and preserved is the summit, not just the area of the project," Hara wrote in an eight-page decision (Civ. No. 04-1-397, *Mauna Kea* v. *BLNR*). Although only Outrigger has been canceled, the ruling will affect all future development on Mauna Kea.

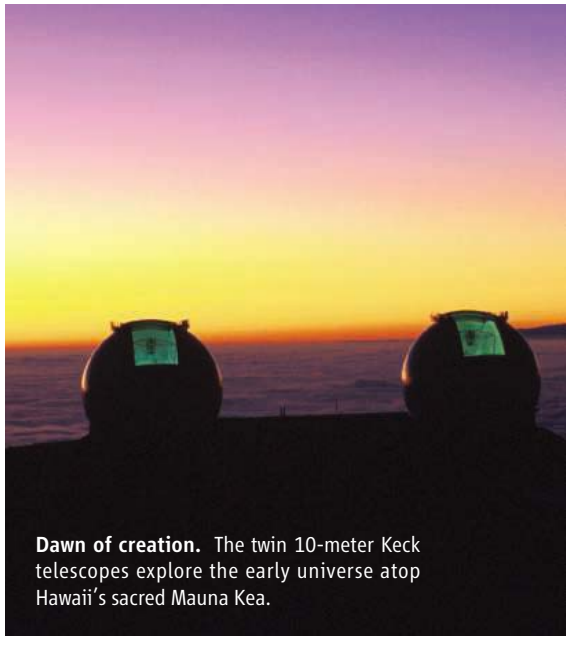

Dawn of creation. The twin 10-meter Keck telescopes explore the early universe atop Hawaii's sacred Mauna Kea.

"Astronomers always want the next best thing, and they don't want any restrictions placed on them," says Lea Hong, a Honolulu attorney who represented the plaintiffs, which included local groups and the Sierra Club. "My clients aren't antiastronomy. But they do want meaningful community representation in a process that respects the environmental, cultural, and aesthetic aspects of the mountain."

The judge's ruling "highlights an ambiguity" in the current procedures, admits Frederic Chaffee, director emeritus of the Keck Observatory. The university, which manages activities at the summit, adopted a Mauna Kea master development plan in 2000, Chaffee notes, but the state never approved it or any similarly comprehensive plan. That loophole allowed critics of the Outrigger telescope project to argue successfully that the state was ignoring its own rules for managing the summit.

"The board needs to adopt a master plan," agrees BLNR chair Peter Young, adding that there's no time to waste because a U.S. government-funded panoramic survey telescope (Pan-STARRS 4) project is moving ahead quickly (*Science*, 12 May, p. 840) and the enormous Thirty-Meter Telescope, being planned by a public-private consortium, is waiting in the wings (www.tmt.org). "We plan to work with the university to come up with something that would incorporate both those projects and others down the road."

IFA Director Rolf Kudritzki says that, in retrospect, the process used for the Outrigger project "wasn't the best way to proceed." But he says, "I don't see a problem for astronomy" in the wake of the judge's ruling. Chaffee estimates that "we've already done 80% of the work" on a comprehensive plan for the summit in preparing the Outrigger permit.

–JEFFREY MERVIS

SCIENTIFIC EXCHANGES

U.S. Loosens Policy on Ties to UNESCO

The United States government has withdrawn restrictions it placed a year ago on contact between U.S. citizens and the United Nations Educational, Scientific, and Cultural Organization (UNESCO). U.S. scientific societies are relieved by the move, which they say should help restore free exchange between U.S. researchers and the international body.

In May 2005, Louise Oliver, the U.S. ambassador to UNESCO, sent a memo to UNESCO Director General Koichiro Matsuura asking the organization to consult U.S. officials before partnering with anybody in the United States or planning any U.S. events. Last month, in a memo to Matsuura, Oliver effectively retracted that directive by explaining that the U.S. government merely wants to stay informed about contacts between UNESCO and U.S. entities.

Last year's memo seems to have been "misinterpreted by some individuals within the UNESCO Secretariat," Oliver says in her 25 July letter. "We understand that there have been instances where UNESCO staff informed U.S. individuals and nongovernmental organizations that they were required to obtain U.S. government approval before making contact with UNESCO or before entering into any contracts with UNESCO."

Wendy White of the U.S. National Academies, which last year wrote to Oliver expressing its concern, says she hopes the new memo will repair any breaches between the U.S. scientific community and UNESCO caused by last year's memo. But Irving Lerch, of the American Physical Society and Americans for UNESCO, wonders if the status quo can be restored. "Some links between U.S. organizations and UNESCO have already snapped as a result of last year's directive," he says, noting that a UNESCO staffer recently declined a meeting invitation that had not been routed through the U.S. government. Moreover, Lerch says, the U.S. government still wants UNESCO to give it advance notification of any contacts with U.S. organizations—a step that he says hinders free exchange.

–YUDHIJIT BHATTACHARJEE

CREDIT: W.M. KECK OBSERVATORY

CLINICAL RESEARCH

Lessons From a Failed Drug Trial

Doctors who treated the six young men who became desperately ill in a botched U.K. clinical trial last spring have released an in-depth record of the catastrophe. They confirm, for example, that the volunteers were given intravenous doses of a test drug in quick succession (10 minutes apart), even though the drug had never been given to humans before. The subjects began to show signs of illness within 50 to 90 minutes, according to the report. And within 12 to 16 hours, all six were transferred from a company research site, which couldn't handle the emergency, to the Northwick Park and St. Mark's Hospital in London, which rescued them. The men appear to have recovered. But even 30 days after the test, according to a paper released this week from the 7 September *New England Journal of Medicine* (*NEJM*), some had "short-term difficulties in finding words (particularly names)."

This detailed account—by Ganesh Suntharalingam and colleagues in Northwick Park's intensive care unit—fills gaps in an earlier report on the incident by an expert panel advising the U.K. government.* The *NEJM* paper confirms that the drug in this trial, a monoclonal antibody called TGN1412, caused a massive immune response that flooded the volunteers' blood with inflammatory agents, triggering systemic organ damage (*Science*, 24 March, p. 1688). The doctors do not attempt to explain why this happened. But they conclude that TGN1412 itself, not an impurity, caused the injuries. They also speculate that TGN1412, which was designed to activate T cells and regulatory T cells at the same time, also may have directly injured the immune system and focused inflammation in the lungs. Four patients had to receive oxygen by mask, and two had to be put on mechanical ventilators. All six experienced severe and "unexpected" depletion of lymphocytes, cells that are essential to the immune system. The likely long-term consequences are not known.

A Flood of Inflammatory Responses

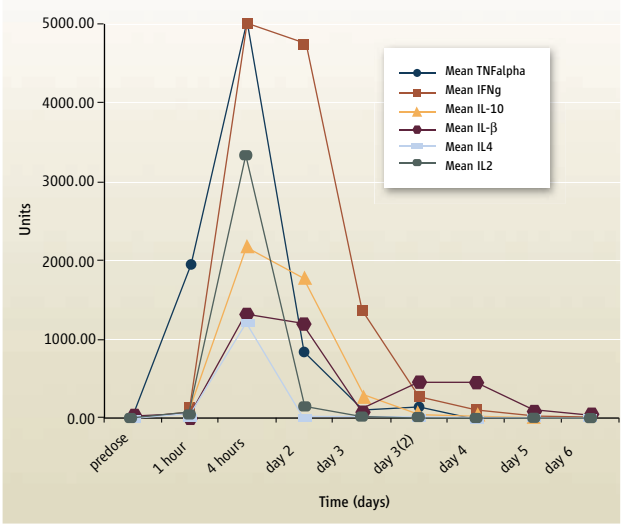

SOURCE: U.K. EXPERT SCIENTIFIC GROUP ON PHASE ONE CLINICAL TRIALS INTERIM REPORT

* Expert Scientific Group on Phase One Clinical Trials, Interim Report (www.dh.gov.uk/assetRoot/04/13/75/69/04137569.pdf)

Others say that data in hand before the trial make it clear that TGN1412 should have been tested with more caution. Nirmala Bhogal, a molecular pharmacologist who has analyzed the trial for FRAME, a nonprofit in Nottingham, U.K., that advocates substitutes for animal testing, says that one preclinical study of TGN1412 in monkeys revealed a proinflammatory response that peaked at 2 hours. The drug company that owns TGN1412—TeGenero of Wurzburg, Germany—discounted this before the clinical trial as a minor effect. However, Bhogal says, in light of the monkey data, "it defies all logic" to dose human volunteers at intervals shorter than 2 hours. TeGenero filed for insolvency in July, and company officials could not be reached for comment.

In its draft report issued last month, the expert panel advising the government, chaired by Gordon Duff, a University of Sheffield specialist in genetics and the human inflammatory response, suggested that when drugs are given to human subjects for the first time, there should be a pause for "an appropriate period of observation" before the next person is dosed.

The Duff panel also offered specific ideas for improving dose-risk calculations. Its broadest proposal is that drug companies and regulators around the world should collect and share unpublished data on human drug reactions. The panel suggested creating a new, open access database for everyone's use. The panel is gathering comments on these and other ideas before issuing a final report to the U.K. government in September. **–ELIOT MARSHALL**

Biopharming Rules Broken

The first U.S. biopharming field trials to undergo legal scrutiny weren't kosher, says a U.S. Hawaiian district judge who ruled last week in a case involving research done several years ago in Hawaii.

The Department of Agriculture (USDA) broke national environmental laws when it allowed four companies to grow HIV vaccines and other pharmaceuticals in genetically modified (GM) crops on four Hawaiian islands, explained Judge J. Michael Seabright in a 10 August ruling. Environmental groups argued successfully that USDA should have considered the potential impact on endangered species and other questions. The agency, Seabright said, showed an "utter disregard for this simple investigation requirement."

Next week, Seabright will hear arguments for a moratorium on field trials while the USDA reviews its biopharming permit program. In the meantime, Paul Achitoff, a plaintiff representing the advocacy group Earthjustice in Oakland, California, says the ruling puts USDA on notice that ignoring the environmental impacts of biopharm GM crops makes it "a sitting duck for future lawsuits." **–ERIK STOKSTAD**

A Mighty Wind Blowin'

The U.S. government should consider a 10-fold increase in research to help understand and protect against hurricanes, according to an upcoming report from a task force of the National Science Board convened in response to Katrina's devastation of the Gulf Coast last August.

Panel chair Kelvin Droegemeier, a meteorologist at the University of Oklahoma, says the country needs a $300-million-a-year National Hurricane Research Initiative along the lines of the multiagency National Earthquake Hazard Research Program created in the wake of the great 1964 earthquake that struck Alaska. Droegemeier says the panel hopes to capitalize on the current hurricane season to grab the attention of U.S. policymakers. "We're trying to build support for an integrative approach to this phenomenon," he reported last week to the science board, which sets policy for the National Science Foundation. **–JEFFREY MERVIS**

MATERIALS SCIENCE

New 'Supercapacitor' Promises to Pack More Electrical Punch

When it comes to powering laptops and hybrid cars, batteries get most of the attention. But these gadgets and myriad others also contain devices known as capacitors that provide quick bursts of energy. Capacitors can't store as much power as batteries, but the latest "supercapacitors" have started to close the gap. Now, their storage capabilities may be about to take another big jump.

In a report published online this week by *Science* (www.sciencemag.org/cgi/content/abstract/1132195), researchers from the United States and France report that by carefully controlling the nanoscale structure of a carbon-based supercapacitor, they've managed to increase the amount of electrical charges it can hold by about 50%. "It looks like they've got something significant there," says John Miller, a physicist who runs JME Inc., a supercapacitor materials evaluation company in Shaker Heights, Ohio. If this performance translates to commercial devices, it could help manufacturers create smaller and cheaper power packs for everything from cameras to cars, Miller says. First, however, researchers need to learn more about how it works.

Typically, a capacitor contains a pair of electrodes surrounded by an electrolyte. When a voltage is applied between the electrodes, oppositely charged ions in the electrolyte snuggle up to each electrode and remain there even when the applied voltage is turned off. When the two electrodes are connected by a wire, electrons flow from the negative electrode to balance the charges in the positive electrode and do work en route.

For many years, carbon has been the electrode material of choice for supercapacitors because it conducts electricity, is light, and can be formed into a meshlike structure that sops up ions like a sponge. The smaller the pores in the material, the larger its surface area and the more charge the capacitor can hold—at least up to a point. When ions move through an electrolyte, other molecules attracted to their charge normally encircle them like groupies mobbing a rock star. Researchers have long thought that if the pores in a carbon supercapacitor got too small—below about 1 billionth of a meter, or nanometer—the ion would not be able to squeeze through with its entourage, and thus the material's overall ability to store charge would drop. But because they had no way to carefully control the pore size throughout a large capacitor, they couldn't test this notion.

Yury Gogotsi and his colleagues at Drexel University in Philadelphia, Pennsylvania, however, came up with a new way to do just that. They started with one of several commercially available compounds called a metal carbide, a mixture of a metal such as titanium and carbon. They then heated their material in a furnace while exposing it to chlorine gas. The gas reacted with the metal, forming volatile compounds that could easily be separated from the mixture, leaving behind carbon shot through with a continuous mesh of voids. By controlling the temperature and other conditions in their reactor, the researchers found they could tailor the holes in their carbon mesh to be a uniform size, between 0.6 and 2.25 nanometers across.

When Gogotsi and his students measured the charge-storing capabilities of the material, they got a shock. "We thought it would be useless" to study the smallest pores, Gogotsi says. But in powdered samples, their carbon with the 0.6-nanometer pores held 50% more charge than powders of standard supercapacitors. Gogotsi's group later teamed up with Patrice Simon, a leading supercapacitor expert at the University of Paul Sabatier in Toulouse, France, whose lab confirmed the results.

On a molecular level, it appeared that ions must be wiggling into the tiny pores, by either squeezing their entourage ions or perhaps abandoning them altogether. But how that could happen remains a puzzle, Miller says. In normal carbon supercapacitors, ions nestling up to an electrode form a layer about 1 nanometer thick. So if there is less space than that in the pores of the new material, it's not clear how they can get in. "That will be a bit controversial," Miller says. But both he and Gogotsi point out that thanks to the newfound control over pore size, researchers should quickly be able to figure out just what is going on.

–ROBERT F. SERVICE

On demand. New supercapacitors store less charge than batteries but can supply it more quickly, making them ideal for hybrid cars.

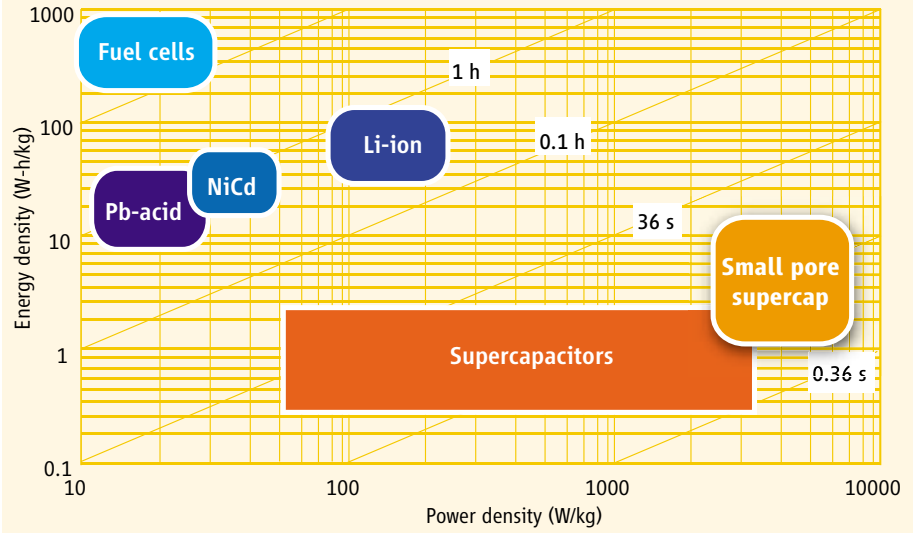

CREDITS: (PHOTO) AP/ROB WIDDIS

CREDIT: NASA/ESA/H. RICHER, UNIVERSITY OF BRITISH COLUMBIA

ASTRONOMY

Nearby Cluster Shows Extremes of Stardom

In the life of every small star, there comes a moment of reckoning when it stands on the edge between burnout and enduring brilliance. If the star's mass lies below a certain value, it runs out of nuclear fuel and begins to fade into a husk known as a brown dwarf. If its mass exceeds that value, the center of the star becomes hot enough to achieve a state of self-sustaining fusion, allowing it to burn merrily for trillions of years.

The critical mass, known as the brown dwarf limit, has been a fundamental prediction of stellar evolutionary theory. Now, for the first time, researchers have identified and measured this threshold in reality. On page 936, Harvey Richer of the University of British Columbia in Vancouver, Canada, and colleagues report the brown dwarf limit for stars in the nearby NGC 6397 globular cluster (above) and show that it matches the predicted value of 0.083 times the sun's mass. The researchers also report that the cluster's faintest white dwarfs—burnt-out remains of massive stars that grow dim as they cool over time—confirm another theoretical prediction, that white dwarfs turn bluer as they age.

The team's observation of the brown dwarf limit is "of prime importance" in helping theorists confirm their account of how stars evolve, says Gilles Chabrier, an astrophysicist at the École Normale Supérieure in Lyons, France. And by identifying the coolest white dwarfs in the population, Chabrier says, the researchers have taken "a key step toward determining the age of the cluster."

For their study, Richer and his colleagues trained the Hubble Space Telescope on a section of NGC 6397 for 5 days at a stretch. "This was a very long exposure, so we could see fainter objects than had been seen before, even with this instrument," says Brad Hansen, an astronomer at the University of California, Los Angeles, and a co-author of the paper. From a computer analysis of the images, the researchers were able to spot stars that were barely alight. Hubble could have detected stars that were fainter still, but the researchers didn't see any. That convinced them that they had identified the smallest stars capable of stably burning hydrogen in their cores.

Using a similar analysis, the researchers identified the faintest—and hence the coldest—white dwarfs. The observation bears out a prediction Hansen made in 1998: As spent stars get cooler, they emit radiation of longer and longer wavelengths, appearing redder in the process. But once a star cools to below 4000 kelvin, its atmosphere forms hydrogen molecules that absorb the redder wavelengths of radiation emanating from its core. As a result, the star's spectrum shifts from red to blue and gets bluer as the temperature falls. The white dwarfs in the study showed exactly that trend. "It's a wonderful illustration of quantum physics taking place in the atmosphere of stars," says Chabrier.

The white-dwarf results open the door to establishing the age of the cluster, Hansen says: "It's like identifying the time of death of a corpse from the body temperature." And because the NGC 6397 cluster is one of the oldest in the galaxy—as determined from the rarity of metals in its composition—learning its history would provide valuable insights into the early formation of the Milky Way, he says. **–YUDHIJIT BHATTACHARJEE**

SCIENCESCOPE

More Questions for NIH

Despite strict new rules on how researchers at the National Institutes of Health (NIH) should interact with industry, the issue hasn't gone away. The latest case, reported last month by the *Los Angeles Times*, involves Thomas J. Walsh of the National Cancer Institute and his role in helping companies developing antifungal drugs.

In a 28 July letter to NIH Director Elias Zerhouni, the House Energy and Commerce Committee asked if there is "a sufficient factual basis to formally investigate [larger] questions about [NIH] policy" raised by Walsh's conduct. The members requested Walsh's financial reports and reviews of his paid and unpaid consulting and other activities, which include discussing some companies' products before the Food and Drug Administration. NIH officials, who tell *Science* that Walsh was already an "open case," are preparing a response.

–JOCELYN KAISER

Agbio Lab List Pared

Eighteen of 29 applicant sites are still in the running for a new $450 million high-security agro-biodefense lab to replace Plum Island Animal Disease Center, the aging facility off Long Island, New York (*Science*, 2 September 2005, p. 1475). The Department of Homeland Security is funding the National Bio-and Agro-Defense Facility to study animal diseases and possibly human illnesses. It plans to name a second round of finalists by the end of this year and choose a winner in early 2008.

–JOCELYN KAISER

Wanted: More Science Students

U.K. companies say a failing education system could make the country a scientific also-ran. On Monday, the Confederation of British Industry (CBI), the U.K.'s biggest business group, outlined its concerns about the sharp decline in students studying physics, chemistry, and maths at A-level, the exams needed for university entry. It faults "a stripped down science curriculum, a lack of specialist teachers, and uninspiring careers advice." In a related development, Alan Smithers and Pamela Robinson of the University of Buckingham last week reported a 50% decline in A-level physics entries since 1982.

Calling the scientific workforce "a priority," Schools Minister Jim Knight points to a $57 million government scheme that includes pay incentives to attract and retain teachers and efforts to build interest among students.

–LAURA BLACKBURN

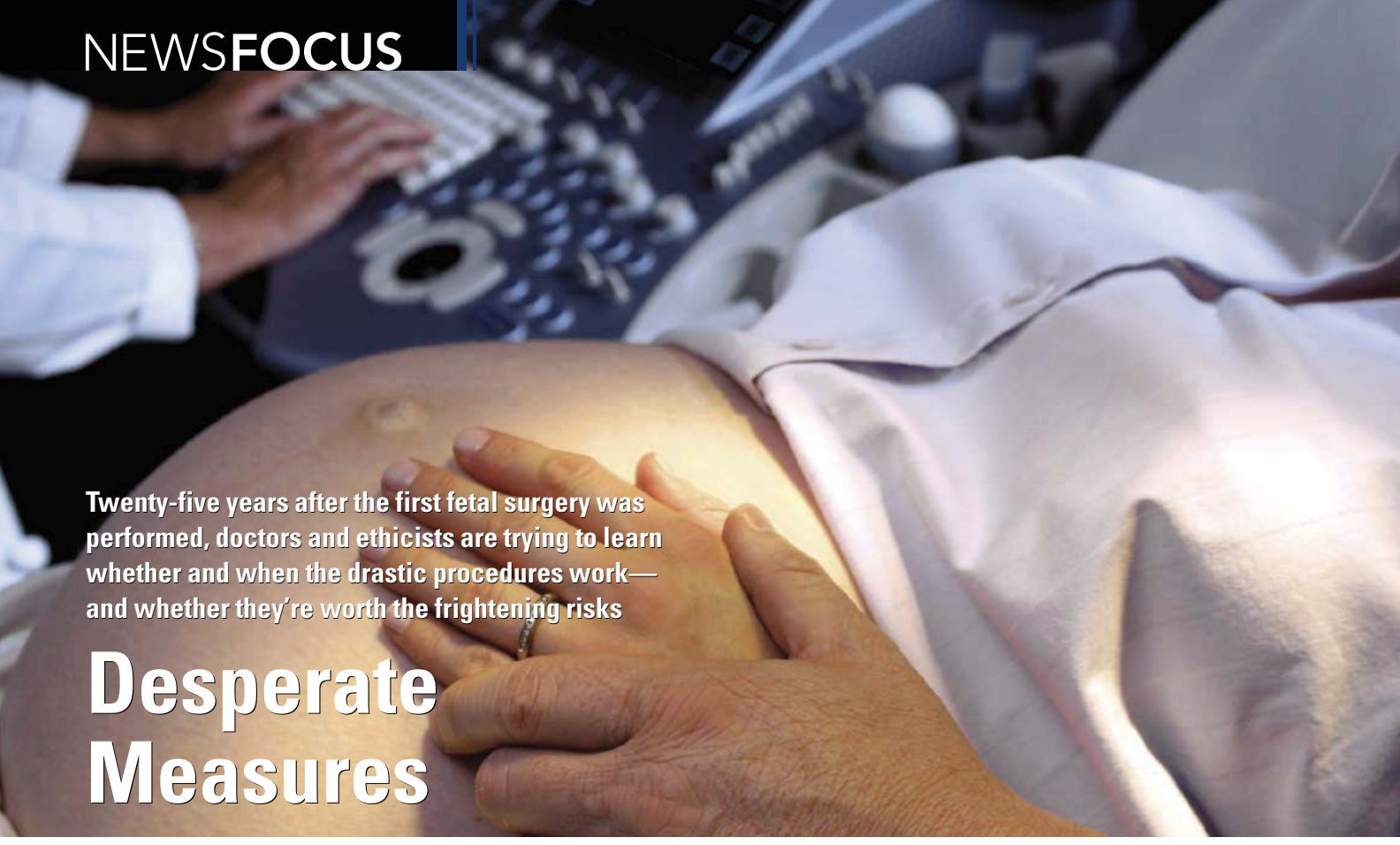

Twenty-five years after the first fetal surgery was performed, doctors and ethicists are trying to learn whether and when the drastic procedures work—and whether they're worth the frightening risks

Desperate Measures

ON 23 JANUARY 2002, SURGEONS CUT A 30-centimeter incision in Lorie Barber's abdomen, peeling away layers of tissue to reach her 23-week-old fetus. Delicately removing the uterus and slitting it open, the doctors at Vanderbilt University Medical Center in Nashville, Tennessee, stitched closed a gaping hole at the base of the fetus's spine. That opening was the signature left by spina bifida, which can cause paralysis, hydrocephalus, and other lifelong disabilities.

Thirteen days after the surgery, Nicole Eva Barber was born, more than 3 months early and weighing in at 1 pound and 10 ounces (740 grams). Nearly all fetal surgeries, the Barbers had been warned, carry a risk of premature birth. That hadn't deterred them.

Lorie Barber and her husband had come to Vanderbilt from their home in Ohio, desperate and devastated. Weeks earlier, a genetic counselor had discussed the diagnosis and presented two options: terminate the pregnancy or have the baby. The Barbers reached for a third choice they'd learned of over the Internet: fetal surgery that might offer their child a better life.

But for the Barbers, as for hundreds of other couples who have endured fetal surgery for a variety of conditions, there were no guarantees that the benefits of this treatment would outweigh its risks to both mother and fetus. Although roughly a dozen medical centers worldwide now offer fetal surgery, it remains highly experimental. Few fetal surgeries have been tested systematically in clinical trials, and for those that have, the results are decidedly mixed—suggesting anything from no advantage to robust benefit.

Part of the problem is that fetal surgeries are maddeningly difficult to evaluate in clinical trials. That's true of surgical interventions generally, and many enter mainstream practice without rigorous testing. But as diagnostic imaging advances, making it possible to visualize still more fetal anomalies potentially amenable to surgery, a growing number of physicians and ethicists are calling for trials to measure fetal surgery's worth against standard postnatal care. Perhaps more than anything, they fear that fetal surgeries, once confined to the most dismal cases, are becoming routine before their safety and effectiveness can be rigorously tested.

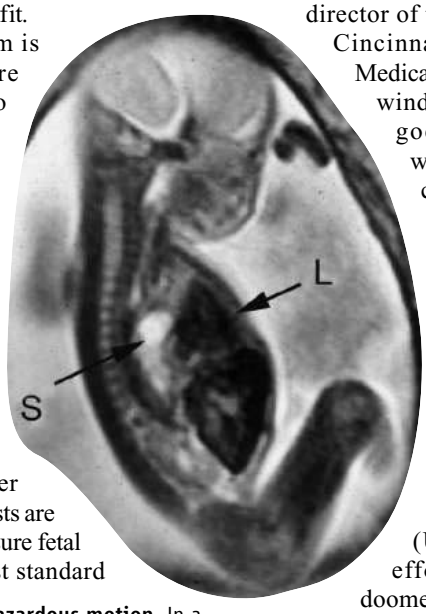

Hazardous motion. In a fetus with congenital diaphragmatic hernia, the stomach (S) and part of the liver (L) have migrated toward the chest, inhibiting lung development.

"Oftentimes, these therapies kind of take on a life of their own," says Timothy Crombleholme, a pediatric surgeon and director of the Fetal Care Center at Cincinnati Children's Hospital Medical Center in Ohio, "and the window to evaluate them … goes away." To keep that window open, fetal surgery centers banded together last spring to form a clinical trials network that they hope will speed testing of various fetal treatments, before they become entrenched.

First breaths

Fetal surgery began in 1981 at the University of California, San Francisco (UCSF), as a last-ditch effort to save otherwise doomed fetuses. The hope was that by correcting a life-threatening defect early, surgeons could prevent further damage and save the fetus's life.

The first successful surgery, to repair a urinary obstruction that triggers kidney and lung failure after birth, resulted in a boy born

CREDIT (TOP TO BOTTOM): ED CUNICELLI; THE CHILDREN'S HOSPITAL OF PHILADELPHIA

Diagnosis. A woman undergoes a high-resolution ultrasound at the Children's Hospital of Philadelphia to help determine whether her fetus could benefit from surgery.

alive who recently celebrated his 25th birthday. In the hands of UCSF pediatric surgeon Michael Harrison and his colleagues, rare conditions considered fatal sometimes proved no longer so. By following the natural history of certain diseases—in other words, how babies fared with standard, postnatal care—the physicians felt they could gauge fetal surgery's effectiveness.

As word spread about what the UCSF team was doing, "people would present [us] with a problem, often in the form of a patient, and say, 'Do something,' " says Mitchell Golbus, an obstetrician and geneticist, now retired, who helped develop the UCSF program. In this way, the surgeries gradually spread to other life-threatening conditions. Among them was twin-twin transfusion syndrome, an often fatal circulatory disorder that strikes twins.

Another, congenital diaphragmatic hernia (CDH), occurs when abdominal organs migrate through a hole in the diaphragm to the chest in utero, compressing lung development and leaving newborns with inadequate lung capacity. The disease afflicts about 1 in 2500 babies worldwide, and all require surgery early in life. Intervening during fetal development, it was thought, might leave babies with larger, healthier lungs at birth and thus a much better chance of survival. When pediatric surgeons first began exploring fetal surgeries for CDH, about 30% of infants born with the condition survived.

In 1989, after 5 years of failed attempts in fetuses who died from the disease, UCSF performed the first successful CDH fetal surgery, closing the hole in the diaphragm. Although buoyed by their victories, even the most enthusiastic recognized that although they might be saving some very sick fetuses, the early surgeries had unsettling downsides. Some fetuses died from surgery itself, and others were born extremely prematurely. Moreover, some of the healthy women who underwent fetal surgery ended up in intensive care, hit dangerously hard by side effects from drugs given to prevent early labor.

"You have to make sure you have very good justification" for these surgeries, says Golbus, "because you're taking a healthy mother and running the risk of making her unhealthy."

With that in mind, Harrison pushed for and led the first-ever clinical trial of fetal surgery. Begun in the early 1990s, the trial was designed to test so-called open surgery for CDH, the surgical approach that Lorie Barber endured for spina bifida. In CDH cases, the mother's womb is opened and the fetus partially removed for the operation.

Behind the scenes, the trial was a nightmare. Uneasy about the treatment's novelty, officials at the National Institutes of Health (NIH), which funded the trial, and UCSF's human subjects oversight committee took 2 years to approve it. Soon after the trial began, it was abruptly halted amid reports that women inside and outside the study who had undergone fetal surgery suffered pulmonary edema. The cause was traced to nitroglycerin, given experimentally to prevent early labor. The study restarted, finally ending 8 years after Harrison first proposed it. The randomized trial eventually compared the survival of four fetuses who had open surgery with seven who did not.

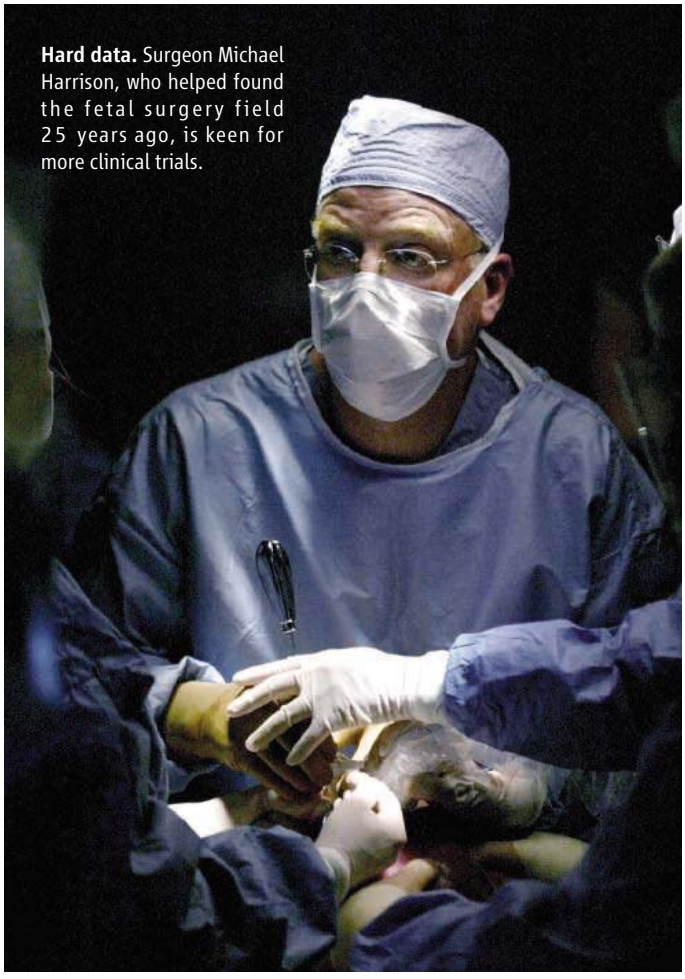

Hard data. Surgeon Michael Harrison, who helped found the fetal surgery field 25 years ago, is keen for more clinical trials.

CREDIT: LEA SUZUKI/*SAN FRANCISCO CHRONICLE*

Logistics aside, Harrison and colleagues were convinced going in that CDH surgery would prove beneficial. "We thought for sure the randomized trial couldn't fail," says Russell Jennings, then a fellow with Harrison and now head of the Advanced Fetal Care Center at Children's Hospital Boston. The truth was less kind. In a paper published in 1997 in *The Journal of Pediatric Surgery*, Harrison and colleagues reported that survival rates were 75% in the treated group and 86% in the control group, a difference that was not statistically significant, given the small numbers involved. One baby in each group died.

But around that time, two teams working with fetal lambs—one led by Harrison and the other by Jay Wilson of Children's Hospital Boston—found that they could correct the defect by blocking the trachea. This less invasive mechanical fix had a dramatic effect, keeping fluid pressure in the lungs high and forcing them to grow more rapidly. (The herniated diaphragm, surgeons found, could be repaired after birth.) "Right after our first sheep, we said, 'This is it; we have cured diaphragmatic hernia,' " recalls Jennings.

A second trial testing this endoscopic technique, however, met with disappointment. Published in 2003 in *The New England Journal of Medicine*, that study found that 8 of 11 treated fetuses survived. But so did 10 of 13 in the control group. The treated babies who lived did have larger, healthier lungs, as the sheep studies had predicted, but those benefits were often muted by prematurity.

Although they didn't show survival advantages from fetal surgery, the trials did underscore risks to the fetus and the mother. Both open and endoscopic surgery greatly boosted the chance of premature birth. Babies in the open-surgery trial were born at 32 weeks, on average, and at 31 weeks in the endoscopic trial, roughly 6 weeks earlier than babies in both control groups. Since then, other risks have surfaced. Roughly 5% to 15% of women undergoing endoscopic fetal surgery experience a rupture in their uterine membrane, which puts the mother at risk of

infection and may force early delivery of the baby—a complication that can also strike subsequent pregnancies. The risk is lower, about 4%, in open surgeries, says Scott Adzick, who runs the Center for Fetal Diagnosis and Treatment at the Children's Hospital of Philadelphia (CHOP).

Another reason for the confounding CDH results is that while the trials chugged along, survival odds were trending upward for CDH babies given postnatal respiratory support and surgery. At major pediatric centers such as Children's Hospital Boston, 95% of babies with CDH now survive, says Wilson, although many suffer long-term gastrointestinal and respiratory complications.

At least some surgeons still believe CDH fetal surgery offers the best hope for a healthy life. A variant on the endoscopic surgery tested in the second trial is now practiced regularly in Europe. More than 90 fetuses have been operated on so far, says Jan Deprest, a gynecologist at University Hospital Gasthuisberg Leuven in Belgium. Deprest says that his technique improves survival by 50%—but in Europe, say U.S. surgeons, CDH survival rates are lower than in North America (an assertion Deprest disputes). The surgeries, which focus on fetuses with the worst prognoses, have generated controversy, in part given the failure of other CDH fetal surgeries to show benefit. Both Deprest and Harrison are eager for yet another trial, to, as Deprest puts it, "have this discussion finished."

Regardless, as postnatal medical care advances, many babies with CDH and other conditions who once perished now pull through. But often, they're left with lingering disabilities. That has physicians considering fetal surgery's power to enhance life's quality.

A better life?

As the CDH trials continued, fetal surgery was stretching to accommodate its first non–life-threatening defect, spina bifida. "It really shifted … fetal treatment into another realm," recasting the benefit-risk balance irrevocably, says Nancy Chescheir, an obstetrician at Vanderbilt.

Spina bifida arises very early in pregnancy, when the fetus's spinal cord fails to close. Children with the disability rarely die from it, but they often need shunts to drain fluid from their brains and suffer mobility, learning, and bladder and bowel problems.

Experiments on fetal lambs in the 1980s and early 1990s suggested that closing the wound in utero could reduce these complications. Fetal surgeons believe that sealing the opening may protect the spinal cord from continuing damage, perhaps by preventing exposure to amniotic fluid and normalizing fluid dynamics in the fetus's brain. Physicians at Vanderbilt proclaimed the first open fetal surgery for spina bifida in 1997, and hundreds of families streamed into Nashville.

The University of North Carolina, Chapel Hill, also offered the surgery. Sue Estroff, an anthropologist who chairs the university's maternal-fetal intervention advisory group, says that families typically came determined to proceed and weren't swayed by discussions of risks and benefits. "Our concepts of [informed] consent didn't fit what we saw," she says. "People brought ideas about what it means to be a good parent."

One was Lorie Barber. She imagined eschewing the surgery, only to have her child later grow up to say, "Mom, you knew about this, and it was available back then. Why didn't you try, why didn't you go for it?"

Barber was also encouraged by preliminary data from Vanderbilt suggesting that surgery might lessen the need for a shunt. In a paper published 2 years ago (although details were shared with families earlier as they accrued), Joseph Bruner, who oversaw spina bifida fetal surgeries at Vanderbilt and now works in Tennessee, and his colleagues reported that of 116 fetuses who had the surgery, 54% required a shunt before 1 year of age. The shunt rate for children who don't have fetal surgery has been estimated at as high as 85%, although it's thought to be drifting downward as neurosurgeons shunt more conservatively.

Riding high. Born 3 months early after spina bifida fetal surgery, 4-year-old Nicole Barber has few spina bifida symptoms—but it's difficult to know whether the experimental procedure made a difference.

CREDIT: COURTESY OF THE BARBER FAMILY

Even so, substantial questions about the surgery's benefit remained. For one, "spina bifida in humans happens at 8 weeks' gestation," says Harrison. "We cannot work [on a fetus] at 8 weeks." It's possible that by the time technology permits surgeons to operate—at about 20 weeks—the bulk of the damage has already occurred, making the drastic surgery largely futile. At the same time, because babies with spina bifida have an excellent chance of survival, life-threatening fetal surgery was creating ethically tenuous scenarios. At CHOP, says Crombleholme, who trained there before moving to Cincinnati, three babies with spina bifida who underwent fetal surgery were born so prematurely that they died. "These are three patients who would have survived," he says.

Many physicians and ethicists became convinced that the only way to assess this surgery was in a clinical trial with a control group. With that in mind, NIH launched a trial in 2003, based at Vanderbilt, CHOP, and UCSF. Originally slated to end next year, the trial randomly assigns 100 mothers to surgery and 100 more to standard care. Success is measured by survival, the need for a shunt in the baby's first year, and neurologic function at 30 months.

By the time the trial began, physicians had performed more than 200 spina bifida fetal surgeries, and demand showed no signs of abating. To ensure that women would sign up for the trial, all hospitals halted spina bifida fetal surgeries outside the study.

Despite these efforts, recruitment has been sluggish. The trial was supposed to have begun a full year ago, but so far just 99 women have signed on. Explanations include a reluctance to be randomly assigned to either fetal surgery or a control group and a mother's unwillingness to remain at the surgical center until birth, as the trial mandates. But one thing is apparent: Continuing to recruit at this pace, "we're up to a 10-year trial," double the time anticipated, says Chescheir. So far, NIH has alloted more than $14 million to it.

Some surgeons quietly question whether spina bifida fetal surgery will survive. "The surgery itself is dying a slow death because of the length of the trial," says Bruner. Unlike a drug, "surgery is a living, evolving entity," he says. Doing a trial means "you have to freeze it in time," halting the subtle enhancements surgeons routinely make. Safer, endoscopic

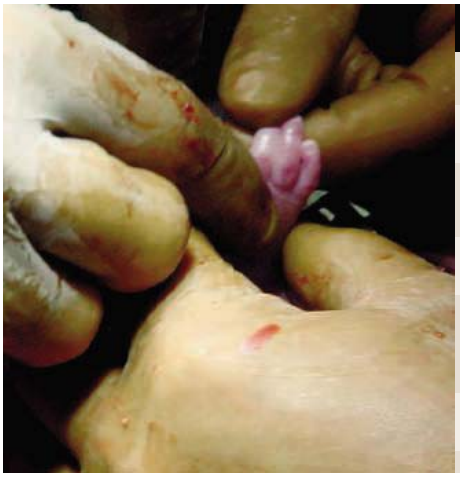

Fetal Surgery Trials

Disease	Lead Clinical Site(s)	Surgery Type	Total Size (women)	Status
Congenital Diaphragmatic Hernia	UCSF	Open surgery	11	Published in 1997, no survival benefit
Congenital Diaphragmatic Hernia	UCSF	Endoscopic	24	Published in 2003, no survival benefit
Twin-Twin Transfusion Syndrome	Hospitals in France, Belgium, and the U.S.	Endoscopic	142	Published in 2004, fetal surgery helped survival
Twin-Twin Transfusion Syndrome	*Children's Hospital Medical Center, Cincinnati	Endoscopic	42	Halted early after European trial
Spina Bifida	UCSF, Vanderbilt, CHOP	Open surgery	200	Still recruiting

* Trial began at CHOP.

approaches have not yet been effective at repairing spina bifida lesions, for example. As a result, in Europe, where open fetal surgeries are considered too aggressive to the mother, the procedure is not offered.

The heart of the matter

Some physicians are converging instead on another new frontier: fetal heart surgery. In the operating suites at Children's Hospital Boston, doctors now regularly perform procedures on fetuses with heart defects, 77 and counting since 2000. Although Boston is the only center in the world to have done more than a handful of these surgeries, says Wayne Tworetzky, a cardiologist there, other centers are considering whether to follow suit. Heart defects are ideal candidates for fetal surgery, Tworetzky and others say. High-tech fetal imaging has made diagnosis easier, and heart defects are a common and serious scourge in babies. The surgery to address them involves inserting a needle into the mother's abdomen and guiding it via ultrasound into the fetus's heart.

But as with other fetal surgeries, the cardiac procedures are raising difficult questions of their own—in particular, whether cardiologists understand enough about the defects they're trying to fix in utero. Nor is it clear that they can identify the fetuses most likely to benefit.

Take hypoplastic left heart syndrome (HLHS), the defect that the Boston team most commonly targets. Babies with HLHS are born lacking a functioning left ventricle, which leaves them with "only one pumping chamber," says Tworetzky. Soon after birth, the infants turn ashen and struggle to breathe and feed normally. HLHS is not curable, and although most children can be treated with a series of operations or a heart transplant, their long-term prognosis is still shaky.

Strategies to fix HLHS in utero, however, are complicated by questions about what's driving the disease. In some babies, HLHS seems to begin with a problem that is straightforward enough to fix: a blocked heart valve. Sophisticated tests on a pregnant woman can determine whether her fetus has this blocked valve. The surgery targets this obstruction in the hope that clearing it gives the left ventricle time to develop.

However, although a blocked valve is certainly associated with the heart defect, it's not yet clear that it's the key culprit. Fixing it, then, might be less likely to help than it would be if the blocked valve were causative. "It's possible that these lesions which we consider primary … could be secondary, [and] relieving those would not necessarily improve muscle growth," says Abraham Rudolph, a former chief of pediatric cardiology at UCSF who spent decades studying fetal circulation.

> "Oftentimes, these therapies kind of take on a life of their own, **and the window to evaluate them … goes away.**"
>
> —Timothy Crombleholme, Cincinnati Children's Hospital Medical Center

And there's a second catch. Only a subset of fetuses with the blocked valve develop HLHS. Others are born with just the blockage, which can be corrected postnatally. Physicians at Children's Hospital Boston such as Tworetzky and cardiologist James Lock have done a number of studies to try to identify which fetuses with blocked heart valves go on to develop HLHS, because the risks of fetal surgery cannot currently be justified for the others. "We have strict criteria; you have to have this and this and not that," says Tworetzky. In March, he and his colleagues published a paper in *Circulation* suggesting that certain types of blood flow in fetal hearts can predict HLHS—and thus which mothers and their fetuses are best suited for surgery.

But other hospitals are hanging back. "There's logic to it, it makes sense, but it hasn't been rigorously tested," says Jack Rychik, the head of CHOP's Fetal Heart Center, of the work in Boston. Last month, CHOP performed its first fetal heart procedure—but that fetus had multiple heart defects and an especially poor prognosis. Rychik wants firmer guarantees that he can pick the right mothers and fetuses for surgery and for now is not comfortable operating on all the same classes of women and fetuses treated in Boston.

Instead, Rychik is working to bring together eight centers, including Boston, to create a registry of fetuses with various heart defects who would be followed until birth. "The Boston experience has given us a kick in the pants" to examine the natural history of HLHS and other defects before fetal heart surgery becomes routine, says Rychik, who adds that the therapy may soon merit a clinical trial. In April, 17 centers in North America launched the North American Fetal Therapy Network to create a single voice to advocate for and help develop fetal treatment trials. It hopes its endorsement of certain trial proposals will encourage NIH and other funders to supply the millions of dollars these studies can cost.

Rychik and others are treading cautiously in part because families seek fetal surgery wherever possible. Even the Barbers, whose daughter spent 6 weeks on a ventilator and 103 days in a neonatal intensive care unit, say the price of surgery was worth it. Now 4 years old, Nicole's moderate hydrocephalus has not required a shunt. She's a strong-willed, talkative little girl who walks unassisted, attends a typical preschool, and enjoys bringing in the mail. Her mother has no regrets.

–JENNIFER COUZIN

CREDIT: (PHOTO) FETAL TREATMENT CENTER, UNIVERSITY OF CALIFORNIA, SAN FRANCISCO

Widening the Attack on Combat-Related Mental Health Problems

The lessons of Vietnam have prompted U.S. military leaders to do more to protect the mental health of troops in Iraq and Afghanistan. But will these efforts be effective?

Airman C couldn't shake the image of the young Iraqi boy. Days earlier, a car bomb went off as his convoy drove down a busy city street, injuring three fellow soldiers and killing perhaps 10 Iraqi civilians. The boy sat at the edge of a street near a light pole. The explosion had torn off the right side of his jaw and opened his neck, exposing his esophagus. He reached up to Airman C, as if to ask for help, and called out "American, American, American." But the word had just come in that the convoy was in danger of a second attack, and Airman C had to move on.

Stressful job. The constant threat of car bombs and other attacks can take a toll on troops' mental health.

After the attack, the image of the boy kept replaying in Airman C's mind throughout the day and at night, in frequent nightmares, says Alan Peterson, a clinical psychologist who treated the 22-year-old airman in the field for symptoms of posttraumatic stress disorder (PTSD).

Peterson, who served with the U.S. Air Force as the chief psychologist at Balad Airbase near Baghdad until January 2005, knows firsthand how the tremendous stress and horrific situations faced by the troops can affect their mental health. And increasingly, he and others say, U.S. military leaders are showing a much greater willingness to acknowledge—and address—these problems than in the past. More psychologists and other mental health professionals have, like Peterson, been deployed to the frontlines of Iraq and Afghanistan. The Department of Defense (DOD) has instituted a universal screening program to monitor the health, including the mental health, of troops returning from combat. And several innovative programs aim to ease their transition to civilian life.

Although it's too early to gauge the effectiveness of these interventions—and the screening program, in particular, has its detractors—many observers see them as a welcome sign of progress. "The leadership has taken a very proactive stance toward mental health issues," says Charles Hoge, a psychiatrist at Walter Reed Army Medical Center in Washington, D.C. "We're well aware this time that there's an expected psychological cost of war."

Lingering effects

War has always taken a toll on soldiers' psyches. After the Vietnam War, the chronic difficulties suffered by many returning troops—including flashbacks, nightmares, and feelings of detachment—inspired a new psychiatric diagnosis, PTSD, which officially entered the psychiatric lexicon in 1980 as an entry in the *Diagnostic and Statistical Manual of Mental Disorders*, third edition. From the start, however, gauging the prevalence of PTSD in combat veterans has been difficult and controversial.

A study of Vietnam vets by the Centers for Disease Control and Prevention in Atlanta, Georgia, in 1988 put the prevalence of PTSD at 15%. But a short time later, the National Vietnam Veterans Readjustment Study (NVVRS), commissioned by Congress, doubled that estimate—concluding that 31% of Vietnam vets had suffered from PTSD at some point in their lives. Many researchers suspected that the NVVRS number was too high: Critics pointed out that the proportion of vets who'd suffered PTSD was twice the proportion who'd served in combat roles. A reanalysis of the NVVRS, which attempts to exclude vets whose symptoms weren't severe enough to interfere with daily living, now puts the figure at about 19% (see Report on p. 979 and Perspective on p. 923). But even that figure translates to more than 500,000 cases among Vietnam vets.

Experts say it's impossible to know how many of the troops serving in Iraq or Afghanistan will develop PTSD or other combat-related mental problems, but preliminary data hint at a prevalence similar to the new figure for Vietnam. Soldiers in all three conflicts have faced similar stressors: a constant threat of ambush, a high casualty rate among both soldiers and civilians, and a difficulty distinguishing friend from foe. More frequent and more intense combat experiences raise the risk of PTSD, and there is no shortage of these, especially in Iraq. In the 1 July 2004 issue of *The New England Journal of Medicine* (*NEJM*), Hoge and colleagues reported that among 894 members of an Army combat unit that had recently returned from Iraq, 89% reported being attacked or ambushed, and 95% reported seeing dead bodies or human remains.

This *NEJM* paper also provided one of the first looks at how soldiers are holding up under such conditions. In an anonymous survey, 17% of members of the same Army unit reported symptoms of PTSD, generalized anxiety, or depression. The researchers found a somewhat lower prevalence of such symptoms, about 11%, in 1962 soldiers deployed to Afghanistan, presumably reflecting their lower levels of reported combat experience.

A second study by Hoge and colleagues, based on an abbreviated survey but a much larger sample of 238,938 Army and Marine personnel returning from Iraq and Afghanistan, produced similar findings. In the 1 March 2006 issue of *The Journal of the American Medical Association* (*JAMA*), they reported that 19% of those serving in Iraq and 11% of those serving in Afghanistan reported symptoms of PTSD or other mental health problems (see table, p. 909).

Although the figure for Iraq troops seems similar on the surface to the new figure for Vietnam, there's no way to make a definitive comparison, says Bruce Dohrenwend, a psy-

CREDIT: GHAITH ABDUL-AHAD/GETTY IMAGES

chiatric epidemiologist at Columbia University who led the new reevaluation of the NVVRS. Whereas the raw data for NVVRS was collected in one-on-one clinical interviews lasting an hour or more, the data in Hoge's studies come from soldiers ticking off symptoms on a questionnaire. "I don't know how symptom scales compare to a rigorous diagnosis by a trained clinician," Dohrenwend says.

Concerns about the reliability of using surveys to detect mental problems have led some experts to question the effectiveness of DOD's new postdeployment health assessment program, instituted at the onset of the Iraq War. Every service member must now complete a three-page questionnaire that includes about a half-page of questions on mental health, either immediately before or within 2 weeks of returning home. Those who screen positive for a mental health problem get a follow-up interview with a clinician. The goal is to catch soldiers who need help early on, says Hoge, and get them treatment before their symptoms develop into a full-blown disorder or become compounded by family, alcohol, or drug problems, as happened to many soldiers after Vietnam. The 2006 *JAMA* paper was the first report based on data collected by the health assessment program. DOD recently announced plans to repeat the assessment at 3 and 6 months postdeployment. That's a good idea, Hoge and others say, because little is known about the time course of PTSD and because some problems might be masked by soldiers' initial euphoria over returning home.

But Simon Wessely, a psychiatrist at Kings College London and civilian adviser to the British Army, dismisses the DOD screening effort as scientifically unfounded and a likely waste of resources. The main problem, he and others say, is that such surveys haven't proven effective at predicting which individuals will need mental health help. On one hand, the screen may tend to exaggerate problems by only tallying symptoms, says Richard McNally, a psychologist at Harvard University. It's possible to have a couple of symptoms of PTSD but not a full-blown disorder that requires intervention, he says: "Almost everybody is changed by the experience of fighting in a war. You have to draw a distinction between normal human emotions that are evoked by a horrible experience and things that impair daily life." The follow-up interviews should help cut down on false positives, however, McNally says.

A greater concern, in his view, is that the survey may fail to identify some veterans who need assistance. Peterson agrees. "The word on the street is, 'Don't tell them you have symptoms, or you'll have to see a shrink,' " he says. Soldiers who take the survey before returning stateside are often tempted to hide symptoms to avoid delaying their return, and worries about the confidentiality are also widespread, Peterson says. Many soldiers may not check the box because they fear negative ramifications on their careers. The recent *JAMA* paper seems to bolster concerns that the screening isn't very accurate at identifying individuals who need help. Hoge's team found, for example, that fewer than 8% of servicemen seeking mental health care in the first year after their return had been referred by the screening program, suggesting that the vast majority of those who sought help weren't flagged by the program. At the same time, fewer than 20% of those who did report mental health concerns on the survey were referred to a mental health professional for further evaluation. In a May 2006 report, the U.S. Government Accountability Office chastised DOD for failing to get veterans mental health care when they need it. "The drive to do widespread screening is a laudable ambition, but it's driven largely by politics and the desire to be seen to be doing something and not by any evidence I've seen that it's doing any good," says Wessely.

CREDIT: SCOTT OLSON/GETTY IMAGES

U.S. Soldiers at Risk	In Iraq (222,620)	In Afghanistan (16,318)
Screened positive for PTSD	9.8%	4.7%
Screened positive for any mental health concern	19.1%	11.3%
Visited mental health clinic within first year home	34.6%	21.5%
Diagnosed with mental disorder within first year home	11.9%	9.7%

SOURCE: HOGE *ET AL.*, *JOURNAL OF THE AMERICAN MEDICAL ASSOCIATION* **295**, 9 (2006)

In their own terms

Wessely says he's advised the U.K. government that money and effort would be better spent on expanding mental health services and making them more amenable to veterans than on screening. He cites a U.S. DOD program called Battlemind, started by Hoge, as "a promising way forward." In presentations to returning combat units and in videos and other materials available online for soldiers and their families, Battlemind explains how the combat-zone mindset can lead to problems at home. For example, in a combat zone, constant awareness of the surroundings is crucial for survival. But once soldiers return home, such heightened attention can leave them anxious and easily startled—a PTSD symptom called hypervigilance. The program appeals to soldiers because it uses language they understand and steers clear of mental health jargon, says Hoge: "We don't talk about hypervigilance; we talk about tactical awareness."

Meanwhile, Peterson, who has retired from the military and is now at the University of Texas Health Science Center in San Antonio, is developing a training program for Air Force mental health providers to teach them how to treat PTSD symptoms in the field. Airman C's symptoms were severe, and in previous conflicts, he would likely have been evacuated. But Peterson used a type of exposure therapy with him that has also proven useful with civilian rape and accident victims. In four sessions over the course of several weeks, Airman C talked through his ordeal in excruciating detail with Peterson, who made an audiotape of the session and asked him to listen to it at least once in the coming week. It's a painful process, but it helps desensitize people to the traumatic event, Peterson says. With time, Airman C's symptoms dissipated, and he began to feel more like himself, Peterson reported in a case study published last year. He now has funding from DOD to evaluate the therapy in a larger trial. "We think part of the key is early intervention," he says.

–GREG MILLER

Karoo contender. The four sites competing for the SKA's core include this stretch of the Karoo semidesert in South Africa.

RADIO ASTRONOMY

Candidate Sites for World's Largest Telescope Face First Big Hurdle

For more than a decade, the Square Kilometer Array has been a paper project, an instrument for astronomers to dream about. Now it's time to start getting real

CAPE TOWN, SOUTH AFRICA—One site is a barren tract of South Africa's Karoo semidesert, so quiet that the only sound is a hawk's cry. Another, 12,000 kilometers away, is an arid plain that stretches to western Australia's horizon. Yet another site is across the Pacific Ocean, in Argentina's high, dry plateaus; the fourth is nestled in natural bowls between the angular karst hills of southeastern China.

The challenge for a select group of radio astronomers this summer is to recommend which site would potentially make a suitable home for the largest astronomical instrument ever built: the International Square Kilometer Array (SKA). Planned as a network of some 4000 radio dishes spread over an area several thousand kilometers across, SKA—whose name refers to the total collecting area of the planned instruments—will be 100 times as sensitive as today's best radio telescopes. In choosing which locations will work, SKA's international steering committee is looking for a stable ionosphere, predictable weather, and good infrastructure. But radio silence, perhaps above all else, is golden, as is the host government's ability to maintain it.

At a meeting in Germany at the end of this month, the committee is to whittle down, on scientific and technical grounds, the current four to a short list of acceptable SKA sites. Then begins the delicate political dance of persuading funders to bankroll it and agreeing on the final site.

With a price tag likely to be at least $1 billion, the SKA collaboration is treading carefully. The project has already been working for more than a decade; a reference design for the telescope was completed only this year, and the array itself is unlikely to be finished before 2020. But the team doesn't want to force the pace and fall into the traps that have beset other recent international collaborations such as the International Thermonuclear Experimental Reactor (*Science*, 1 July 2005, p. 28) and the Atacama Large Millimeter Array (ALMA), a telescope under construction in Chile (*Science*, 19 May, p. 990).

From the start, SKA has been a grassroots project, and with scientists at more than 50 institutes in 17 countries involved, there is a strong emphasis on collaboration. Bo Peng of China's National Astronomical Observatories in Beijing says that SKA "has been a very successful international project for a decade, on the basis of cooperation, not so much competition for SKA science, technology, and even site ranking."

In the competing regions, the site selection has energized radio astronomy and engineering with new instruments, more government backing, and scientific networking. "It is having a tremendous focusing impact on scientists," says Netherlands-based astronomer Richard Schilizzi, director of the SKA project.

"The collaboration is fantastic," agrees Australia's SKA planning office chief, astrophysicist Michelle Storey, "not only within Australia's radio community but also among astronomers from all the countries involved in the SKA." Astronomer Justin Jonas, South Africa's SKA project scientist, foresees "a tremendous boost to astronomy and to science in general in southern Africa." Jin Chengjin of the National Astronomical Observatories says his nation's radio-astronomy community is being opened up by the SKA effort because "the competition helps us in communicating with international astronomical and technological communities." Ricardo Morras of the Argentine Radio Astronomy Institute says winning the SKA site would be "a major breakthrough in the history of radio astronomy in Latin America."

What a dish. China's proposed SKA site lies in a lush valley surrounded by karst hills. Proponents say natural depressions there are ideal for building fixed dish antennas.

Probing dark matter and energy

SKA's main aim is to search for faint radio signals from the most distant reaches of the universe, helping scientists examine clues to what existed before the first stars were born and to probe the nature of dark matter and dark energy.

CREDITS (TOP TO BOTTOM): ROB MILLENAAR; CHINESE NATIONAL ASTRONOMICAL OBSERVATORIES

George Miley of Leiden University in the Netherlands says the instrument has the potential to be "a giant step forward for radio astronomy." By exploiting new technologies such as steering the observing direction electronically instead of by moving the dish, unprecedented supercomputing power, and multibeaming—observing several regions of the sky simultaneously—SKA will attain orders-of-magnitude improvement in frequency resolution and the area of sky that can be observed at any given time.

Astronomer James Cordes of Cornell University, head of the U.S. SKA team, agrees that the telescope "will be a fantastic discovery instrument." Schilizzi points out that "radio astronomy over the years has resulted in many unexpected discoveries, from the cosmic microwave background to pulsars to quasars to dark matter in galaxies." By peering into the early universe, SKA "will give us a handle on the effects of dark energy and its evolution as the universe expands," he adds.

Miley says data from SKA would help scientists study astrophysical phenomena that are impossible to probe using optical telescopes or millimeter arrays such as ALMA. Examples include neutral hydrogen, a diagnostic of the early universe in an era before the first galaxies formed, and synchrotron emission, radiation given off when electrons are accelerated—a unique probe of magnetic fields throughout the universe.

Site competition, science cooperation

But there is much still to do before observations can begin. Officials of the four national site planning offices have been competing hotly behind the scenes. On 4 July, a parade of these officials presented their proposals separately at a meeting in Cambridge, U.K.

The Australians argue that their core site in Mileura and their proposed remote sites have the lowest radio frequency interference (RFI) and that all are located in Australia, with the option of extra stations in New Zealand. Australia has a "very strong tradition in radio astronomy," Storey says, and several of its leading universities already are intensely involved in SKA research and development.

The South Africans contend that their site, northwest of the town of Carnarvon in the arid Karoo region, offers "very good radio-quiet status, excellent ionospheric and tropospheric conditions, strong government support and infrastructure," says former astronomer Bernie Fanaroff, South Africa's SKA chief. Remote array stations would be located in seven other African countries, bolstering astronomy and engineering across the southern part of the continent.

The Chinese say their bid is strong because of the site's relatively quiet electromagnetic environment and because the karst depressions offer the possibility of building a smaller number of huge static dishes, which would "ease the correlation process and help in calibrating the network effectively," Jin says. He adds that the valleys offer "good local shielding against radio interference from outside."

The Argentineans maintain that their site, in a high, arid plain about 1100 kilometers west of

From KAT to FAST, Telescope Project Sprouts Test Beds

High-tech radio-astronomy dishes are popping up in several remote areas of the world as demonstrators for the International Square Kilometer Array (SKA). Although each will be only a tiny fraction of the size of the planned SKA, the instruments will be capable of conducting cutting-edge science. Scientists in three of the candidate countries—Australia, China, and South Africa—have persuaded their governments to back the design and initial construction of prototype projects that are roughly 1% of SKA's dish area or smaller but that would demonstrate key technologies near the same core sites that are proposed for SKA itself.

Australia's Extended New Technology Demonstrator (xNTD) is planned as a full-system prototype, making use of an innovative phased focal-plane array, a detector made of a patchwork of antenna elements that can steer its field of view electronically. The demonstrator, operating over the frequency range of 0.8 to 1.8 gigahertz, will be built at the Mileura site, with completion targeted for 2009. Others are in the works too: the SKA Molonglo Prototype from the University of Sydney for low-frequency radio astronomy, and the Mileura Widefield Array–Low Frequency Demonstrator, built in partnership with the Massachusetts Institute of Technology's Haystack Observatory.

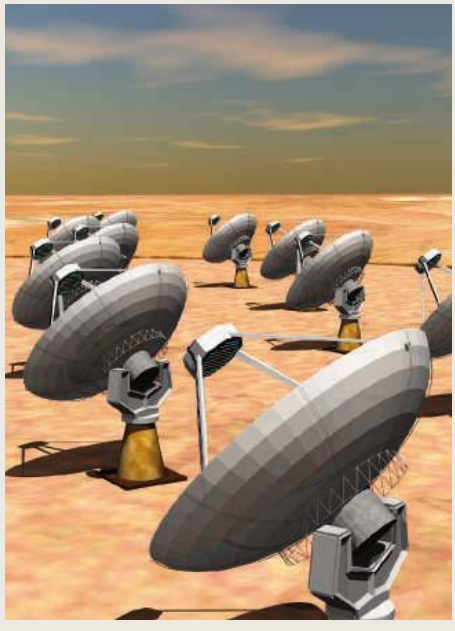

Aussie array. Artist's drawing shows part of the array of dishes planned for Australia's Extended New Technology Demonstrator (xNTD).

Meanwhile, South Africa's planned Karoo Array Telescope (KAT) is expected to have 20 dishes, each 15 meters in diameter, with innovative "smart" feeds in the focal plane. The South African government has committed the equivalent of about $50 million so far, and the prototype dish will be ready next year, with first light in 2009.

China's planned demonstrator instrument, the 500-meter-diameter Aperture Spherical Radio Telescope (FAST), would have a cable-supported reflector made up of 1800 hexagons—the world's largest single dish. Built in one of the karst depressions in Guizhou Province that are envisioned to be part of SKA, FAST "may be seen as a forerunner or prototype of the Chinese SKA concept," says Jin Chengjin of the National Astronomical Observatories in Beijing.

Although FAST is a somewhat different design, astrophysicist Michelle Storey, head of Australia's SKA planning office, says KAT and xNTD "are similar in many ways." That's a reason to be cautious, says Renee C. Kraan-Korteweg, who heads the University of Cape Town's astronomy department. It is important for the SKA competitors to make sure their demonstrator instruments and scientific goals complement one another. "Both the KAT and xNTD are interesting scientific instruments. But we need to communicate and avoid doing the same things," Kraan-Korteweg says.

No matter where SKA itself is eventually located, director Richard Schilizzi says, "all of these projects will generate great science, and technically they are taking innovative approaches, for example in terms of utilizing focal-plane arrays." They are also fostering a sense of community, says Kraan-Korteweg: "There is competition at one level, but there also is a great deal of collaboration, especially with the Australians and the groups at ASTRON [in the Netherlands] and in England. The Australian and South African groups have been sharing information in a cooperative way." **–R.K.**

CREDIT: CENTRE FOR ASTROPHYSICS & SUPERCOMPUTING, SWINBURNE UNIVERSITY OF TECHNOLOGY

Buenos Aires, offers the best combination of key factors. Morras says the proximity of existing or planned "frontline 21st century astronomical facilities," such as ALMA, the European Southern Observatory's Very Large Telescope, and the Magellan 6-meter telescopes, all sited in Chile, "will allow simultaneous observations with a great number of telescopes operating on a wide range of different frequencies."

Each site also has its drawbacks. Some astronomers worry that the ionosphere above the proposed Argentine location is less stable than that over the others. Morras concedes that "there are signal fluctuations, known as ionospheric scintillation, in that region." But he says the Argentinean site's core "is near the southern limit" of the scintillation phenomenon.

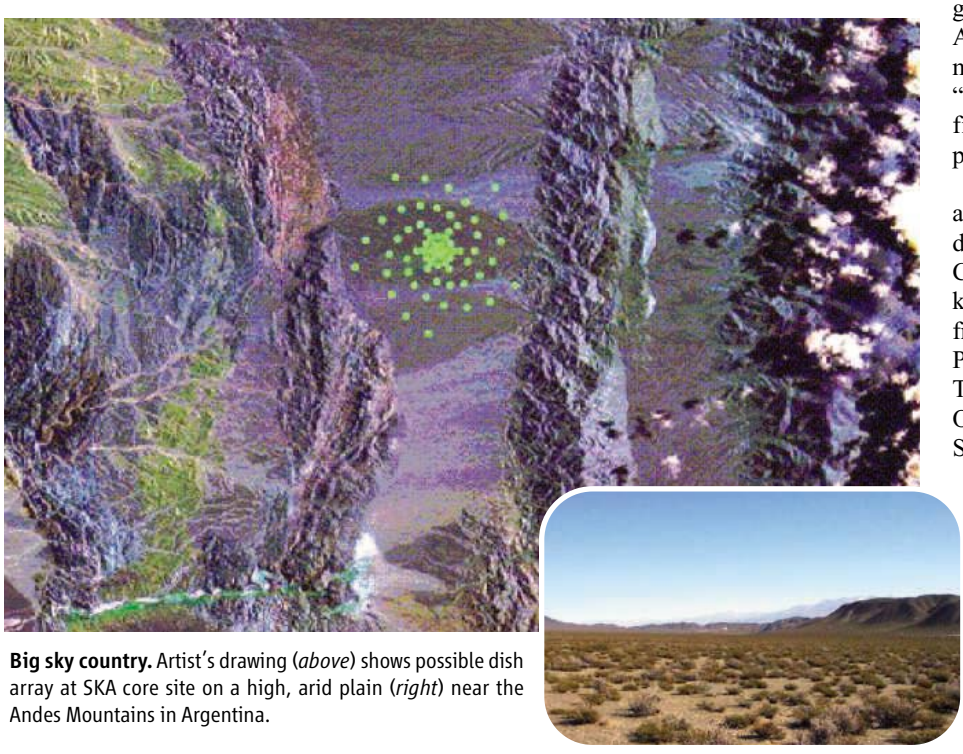

Big sky country. Artist's drawing (*above*) shows possible dish array at SKA core site on a high, arid plain (*right*) near the Andes Mountains in Argentina.

The China site, meanwhile, is in the Northern Hemisphere, which would limit SKA's ability to observe our Milky Way galaxy, whose center is visible in the Southern Hemisphere. Another possible disadvantage, Jin concedes, is that the site's humid climate "is not suitable for observations at frequencies higher than 10 gigahertz."

Regional politics may also become an issue. South Africa's roping in of Namibia, Botswana, Mozambique, Kenya, Madagascar, Ghana, and Mauritius has the advantage of boosting the bid's political clout but could also increase the risk that politics or economic problems might affect the remote stations. The Australian site, meanwhile, does not share any part of the sky with Europe and may involve higher construction costs.

In an effort to keep down levels of RFI from humanmade sources such as cell phones, TV transmitters, car ignitions, and power lines, Australia, South Africa, and Argentina are establishing "radio-astronomy reserves" around their candidate sites. Proximity to major cities could be another big RFI headache; one analysis suggests that the SKA core site would need to be at least 500 kilometers away from major urban centers. This could be another problem for the Argentinean site, which has two cities located about 100 kilometers away.

Power and money

Although the details of the final design cannot be fixed until the site is known, SKA will likely include a network of 4000 or more small dishes (each about 10 meters in diameter) operating at frequencies from 1 to 25 GHz and aperture arrays (flat collections of detectors, looking a bit like solar panels, that can see many parts of the sky at once) operating from 100 MHz to 1 GHz, all connected together in a giant interferometer. Half of the total collecting area will be concentrated in the 5-kilometer-wide core, with the rest spread over several thousand kilometers.

SKA's current timeline calls for system design to begin in 2008—by which time the final site should have been chosen—and for construction to start on the first 10% of the collecting area in 2011. SKA would start collecting data in 2014 and would be fully operational by 2020. That scope and schedule depends on funding. So far, the largest contributions in the current Pathfinder phase have come from Europe (€10.4 million from the European Union and €28 million from national funding agencies) and from in-kind R&D contributions from South Africa and Australia related to their demonstrator projects (see sidebar, p. 911).

The biggest funding question mark is the U.S. National Science Foundation (NSF), which so far has avoided making a firm commitment. "We foresee that this will be an issue for the next Decade Survey, which is likely to start in about a year from now," says the director of NSF's astronomical sciences division, Wayne Van Citters. He adds that, given NSF's commitment to complete ALMA and other major projects "that are more advanced in planning" than is SKA, "we are realistically quite a few years away from any consideration of a construction project of this magnitude."

Over the past 4 years, NSF has provided about $1.8 million for SKA "technology development" in grants to Cordes's team at Cornell. The U.S. SKA team has also been kept busy with university funding and money from the likes of Microsoft Corp. co-founder Paul Allen. Allen has part-funded the Allen Telescope Array (ATA), formerly called the One Hectare Telescope, a joint effort by the SETI Institute and the University of California, Berkeley. The ATA project has involved developing many components relevant to SKA, such as relatively inexpensive antennas and mounts, broadband feeds, and some signal-processing hardware. Schilizzi says the American work on the Allen instrument "will be of crucial importance to the technology of the SKA."

NSF's initial reluctance to commit large sums to SKA was a major reason why the U.S. SKA consortium opted last year not to submit a site proposal, Cordes says. But Schilizzi says he is "still hopeful" that NSF eventually will allocate substantial money to the project. "It may be that funding will come in a phased way, with one region dominating the early funding and another region contributing more later," he says.

Such staggered funding would not be at odds with the slow but steady approach that SKA researchers have adopted. Despite the uncertainties, team members remain confident. Miley says that funding for large telescopes always seems to be up in the air: "In my view, the question is not whether SKA will be funded but rather *when* this will occur."

–ROBERT KOENIG

CREDIT: SKA

Two Cultures

DUAL NATURE. A wave-particle duality runs through Julian Voss-Andreae's life. He was a budding painter before opting for a graduate program in physics at the University of Vienna in Austria. But before long, Voss-Andreae's artistic nature reasserted itself. Since graduating 2 years ago from the Pacific Northwest College of Art in Portland, Oregon, Voss-Andreae has focused on abstract sculptures of hemoglobin and other proteins. "My interest is really nature," he says. "One way to explore it is through science. Another is through intuitive sense and a search for metaphors."

His latest sculpture, titled *Quantum Man*, will be unveiled next month in Moses Lake, Washington. The 2.5-meter sculpture is made of 115 thin steel slabs connected and spaced apart by 1000 short steel rods. Seen from the front, the figure looks dark and solid. But from the side the quantum walker nearly disappears, as light shines through the spaces between the slabs. "It shows that when you look at things from a different perspective, they can look extremely different," says Anton Zeilinger, a physicist at the University of Vienna and Voss-Andreae's former group leader. "That's part of the quantum message."

ON CAMPUS

TERRORIZED. A failed attempt to bomb the home of a colleague was apparently the last straw for Dario Ringach, a primate neurobiologist at the University of California, Los Angeles (UCLA). "You win," he wrote earlier this month in an e-mail to several animal-rights groups that says he plans to stop doing animal research immediately. "Please don't bother my family any more."

Marie-Francois Chesselet, chair of the school's neurobiology department, says Ringach was shaken by a recent attempted bomb attack on the home of another UCLA researcher (*Science*, 28 July, p. 437). Ringach continued his work on visual object recognition in monkeys even after animal-rights activists had previously vandalized and staged demonstrations at Ringach's home, frightening his children, Chesselet says. But when the FBI told him the explosive could have blown up a house, Ringach decided to remove his family from the line of fire. "It was his responsibility to do whatever it took to protect them," Chesselet says.

Some of Ringach's colleagues have expressed surprise at his decision to abandon his monkey research. "Everyone is concerned that his gesture will empower the activists," says Chesselet. "Of course it will. But he shouldn't be blamed for that."

IN THE COURTS

JUSTICE, IN SECRET. A Russian scientist has received a 6-year suspended prison sentence for selling dual-use technology to a South Korean company. Oskar Kaibyshev, 66, who directed the Institute for Metals Superplasticity Problems in Ufa until he was fired by the institution last year, has also been banned from holding positions of authority for 3 years and fined $131,000.

During a closed-door trial last week in a Bashkortostan court, prosecutors argued that the technology that Kaibyshev sold to a subsidiary of the Hankook Tire Manufacturing Co. in South Korea could also be used to produce weapons. Kaibyshev plans to appeal the sentence. Prosecutors, who argued for a 10-year prison term, are also considering an appeal.

They Said It

"How could it be that the Romans built aqueducts 2000 years ago that are still standing today while the ceiling on the Big Dig tunnel came down in 2 years?"*

—Bernard Gordon, an electrical engineer and founder of Analogic Corp., citing last month's collapse of concrete panels in the recently completed $15 billion Boston tunnel project as a sign that the United States was losing its engineering prowess. To stem the decline, Gordon last week gifted $40 million to support engineering education and research at Boston's Museum of Science and Northeastern University.

* Source: *The Boston Globe*

Pioneers >>

ANCIENT MARINER. Few people know much about Zheng He, an accomplished Chinese seafarer who led major voyages in the early 15th century. Jin Wu, an ocean scientist and former education minister in Taiwan, hopes to change that—and drum up interest in science in the process.

Wu, who studied antisubmarine warfare for a U.S. defense contractor before spending 20 years at the University of Delaware, was inspired to learn more about He from a Taiwanese documentary that referred to his seven expeditions, with 200 ships and 28,000 men.

The historical record is sparse because the Ming Dynasty decided to destroy the ships and cancel ocean exploration. But last month, Wu began a 4-month fellowship at the Library of Congress in Washington, D.C., to study questions such as whether the wooden boats were really 144 meters long and how the fleet supported a crew of 28,000. Wu also hopes China will rebuild one of He's vessels. Wu has already organized Zheng He societies in six U.S. cities, and he says a recent bout with cancer won't prevent him from sailing full steam ahead on the project.

Got a tip for this page? E-mail people@aaas.org

CREDITS (TOP TO BOTTOM): JULIAN VOSS-ANDREAE; NATIONAL CHENG KUNG UNIVERSITY

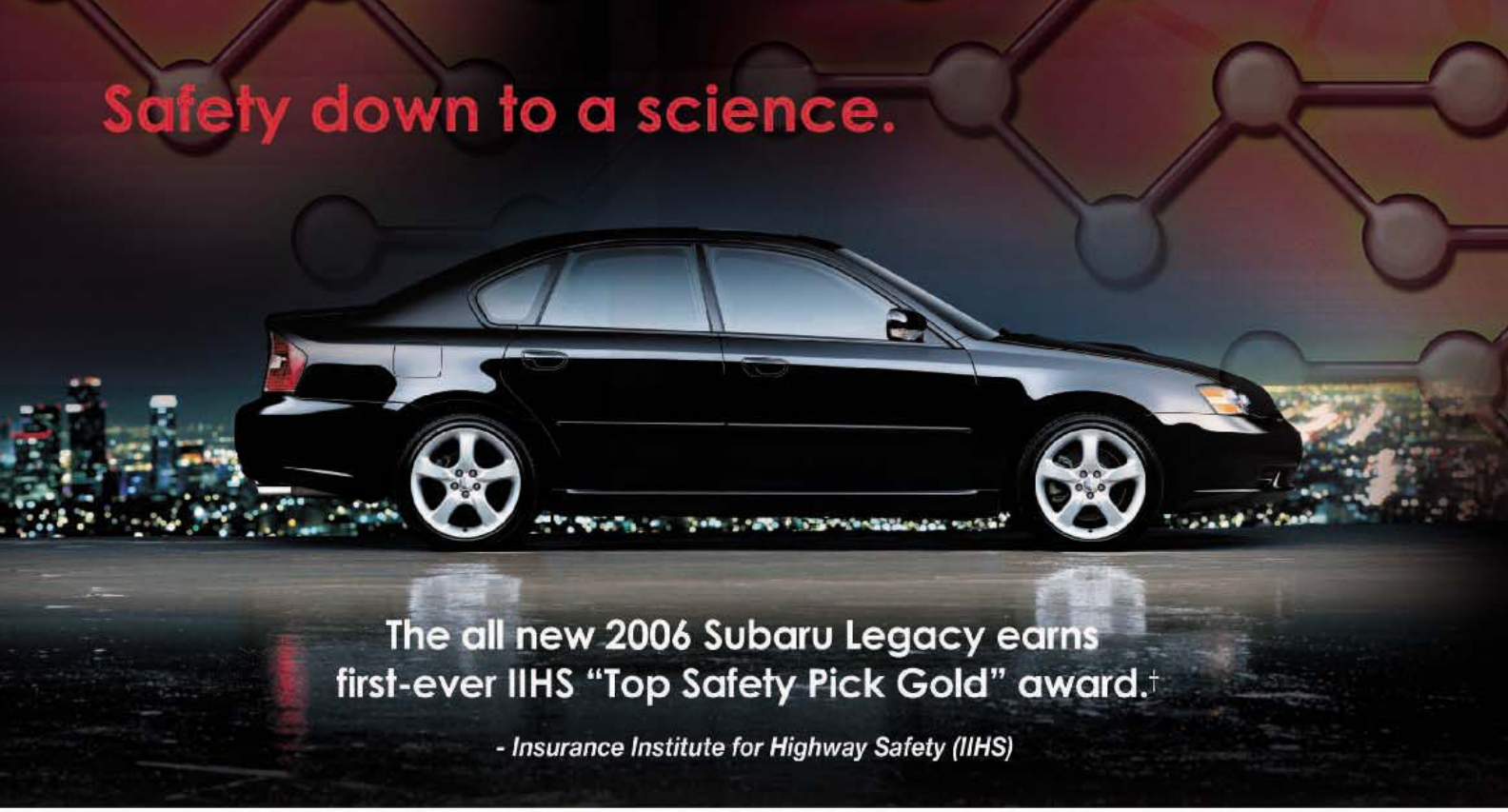

Subaru's sponsorship of the American Association for the Advancement of Science (AAAS) highlights our advanced design of symmetrical all-wheel drive technology to our target markets and underscores Subaru's commitment to further science, engineering and technology education both at the annual meeting and programs throughout the year. Subaru is proud to be the Premier Automotive Sponsor of the AAAS.

In a continuing effort to offer our partners unique and valuable benefits, we provide special offers for AAAS Members, the Subaru VIP Partners Program. AAAS Members can **save up to $3,000*** off the manufacturer's suggested retail price (depending on model and accessories) on the purchase or lease of a new Subaru from participating dealers. To qualify, you must be a AAAS member in good standing for at least six consecutive months prior to participation in this program. Please contact AAAS Member Services at 202.326.6417 or e-mail membership@aaas.org **BEFORE** visiting your local Subaru dealer. Access subaru.com to find a nearby dealer or learn more about Subaru vehicles.

Science
AAAS

Think. Feel. Drive.™

SUBARU

*From MSRP to dealer invoice. MSRP does not include tax, title, and registration fees. Limited time offer subject to change without notice. Terms and conditions apply. This offer replaces all other existing offers, cannot be redeemed for cash and is not applicable in Canada and Hawaii. † Based on Insurance Institute for Highway Safety 40 mph offset frontal crash test, 31 mph side impact test, and 20 mph rear impact test.

LETTERS

edited by Etta Kavanagh

A *G. luii* gecko

Captive Breeding and a Threatened Gecko

IN THEIR LETTER "SCIENTIFIC DESCRIPTION CAN IMPERIL SPECIES" (26 MAY, p. 1137), B. L. Stuart *et al*. warn that scientific description can draw attention to newly described species attractive for hobbyists, which could lead to their overexploitation or even extinction. Although this scenario sounds plausible, and taxonomists should keep in mind the conservation impacts of their work, at least one of the three examples given is incorrect. The gecko *Goniurosaurus luii* from southeastern China was heavily threatened by hunting for pet trade and local medicine purposes and was probably extirpated from its type locality before it was scientifically described. The specimens of *G. luii* obtained from pet dealers and listed as *Goniurosaurus* sp. were studied by Japanese molecular phylogenetics before the official description (*1*). Lui, the collector of the holotype of *G. luii*, himself "became aware of the existence of *Goniurosaurus luii* and *G. araneus*" from "individuals who specialise in gecko collecting for commercial purposes" (*2*).

Stuart *et al.* also claim that immediately after being described in 1999, *G. luii* reached a breathtaking price of $1500 to $2000 per individual in importing countries. During the last few years, hobbyists perfectly mastered the keeping and breeding of *G. luii* and closely related *G. araneus* and established numerous breeding colonies of both species. Recently, hundreds of captive-born juveniles have been available on the world pet market every year for about $40 each, which has two important conservation consequences. First, there is no further demand on the imported, wild-caught animals. Second, as *G. luii* is a species with limited range still hunted for local medicine trade (*3*) and endangered by habitat damage (*2*), the captive population will soon outnumber the wild one and can serve as a guarantee that this species will survive at least in captivity with a potential chance for re-introduction.

LUKÁŠ KRATOCHVÍL

Department of Ecology, Faculty of Science, Charles University, Viničná 7, 128 44 Praha 2, Czech Republic. E-mail: kratoch1@natur.cuni.cz

References

1. H. Ota, M. Honda, M. Kobayashi, S. Sengoku, T. Hikida, *Zool. Sci.* **16**, 659 (1999).
2. L. L. Grismer, B. E. Viets, L. J. Boyle, *J. Herpetol.* **33**, 382 (1999).
3. K. S. Lee, M. W. N. Lau, B. P. L. Chan, "Wild Animal Trade Monitoring in Selected Markets in Guangzhou and Shenzhen, South China 2000–2003" (Kadoorie Farm and Botanic Garden Corporation, Tai Po, Hong Kong SAR, 2004).

Response

OUR LETTER USED THREE ASIAN HERPETOlogical examples to illustrate the point that publishing scientific descriptions of new species may inadvertently facilitate their overexploitation by advertising "novelties" to hobbyists and providing detailed locality information to commercial collectors. Kratochvíl correctly notes that one of our examples, the gecko *Goniurosaurus luii*, was already being heavily harvested in China for sale in the international pet trade (*1*, *2*) prior to its description as a new species (*1*). However, immediately after being described, its value in the U.S. pet trade jumped from approximately $500 under an older name to approximately $1500 under its new name as a result of increased demand from hobbyists seeking a unique addition to their collections (the $2000 quote in our Letter referred to a second reptile example, *Chelodina mccordi*, provided in the same sentence). Thus, we feel that *G. luii* remains an appropriate example of how scientifically describing a new species can unintentionally fuel its commercial exploitation (*3*). It is fortunate for *G. luii* that demand for wild-caught individuals has now diminished, owing to the availability of inexpensive, captive-born individuals produced by hobbyists. The conservation merits of unregulated, private, captive breeding programs are beyond the scope of our Letter, but it does seem that *G. luii* paid a high cost for the end result of inexpensive, captive-born substitutes in the pet trade.

BRYAN L. STUART[1,2] AND L. LEE GRISMER[3]

[1]Department of Zoology, The Field Museum, 1400 South Lake Shore Drive, Chicago, IL 60605–2496, USA. [2]Department of Biological Sciences, University of Illinois at Chicago, 845 West Taylor Street, Chicago, IL 60607–7060, USA. [3]Department of Biology, La Sierra University, 4500 Riverwalk Parkway, Riverside, CA 92515, USA.

References

1. L. L. Grismer, B. E. Viets, L. J. Boyle, *J. Herpetol*. **33**, 382 (1999).
2. H. Ota, M. Honda, M. Kobayashi, S. Sengoku, T. Hikida, *Zool. Sci*. **16**, 659 (1999).
3. For additional plant and animal examples, see L. Guterman, *Chron. Higher Educ.* **52**, A12 (21 July 2006).

Roles of CITES in Protecting New Species

IN THEIR LETTER "SCIENTIFIC DESCRIPTION can imperil species" (26 May, p. 1137), B. L. Stuart *et al.* warn of a dilemma faced by scientists who publish the first scientific description of a new species. Revealing geographical locations in the publication can guide unscrupulous collectors from the international pet trade to the species, which could lead to a rapid decline in population size and even extinction.

To prevent this, Stuart *et. al.* suggest that taxonomists should work closely with relevant governmental agencies. The problem

with governmental agencies, however, is that the protection is local, not global. Once the species is illegally exported from the country of origin, it can be legally imported into most other countries. For example, the snake species *Bothrops insularis* occurs solely on Queimada Grande, a small island (of 43 ha) off the Brazilian coast, where it could potentially be collected in large numbers. This species is protected by Brazilian law and listed as "Critically Endangered" in the IUCN Red List. However, once illegally exported from South America, the species is completely legal in Europe. No law or convention protects this species from the trade there.

If newly described species are to be protected from international trade, it must be at a global level through CITES (Convention on International Trade in Endangered Species of wild fauna and flora) registration. Before scientists publish their descriptions of new species, population sizes and potential vulnerability to trade should be carefully assessed against the relevant criteria for amendments on the CITES list (with the CITES secretariat in Geneva probably being the best contact point), and the process of listing the species initiated in conjunction with the preparation of its formal scientific description.

FREEK J. VONK[1] AND WOLFGANG WÜSTER[2]

[1]Department of Integrative Zoology, Institute of Biology, Leiden University, Post Office Box 9516, 2300 RA, Leiden, the Netherlands. [2]School of Biological Sciences, University of Wales, Bangor LL57 2UW, Wales, UK. E-mails: F.J.Vonk@umail.leidenuniv.nl; W.Wuster@bangor.ac.uk.

A Problem in Archaeology Too

THE LETTER "SCIENTIFIC DESCRIPTION CAN imperil species" (B. L. Stuart *et al.*, 26 May, p. 1137) notes that formal publications of new species "advertise 'novelties' for hobbyists and drive new markets." The authors document tragically increased commercial exploitation of reptiles and amphibians following publication in the literature. Ironically, this same "dual-use dilemma," as they term it, has also followed formal publication in another discipline: archaeology. Site location data have stimulated pothunters and collectors who use the reports as veritable guidebooks to further their illegal activities. This has been particularly the case in Americanist studies, and I have little doubt of its foreign analogs.

BERNARD W. POWELL

Chuluota, FL, USA.

Photosynthesis in Balance with Respiration?

AS AN ORDINARY BIOLOGIST, I ASSUMED THAT living organisms' impacts on atmospheric CO_2 and O_2 levels were more or less "in balance," with plant photosynthesis being equalled by the summed respiration of plants, animals, and soil and aquatic microbes.

Thus, I find puzzling the attempt by A. W. King *et al.* ("Plant respiration in a warmer world," Perspectives, 28 Apr., p. 536) to use an adaptation of plant respiration to higher temperatures as compensation for increased CO_2 production owing to temperature-stimulated increases in photosynthesis. Surely, temperature also affects rates of respiration in almost all organisms that utilize photosynthates for their energy source? Thus, only the small handful of animals capable of thermal control of body temperature could effectively offset rises in body temperature to lower respiration rates—and even those capacities can add to respiration-derived energy demands. Why is plant adaptation by lowering temperature-induced increases in respiration a necessary hypothesis to offset higher photosynthetic rates?

Surely, if we are to estimate the production of CO_2 as a function of ambient temperatures, we must also consider the impacts of such temperatures on photosynthesis, as well as on the rates of respiration not only of plants, but also of all other lifeforms—from microbes to humans. How well do they adapt their metabolic needs to persistent temperature increases? On balance, over eons of time, the photosynthate has more or less been "in balance" (once the great quantities of reduced carbon were sequestered in fossil fuels, creating an oxygen-rich atmosphere)—through periods of warming and cooling—to provide relatively stable CO_2 to O_2 ratios in the atmosphere. Shouldn't the temperature-dependent responses of all these metabolic regimes be part of any meaningful analysis? If all reactions are more or less equally affected by temperature, how can there be a net "problem" from increased plant respiration?

MARY E. CLARK

Professor of Biology, Emerita, San Diego State University; Professor of Conflict Resolution, Emerita, George Mason University; 780 Girard Court, Cottage Grove, OR 97424, USA. E-mail: meclark@efn.org

Response

CLARK'S ASSUMPTION THAT GLOBAL PHOTOsynthesis is more or less "in balance" with total plant and animal respiration holds as an approximation only when those processes are not being forced from their quasi-equilibrium by disturbance. The ongoing anthropogenic perturbation of the atmosphere by fossil-fuel burning is a major disturbance of Earth's carbon cycle (*1*). Rising atmospheric CO_2 increases photosynthesis. The concurrent increases in temperature alter photosynthesis and respiration, but with different sensitivities. These perturbations, combined with deforestation accompanying large-scale agriculture, are large enough that the world's terrestrial ecosystems are not in equilibrium with respect to CO_2 and O_2 fluxes.

We did not investigate "adaptation" of plant respiration, as suggested by Clark, but rather acclimation to higher temperatures. Acclimation commonly refers to physiological and metabolic adjustments to environmental change, distinguishing these responses from genetic adaptation. Nor did we examine "photosynthesis," but rather temperature-stimulated respiration. Clark asks, "Surely, temperature also affects rates of respiration in almost all organisms…?" Yes, it does, and all rates of metabolic respiration in our model are functions of temperature (*2*, *3*). Furthermore, organisms can indeed lower respiration rates in the facing of rising temperatures. The concept of thermal acclimation applies to respiratory rates (and rates of other enzymatic-based processes) in any poikilothermic organism (*4*, *5*), which includes plants. Acclimation of plant respiration to warmer temperatures is not included in global models of carbon cycle response and feedback to climate change. It is important to understand how including or not including it influences the simulation and interpretation of positive feedback between Earth's carbon cycle and future climate change.

The argument can be made that if one's purpose is to estimate the production of CO_2 as a function of changes in temperature, then one must consider the impacts of temperature (and temperature acclimation) not only on plant respiration, but also photosynthesis and respiration of all lifeforms. The respiration of all lifeforms in the simulations was modeled as a function of temperature, but we purposefully designed the simulation experiments to isolate the contribution of acclimation of plant (leaf) respiration to temperature. Nonetheless, the differential effects of increases in atmospheric CO_2 and changes in climate on cellular reactions could result in plants making an additional net contribution to the imbalance in atmospheric CO_2.

ANTHONY W. KING, CARLA A. GUNDERSON,

WILFRED M. POST, DAVID J. WESTON, STAN D. WULLSCHLEGER

Environmental Sciences Division, Oak Ridge National Laboratory, Oak Ridge, TN 37831, USA.

References

1. J. T. Houghton *et al.*, Eds., *Climate Change 2001: The Scientific Basis* (Cambridge Univ. Press, Cambridge, 2001).
2. A. W. King, W. M. Post, S. D. Wullschleger, *Clim. Change* **33,** 199 (1997).
3. J. S. Amthor *et al.*, *J. Geophys. Res.* **106**, 33623 (2001).
4. A. Pisek, in *Temperature and Life*, H. Precht, J. Christophersen, H. Hensel, W. Larcher, Eds. (Springer-Verlag, New York, 1973), pp. 102–194.
5. K. Y. H. Lagerspetz, *J. Thermal Biol.* **31**, 332 (2006).

TECHNICAL COMMENT ABSTRACTS

Comment on "Computational Improvements Reveal Great Bacterial Diversity and High Metal Toxicity in Soil"

Igor Volkov, Jayanth R. Banavar, Amos Maritan

Based on analysis of the reassociation kinetics of bacterial DNA in soil, Gans *et al*. (Reports, 26 August 2005, p. 1387) claimed that millions of microbe species existed in 10 grams of pristine soil and that 99.9% of the diversity was lost as a result of toxic metals. We show that the data do not support these startling conclusions unambiguously.

Full text at www.sciencemag.org/cgi/content/full/313/5789/918a

Response to Comment by Volkov *et al.* on "Computational Improvements Reveal Great Bacterial Diversity and High Metal Toxicity in Soil"

Jason Gans, Murray Wolinsky, John Dunbar

Volkov *et al*. claim that significant conclusions about the total number of species (*S*) cannot be made because different abundance models cannot be distinguished and the sensitivity of the chi-square measure to changes in estimates of *S* is low. We point out that currently available data do not support these claims.

Full text at www.sciencemag.org/cgi/content/full/313/5789/918b

Comment on "Computational Improvements Reveal Great Bacterial Diversity and High Metal Toxicity in Soil"

John Bunge, Slava S. Epstein, Daniel G. Peterson

Gans *et al*. (Reports, 26 August 2005, p. 1387) provided an estimate of soil bacterial species richness two orders of magnitude greater than previously reported values. Using a rederived mathematical model, we reanalyzed the data and found that the statistical error exceeds the estimate by a factor of 26. We also note two potential sources of error in the experimental data collection and measurement procedures.

Full text at www.sciencemag.org/cgi/content/full/313/5789/918c

Response to Comment by Bunge *et al.* on "Computational Improvements Reveal Great Bacterial Diversity and High Metal Toxicity in Soil"

Jason Gans, Murray Wolinsky, John Dunbar

Bunge *et al*. claim that we underestimated the error in our analysis of bacterial diversity in noncontaminated soil. However, they used an unsatisfactory model that exhibited pathological behavior and consequently led to an exceptionally high calculated error. In contrast, the zipf distribution yielded an error estimate only 0.7 times the estimate of the total number of species (*S*), and it is more biologically relevant.

Full text at www.sciencemag.org/cgi/content/full/313/5789/918d

Letters to the Editor

Letters (~300 words) discuss material published in *Science* in the previous 6 months or issues of general interest. They can be submitted through the Web (www.submit2science.org) or by regular mail (1200 New York Ave., NW, Washington, DC 20005, USA). Letters are not acknowledged upon receipt, nor are authors generally consulted before publication. Whether published in full or in part, letters are subject to editing for clarity and space.

NEUROSCIENCE

From Austria, Through *Aplysia*, Toward the Mind

Nancy C. Andreasen

Eric Kandel's *In Search of Memory* is an enchanting book that has a broad historical and conceptual sweep reminiscent of a David Lean film. It takes us on a journey through the life of one of our greatest neuroscientists, intertwining his personal intellectual history with the events that were simultaneously occurring on the world stage. In the process we meet not only Eric but his many compatriots, who have shared the journey with him.

In Search of Memory
The Emergence of a New Science of Mind
by Eric R. Kandel
Norton, New York, 2006. 526 pp. $29.95, C$42, £19.99. ISBN 0-393-05863-8.

The fascinating read begins with Eric's memories of young Erich (his German first name) on his ninth birthday, in November 1938. He is playing with a much-craved toy: a battery-operated, remote-controlled model car, received as a birthday gift from his parents, who owned a small toy store. Two days later, a shattering new memory is encoded in Erich's mind alongside this idyllic one. Austrian Nazis invade the small Kandel apartment, arrest Erich's father, and remove the rest of the family to a stranger's apartment. After many anxious days, his father is released and the family is allowed to return home. They find it ransacked and all the valuables stolen, including Erich's coveted toy car. The following months are marked by more traumata, as Austrian Jews are subjected to vicious humiliations that forebode a dangerous future. The Kandel family finds a way to escape to a Promised Land in New York. There Erich changes his name to Eric and begins a new life as a young American boy entranced by endless opportunities and freedoms, ultimately becoming a psychiatrist, a neuroscientist, and a Nobel laureate.

This autobiography will be interesting to both scientists and general readers for many reasons. The book provides a lucid and comprehensive overview of developments in neuroscience during the 20th century. Kandel consistently places his work within the context of his predecessors as a reminder that he too has stood on the shoulders of giants in the field. The early pages are filled with summaries of the contributions of such figures as Santiago Ramón y Cajal, Charles Sherrington, Edgar Adrian, Alan Hodgkin and Andrew Huxley, Bernard Katz, Otto Loewi and Henry Dale, and John Eccles. Their findings constitute the basics of contemporary neurophysiology, but Kandel describes these giants with a freshness and drama that portrays them as real people, identifying and struggling to answer early crucial questions of neuroscience.

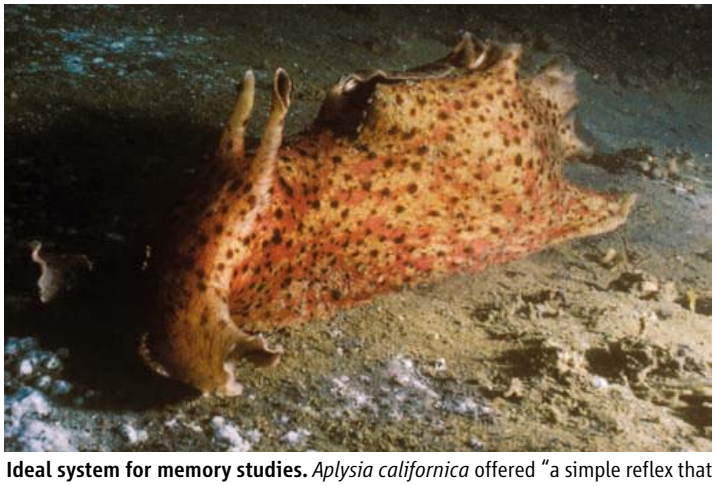

Ideal system for memory studies. *Aplysia californica* offered "a simple reflex that could be modified by learning and that was controlled by a small number of large nerve cells whose pathway from input to output could be identified."

The book also provides a wonderful reminder of the importance of mentors in shaping the careers of scientists. Very early in his career, Kandel became interested in Freud, and he was encouraged to become a psychoanalyst-psychiatrist by the prominent analysts Ernst and Marianne Kris, the parents of a friend. Eric changed his career interests from history to medicine, because that was the pathway to becoming an analyst. While a medical student (like many of us future neuroscientists), he would look at model brains and neuroanatomical specimens and wonder where thoughts arise. In his case, the question was, Where in the brain are the id, the ego, and the superego? So he sought out his first mentor, Harry Grundfest of Columbia University. With the hubris of youth, he animatedly explained his vast and lofty goals. Grundfest's reply: Study the brain one cell at a time. Offering Kandel his first experiences with the joys of doing research, Grundfest proved an inspiring and supportive mentor. He was followed by many others—Dominick Purpura, Wade Marshall, Stephen Kuffler, and Ladislav Tauc—who served as role models, taught Kandel new methods and ways of thinking, shared their excitement and questions with him, and ultimately helped him grow into a creative independent scientist who questioned and answered with his own individual voice. The author's love, appreciation, and admiration for his mentors pervade the book and give it a warm and mature tone.

At the heart of *In Search of Memory* lies the story of how colleagues, and subsequently students, became Kandel's companions in his "search for memory." An adventurous band of friends and students—working amidst the kaleidoscope of new findings that occurred in neuroscience and molecular biology in the second half of the 20th century—created new ideas and methods, shared them with one another, and relentlessly pursued the question of how memories are formed, preserved, and discarded. Kandel's work with the sea hare (marine slug) *Aplysia* produced ground-breaking discoveries: that synapses (of the gill withdrawal reflex) are modified by learning, that the same synapse can be modified in different ways by different forms of learning, and that long-term memory differs from short-term memory in requiring the use of gene expression to lead to the growth of new synapses. The book details how collaborations with friends enriched Kandel's work and how one student after another made creative and original contributions to his laboratory. The tales of doing science will be a familiar one to many. To do high-quality, original research, Kandel continually remade himself, learned new techniques, and adapted to advances in the field. The long and arduous road that began with inserting microelectrodes into

The reviewer is at the Department of Psychiatry, University of Iowa Hospital and Clinics, Iowa City, IA 52242, USA. E-mail: nancy-andreasen@uiowa.edu

Aplysia neurons has helped move our understanding of the formation of memories from behavioral conditioning to elegant molecular biology.

The author's own memories help make his account special. Kandel is a confident and persistent man with a hearty sense of humor. (As those who know him have found, his laughter is both infectious and unique.) But the book is marked with introspection and is sometimes haunted by the pain of loss—of his friends, parents, and brother through disease and death (sometimes cruelly premature). His connections with Vienna and its culture—and the near-destruction of that culture in the Holocaust—are very much part of his search of his personal memories. His wife, Denise, is beside him throughout the journey, providing love and support, while his children provide corrective critiques.

In short, *In Search of Memory* is a must-read account of science and a life, with all the associated joys and sorrows. It provides an insightful perspective on how first-rate research is carried out. One encounters a fascinating and persistent person who pursued the quest for his own Holy Grail (or, more appropriately, Ark of the Covenant) and found it.

10.1126/science.1127774

HUMAN EVOLUTION

Seeking the Base of Our Branch

David R. Begun

In *The First Human*, Ann Gibbons, a contributing correspondent who covers human evolution for *Science*, offers a wonderful, balanced, and accurate account of the search for the oldest human ancestors and the personages involved in this quest. Gibbons provides a revealing window into the house of horrors that can be human origins research. The descriptions of the protagonists' personalities, which in every case conform to my own perceptions, are insightfully woven into the main fabric of the book: the immensely engaging, and sometimes self-destructive, effort to find the first human.

At the same time, there is not a word of gossip in this book. Although the strengths and weaknesses of various researchers are described with no pulled punches, Gibbons sticks to their professional behavior and does not get personal. This respectful detachment was a great relief, as I initially feared the book might be a soap opera of the type written by some previous authors (including some people featured in the book), which would have done a disservice to the field. Other researchers might still feel that a disservice has been done, but I disagree. Gibbons profiles in some detail a dozen among the hundreds of past and present paleoanthropologists. In an even-handed manner, she presents both sides of each conflict, a few cases of which are highly acrimonious, if not borderline criminal, in nature. Some would say she is in places a bit too kind, but that is for the reader to judge. Paleoanthropologists will understand that the conflicts and dubious activities the author describes are not typical of their field, and other scientists will recognize that their own ponds have a film of prima donnas sometimes behaving badly that rises to the surface and comes to the attention of outsiders. I knew something of these battles from chats with those involved, but reading the book has given me a much more detailed understanding of what actually happened and the participants' motivations. Nonetheless, for the most part paleoanthropologists do not eat their young, and we usually get along quite well.

Gibbons provides a multifaceted view of paleoanthropology, one that will serve as an excellent introduction for nonspecialists. Combining science, the history of ideas, and current events, her account allows the reader to virtually live the events as they unfold. Interesting portrayals of historic luminaries such as Eugène Dubois, Raymond Dart, and Louis Leakey accompany insightful analyses of contemporary researchers. Smoothly written, informative, and easy-to-understand asides, which focus on paleoanthropological methods and theory, place everything in perspective. The reader should come away with a sense of why the field is so important and engaging—as well as why some of its practitioners occasionally go mad.

The book brings to mind a number of interesting problems. How will we know when we have found the earliest human (that is, a member of the earliest population more closely related to humans than to chimpanzees)? Necessarily, this fossil will most likely be indistinguishable from the earliest member of the chimpanzee and bonobo clade. How should we interpret the conflict (to which Gibbons devotes some attention) between molecular and morphological approaches to human origins? This issue has again come to the attention of a broad audience with the recent publication of a comparative analysis of DNA from African apes and humans that suggests chimps and humans experienced a lengthy and complex period of hybridization before finally going their separate ways, sometime after the age of the earliest human fossils Gibbons discusses (*1*). Whether or not *Sahelanthropus, Orrorin,* and *Ardipithecus* can be described as the love children of unions between ancestral chimps and human ancestors remains to be seen, but the paper raises stimulating questions about the sometimes curious mixture of African ape and human traits in all of these fossils.

The First Human
The Race to Discover Our Earliest Ancestors
by Ann Gibbons
Doubleday, New York, 2006. 341 pp. $26, C$37. ISBN 0-385-51226-0.

I have a few quibbles. Molecular dates of human origins are not so consistent as Gibbons suggests. They range from 3 million to 12 million years ago (Ma), though it is true that most converge around the 5 to 7 Ma range. Younger dates have been used to disqualify certain fossils from membership in the human club, and older dates have been used to nominate much older fossils. I was saddened to see Leonard Greenfield's contribution to the *Ramapithecus* debate again ignored. It was Greenfield who first published a detailed rationale for the interpretation that *Ramapithecus* is in fact a female *Sivapithecus* and not a human ancestor (*2*); David Pilbeam only later reached that same conclusion. Lastly, it is probably an overstatement to say that the monumental discovery of Lucy sealed the deal for the view that humans originated in Africa. That view gained wide acceptance after work in South Africa by Robert Broom and John Robinson in the 1930s and 1940s. Their efforts also led to the discovery of a "skeleton" (STS 14), so Lucy was not the first.

In spite of these minor complaints, readers should enjoy Gibbons's compelling and informative account of recent research on hominin origins.

References

1. N. Patterson, D. J. Richter, S. Gnerre, E. S. Lander, D. Reich, *Nature* **441**, 1103 (2006).
2. L. O. Greenfield, *Am. J. Phys. Anthropol.* **50**, 527 (1979).

10.1126/science.1130116

The reviewer is at the Department of Anthropology, University of Toronto, 100 St. George Street, Toronto, ON M5S 3G3, Canada. E-mail: begun@chass.utoronto.ca

SCIENCE AND LAW

Integrity in International Stem Cell Research Collaborations

Although countries with different traditions, laws, and cultures may not agree on standards for stem cell research, a set of principles could clarify terms of collaboration.

Debra J. H. Mathews,[1]* Peter Donovan,[2] John Harris,[3] Robin Lovell-Badge,[4] Julian Savulescu,[5] Ruth Faden[1]

International collaborations in human embryonic stem cell research (hESCR) currently face ethical and policy challenges resulting from conflicting national regulations. To address these challenges, we convened more than 50 scientists, ethicists, journal editors, lawyers and policy-makers from 14 countries, in Hinxton, Cambridge, UK (*1*). Through exploration of case studies (see Supporting Online Material) and deliberations, we came to consensus on guiding principles (see table, page 922) for international collaborations in hESCR (*1*).

Science, Society, and the Law

Society has the authority to regulate science, and scientists have moral and legal duties to obey the law. The Hinxton Group engaged in discussion about the power of law to facilitate or to restrict hESCR and about the need, given the critical contribution science makes to the public good, for lawmakers to be circumspect in regulating science.

Even apparently well-crafted laws can have unintended consequences as science progresses. Since enacted legislation is difficult to change, a premium should be placed on flexible regulatory structures that can respond to the rapid evolution of scientific understanding. To strike the best possible balance between free scientific inquiry and social values, it is essential that lawmakers and scientists consult with each other and with the public.

We also call for clarity in the law. Scientists and clinicians have the right to know what is, and is not, permitted with respect to their research, the jurisdiction of any prohibitions, and related penalties so that they and their research institutions can regulate their behavior accordingly. The lack of clarity in laws, for example, due to the ambiguous use of technical language [e.g. (*2*)], may have unintended chilling effects on science. It can lead to costly and time-consuming legal challenges, and in the face of ambiguity, scientists and research institutions may choose not to pursue a particular line of investigation or collaboration.

Governments have the authority to regulate science according to the values and histories of their nations. One of the most contested issues the Hinxton Group discussed was whether or under what conditions governments should exert extraterritorial jurisdiction over hESCR. One case study that we debated involved an Italian scientist traveling to England to pursue collaborative work in which nuclear transfer will be used to develop patient-specific hESC lines. This is legal in England but illegal in Italy. Because Italian law does not address conduct of its scientists outside its borders, it appears that the Italian investigator would not be violating her country's laws. A second case study involved a German scientist planning travel to the United States to collaborate with a California colleague on research involving derivation of hESC lines from supernumerary in vitro fertilization (IVF) embryos. This is legal in California but illegal in Germany. In contrast to Italy, Germany appears to claim extraterritorial jurisdiction, regulating conduct of German scientists outside Germany.

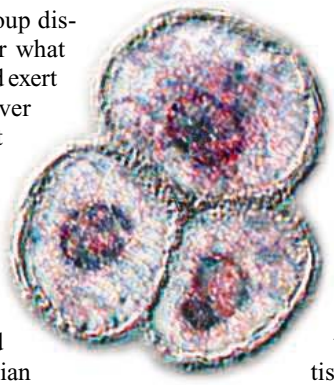

The Hinxton Group calls on lawmakers to be circumspect in restricting citizens' conduct extraterritorially with regard to hESCR. We agreed that if scientifically and ethically defensible hESCR is undertaken in a country in which it is legal, scientists should be free to participate without fear of being liable to prosecution, restriction, or discrimination in another jurisdiction. There was not, however, unanimity in the group on how far this point should be extended. For example, the apparent extraterritorial reach of German law is embedded in the German constitution and is not specific to hESC research or scientists, but rather applies to the conduct of federal employees, which includes most scientists. Insofar as this is a basic principle of German law, it may be inappropriate, and unrealistic, to expect that science should be treated as an exception.

In countries with laws that restrict elements of hESCR but that do not expressly prohibit citizens' participation in these practices abroad, research institutions should neither discriminate against nor restrict the freedom of investigators who want to travel to do scientifically and ethically defensible research. For example, when the traveling Italian scientist is evaluated for promotion, his home institution should include in its assessment any publications that come from his collaboration in England. By contrast, the home institution of the German scientist, even if she is not prosecuted, may be legally constrained from including in her review any publications that emerged from her work in California.

In some cases, scientists who are citizens of countries with restrictive laws may wish to collaborate with colleagues in more permissive countries without personally engaging in the activities that are illegal in their home countries. Particularly for such scientists, and also generally, journal editors should encourage authors to include in manuscripts explicit descriptions of their specific roles in the collaboration that led to the published research.

Promoting Integrity

Scientific and ethical integrity are crucial to scientific progress, which depends not only on the replication of results, but also on the public's trust. The Hinxton Group proposed that scientists should submit stem cell lines they derive to national or international depositories (e.g., the U.K. Stem Cell Bank) that subscribe to internationally accepted standards of quality and that make cell lines and relevant information (e.g., DNA fingerprinting and microsatellite data) (*3*) publicly available. Journal editors should require authors

[1]Phoebe R. Berman Bioethics Institute, The Johns Hopkins University, Baltimore, MD 21205, USA. [2]Stem Cell Research Center, University of California, Irvine, CA 92697, USA. [3]Institute of Medicine, Law, and Bioethics, University of Manchester, Manchester M13 9PL, UK. [4]Division of Developmental Genetics, Medical Research Council (MRC) National Institute for Medical Research, London NW7 1AA, UK. [5]Oxford Uehiro Centre for Practical Ethics, University of Oxford, Oxford OX1 1P, UK.

*Author for correspondence. E-mail: dmathews@jhmi.edu

HINXTON GROUP PRINCIPLES AND A SAMPLING OF NATIONAL POLICIES

	Hinxton Group	Australia	China	United Kingdom	Germany	Israel
Flexible regulatory structures	Flexibility in hESC policy.	Relevant Acts were reviewed by the Lockhart Committee in 2005 and are awaiting government response.	Not addressed in the relevant policy.	Licensure guidelines are broadly written, allowing flexibility in case-by-case assessment of research proposals.	Not addressed in the relevant policy.	Current law is valid only until 1 March 2009. "Existing regulations… [to be] respected, and when necessary changed."
Consultation with scientists and the public	Consultation between lawmakers, scientists, and the public.	Extensive consultation was undertaken by the Lockhart Committee — over 1000 submissions.	Not addressed in the relevant policy.	An annual report from HFEA (focuses on its own activities).	Not addressed in the relevant policy.	Public discussion and an annual report from the advisory committee (issues include medicine, science, biotech, bioethics, and law)
Extraterritorial jurisdiction	Circumspection in exerting extraterritorial jurisdiction.	Jurisdiction is limited to Australia.	The Guiding Principle applies to "research activity related to [hESCs] conducted in the territory of the People's Republic of China."	Regulations extend to Northern Ireland and the Channel Islands.	The Embryo Protection Act and the German Penal Code imply that prohibited actions are illegal—and prosecutable—regardless of location of the transgression.	Not addressed in the relevant policy.
Human materials donors	Classification and protection as human research subjects.	Protections and procedures required for human subjects research. The Lockhart Committee recommended that the NHMRC develop guidelines for egg donation.	Protections and procedures required for human subjects research.	Implies that prohibited actions are illegal. Protections and procedures required for human subjects research.	Defers to national policies for the countries where stem cell lines were derived.	Informed consent for gamete donors in relation to IVF. (Oocyte donation is accepted only for cases of infertility.)

Last updated 24 July 2006; for source documents, see (*9*). HFEA, Human Fertilisation and Embryology Authority; NHMRC, National Health and MRC.

(i) to provide specific information about the source of the cells used in research, (ii) to submit data verifying the authenticity of new hESC lines, and (iii) to explain how they have complied with accepted standards of good cell culture practice.

Journal editors and reviewers have a responsibility to promote ethical, as well as scientific, integrity. Journal editors should require a statement from scientists that their research conforms to local laws and policies and has been approved by all applicable oversight committees. Scientists should also be ready and willing to provide approved protocols, consent forms, and other related information that may bear on the ethics of their research.

The Hinxton Group is creating a public database for the deposition of relevant policies, information provided to potential human subjects and tissue donors, and other documents that bear on the ethics of hESCR. This site will also provide a forum for international conversation among scientists and the broader society. It should be available in the fall of 2006 (*4*).

Some ethical challenges facing hESCR can be addressed through national regulatory mechanisms and international norms of ethics for conduct of research involving human subjects. Although human materials donors in the context of hESCR may not normally be considered research subjects, for ethical oversight, we believe that they should be treated as such. Currently, the status of human materials donors and the policies that pertain to their participation as donors in hESCR varies between countries (see table, above).

However, many ethical challenges in hESCR fall outside the traditional human subjects framework. As the science evolves, academies of science and relevant professional organizations, in consultation with the public, should continue to develop guidelines for the ethical conduct of hESC research and clinical trials. Several national and international bodies are currently attempting this (*5*–*8*). The process should include concerted efforts to engage people worldwide in honest and realistic conversations about the science and ethics of hESCR. Research institutions should create opportunities for scientists and trainees to learn about the social context and implications of research and to engage in ethical discussion and reflection among themselves and with the public. Funders of hESCR must satisfy themselves that the scientists they fund conduct their research ethically and in accordance with national regulations and international guidance.

Although we should not expect harmonization of international laws with respect to hESCR, we should strive to develop international consensus on ethical and scientific standards and practices. Stem cell scientists should be vigilant in anticipating coming ethical challenges to ensure that the science proceeds in an acceptable fashion.

References and Notes

1. See (www.hinxtongroup.org).
2. B. Hansen, *Med. Law* **23**, 19 (2004).
3. I. Wilmut *et al.*, *Science* **310**, 1903 (2005).
4. Public database (www.hinxtongroup.org) in design stage.
5. U.K.'s Human Fertilisation and Embryology Authority (www.hfea.gov.uk).
6. U.S. National Academy of Sciences (http://dels.nas.edu/bls/stemcells/).
7. International hESCR Guidelines Task Force of the International Society for Stem Cell Research (www.isscr.org/scientists/guidelines.cfm).
8. International Stem Cell Forum (www.stemcellforum.org/).
9. Country-specific sources that formed the basis for the table were as follows. **Australia**: Human Cloning Prohibition Act (2002); Research Involving Human Embryos Act (2002); National Health & Medical Research Council's Ethical Guidelines on the Use of Assisted Reproductive Technology in Clinical Practice and Research. **China**: Ethical Guiding Principles for Research on Human Embryonic Stem Cells (2003); The Guidelines on Human Assisted Reproductive Technology (July 2003), promulgated by the Ministry of Health. **United Kingdom**: Human Fertilisation and Embryology Act, Schedules 2 and 3 (1990); Human Fertilisation and Embryology (Disclosure of Information) Act (1992); Human Fertilisation and Embryology (Research Purposes) Regulations (2001). **Germany**: StGB (German Penal Code); Embryonenschutzgesetz—ESchG (1990); Stammzellgesetz—StZG (2002). **Israel**: Prohibition of Genetic Intervention (Human Cloning and Genetic Manipulation of Reproductive Cells) Law, 5759-1999 (this law was renewed, and slightly amended, in 2004, with the same sunset clause established for another 5 years); Report of the Bioethics Advisory Committee of the Israel Academy of Sciences and Humanities: The Use of Embryonic Stem Cells for Therapeutic Research (2001); Public Health Regulations (1979).

10. Supported by the Greenwall Foundation; the Wellcome Trust; the British Embassy in Washington, DC; and the Juvenile Diabetes Research Foundation.

Supporting Online Material

www.sciencemag.org/cgi/content/full/313/5789/921/DC1

10.1126/science.1127990

PSYCHOLOGY

Psychiatric Casualties of War

The prevalence of posttraumatic stress disorder in Vietnam veterans has been a controversial medical and political issue. A new analysis provides better data and more robust conclusions.

Richard J. McNally

The Vietnam War ended more than 30 years ago, but controversy concerning its psychiatric cost continues today. On page 978 of this issue, Dohrenwend *et al.* (*1*) have reanalyzed the prevalence of posttramatic stress disorder (PTSD) among U.S. male veterans of the war, further adding to the debate about the psychological trauma incurred during exposure to military combat.

According to the U.S. Centers for Disease Control and Prevention (CDC), 14.7% of male veterans developed PTSD after serving in Vietnam, but only 2.2% still had the illness by the late 1980s (*2*). Clinical experts on PTSD disputed this conclusion, arguing that flawed methods underestimated the true prevalence of the problem. To resolve the issue, Congress authorized the National Vietnam Veterans' Readjustment Study (NVVRS) (*3*). Its results indicated that 30.9% of male veterans developed PTSD, and an additional 22.5% developed partial PTSD. Moreover, 15.2% still suffered from the disorder in 1990, a prevalence rate nearly seven times as high as that determined by the CDC. Congress had been poised to phase out counseling and other services for Vietnam veterans, but the NVVRS triggered an abrupt about-face. The government poured funds into clinical services and research designed to cope with an apparent epidemic of chronic PTSD among Vietnam veterans.

Clinical workers and researchers in the trauma field accepted the NVVRS at face value, assuming that the CDC got it wrong. But in recent years, skeptics, often historians of military psychiatry, have expressed doubts about the NVVRS (*4*). They noted that only about 15% of those who served in Vietnam had been assigned to combat units (*5*), yet the NVVRS indicated that 53.4% of all men who served in any capacity had developed either full-blown or partial PTSD. Ben Shephard, the preeminent historian of military psychiatry, suspected that the NVVRS interviewers misconstrued expectable symptoms of emotional distress as indicative of mental illness (*4*). Indeed, the diagnostic criteria for PTSD used by the NVVRS did not require that symptoms produce functional impairment. Others observed how the pattern of psychiatric casualties in Vietnam differed from the shell shock of World War I and the battle fatigue of World War II. Another expert on the psychiatric consequences of war pointed out that "Vietnam produced an extremely low proportion of proximate combat stress casualties and produced or is claimed to have produced massive numbers of postcombat casualties. Therefore, Vietnam breaks with the past normative pattern of combat and war zone stress casualty production" (*6*). For reasons that remain unclear, psychiatric problems in many Vietnam veterans became evident years after their return to civilian life.

The consequences of war. The Vietnam Veterans Memorial in Washington, D.C.

Directly addressing concerns raised by the skeptics, Dohrenwend *et al*. reanalyzed data from the NVVRS. They consulted archival records, personnel files, and other historical sources to verify reports of traumatic events, and they ensured that PTSD symptoms produced impairment before accepting the diagnosis of PTSD. The authors confirmed the suspicions of the skeptics: The NVVRS overestimated the rate of PTSD by 40%. Although their recalculation produced plummeting prevalence rates, Dohrenwend *et al*. emphasized that 9.1% of all Vietnam veterans still suffered from the disorder as of 1990.

Dohrenwend *et al*.'s most newsworthy finding is that the NVVRS markedly overestimated the prevalence of PTSD. But two other findings also deserve mention. They confirmed the dose-response effect: The more trauma exposure a veteran had experienced, the more likely he was to develop PTSD. Also, by adopting a method known to all historians—the study of archives—Dohrenwend *et al*. verified nearly all the reports of trauma exposure mentioned by the veterans. Indeed, motives to fabricate trauma histories and PTSD symptoms are nearly nonexistent in an epidemiologic study. However, consulting the same archival sources as Dohrenwend *et al*., Frueh *et al*. (*7*) could verify reports of combat exposure in only 41% of 100 men recently seeking treatment and service-connected disability for Vietnam-related PTSD. Just as Dohrenwend *et al*. emphasized that one cannot generalize from a treatment or compensation-seeking sample to an epidemiologic sample, one cannot generalize from an epidemiologic sample to a clinical one, either. Archival sources are important in both contexts.

Both the NVVRS results and Dohrenwend *et al*.'s reanalysis show that many men who developed PTSD since the Vietnam war no longer had the disorder by the late 1980s. One might have predicted that the number of men suffering from PTSD would have declined further since then. But a recent investigation by the Department of Veterans Affairs suggests otherwise (*8*). In fact, the number of veterans seeking treatment and service-connected disability payments has been skyrocketing. During fiscal years 1999 to 2004, the total number of veterans receiving disability compensation for PTSD increased by 79.5%, whereas the total number receiving disability compensation for all health problems increased by only 12.2%. During this period, PTSD disability payments increased by 148.8%. Does this indicate an upsurge of delayed-onset PTSD, a reactivation of symptoms among veterans approaching retirement, or delayed presentation of PTSD among those who have suffered for decades and are only now seeking the help they need?

The field of psychological trauma is notable for the moral passion it mobilizes and the controversies that erupt within it (*9*). Critics who question cherished assumptions are often accused of harboring political agendas, inadvertently silencing the voices of survivors, or downplaying the psychic consequences of traumatic stress. Indeed, the president of the International Society for Traumatic Stress Studies recently urged critics to muffle their dissent, lest the intensity of

The author is in the Department of Psychology, Harvard University, Cambridge, MA 02138, USA. E-mail: rjm@wjh.harvard.edu

scientific controversy distract us from attending to the needs of trauma victims (*10*). But criticism is vital for any scientific field, and discovering new facts, however politically incorrect they may seem, provides the best basis for helping victims. The new study's conclusion that the NVVRS overestimated the rate of PTSD by 40% will upset some people. Yet by increasing the accuracy of our prevalence estimates, Dohrenwend *et al*. have performed a valuable service. Advocacy for victims must rest on the best science possible.

References

1. B. P. Dohrenwend *et al.*, *Science* **313**, 978 (2006).
2. Centers for Disease Control Vietnam Experience Study, *J. Am. Med. Assoc.* **259**, 2701 (1988).
3. R. A. Kulka, W. E. Schlenger, J. A. Fairbank, R. L. Hough, B. K. Marmar, D. S. Weiss, *Trauma and the Vietnam War Generation: Report of Findings from the National Vietnam Veterans Readjustment Study* (Brunner/Mazel, New York, 1990).
4. B. Shephard, *A War of Nerves: Soldiers and Psychiatrists in the Twentieth Century* (Harvard Univ. Press, Cambridge, MA, 2001).
5. E. T. Dean Jr., *Shook Over Hell: Post-traumatic Stress, Vietnam, and the Civil War* (Harvard Univ. Press, Cambridge, MA, 1997).
6. D. H. Marlowe, *Psychological and Psychosocial Consequences of Combat and Deployment with Special Emphasis on the Gulf War* (RAND, Santa Monica, CA, 2001).
7. B. C. Frueh *et al.*, *Brit. J. Psychiat.* **186**, 467 (2005).
8. Department of Veterans Affairs, Office of the Inspector General, *Review of State Variances in VA Disability Compensation Payments (Report #05-00765-137)* (2005); www.va.gov/foia/err/standard/requests/ig.html.
9. R. J. McNally, *Remembering Trauma* (Harvard Univ. Press, Cambridge, MA, 2003).
10. D. Kilpatrick, *Traumatic StressPoints* **20**, 2 (2006); www.istss.org.

10.1126/science.1132242

EVOLUTION

Traversing the Adaptive Landscape in Snapdragons

The genetic changes that underlie adaptive evolution of species are not easy to determine. Snapdragon species with different flower colors that coexist in the Pyrenees offer a promising system for analyzing them.

Elena M. Kramer and Kathleen Donohue

How does one species become two species? Species appear to be stable, adapted entities reproductively isolated from related species, but how did this isolation appear? We can view species in terms of populations in an adaptive landscape—a topographical plot of fitness as a function of combinations of characteristics. Each species then sits on its own high ground, sporting adaptive characteristics (collectively, their phenotypes), while they tower over valleys of maladaptive phenotypes. Does this high ground represent isolated peaks, each species inhabiting one of them, or are the areas of high ground connected by an equally high ridge, long and circuitous though it may be?

Distinguishing between these two possibilities is fundamental to understanding speciation. With two isolated peaks, there is no way to get from one to the other except through great mutational leaps, tromping through a valley of low fitness, or waiting for the environment (the landscape itself) to change. In the alternative case, one can simply walk randomly along a ridge. The evolutionary mechanisms are very different between those two scenarios, including the roles of natural selection, drift, migration, and mutation. On page 963 of this issue, Whibley *et al.* provide evidence that speciation in snapdragons may have occurred through a walk along an adaptive ridge (*1*).

Since Wright first introduced the concept of the adaptive landscape in 1932 (*2*), it has become one of the most important heuristic tools in evolutionary biology. The original formulation plotted fitness in a population as a function of the frequency of different forms of specific genes (alleles), resulting in a contoured landscape where the peaks represent local optima that correspond to a particular genotype. This concept was modified by Simpson (*3*) and Lande (*4*) to yield an alternate landscape that plots fitness as a function of phenotypic values, where the surface represents the relative fitness of particular phenotypes in a population. Given that many phenotypes are quite complex at the genetic level, however, the relationship between genotype and phenotype has often proven difficult to quantify. As Wright himself pointed out, the true adaptive landscape exists in thousands of dimensions, with many genes sometimes contributing to a single phenotype under selection. Thus, many authors have debated the true nature of an adaptive landscape: whether it is smooth or rugged, with many isolated peaks or few, with the highest level of adaptation represented by single points or by continuous ridges [see the review by Schluter (*5*)].

A classic model of speciation along an adaptive ridge is the Dobzhansky-Muller model. Imagine a population with individuals that have the two-locus (two-gene) genotype *rrSS* (where upper and lower case denote different alleles), and the population divides into two. In one population, a new *R* allele arises and replaces *r*, so the population now has genotype *RRSS*. In the other, a new *s* allele arises and replaces *S*, and the population has the genotype *rrss*. Note that the *R* allele has never occurred with the *s* allele during this

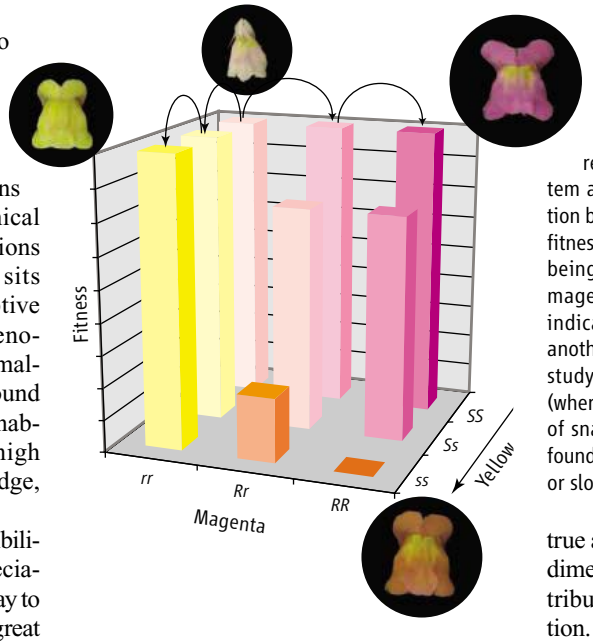

Evolution along an adaptive ridge. Whibley *et al*. found three loci associated with floral color, two being tightly linked and virtually inherited as one. The diagram represents their results in terms of evolution of a two-gene system along a ridge that creates reproductive isolation between the subspecies. The *z* axis indicates the fitness of flowers with different colors, with orange being in the valley of low fitness and yellow and magenta along the ridge of high fitness. Arrows indicate stepwise changes from one genotype to another, starting with *rrSS*. One subspecies in their study had genotype *RRSS* and the other had *rrss* (where *R* = *ROS*, *S* = *SULF*). Other extant subspecies of snapdragon are expected to contain genotypes found along the ridge but not genotypes in the valley or slopes.

PHOTO INSETS: WHIBLEY *ET AL.* (*1*)

The authors are in the Department of Organismic and Evolutionary Biology, Harvard University, Cambridge, MA 02138, USA. E-mail: ekramer@oeb.harvard.edu

process. If the combination of *R* and *s* results in low fitness, then the two new populations would be reproductively isolated (their offspring would have low fitness because they would contain both *R* and *s*), even though neither population went through any stage of low fitness itself.

Whibley *et al*. provide a possible real-world example of this process (see the figure). The authors conducted a study of naturally hybridizing subspecies of *Antirrhinum majus*, a snapdragon. The yellow-flowered *A. m. striatum* and magenta-flowered *A. m. pseudomajus* form a narrow hybrid zone where their ranges meet in the Pyrenees. Whibley *et al.* were able to identify three loci that contribute significantly to the flower color differences between the two morphs. To further investigate the evolutionary interactions of the yellow and magenta floral forms, Whibley *et al*. combined an elegant digital color quantification technique with principal components analysis to define a phenotypic space for flower color. Although the F_2 (second generation and offspring of interbred hybrids) plants from a *striatum-pseudomajus* cross occupied a relatively large portion of the space, variation observed in natural subspecies was restricted to a narrower domain. In particular, an orange-colored form obtained in the F_2 crosses was never observed in natural populations. The authors suggest that this result reflects reduced fitness due to pollinator aversion and conclude that lowered fitness among the hybrids has helped to isolate the parental genotypes. Moreover, the seemingly disjunct yellow and magenta forms are found to occupy the extremes of a contiguous domain in genetically determined phenotypic space. If the maintenance of these colors in nature reflects their higher fitness, the connection between the two extremes can be interpreted as a route for the transition from yellow to magenta while avoiding the fitness valley represented by the orange genotypes. This connection can be thought of as an adaptive ridge in which the magenta/yellow domain of genotype space represents a continuous ridge of high fitness. Populations or species tend to evolve upward toward the ridge crest, resulting in a random distribution along the ridge. In this case, it appears that one defining feature of the ridge is that when two populations come into contact, their hybridization produces some phenotypes that "fall off" the ridge, resulting in lower fitness.

The current study is possible because the authors can make accurate predictions about the relationships between color and genotype, allowing the conversion between phenotypic and genotypic space. The genetic simplicity of the system makes it irresistible for actual tests of the Dobzhansky-Muller dynamic through measures of natural selection on the different genotypes. Note that an adaptive landscape describes the relationship between genotypes and fitness in a single environment. The model therefore would make the simple and testable prediction that all extant floral color genotype combinations would have comparable fitness across the entire geographical range of distribution, and all missing phenotypes (presumably those carrying the incompatible combination of *R* and *s*) would have equally low fitness across the range. The alternative hypothesis is that each color morph is locally adapted to its own local environment. Such measurements would address a fundamental question regarding speciation, namely whether environment-independent genetic incompatibilities alone account for reproductive isolation between species that have diverged essentially through drift along a ridge, or whether divergent adaptation to different environments is the cause. In short, just what is the role of natural selection in speciation?

References

1. A. C. Whibley *et al*., *Science* **313**, 963 (2006).
2. S. Wright, in *Proceedings of the Sixth International Congress of Genetics*, D. F. Jones, Ed. (Brooklyn Botanic Garden, Menasha, WI, 1932), vol. 1, pp. 356–366.
3. G. G. Simpson, *Tempo and Mode in Evolution* (Columbia Univ. Press, New York, 1944).
4. R. Lande, *Evolution* **33**, 402 (1979).
5. D. Schluter, *The Ecology of Adaptive Radiation* (Oxford Univ. Press, Oxford, 2000).

10.1126/science.1130958

ASTRONOMY

A Journey Through Time

Joseph Silk

Small variations in the temperature and density of matter just after the Big Bang are thought to have been the seeds for the galaxies we see today. This picture has been confirmed by observational evidence.

The cosmic microwave background radiation left over from the Big Bang provides a unique window on the very early universe. We believe now that galaxies formed as small variations in matter density evolved under the influence of gravity. If so, then the primordial fluctuations had to have a finite amplitude given the limited time available for fluctuation growth. An inevitable consequence is that temperature fluctuations must be generated in the cosmic microwave background. Recent observations of the background radiation confirm this picture of the gravity-induced growth of structure in the early universe.

Enhanced online at www.sciencemag.org/cgi/content/full/313/5789/925

The first predictions of cosmic temperature fluctuations were made in 1967 by Sachs and Wolfe (*1*). It was not until 1992 that NASA's Cosmic Background Explorer (COBE) verified, to within a factor of 2, the predicted effect (*2*). This is with hindsight also the prediction of the inflationary theory of cosmology of large–angular scale temperature fluctuations generated in the first 10^{-36} s of the Big Bang. It was to take more than a decade, however, before the fine-scale anisotropy predictions (*3*, *4*) associated with galaxy formation were confirmed (*5*).

Each time there was a major experimental improvement, the theoretical hurdle was raised as the predictions were refined. The ultimate prediction of temperature fluctuations arising from structure formation, made in 1984 (*6, 7*), was only 3 parts in 100,000, at an angular scale of about 30 arc min, and substantially lower on smaller angular scales. Eventually, ground-based and balloon-borne experiments provided strong confirmation of the elusive signal. But it was the release of first-year data from the Wilkinson Microwave Anisotropy Probe (WMAP) satellite in 2003 that provided the first high-precision measurements (*8*). Cosmology would never be the same again with the new refined measurements.

There were several dramatic results. The universe had to be flat, and at the critical density. Most of its mass-energy density was in the form of dark energy. One-third of the critical density was in nonbaryonic matter, and only 15% of that was in baryons (such as neutrons and protons). The primordial fluctua-

The author is in the Department of Physics, University of Oxford, Oxford OX1 3RH, UK. E-mail: silk@astro.ox.ac.uk

tions were scale-invariant, with just one number describing their amplitude. And the universe was reionized at the unexpectedly high redshift of 17 (corresponding to 400 million years after the Big Bang) when newly forming galaxies emitted strong ionizing radiation. Cosmologists were jubilant. The standard model of cosmology was confirmed to unprecedented precision. However, the theorists still had work to do, as the power distribution of fluctuations on different scales, characterized by the spectral index n_s, was uncomfortably close to unity, corresponding to perfect scale invariance.

The original preinflationary cosmology prediction for n_s by Zeldovich and Harrison was indeed unity (*9, 10*). However, as inflation peters out during the first 10^{-36} s, smaller and smaller scales successively become causally disconnected but with slightly suppressed amplitude. Inflation predicts a rollover as progressively smaller scales inflated, so that n_s is ~0.95.

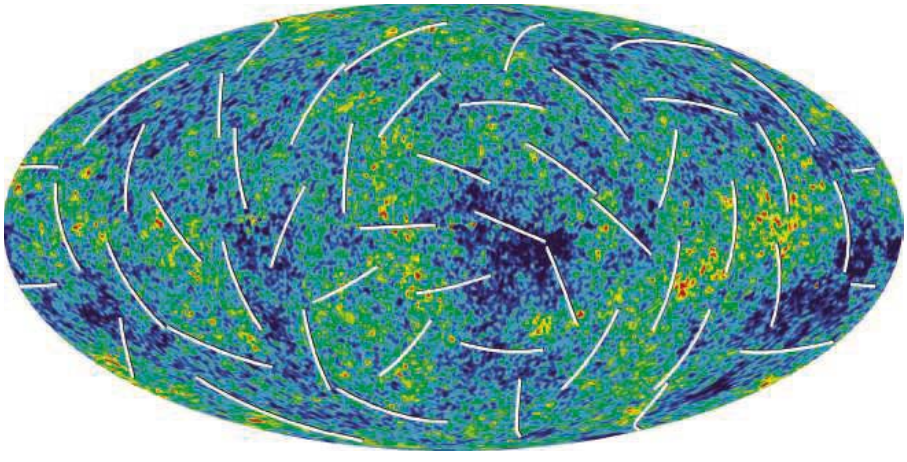

Microwave sky. Data from WMAP after 3 years of collection showing hotter (red) and cooler (blue) regions of the universe, along with directions of microwave polarization (white bars).

Moreover, the detection of polarization of the cosmic microwave background indicated the effects of scattering of photons by free electrons when the universe was reionized. The first-year data found an unexpectedly large amount of polarization, although the uncertainties were large because only the correlation between temperature and polarization was measured. The inferred epoch of reionization at a redshift of 17 could not be explained by known sources such as the first stars or quasars.

Earlier this year, the WMAP team released its full 3-year data set (*11–14*). So what has changed? The big improvement over the first year of data was the addition of the more accurate all-sky polarization data (see the figure). Previously only the polarization-temperature correlation power was available, with correspondingly large uncertainties. The optical depth of the universe τ (that is, the probability that a cosmic microwave background photon is scattered) was now measured with higher precision, and was found to be substantially lower than previously thought. Reionization now appears to have occurred at a redshift of 10 (corresponding to a billion years after the Big Bang), altogether a more acceptable epoch for cosmology.

There is a degeneracy between τ and n_s: The smaller τ is, the bluer is the inferred spectrum, and the smaller is n_s. The amplitude of the pure polarization power signal is proportional to τ^2 so that the new measurement strongly constrains the optical depth. This broke the degeneracy and led to a substantial reduction in n_s. In fact, τ came down and so did n_s, so that the new result is that n_s is about 0.95. The previous result that n_s is close to 1 can now be rejected in favor of the inflationary cosmology prediction. These changes have brought the cosmological parameters much closer to theoretical expectations. Lowering τ meant that the fluctuation amplitude had to be lowered to give the measured temperature fluctuations.

Moreover, the strength of the density fluctuations (denoted by σ_8) was reduced by 15%, which has dramatic implications. The contribution of hot intracluster gas scattering to the very fine-scale cosmic microwave background fluctuations by Compton interactions, known as the Sunyaev-Zeldovich effect, depends on a very high power of σ_8. If the detection by the CalTech-led Cosmic Background Imager experiment of excess power at small angular scales relative to the primary cosmic microwave background fluctuations holds up, some novel interpretation may be needed for the excess signal. This could, for example, be due to a nongaussian distribution of primordial fluctuations on galaxy-cluster scales, a result that would have profound implications for structure formation and for inflation. A more mundane interpretation may be the contribution of a hitherto unidentified population of radio galaxies with flat spectra. Also, on the galaxy-formation front, the lowering of the fluctuation strength means that the number of late mergers is considerably reduced. This is good news for helping understand the fragile nature of galactic disks, and bad news for the large-scale simulators who will need to repeat their calculations.

The solutions for the cosmological parameters are still not completely definitive. In the cosmic microwave background alone, there are notable parameter degeneracies. However, specifying the measured value of the Hubble constant leads to the highly significant inference that the universe is flat. The spatial curvature is close to zero. This reinforces the need for dark energy to make up the shortfall of dark matter to generate the critical density for a flat universe.

Perhaps the most important WMAP inference is that the primordial density fluctuations are nearly but not quite scale-invariant. This new result has been greeted with jubilation by many theorists who regarded it as a prediction of inflationary cosmology. I am less convinced by the predictive power of inflation, recalling the equally vocal band of inflationary theorists in the 1990s who tuned inflationary models to welcome the low-density universe then favored by observational cosmologists but that now are history. Nevertheless, it seems fair to conclude that the ultimate theory of cosmology will most likely include both the emerging standard cosmological model and inflation as key ingredients.

References

1. R. K. Sachs , A. M. Wolfe, *Astrophys. J.* **147**, 73 (1967).
2. G. F. Smoot *et al.*, *Astrophys. J. Lett.* **396**, L1 (1992).
3. J. Silk, *Nature* **215**, 1155 (1967).
4. J. Silk, *Astrophys. J.* **151**, 459 (1968).
5. L. Knox, L. Page, *Phys. Rev. Lett.* **85**, 1366 (2000).
6. N. Vittorio, J. Silk, *Astrophys. J. Lett.* **285**, L39 (1984).
7. J. R. Bond, G. Efstathiou, *Astrophys. J. Lett.* **285**, L45 (1984).
8. C. L. Bennett *et al.*, *Astrophys. J. Suppl.* **148**, 1 (2003).
9. E. Harrison, *Phys. Rev. D* **10**, 2726 (1970).
10. Ya. B. Zeldovich, *Mon. Not. R. Astron. Soc.* **160**, 1P (1972).
11. D. N. Spergel *et al.*, http://arxiv.org/abs/astro-ph/0603449.
12. L. Page *et al.*, http://arxiv.org/abs/astro-ph/0603450.
13. G. Hinshaw *et al.*, http://arxiv.org/abs/astro-ph/0603451.
14. N. Jarosik *et al.*, http://arxiv.org/abs/astro-ph/0603452.

10.1126/science.1127780

CREDIT: NASA/WMAP SCIENCE TEAM

CLIMATE CHANGE

Is Global Warming Causing More, Larger Wildfires?

Higher spring and summer temperatures and earlier snowmelt are extending the wildfire season and increasing the intensity of wildfires in the western United States.

Steven W. Running

On 3 April 2006, the U.S. weekly news magazine *Time* ran a report on global warming with the cover title "Be worried, be very worried." Similar coverage of global warming has emerged in other general-interest magazines in recent months, triggered by scientific studies that are finding evidence for adverse impacts of global warming occurring today, not merely projected for future decades. These adverse impacts—from higher probabilities of category 4 and 5 hurricanes (*1*, *2*) to higher rates of sea-level rise (*3*)—are found not in some distant unpopulated region, but rather right in our own back yards.

On page 940 of this issue, Westerling *et al.* (*4*) come to a similarly discomforting conclusion for wildfires. They show that warmer temperatures appear to be increasing the duration and intensity of the wildfire season in the western United States. Since 1986, longer, warmer summers have resulted in a fourfold increase of major wildfires and a sixfold increase in the area of forest burned, compared to the period from 1970 to 1986. A similar increase in wildfire activity has been reported in Canada from 1920 to 1999 (*5*).

Westerling *et al.* used the most comprehensive data set of wildfire occurrences yet compiled for the western United States to analyze the geographic location, seasonal timing, and regional climatology of the 1166 recorded wildfires with an extent of more than 400 ha. They found that the length of the active wildfire season (when fires are actually burning) in the western United States has increased by 78 days, and that the average burn duration of large fires has increased from 7.5 to 37.1 days. Based on comparisons with climatic indices that use daily weather records to estimate land surface dryness, Westerling *et al.* attribute this increase in wildfire activity to an increase in spring and summer temperatures by ~0.9°C and a 1- to 4-week earlier melting of mountain snowpacks. Snow-dominated forests at elevations of ~2100 m show the greatest increase in wildfire activity.

The hydrology of the western United States is dominated by snow; 75% of annual streamflow comes from snowpack. Snowpacks keep fire danger low in these arid forests until the spring melt period ends. Once snowmelt is complete, the forests can become combustible within 1 month because of low humidities and sparse summer rainfall. Most wildfires in the western United States are caused by lightning and human carelessness, and therefore forest dryness and hot, dry, windy weather are the necessary and increasingly common ingredients for wildfire activity for most of the summer. Snowpacks are now melting 1 to 4 weeks earlier than they did 50 years ago, and streamflows thus also peak earlier (*6*, *7*).

Westerling *et al.* found that, in the 34 years studied, years with early snowmelt (and hence a longer dry summer period) had five times as many wildfires as years with late snowmelt. High-elevation forests between 1680 and 2690 m that previously were protected from wildfire by late snowpacks are becoming increasingly vulnerable. Thus, four critical factors—earlier snowmelt, higher summer temperatures, longer fire season, and expanded vulnerable area of high-elevation forests—are combining to produce the observed increase in wildfire activity.

The fires in Yellowstone Park in 1988 (see the first figure) seemed to inaugurate this new era of major wildfires in the western United States. The fires lasted more than 3 months, burning 600,000 ha of forest, and—despite the investment of $120 million and deployment of 25,000 firefighters—were only extinguished when snow began to fall in mid-September (*8*).

Too close for comfort. Wildfire is seen approaching Old Faithful Village, Yellowstone National Park, in 1988.

The Yellowstone fires exemplify a common statistic of wildfires: Less than 5% of all wildfires account for more than 95% of the area burned. A small fraction of fires get very large and become uncontrollable despite human efforts to suppress them, regardless of money expended. Such efforts can cost more than $20 million per day, and seasonal expenditures by governmental agencies in recent years have reached $1.7 billion.

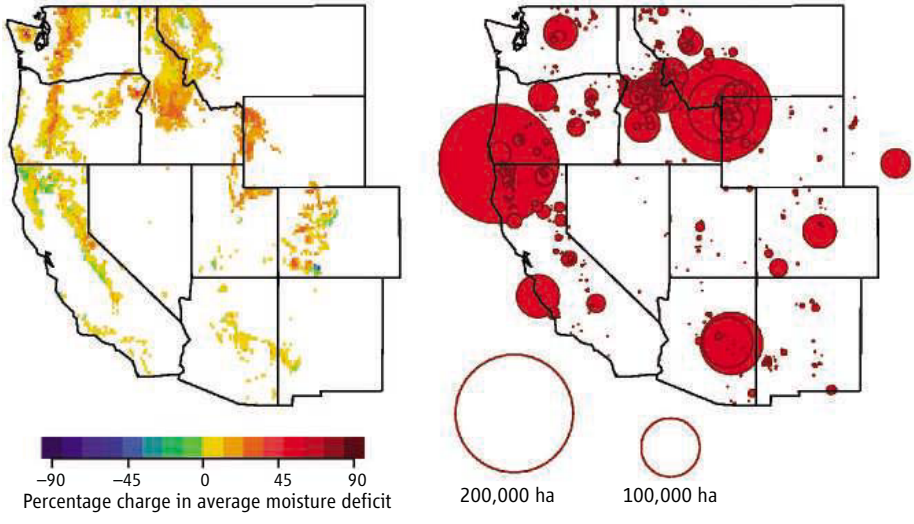

Less moisture—more fires. Between 1970 and 2003, spring and summer moisture availability declined in many forests in the western United States (**left**). During the same time span, most wildfires exceeding 1000 ha in burned area occurred in these regions of reduced moisture availability (**right**). [Data from (*4*)]

The author is with the Numerical Terradynamic Simulation Group, University of Montana, Missoula, MT 59812, USA. E-mail: swr@ntsg.umt.edu

CREDIT: (TOP) NPS PHOTO

Fire is an important process for recycling dead biomass in the arid west, where natural decomposition rates are extremely slow (historical repeat photography has shown untreated wooden fenceposts still intact after 100 years). However, this benefit is balanced by the annual damages in the western United States from wildfires that have exceeded $1.0 billion in 6 of the past 15 years (*9*).

In 2002, the U.S. Departments of Agriculture and the Interior embarked on a controversial new land management policy called "Healthy Forests," whose stated objective is to clean out dead and dying trees in the west to reduce the risk of wildfires. This initiative blames increasing wildfire activity in the western United States solely on increasing stand density and the buildup of dead fuel as a result of fire exclusion policies; it does not acknowledge any role of changing climate in recent wildfire trends. In contrast, the analysis of Westerling *et al.* suggests that observed increased wildfire activity is at least partially the result of a longer wildfire season acting over a larger forested area. This increased wildfire trend correlates with observed higher temperatures and reduced moisture availability (see the second figure).

As part of the upcoming 4th Assessment of the Intergovernmental Panel on Climate Change (IPCC) (*10*), seven general circulation models have run future climate simulations for several different carbon emissions scenarios. These simulations unanimously project June to August temperature increases of 2° to 5°C by 2040 to 2069 for western North America. The simulations also project precipitation decreases of up to 15% for that time period (*11*). Even assuming the most optimistic result of no change in precipitation, a June to August temperature increase of 3°C would be roughly three times the spring-summer temperature increase that Westerling *et al.* have linked to the current trends. Wildfire burn areas in Canada are expected to increase by 74 to 118% in the next century (*12*), and similar increases seem likely for the western United States.

Wildfires add an estimated 3.5×10^{15} g to atmospheric carbon emissions each year, or roughly 40% of fossil fuel carbon emissions (*13*). If climate change is increasing wildfire, as Westerling *et al.* suggest, these new sources of carbon emissions will accelerate the buildup of greenhouse gases and could provide a feed-forward acceleration of global warming.

References and Notes

1. P. J. Webster *et al.*, *Science* **309,** 1844 (2005).
2. K. Emmanuel *et al.*, *Nature* **436**, 686 (2005).
3. E. Rignot, P. Kanagaratnam, *Science* **311**, 986 (2006).
4. A. L. Westerling, H. G. Hidalgo, D. R. Cayan, T. W. Swetnam, *Science* **313**, 940 (2006); published online 6 July 2006 (10.1126/science.1128834).
5. N. P. Gillett *et al.*, *Geophys. Res. Lett.* **31**, L18211 (2004).
6. P. W. Mote *et al.*, *Bull. Am. Meteorol. Soc.* **86**, 39 (2005).
7. I. T. Stewart *et al.*, *J. Clim.* **18**, 1136 (2005).
8. See www.nps.gov/yell/nature/fire/index.htm.
9. See www.ncdc.noaa.gov/img/reports/billion/billion2005.pdf.
10. See www.ipcc-wg2.org/authors/index.html.
11. K. Rousteenoja *et al.*, *Finn. Environ. Inst.* #644 (2003); see www.ymparisto.fi/download.asp?content id=25835&lan=EN.
12. M. D. Flannigan *et al.*, *Clim. Change* **72**, 1 (2005).
13. G. R. van der Werf *et al.*, *Science* **303**, 73 (2004).

Published online 6 July 2006;
10.1126/science.1130370

NEUROSCIENCE

No More Cortical Neurons for You

Pasko Rakic

Are new neurons born in the cortex of the adult human brain? An advanced method of cell birth dating appears to answer this contentious question in the negative.

The cerebral cortex is the seat of human intelligence, language, and creativity. This may be why the question of whether new cortical neurons are generated during a person's life span is so fascinating. In particular, whether the human neocortex (see the figure) receives new neurons during adulthood has remained highly controversial. In a recent issue of the *Proceedings of the National Academy of Sciences U.S.A.*, Bhardwaj *et al.* (*1*) add to the evidence that establishes the absence of neurogenesis in this region of the adult human brain. They accomplish this by using an advanced approach based on the carbon-14 (^{14}C) assay for determining the age of cells in the human body.

Over the past 120 years, numerous histological, silver impregnation, and electron microscopic studies have not displayed morphological evidence of new neurons in adult mammalian cortical tissue. More indirect methods, such as radiolabeling the replication of genomic DNA during cell division, have indicated that the cerebral cortex in all mammals so far examined, including rodents and nonhuman primates, is generated during a well-defined developmental period (*2*–*4*). On the other hand, it was reported that a large number of neurons stream daily from proliferative layers near the cerebral ventricle to the overlaying neocortex in adult nonhuman primates (*5*), raising speculation that new neurons are continuously added to the adult human cerebral cortex. However, this finding could not be confirmed in either the primate (*6*, *7*) or rodent cortex (*8*, *9*), making this issue controversial (*9*, *10*).

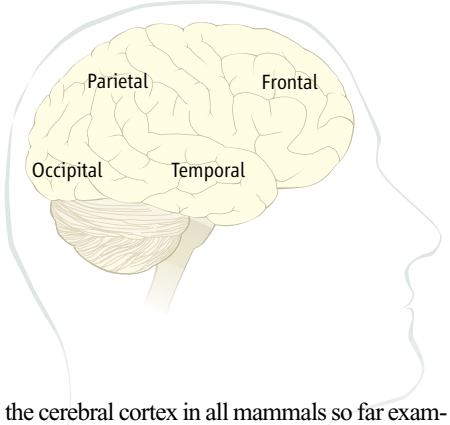

The adult human brain. The surface of the human neocortex is about 10 times as large as that of a macaque monkey and 1000 times as large as that of a mouse. The neocortex consists of the frontal, parietal, temporal, and occipital lobes. It can be further subdivided into structurally and functionally distinct areas that mediate our most important mental capacities.

The innovative study by Bhardwaj *et al.* demonstrates with advanced methodology—^{14}C dating of cell births—that no new neurons are added to the human neocortex after birth. The authors take advantage of a transiently sharp increase in the level of the radioactive carbon isotope, ^{14}C, in Earth's atmosphere during the era of aboveground testing of nuclear weapons between the mid-1950s and the time of the nuclear Test Ban Treaty in 1963. In the years following these events, the level of ^{14}C in the atmosphere declined to preexisting low background levels. The authors acquired cortical tissue from the autopsies of seven individuals born in Sweden between 1933 and 1973, and examined the level of ^{14}C in individual cells by accelerator mass spectrometry. The presence of ^{14}C in genomic DNA indicates that cells passed through their last cell division

CREDIT: P. HUEY/*SCIENCE*

The author is in the Department of Neurobiology, Yale University School of Medicine, New Haven, CT 06520–8001, USA. E-mail: pasko.rakic@yale.edu

at a time when the atmospheric level of this isotope was high. The authors previously tested the validity of their approach in other tissue samples known to be renewable (intestine and skeletal muscle) and showed that the technique detected ^{14}C accurately in these cells, even in specimens collected 50 years after DNA replication had occurred (*11*).

In the present study, the authors found numerous ^{14}C-positive nonneuronal cell types, such as glial and endothelial cells, in all cortical specimens. However, no neurons were labeled in the several structurally and functionally distinct areas of the frontal, parietal, temporal, and occipital lobes of the neocortex of adult specimens. For optimal precision, the authors examined more than 100 million cells in most samples. Because ^{14}C assays theoretically may leave a minute number of labeled cells undetected, the authors also labeled DNA with 5-bromo-2′-deoxyuridine (BrdU, a thymidine analog) in cortical tissue from volunteers afflicted with terminal cancer. These patients were injected with BrdU and died between 4 months and 4 years afterward. Although cortical tissue from these patients exhibited labeling of neuronal and nonneuronal cells (glial and granule cells, respectively) in the hippocampus (*12*), none of the labeled cells in neocortical tissues were neurons.

The lack of addition of new neurons to the adult human neocortex agrees with the progressive decrease in adult neurogenesis that occurred during evolution. Although it was shown that new neurons are added to the mammalian hippocampus and olfactory bulb (*13*) in nonhuman primates, their number is both relatively and absolutely smaller than in rodents (*14*, *15*), and the migratory stream that supplies neurons to the olfactory bulb is absent and/or undetectable in the adult human (*16*). The decrease in neurogenesis in adult primates contrasts with the large addition and/or renewal of neurons in the brains of nonmammalian vertebrates such as fish, frogs, reptiles, and birds, which usually correlates with their capacity for regeneration (*13*). Why is such a useful capacity lost during mammalian evolution? One hypothesis is that preservation of acquired information within a permanent population of cortical neurons may be more valuable for the survival of an organism than the introduction of "naïve" neurons that have not been exposed to experience (*17*). Thus, lack of neurogenesis in the cerebral cortex may be a critical step in the evolution of mental prowess in *Homo sapiens*.

The absence of neurogenesis in the adult human cortex is not a reason to decrease research efforts that seek ways of replacing neurons lost due to trauma, stroke, infection, degeneration, or aging. Various therapies, including cell transplantation, are being explored precisely because neurons are not normally regenerated. However, at present, we lack the knowledge of how to direct endogenous or transplanted neural stem cells to their desired position, and to assume their correct phenotype, functionality, and ability to form cellular connections. Accumulating evidence suggests that the timing of neuron formation, laminar specificity, and phenotypes of cortical neurons are encoded within lineages of individual progenitor cells in the ventricular zone (*18*), making transplantation of stem cells a formidable task. Furthermore, the resistance of mature neurons to multiplication appears to be so powerful that, remarkably, no malignancy of mature neurons has occurred spontaneously or been induced by carcinogens in the adult cortex, although glioma and other types of brain tumors are frequent. Thus, identification of the mechanism that inhibits neuronal proliferation in the adult cortex may provide new insight into how to prevent unwanted cell divisions in various carcinomas.

References and Notes

1. R. D. Bhardwaj *et al.*, *Proc. Natl. Acad. Sci. U.S.A.* **103**, 12564 (2006).
2. J. B. Angevine, R. L. Sidman, *Nature,* **192**, 766 (1961).
3. M. B. Luskin, C. J. Shatz, *J. Comp. Neurol.* **242**, 611 (1985).
4. P. Rakic, *Science* **183**, 425 (1974).
5. E. Gould *et al.*, *Science* **286**, 548 (1999).
6. R. D. Kornack, P. Rakic, *Science*, **294**, 2127 (2001).
7. D. Koketsu *et al.*, *J Neurosci.* **23**, 937 (2003).
8. S. S. Magavi, B.R. Leavitt, J. D. Macklis, *Nature* **405**, 951 (2000).
9. R. S. Nowakowski, N. L. Hayes, *Science* **288**, 771a (2000).
10. P. Rakic, *Nat. Rev. Neurosci.* **3**, 65 (2002).
11. K. Spalding *et al.*, *Cell* **122**, 133 (2005).
12. P. S. Eriksson *et al.*, *Nat. Med.* **4**, 1313 (1998).
13. G. Kempermann, *Adult Neurogenesis* (Oxford University Press, Oxford, 2006).
14. R. D. Kornack, P. Rakic, *Proc. Natl. Acad. Sci. U.S.A.* **96**, 5768 (1999).
15. R. D. Kornack, P. Rakic, *Proc. Natl. Acad. Sci. U.S.A.* **98**, 4752 (2001).
16. N. Sanai, *Nature* **427**, 740 (2004).
17. P. Rakic, *Science* **227**, 1054 (1985).
18. Q. Shen *et al.*, *Nat. Neurosci.* **9**, 743 (2006).

10.1126/science.1131713

CHEMISTRY

Dendrimers at Work

Brett Helms and E. W. Meijer

Highly branched dendrimer molecules are being used increasingly for such biomedical applications as molecular imaging and drug delivery.

Dendrimers are synthetic polymers with a highly branched architecture and nearly perfect molecular structure (see the figure). They are identical, monodisperse macromolecules that expose many end groups at their globular periphery. In academic laboratories, dendrimers have been used as light- and energy-harvesting materials, for drug delivery, as catalysts, and in optoelectronic applications. Yet they have not been widely introduced commercially. This situation is about to change, with several dendrimers now entering the market.

Paul Flory first envisaged dendrimers in 1941 (*1*), but four decades passed before chemists could produce these materials with high precision (*2*–*4*). These early dendrimers were prepared in an iterative sequence of steps to achieve growth and branching, starting from a central core unit; this approach would later be termed "divergent." A paradigm shift occurred in the early 1990s, when Hawker *et al.* constructed dendritic materials from the periphery inward (*5*). This "convergent" approach provided access to dendrimers of unprecedented purity and offered greater control over the placement of functional groups in the macromolecule than could be achieved with divergent methods.

Since then, many new dendrimers have been reported, using both divergent and convergent synthesis methods (*6*), but commercialization has been slow to follow. It was not until 1993 that de Brabander-van den Berg *et al.* described a divergent industrial-scale synthesis that allowed the preparation of kilogram quantities of the poly(propylene imine) dendrimer (*7*).

Today, a wide range of dendrimers are commercially available and tuned for specific applications. However, for large-scale applications, the focus has switched to hyperbranched polymers, which are easy to manufacture. They share some of the key properties of dendrimers, including a large number of end

The authors are in the Laboratory of Macromolecular and Organic Chemistry and Department of Biomedical Engineering, Eindhoven University of Technology, 5600 MB Eindhoven, Netherlands. E-mail: e.w.meijer@tue.nl

groups and a globular conformation, but have an ill-defined microstructure with irregular branches. They are increasingly used in coatings, as viscosity mediators, and to prevent gas hydrate–ice crystal formation in oil pipelines (*8*). For such bulk applications, hyperbranched polymers are more cost-effective than dendrimers and have become the industry standard.

For smaller scale applications, especially in the biomedical sector, many companies have continued to develop products based on dendrimers. With their unique and perfect molecular composition, dendrimers are more likely than other polymers to meet the strict regulatory requirements for polymer-based materials intended for use in humans. Moreover, the biocompatibility and toxicity of dendrimers can be regulated by synthesis, especially through the judicious choice of functional groups at the periphery (*9*).

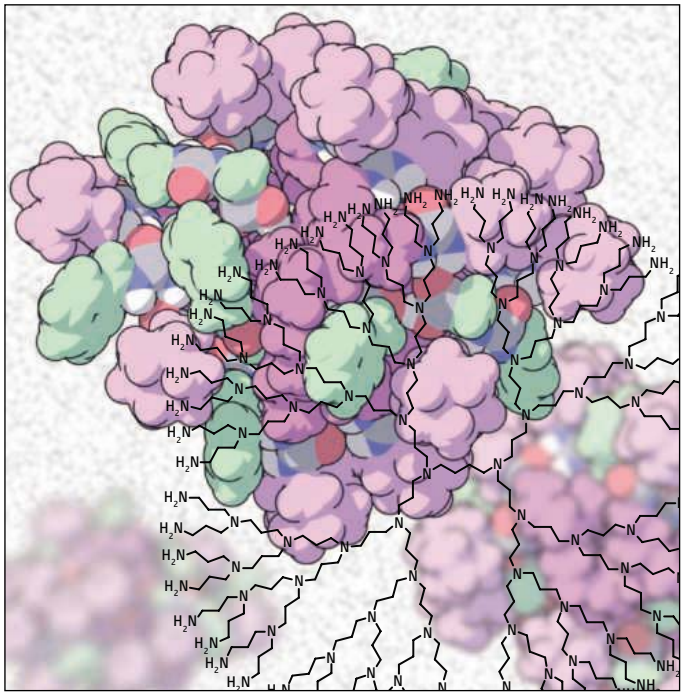

Dendrimer structure. The molecular structure of a dendrimer resembles a tree. The globular molecules expose many end groups at their periphery.

For example, Starpharma (Australia) has used a dendrimer as the active pharmaceutical ingredient in VivaGel, a topical vaginal microbicide for HIV prevention (*10*). Their polylysine dendrimer displays 32 naphthalene disulfonate units at its periphery. The dendrimers prevent infection by binding to receptors on the viral coat of HIV-1, which in turn prevents the virus from entering target cells. VivaGel has entered phase II clinical trials in humans. The company expects to introduce the product to the market by 2008.

Dendrimers have also been used to improve existing molecular imaging technologies. Schering AG (Germany) introduced Gadomer-17 as a magnetic resonance imaging (MRI) probe. The polylysine dendrimer is functionalized at its periphery with gadolinium chelates, which act as intravascular contrast agents. Gadomer-17 has been particularly effective in magnetic resonance angiography and tumor differentiation, because its moderate size limits the material to the vascular space and slows renal clearance.

Building on the success in MRI contrast agents, self-assembly may play an increasingly important role in emerging technologies for molecular imaging. Encapsulation of guest molecules in dendrimers via self-assembly was first demonstrated more than 10 years ago (*11*). Since then, researchers in biomedical imaging have used the void spaces within dendrimers to localize contrast agents for MRI. Guest molecules have included paramagnetic gadolinium chelates, such as Magnevist (*12*), and molecular cages for localizing polarized xenon, a relatively new contrast agent (*13*). In these applications, the contrast agent is bound to a generic, nontoxic dendrimer through relatively weak noncovalent interactions. The assembly must be stable only for the duration of the MRI experiment, after which the assembly falls apart into nontoxic species that can be easily filtered through the kidneys.

Encapsulation of guest molecules in dendrimers can also be used to deliver therapeutic agents throughout the body. The dendrimer can improve the solubility, efficacy, toxicity, and targeting ability of many drugs. For example, Dendritic Nanotechnologies uses the voids in a polyamidoamine dendrimer to host cisplatin or carboplatin anticancer drugs (*14*). The dendrimer-drug conjugates are active against aggressive tumor models that are resistant to cisplatin at its maximum tolerated dose via intravenous administration. They are less toxic than the unbound drug, water soluble, and stable on storage.

In 1993, Szoka and co-workers showed that dendrimers can be used as vehicles to introduce a gene into a cell (*15*). In this case, positively charged dendrimers cause negatively charged DNA to condense into highly compact structures, resulting in supramolecular assemblies that can be delivered to cells (*16*). Commercial kits using similar cationic dendrimer-based materials are available from Qiagen (Germany). Their SuperFect reagent should provide the means for various high-throughput transfection schemes that use recombinant DNA technology for drug discovery and development (*17*–*19*).

Dendrimer formulations used in humans must conform to current Good Manufacturing Practice (cGMP) to ensure the correct identity, strength, quality, and purity. These regulatory hurdles are often difficult to overcome. In contrast, some ex vivo applications can enter the market quite rapidly. For example, Dade Behring has used dendrimer technology in a biosensor for cardiac markers. Their Stratus CS provides quantitative determination of chemical indicators of impending heart damage from whole blood or plasma within 15 min with excellent sensitivity and reproducibility (*20*). The U.S. Army Research Labs are exploring similar techniques for anthrax detection (*21*). Dendrimer technology has also moved beyond the life sciences. Cambridge Display Technology has developed an energy-efficient dendrimer-based diode that emits red light (*22*).

As specialty polymers, dendrimers can be prepared with the precision of small organic molecules, yet they behave like macromolecules. Early successes in dendrimer technology have relied on covalent modification of dendrimers to generate active pharmaceutical ingredients. In the future, more products may use the encapsulation of biologically active agents in dendrimers. Formulations based on simple universal dendrimers may conform more easily with regulations and may be the key to the further success of these materials.

References

1. P. J. Flory, *J. Am. Chem. Soc.* **63**, 3083 (1941).
2. R. G. Denkewalter *et al.*, U.S. patent 4,289,872 (1981).
3. D. A. Tomalia *et al.*, *Polym. J.* **17**, 117 (1985).
4. G. R. Newkome *et al.*, *J. Org. Chem.* **50**, 2003 (1985).
5. C. J. Hawker *et al.*, *J. Am. Chem. Soc*. **112**, 7638 (1990).
6. D. K. Smith, *Chem. Commun.* **2006**, 34 (2006).
7. E. M. M. de Brabander-van den Berg *et al.*, *Angew. Chem.* **105**, 1370 (1993).
8. P. Froehling, *J. Polym. Sci. A* **42**, 3110 (2004).
9. N. Malik *et al.*, *J. Control. Release* **65**, 133 (2000).
10. Y.-H Jiang *et al.*, *AIDS Res. Hum. Retroviruses* **21**, 207 (2005).
11. J. F. G. A. Jansen *et al.*, *Science* **266**, 1226 (1994).
12. H. Gries *et al.*, U.S. patent 4,957,939 (1990).
13. J. L. Mynar *et al.*, *J. Am. Chem. Soc.* **128**, 6334 (2006).
14. N. Malik *et al.*, U.S. patent 7,005,124 (2006).
15. J. Haensler *et al.*, *Bioconjugate Chem.* **4**, 372 (1993).
16. M. Tang *et al.*, *Bioconjugate Chem.* **7**, 703 (1996).
17. T. Hudde *et al.*, *Gene Ther.* **6**, 939 (1999).
18. J. Zhou *et al.*, *Chem. Commun.* **2006**, 2362 (2006).
19. F. Tack *et al.*, *J. Drug Target.* **14**, 69 (2006).
20. S. Altinier *et al.*, *Clin. Chem.* **46**, 991 (2000).
21. R. Yin *et al.*, *Polym. Mater. Sci. Eng.* **84**, 856 (2001).
22. D. Ma *et al.*, *Appl. Phys. Lett.* **81**, 2285 (2002).

10.1126/science.1130639

CREDIT: KOEN PIETERSE

The First Stars in the Universe and Cosmic Reionization

Rennan Barkana

The earliest generation of stars, far from being a mere novelty, transformed the universe from darkness to light. The first atoms to form after the Big Bang filled the universe with atomic hydrogen and a few light elements. As gravity pulled gas clouds together, the first stars ignited and their radiation turned the surrounding atoms into ions. By looking at gas between us and distant galaxies, we know that this ionization eventually pervaded all space, so that few hydrogen atoms remain today between galaxies. Knowing exactly when and how it did so is a primary goal of cosmologists, because this would tell us when the early stars formed and in what kinds of galaxies. Although this ionization is beginning to be understood by using theoretical models and computer simulations, a new generation of telescopes is being built that will map atomic hydrogen throughout the universe.

Astronomers engage in cosmic archaeology. The farther away they look in distance, the further back in time they see, because of the time it takes light to travel from distant stars and galaxies to Earth today. In principle, this allows the entire 13.7-billion-year cosmic history of the universe to be reconstructed by surveying the galaxies and other sources of light to large distances (Fig. 1). To measure distance, astronomers use the characteristic emission patterns of hydrogen and other chemical elements in the spectrum of each galaxy to measure its cosmological redshift z. As the universe expands, light wavelengths get stretched as well, so that the spectrum we observe today is shifted from the emitted one by a factor of $1 + z$ in wavelength. This then implies that the universe has expanded by a factor of $1 + z$ in linear dimension since that time, and cosmologists can calculate the corresponding distance and cosmic age. Large telescopes have allowed astronomers to observe faint galaxies that are so far away that we see them more than ten billion years in the past, so we know that galaxies were in existence as early as 850 million years after the Big Bang, at a redshift of $z \sim 6.5$ (*1*, *2*).

In addition to galaxies, the other major probe of observational cosmology is the cosmic microwave background (CMB), a radiation relic from the fiery beginning of the universe. The universe cools as it expands, so it was initially far denser and hotter than it is today. For hundreds of thousands of years, the cosmic gas consisted of a plasma of protons, electrons, and light nuclei, sustained by the intense thermal motion of these particles. Just like the plasma in our own Sun, the ancient cosmic plasma emitted and scattered a strong field of visible and ultraviolet photons. About 400,000 years after the Big Bang, however, the temperature of the universe dipped for the first time below a few thousand degrees Kelvin. The protons and electrons were now moving slowly enough that they could attract each other and form hydrogen atoms, in a process known as cosmic recombination. With the scattering of the energetic photons now much reduced, the photons continued traveling in straight lines, mostly undisturbed except that cosmic expansion has redshifted them into the microwave regime. The emission temperature of the observed spectrum of these CMB photons is the same in all directions to one part in 100,000, which reveals that conditions were extremely uniform in the early universe.

It was at the moment of cosmic recombination that gravity entered the scene. Since that time, gravity has amplified the tiny fluctuations in temperature and density observed in the CMB data (*3*). Regions that started out slightly denser than average began to contract because the gravitational forces were also slightly stronger than average in these regions. Eventually, after millions of years of contraction, galaxies and the stars within them were able to form. This process, however, would have taken too long to explain the abundance of galaxies today, if it involved only the observed cosmic gas. Instead, gravity is strongly enhanced by the presence of dark matter—an unknown substance that makes up the vast majority (85%) of the cosmic density of matter. The motion of stars and gas around the centers of nearby galaxies indicates that each is surrounded by an extended mass of dark matter, so dark matter concentrations are generally referred to as halos.

Gravity explains how some gas is pulled into the deep potential wells within dark-matter halos and forms the galaxies. On the other hand, cosmologists at first expected the gas outside halos to remain mostly undisturbed. However, observations show that it has not remained neutral (i.e., in atomic form) until the present. To learn about diffuse gas pervading the space outside and between galaxies (referred to as

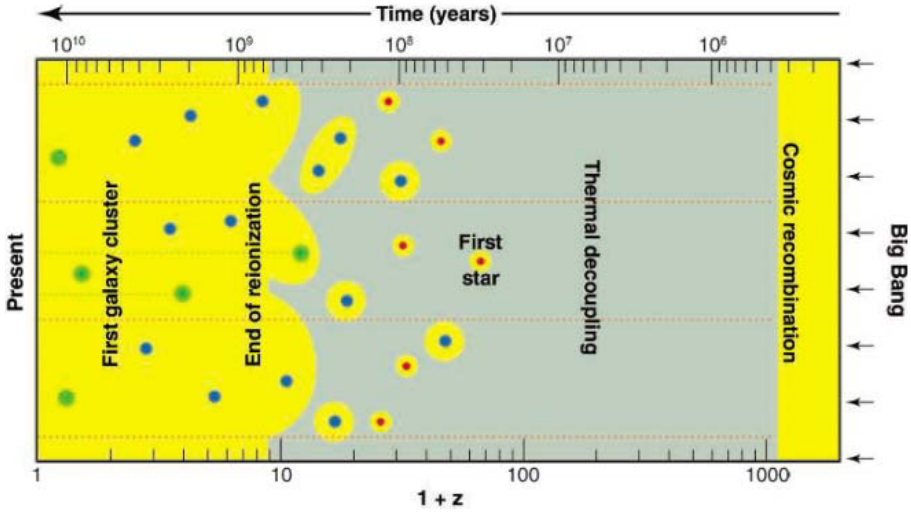

Fig. 1. Overview of cosmic history, with the age of the universe shown on the top axis and the corresponding redshift on the bottom axis. Yellow represents regions where the hydrogen is ionized; gray represents neutral regions. Stars form in galaxies located within dark matter concentrations whose typical size grows with time, starting with 300 light years (red circles) for the host of the first star, rising to 3000 light years (blue circles) for the sources of reionization, and reaching 600,000 light years (green circles) for present-day galaxies like our own Milky Way. Astronomers probe the evolution of the cosmic gas using the absorption of background light (dotted lines) by atomic hydrogen along the line of sight. The classical technique uses absorption by the Lyα resonance of hydrogen of the light from bright quasars located within massive galaxies, whereas a new type of astronomical observation will use the 21-cm line of hydrogen with the CMB as the background source.

School of Physics and Astronomy, Raymond and Beverly Sackler Faculty of Exact Sciences, Tel Aviv University, Tel Aviv 69978, Israel. E-mail: barkana@wise.tau.ac.il

the intergalactic medium, or IGM), astronomers study its absorption against distant quasars, the brightest known astronomical objects. Quasars' great luminosities are believed to be powered by black holes weighing a billion times the mass of the Sun that are situated in the dense centers of massive galaxies. As the surrounding gas falls in toward the black hole, violent collisions within the gas blast radiation into space, creating a beacon visible from afar.

The Lyman-alpha (Lyα) resonance line of hydrogen at a wavelength of 1216 Å has been widely used to trace hydrogen gas through its absorption of quasar light (*4*). The expansion of the universe gives this tool an important advantage common to all spectral absorption probes. Because the wavelength of every photon grows as the universe expands, the rest-frame absorption at 1216 Å by a gas element at redshift z is observed today at a wavelength of 1216 $(1 + z)$ Å. The absorptions of the different gas elements along the line of sight are therefore distributed over a broad range of wavelengths, making it possible to measure the distribution of intergalactic hydrogen.

Lyα absorption shows that the IGM has been a hot plasma at least from a cosmic age of 850 million years ($z \sim 6.5$) until today (*2*). Thus, the hydrogen must have been ionized for a second time after it became neutral at cosmic recombination. Radiation from the first generations of stars is a plausible source for the ionizing photons that transformed the IGM by reionizing the hydrogen throughout the universe.

Absorption at Lyα is so efficient that it becomes difficult to use as observations approach the reionization epoch where the density of neutral hydrogen is higher than at more recent times (*2*). As described below, cosmologists believe that the new technique of "21-cm cosmology" will allow them to measure how the reionization process developed over time and to test theoretical predictions of the properties of the first stars (*5*).

The First Stars

The most distant galaxies that we can see today were already shining brightly when the universe was just a billion years old. In the "hierarchical model" of galaxy formation—in which small galaxies form first and then merge or accrete gas to form larger galaxies—smaller objects should have formed even earlier. So, what were the smallest units within which the first stars formed?

Stars form when huge amounts of matter collapse to enormous densities. However, the process can be stopped if the pressure exerted by the hot intergalactic gas prevents outlying gas from falling into dark-matter concentrations. As the gas falls into a dark-matter halo, it forms shocks due to unstable supersonic flow and in the process heats up and can only collapse further by first radiating its energy away. This restricts the process of collapse to very large clumps of dark matter that are ~100,000 times the mass of the Sun. Inside these clumps, the shocked gas loses energy by emitting radiation from excited molecular hydrogen that formed naturally within the primordial gas mixture of hydrogen and helium (*6*, *7*).

Advances in computing power have made possible detailed numerical simulations of how the first stars formed (*8*, *9*). These simulations begin in the early universe, in which dark matter and gas are distributed uniformly, apart from tiny variations in density and temperature that are statistically distributed according to the patterns observed in the CMB. To span the vast range of scales needed to simulate an individual star within a cosmological context, the newest code follows a box a million light years in length and zooms in repeatedly on the densest part of the first collapsing cloud that is found within the simulated volume. The simulation follows gravity, hydrodynamics, and chemical processes in the primordial gas and resolves a scale 10 orders of magnitude smaller than that of the simulated box. Although the resolved scale is still three orders of magnitudes larger than the size of the Sun, the simulations indicate that the first stars most likely weighed ~100 $M_\odot$ each.

To estimate when the first stars formed, we must remember that the first 100,000 solar mass halos collapsed in regions that happened to have a particularly high density enhancement very early on. There were initially only a few such regions in the entire universe, so a simulation that is limited to a small volume is unlikely to find such halos until much later. Simulating the entire universe is well beyond the capabilities of current simulations, but analytical models predict that the first observable star in the universe probably formed 30 million years after the Big Bang (*10*), less than a quarter of 1% of the universe's total age of 13.7 billion years.

Although stars were extremely rare at first, gravitational collapse increased the abundance of galactic halos and star formation sites with time (Fig. 1). The sources of reionization were most likely a second generation of larger galaxies that formed in halos of mass above ~ 10^7 $M_\odot$ (*11*). The first Milky-Way–sized halo $\boldsymbol{M} = 10^{12}$ $M_\odot$ is predicted to have formed 400 million years after the Big Bang (*10*), but such halos have become typical galactic hosts only in the past 5 billion years.

Cosmic Reionization

Given the understanding described above of how many galaxies formed at various times, the course of reionization can be determined universe-wide by counting photons from all sources of light (*12*–*17*). Both stars and black holes contribute ionizing photons, but the early universe is dominated by small galaxies that, in the local universe, have central black holes that are disproportionately small. Thus, stars most likely dominated the production of ionizing photons during the reionization epoch. If the stars within the early galaxies were similar to those observed today, then each star produced ~4000 ionizing photons per baryon, which means that it was sufficient to accumulate a small fraction (on the order of 0.1%) of the total gas mass in the universe into galaxies in order to ionize the entire IGM. Because most stellar ionizing photons are only slightly more energetic than the 13.6-eV ionization threshold of hydrogen, they are absorbed very quickly once they reach a region with substantial neutral hydrogen. This makes the IGM during reionization a two-

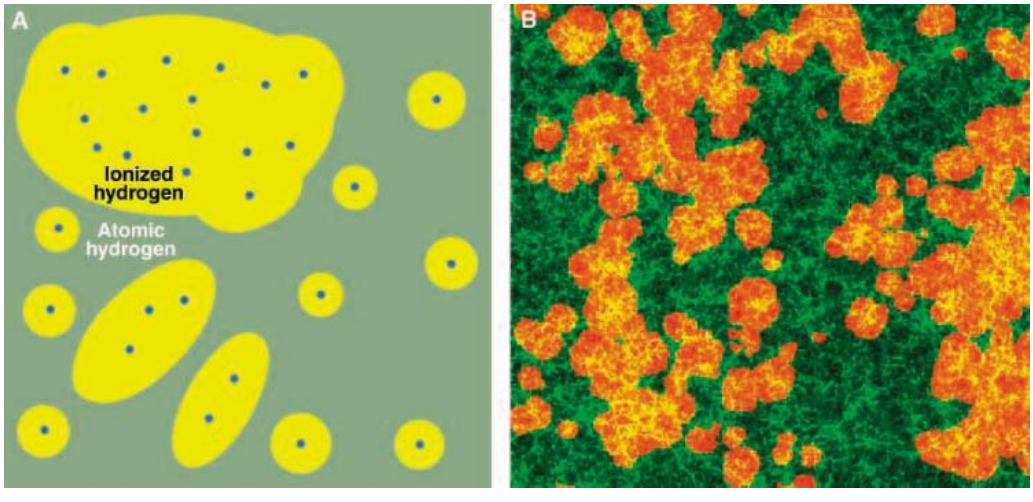

Fig. 2. The spatial structure of cosmic reionization. (**A**) The illustration shows how regions with large-scale overdensities form large concentrations of galaxies (dots) whose ionizing photons produce enormous joint ionized bubbles (upper left). At the same time, galaxies are rare within large-scale voids, in which the IGM is still mostly neutral (lower right). (**B**) A numerical simulation of reionization [from (*24*)] displays a similar variation in the sizes of ionized bubbles (orange), shown overlayed on the density distribution (green).

phase medium characterized by highly ionized regions separated from neutral regions by sharp ionization fronts (see Fig. 2).

From absorption line work, we see that the IGM is completely ionized toward even the most distant objects known (quasars). There are hints, however, that some large neutral H regions persist at these times (*18*, *19*), which suggests that we may not need to go to much higher redshifts to begin to see the last stages of reionization. We know that the universe could not have fully reionized earlier than an age of 300 million years, because the freshly created plasma at reionization rescattered some of the CMB photons and created a clearly detected polarization signature (*3*) that constrains the reionization redshift; an earlier reionization, when the universe was still relatively dense, would have created stronger scattering than observed.

A detailed picture of reionization as it happens will teach us a great deal, because the spatial distribution of ionized bubbles is determined by clustered groups of galaxies rather than by individual galaxies. At such early times, galaxies were strongly clustered even on very large scales (10 to 100 million light years), and these scales therefore dominate the structure of reionization (*20*). The basic idea is simple (*21*). At high redshift, galactic halos are rare and correspond to rare high-density peaks. As an analogy, imagine searching on Earth for mountain peaks above 5000 m. The 200 such peaks are not at all distributed uniformly but instead are found in a few distinct clusters on top of large mountain ranges. Similarly, to find the early galaxies, one must first locate a region with a large-scale density enhancement, and then galaxies will be found there in abundance.

The ionizing radiation emitted from the stars in each galaxy initially produces an isolated ionized bubble. However, in a region dense with galaxies, the bubbles quickly overlap into one large bubble, completing reionization in this region while the rest of the universe is still mostly neutral (Fig. 2). Most important, because the abundance of rare density peaks is very sensitive to small changes in the density threshold, even a large-scale region with a small enhanced density (say, 10% above the mean density of the universe) can have a much larger concentration of galaxies than in other regions (e.g., a 50% enhancement). On the other hand, reionization is harder to achieve in dense regions, because the protons and electrons collide and reform hydrogen atoms more often in such regions, and newly formed atoms need to be reionized again by additional ionizing photons. However, the overdense regions end up reionizing first because the number of ionizing sources in these regions is increased so strongly (*20*). This is a key prediction awaiting observational testing.

Detailed analytical models that account for large-scale variations in the abundance of galaxies (*22*) confirm that the typical bubble size starts below a million light years early in reionization, as expected for an individual galaxy, rises to 20 to 30 million light years during the central phase (i.e., when the universe is half ionized), and then rises by another factor of ~5 toward the end of reionization. These scales are given in "comoving" units that scale with the expansion of the universe, so that the actual sizes at a redshift z were smaller than these numbers by a factor of $1 + z$. Numerical simulations have only recently begun to reach the enormous scales needed to capture this evolution (*23*–*25*). Accounting precisely for gravitational evolution on a wide range of scales, but still crudely for gas dynamics, star formation, and the radiative transfer of ionizing photons, the simulations confirm that the large-scale topology of reionization can be used to study the abundance and clustering of the ionizing sources (Figs. 2 and 3).

21-cm Cosmology

The prospect of studying reionization by mapping the distribution of atomic hydrogen across the universe using its prominent 21-cm spectral line (*26*) has motivated several teams to design and construct arrays of low-frequency radio telescopes; the Primeval Structure Telescope, the Mileura Widefield Array, and the Low Frequency Array will search over the next few years for 21-cm emission or absorption from $z \sim 6.5$ and above, redshifted and observed today at relatively low frequencies that correspond to wavelengths of 1.5 to 4 m.

The idea is to use the resonance associated with the hyperfine splitting in the ground state of hydrogen. The state with parallel spins of the proton and electron has a slightly higher energy than the state with antiparallel spins, yielding a spin-flip transition that corresponds to 21-cm wavelength radiation. Although the CMB spectrum peaks at a wavelength of 2 mm, it provides a still-measurable intensity at meter wavelengths that can be used as the bright background source against which we can see the expected 1% absorption by neutral hydrogen along the line of sight (*27*, *28*). Because the CMB covers the entire sky, a complete three-dimensional map of neutral hydrogen can in principle be made from the sky position of each absorbing gas cloud together with its redshift z.

Because the smallest angular size resolvable by a telescope is proportional to the observed wavelength, radio astronomy at wavelengths as large as a meter has remained relatively undeveloped. Producing resolved images even of large sources such as cosmological ionized bubbles requires telescopes kilometers in diameter. It is much more cost-effective to use a large array of thousands of simple antennas distributed over several kilometers. The new experiments are being placed mostly in remote sites, because the cosmic wavelength region overlaps with more mundane terrestrial telecommunications.

Because the 21-cm line intensity is observed with the CMB as the bright source, the hydrogen gas produces absorption if it is colder than the CMB and excess emission if it is hotter. The observed intensity I_ν relative to the CMB at a frequency ν is measured by radio astronomers as an effective "brightness temperature" T_b of blackbody emission at this frequency, defined using the Rayleigh-Jeans limit of the Planck radiation formula: $\boldsymbol{I_\nu \equiv 2k_B T_b \nu^2/c^2}$.

In approaching redshifted 21-cm observations, although the first inkling might be to consider the mean emission signal, the signal is weaker by a factor of 100,000 than foreground emission from magnetized plasma in our own Milky Way and other nearby galaxies. Thus, cosmologists have focused on the expected characteristic variations in T_b, both with position on the sky and especially with frequency, which signifies redshift for the cosmic signal but signifies frequency for the foreground, which is expected to have the known smooth spectrum of emission from energetic particles in plasmas (*29*). The 21-cm brightness temperature depends on the density of neutral hydrogen. As explained before, large-scale patterns in the reionization are driven by spatial variations in the abundance of galaxies; the 21-cm fluctuations reach ~5 mK (root mean square) in

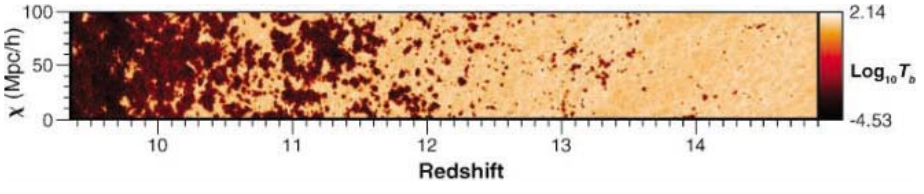

Fig. 3. Close-up of cosmic evolution during the epoch of reionization, as revealed in a predicted 21-cm map of the IGM based on a numerical simulation, from (*24*). This map is constructed from slices of the simulated cubic box of size 450 million light years (in comoving units), taken at various times during reionization, which for the parameters of this particular simulation spans a period of 250 million years from redshift 15 down to 9.3. The vertical axis shows position χ in units of Mpc/h, which equals ~4.5 million light years. This two-dimensional slice of the sky (one linear direction on the sky versus the line-of-sight or redshift direction) shows $\log_{10} T_b$, where T_b (in mK) is the 21-cm brightness temperature relative to the CMB. Because neutral regions correspond to strong emission (i.e., a high T_b), this slice illustrates the global progress of reionization and the substantial large-scale spatial fluctuations in reionization history. Observationally it corresponds to a narrow strip half a degree in length on the sky, observed with radio telescopes over a wavelength range of 2.2 to 3.4 m (with each wavelength corresponding to 21-cm emission at a specific line-of-sight distance and redshift).

brightness temperature (Fig. 3) on a scale of 30 million light years (comoving). Although detailed maps will be difficult to extract due to the foreground emission, a statistical detection of these fluctuations (through the power spectrum) is expected to be well within the capabilities of the first-generation experiments now being built (*30*, *31*). The key information on the topology and timing of reionization can be extracted statistically, with an important check made possible by measuring the particular form of anisotropy, expected in the 21-cm fluctuations, that is caused by gas motions along the line of sight (*32*–*34*).

The theoretical expectations presented here for reionization and for the 21-cm signal are based on rather large extrapolations from observed galaxies to deduce the properties of much smaller galaxies that formed at an earlier cosmic epoch. Considerable surprises are thus possible, such as an early population of quasars or even exotic particles that emitted ionizing radiation when they radioactively decayed. In any case, a detection of the cosmological 21-cm signal will open a new window on the universe and likely motivate a second generation of more powerful telescopes. These will be used to obtain three-dimensional maps of atomic hydrogen during reionization as well as statistical power-spectrum measurements at even higher redshifts (using wavelengths at which the foregrounds are brighter and thus more difficult to remove). Because the 21-cm measurements are sensitive to any difference between the hydrogen temperature and the CMB temperature, the potential reach of 21-cm cosmology extends down to a cosmic age of ~ 6 million years, when the IGM first cooled below the CMB temperature (an event referred to as "thermal decoupling") as a result of the cosmic expansion. The 21-cm technique may open up entirely new cosmological areas, such as investigations of the primordial origin of spatial density variations by measuring them on very small scales that are washed out in the CMB (*35*), and the detection and study of the galaxies from early times (200 million years) through the effect of their stellar radiation on the intergalactic hydrogen (*36*). Understandably, astronomers are eager to start tuning into the cosmic radio channels of 21-cm cosmology.

References and Notes

1. E. M. Hu *et al.*, *Astrophys. J.* **568**, L75 (2002).
2. R. L. White, R. H. Becker, X. Fan, M. A. Strauss, *Astron. J.* **126**, 1 (2003).
3. D. N. Spergel *et al.*, *Astrophys. J.,* in press; available at www.arxiv.org/abs/astro-ph/0603449.
4. J. E. Gunn, B. A. Peterson, *Astrophys. J.* **142**, 1633 (1965).
5. R. Barkana, A. Loeb, *Phys. Rep.* **349**, 125 (2001).
6. P. J. E. Peebles, *Astrophys. J.* **277**, 470 (1984).
7. M. Tegmark *et al.*, *Astrophys. J.* **474**, 1 (1997).
8. V. Bromm, P. S. Coppie, R. B. Larson, *Astrophys. J.* **527**, 5 (1999).
9. N. Yoshida, K. Omukai, L. Hernquist, T. Abel, *Astrophys. J.,* in press; available at www.arxiv.org/abs/astro-ph/0606106.
10. S. Naoz, S. Noter, R. Barkana, *Mon. Not. R. Astr. Soc. Lett.,* in press; available at www.arxiv.org/abs/astro-ph/0604050.
11. Z. Haiman, M. J. Rees, A. Loeb, *Astrophys. J.* **476**, 458 (1997).
12. J. Arons, D. W. Wingert, *Astrophys. J.* **177**, 1 (1972).
13. P. R. Shapiro, M. L. Giroux, *Astrophys. J.* **321**, L107 (1987).
14. M. Tegmark, J. Silk, A. Blanchard, *Astrophys. J.* **420**, 484 (1994).
15. M. Kamionkowski, D. N. Spergel, N. Sugiyama, *Astrophys. J.* **426**, L57 (1994).
16. M. Fukugita, M. Kawasaki, *Mon. Not. R. Astr. Soc.* **269**, 563 (1994).
17. Z. Haiman, A. Loeb, *Astrophys. J.* **483**, 21 (1997).
18. J. S. B. Wyithe, A. Loeb, *Nature* **427**, 815 (2004).
19. A. Lidz, S. P. Oh, S. R. Furlanetto, *Astrophys. J.* **639**, L47 (2006).
20. R. Barkana, A. Loeb, *Astrophys. J.* **609**, 474 (2004).
21. N. Kaiser, *Astrophys. J.* **284**, L9 (1984).
22. S. R. Furlanetto, M. Zaldarriaga, L. Hernquist, *Astrophys. J.* **613**, 1 (2004).
23. B. Ciardi, A. Ferrara, S. D. M. White, *Mon. Not. R. Astr. Soc.* **344**, L7 (2003).
24. G. Mellema, I. T. Iliev, U.-L. Pen, P. R. Shapiro, *Mon. Not. R. Astr. Soc.,* in press; available at www.arxiv.org/abs/astro-ph/0603518.
25. O. Zahn *et al.*, *Astrophys. J.,* in press; available at www.arxiv.org/abs/astro-ph/0604177.
26. P. Madau, A. Meiksin, M. J. Rees, *Astrophys. J.* **475**, 429 (1997).
27. C. J. Hogan, M. J. Rees, *Mon. Not. R. Astr. Soc.* **188**, 791 (1979).
28. D. Scott, M. J. Rees, *Mon. Not. R. Astr. Soc.* **247**, 510 (1990).
29. T. Di Matteo, R. Perna, T. Abel, M. J. Rees, *Astrophys. J.* **564**, 576 (2002).
30. J. D. Bowman, M. F. Morales, J. N. Hewitt, *Astrophys. J.* **638**, 20 (2006).
31. M. McQuinn, O. Zahn, M. Zaldarriaga, L. Hernquist, S. R. Furlanetto, *Astrophys. J.,* in press; available at www.arxiv.org/abs/astro-ph/0512263.
32. N. Kaiser, *Mon. Not. R. Astr. Soc.* **227**, 1 (1987).
33. S. Bharadwaj, S. S. Ali, *Mon. Not. R. Astr. Soc.* **352**, 142 (2004).
34. R. Barkana, A. Loeb, *Astrophys. J.* **624**, L65 (2005).
35. A. Loeb, M. Zaldarriaga, *Phys. Rev. Lett.* **92**, 211301 (2004).
36. R. Barkana, A. Loeb, *Astrophys. J.* **626**, 1 (2005).

37. The author acknowledges Israel Science Foundation grant 629/05 and Israel–U.S. Binational Science Foundation grant 2004386.

10.1126/science.1125644

Pinwheels in the Quintuplet Cluster

Peter Tuthill,[1]* John Monnier,[2] Angelle Tanner,[3] Donald Figer,[4] Andrea Ghez,[5] William Danchi[6]

The five enigmatic cocoon stars after which the Quintuplet cluster was christened have puzzled astronomers since their discovery (*1*). Hundreds of stars have now been identified within the cluster (*2*, *3*), placing it among the most massive in our Galaxy, yet the nature of the five extremely red stars at the heart of the Quintuplet has remained elusive. Their extraordinary cool, featureless thermal spectra [~780 to 1315 K (*3*)] have been attributed to various stellar types from young to highly evolved, whereas their absolute luminosities place them among the supergiants (10^4 to 10^5 times the luminosity of the Sun). We present diffraction-limited images from the Keck 1 telescope, which resolves this debate with the identification of rotating spiral plumes characteristic of colliding-wind binary "pinwheel" nebulae. These have previously been reported in dust shells around luminous hot Wolf-Rayet stars (*4*, *5*).

By using high-resolution speckle techniques in the near-infrared (*6*), we (at least partially) resolved all five cocoon stars and recovered images of the two presenting the largest apparent size, Q 2 and Q 3 (Fig. 1). Outflow plumes depicted follow the form of an archimedean spiral, thereby establishing the presence of circumstellar dust formed in a colliding-wind binary system. These rare pinwheel nebulae result when dust condensation in the stellar wind is mediated by the presence of a companion star, as established in the prototype systems WR 104 (*4*) and WR 98a (*5*). Dust nucleation is enabled by the wind compression associated with the bowshock between the stellar winds. Newly formed hot dust streaming into the wake behind the companion is wrapped into a spiral by the orbital motion as it is embedded within the expanding Wolf-Rayet wind.

With high-resolution images available from two epochs separated by 357 days, we fitted the dust plume of star Q 3 to an archimedean spiral model with winding angle 110 ± 10 milliarc sec per turn and with an inclination of the rotation axis to the line of sight of 26° (not well constrained; adequate fits are possible in the range 0° to 36°). The proper motion of structures between the two epochs indicates a rotation period of the spiral, and hence the colliding-wind binary, of 850 ± 100 days. Assuming an 8000-pc distance to the Quintuplet (*7*), these measurements constrain the Wolf-Rayet wind velocity to be v_∞ = 1800 ± 300 km/s, which is typical for a late-type carbon-rich (WC-spectrum) star (*8*).

Simple models fall short of reproducing all structures (Fig. 1), particularly near the bright core where multiple knots and streams can exist. This problem has also been noted in WR 98a (*5*), where extra complexity was attributed to optical depth and line-of-sight effects from a three-dimensional (3D) structure (*9*). Q 2 appears to have parameters similar to those of Q 3, although a second image epoch is required to measure the rotation rate. Partially resolved objects Q 1, Q 4, and Q 9 (*6*) (table S1) exhibit colors and surface brightness similar to those of Q 2 and Q 3, and we therefore suggest that they are also pinwheels but with tighter winding angles (shorter periods) or less favorable inclinations. Furthermore, the prototype pinwheel WR 104, with a period of 243 days, would give an apparent size in close accord with measured sizes of Q 1, Q 4, and Q 9 if it were removed to the distance of the Quintuplet.

Given the extreme visible extinction [A_v = 29 ± 5 (*2*)], small separation of the central binary stars (likely ~0.6 milliarc sec or 5 astronomical units), and presence of high-luminosity circumstellar dust shells, it would be extremely difficult to detect or study these systems with other techniques. The most luminous stars in our Galaxy are often surrounded by dusty shells, and the implication that most, if not all, of these harbor massive binaries (not single stars) has important implications for the high-mass tail of the stellar initial mass function. Binarity is also a key element to studies of type Ib/c and type IIb supernovae. There are recent indications that explosion light curves can be modified by the imprint of circumstellar matter, carrying an encoding of the mass-loss history of the supernova precursor star system (*10*, *11*).

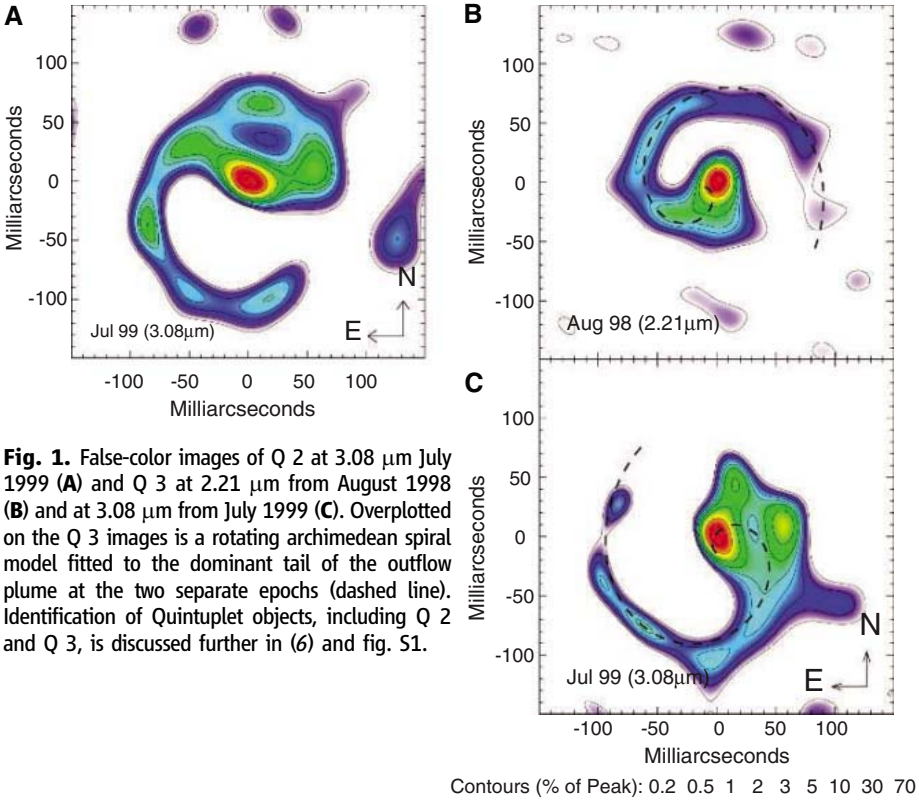

Fig. 1. False-color images of Q 2 at 3.08 μm July 1999 (**A**) and Q 3 at 2.21 μm from August 1998 (**B**) and at 3.08 μm from July 1999 (**C**). Overplotted on the Q 3 images is a rotating archimedean spiral model fitted to the dominant tail of the outflow plume at the two separate epochs (dashed line). Identification of Quintuplet objects, including Q 2 and Q 3, is discussed further in (*6*) and fig. S1.

References and Notes

1. H. Okuda *et al.*, *Astrophys. J.* **351**, 89 (1990).
2. D. F. Figer, I. S. McLean, M. Morris, *Astrophys. J.* **514**, 202 (1999).
3. D. F. Figer *et al.*, *Astrophys. J.* **525**, 750 (1999).
4. P. G. Tuthill, J. D. Monnier, W. C. Danchi, *Nature* **398**, 487 (1999).
5. J. D. Monnier, P. G. Tuthill, W. C. Danchi, *Astrophys. J.* **525**, L97 (1999).
6. Materials and methods are available on *Science* Online.
7. M. J. Reid, *Annu. Rev. Astron. Astrophys.* **31**, 345 (1993).
8. I. D. Howarth, W. Schmutz, *Astron. Astrophys.* **261**, 503 (1992).
9. T. J. Harries, J. D. Monnier, N. H. Symington, R. Kurosawa, *Mon. Not. R. Astron. Soc.* **350**, 565 (2004).
10. J. A. Moran, D. E. Reichart, *Astrophys. J.* **632**, 438 (2005).
11. S. D. Ryder *et al.*, *Mon. Not. R. Astron. Soc.* **349**, 1093 (2004).

12. We thank S. Ryder, C. Townes, E. Becklin, and S. Hornstein for contributions to this paper. This work has been supported by the Australian Research Council and the U.S. NSF. Data presented here were obtained at the W. M. Keck Observatory.

Supporting Online Material

www.sciencemag.org/cgi/content/full/313/5789/935/DC1
Materials and Methods
Fig. S1
Table S1
References

13 April 2006; accepted 12 July 2006
10.1126/science.1128731

[1]Physics Department, University of Sydney, New South Wales 2006, Australia. [2]Astronomy Department, University of Michigan, 500 Church Street, Ann Arbor, MI 48109–1090, USA. [3]Jet Propulsion Laboratory (JPL)–California Institute of Technology (Caltech), Mail Code 100-22, 770 South Wilson Avenue, Pasadena, CA 91125, USA. [4]COS/Center for Imaging Science, 54 Lomb Memorial Drive, Rochester Institute of Technology (RIT), Rochester, NY 14623–5604, USA. [5]Astronomy, University of California Los Angeles, Los Angeles, CA 90095–1547, USA. [6]NASA Goddard, Code 667, Greenbelt, MD 20771, USA.

*To whom correspondence should be addressed. E-mail: p.tuthill@physics.usyd.edu.au

Probing the Faintest Stars in a Globular Star Cluster

Harvey B. Richer,[1]* Jay Anderson,[2] James Brewer,[1] Saul Davis,[1] Gregory G. Fahlman,[3] Brad M. S. Hansen,[4] Jarrod Hurley,[5] Jasonjot S. Kalirai,[6] Ivan R. King,[7] David Reitzel,[4] R. Michael Rich,[4] Michael M. Shara,[8] Peter B. Stetson[3]

NGC 6397 is the second closest globular star cluster to the Sun. Using 5 days of time on the Hubble Space Telescope, we have constructed an ultradeep color-magnitude diagram for this cluster. We see a clear truncation in each of its two major stellar sequences. Faint red main-sequence stars run out well above our observational limit and near to the theoretical prediction for the lowest mass stars capable of stable hydrogen burning in their cores. We also see a truncation in the number counts of faint blue stars, namely white dwarfs. This reflects the limit to which the bulk of the white dwarfs can cool over the lifetime of the cluster. There is also a turn toward bluer colors in the least luminous of these objects. This was predicted for the very coolest white dwarfs with hydrogen-rich atmospheres as the formation of H_2 and the resultant collision-induced absorption cause their atmospheres to become largely opaque to infrared radiation.

When stars are born, they contract under gravity, increasing their central temperatures and densities. If a star is massive enough, at least 0.08 that of the Sun (80 times the mass of Jupiter), the center will eventually get hot enough to allow self-sustaining nuclear energy generation at a level sufficient to halt the contraction. For lower mass objects, the contraction is halted instead by electron degeneracy, the quantum mechanical repulsion between electrons in dense media. For these "brown dwarfs," the rate of energy generation never grows large enough to be self-sustaining, and they fade away within a billion years (*1*). On the other hand, for low-mass stars just above the brown dwarf mass limit, the balance between gravity and thermal equilibrium is long-lived, and these stars are able to shine for much longer than the current age (13.7 billion years) of the universe (*2*). The sharp division between transient and effectively infinite lifetime populations is termed the hydrogen-burning mass limit and is a cornerstone of stellar evolutionary theory. However, because of the faintness of the stars just above the limit, this edge has not previously been solidly identified in any old stellar population such as globular clusters or halo field stars.

At the other end of the stellar mass spectrum, stars with masses ranging from about 1 through 7 solar masses consume their nuclear fuel on a time scale shorter than the age of the universe, burning their original hydrogen to carbon and oxygen, ejecting their outer layers, and becoming white dwarfs. These stellar remnants are also supported by electron degeneracy pressure and slowly cool over time as they radiate their reservoir of thermal energy left over from the previous stages of nuclear burning. The accompanying slow fading, at approximately constant radius, traces out the so-called white dwarf cooling sequence in the color-magnitude diagram (CMD). At faint magnitudes, this sequence is expected to end, with the magnitude of the cutoff indicating the luminosity to which the oldest white dwarfs have faded. With the aid of theoretical models, this luminosity can then be used to derive the age of the cluster (*3*, *4*).

The white dwarf cooling sequence is expected to turn back to the blue at faint magnitudes (*5*–*9*). As white dwarfs with hydrogen-rich atmospheres cool below temperatures of 4000 K, they exhibit the collision-induced absorption (CIA) of molecular hydrogen (*10*). CIA is strongest at near-infrared wavelengths, which suppresses the flux near 1 μm (*11*) and causes the optical colors to become bluer as the star cools, rather than redder, as might be expected from a blackbody. CIA arises because hydrogen molecules can form in these cool atmospheres. Being symmetric, H_2 does not have a dipole moment and will only very weakly absorb radiation via quadrupole transitions (*10*). A dipole moment may be induced, however, during an H_2-H_2, H_2-H, or H_2-He collision (*12*), leading to CIA. The stars continue to get bolometrically fainter and cooler as they evolve on the blueward track in the CMD known as the blue hook. The spectral signature of CIA has been seen in a few individual field white dwarfs (*13*–*15*), but never as a feature in the cooling sequence of a stellar cluster. The expected cluster CIA signature is a blue hook in the cooling sequence. We note that this is a temperature effect, seen at faint magnitudes, and that it is distinct from the feature observed in the open cluster NGC 6791 (*16*). The latter feature occurs in younger populations and is a consequence of the smaller radii and slower cooling of more massive white dwarfs at early times, as shown in figure 17 of (*17*).

Imaging data. In an attempt to locate the limits of both the faint main-sequence star population and the faint white dwarf population, we used the Hubble Space Telescope (HST) to obtain images of the globular star cluster NGC 6397 located in the southern constellation Ara. It is seen projected in the direction of the galactic center, at a distance of about 8500 light-years from Earth (*18*), and its stars have a heavy-element content that is ~1% that of the Sun (*19*). It was discovered by Abbé Nicolas Louis de Lacaille during his sojourn at the Cape of Good Hope in 1751–1752; in his original catalog, it bears the name Lacaille III.11. It was the 12th such cluster discovered. We imaged a single field in NGC 6397 with the Advanced Camera for Surveys (ACS) on the HST for a total of 126 orbits (4.7 days) to characterize the faintest globular cluster stellar populations. Our observations were carried out 5 arc min southeast of the cluster core. They overlap preexisting Wide Field Planetary Camera 2 (WFPC2) images that we used to select, by common proper motion (angular motion in the plane of the sky), a clean sample of cluster stars largely devoid of galactic foreground and background stars. The exposures were taken through two filters, F606W and F814W, where the number indicates the central wavelength of the filter in nanometers.

The data set consists of 252 exposures totaling 179.7 ksec in F814W and 126 exposures totaling 93.4 ksec in F606W. This 2:1 ratio was chosen because the primary science goal of the program was exploration for the coolest white dwarfs. If cool white dwarfs do indeed turn blue at faint magnitudes (*5*–*9*), they will be very faint on the longer wavelength images, thus requiring increased exposure time to detect them. To find the faintest possible sources, we scoured each image for indications of where the faintest stars might be located. The most we could hope for from the very faintest ones is that they would push their central pixels up above the noise in some significant number of images. We studied the noise in the images via artificial star tests, and we concluded that a detection in 90 out of 252 F814W images constituted a 3σ detection above the background.

Figure 1 is an image of part of our field that was constructed by combining the exposures in

[1]Department of Physics and Astronomy, University of British Columbia, Vancouver, British Columbia V6T 1Z1, Canada. [2]Department of Physics and Astronomy, Rice University, Houston, TX 77005, USA. [3]National Research Council, Herzberg Institute of Astrophysics, Victoria, British Columbia V9E 2E7, Canada. [4]Division of Astronomy and Astrophysics, University of California, Los Angeles, CA 90095, USA. [5]Department of Mathematics and Statistics, Monash University, Clayton, Victoria 3800, Australia. [6]Department of Astronomy and Astrophysics, University of California, Santa Cruz, CA 95064, USA. [7]Department of Astronomy, University of Washington, Seattle, WA 98195, USA. [8]Department of Astrophysics, American Museum of Natural History, New York, NY 10024, USA.

*To whom correspondence should be addressed. E-mail: richer@astro.ubc.ca

the two filters. The insets provide expanded views of two stars at the extremities of stellar evolution: the least luminous hydrogen-burning cluster star observed (bottom) and a white dwarf that is cool enough to lie in the blue hook part of the cooling sequence (top).

Cluster CMD. We constructed a CMD (Fig. 2A) from these data, including all sources that (i) generated local maxima in at least 90 out of 252 F814W images, (ii) were the most significant sources within 7.5 ACS pixels, and (iii) passed morphology tests indicating that they are point-like objects. In this diagram, brighter stars have small values of the F814W magnitude and red stars will have larger positive (F606W – F814W) colors. Some unresolved faint blue galaxies likely remain in the sample bluer than (F606W – F814W) = 1 and fainter than F814W = 27. To estimate the photometric errors for white dwarf stars, we used measurements of artificial stars of known magnitude inserted into the individual exposures and recovered by our finding and measuring algorithms. In addition, we considered the completeness for stars as a function of the F814W magnitude—that is, the fraction of stars that we recovered in the ACS images in artificial star tests. The completeness is based solely on the recovery fractions in the F814W data and hence applies equally well to both white dwarfs and main-sequence stars. Completeness fractions in excess of 50% are normally considered acceptable.

Fig. 1. A section of the observed field in NGC 6397 covering 94 arc sec by 127 arc sec. This is 29% of the entire field of our observations. Directions on the sky and a scale bar are shown at the lower right. The image is a composite of exposures from the HST ACS wide-field camera in F606W and F814W. The insets (each 10 arc sec by 10 arc sec) show detail for the faintest hydrogen-burning star observed in the cluster (top) and a white dwarf along the blue hook part of the cooling sequence (bottom). Although the field is in a globular star cluster with many bright stars, the ACS has such a tight point spread function, with relatively little scattered light, that it is still possible to see faint external galaxies right through the cluster.

Figure 2A is dominated by a narrow continuous cluster sequence spanning at least 14 magnitudes in the F814W filter. The sequence extends from a sparse giant branch at the brightest F814W magnitudes, through the main-sequence turnoff near F814W = 15.7, and down the main sequence to faint objects, with a possible termination in a cloud of field stars near F814W = 24. The turnoff region corresponds to stars that have recently completed hydrogen burning in their cores. They will shortly evolve into red giants, a phase of evolution lasting about 100 million years, before they eject their atmospheres and become white dwarfs. The scatter around this narrow sequence is produced by stars not associated with the cluster. These are stars from the galactic disk and bulge that are found along the line of sight to NGC 6397. This population is large because of the low galactic latitude (–12°) of NGC 6397.

The most novel feature of the diagram, however, is the white dwarf cooling sequence, which begins at about F814W = 22.5 and extends to F814W = 27.2, where it then "hooks" toward the blue. The sequence appears to be largely truncated fainter than F814W = 27.8. This truncation reflects the limit to which the bulk of the hydrogen-rich white dwarfs can cool over the lifetime of the cluster. For this reason it will be a powerful diagnostic in determining the age of NGC 6397. However, this truncation does not necessarily mean that there are no white dwarfs in the cluster fainter than this limit. Over a long period of time, both massive white dwarfs (those with masses in excess of about 0.8 that of the Sun) and those with helium-rich atmospheres cool more quickly and to fainter magnitudes than do white dwarfs of modest mass (0.5 to 0.6 solar masses) with hydrogen-rich atmospheres. As a consequence of electron degeneracy, more massive white dwarfs have smaller radii and hence larger densities. They will thus develop a crystallized core earlier than low-mass white dwarfs, causing them to enter a regime known as Debye cooling before the lower mass ones do. In this phase of evolution, the star effectively loses its ability to store thermal energy and it cools very rapidly. Because helium does not form molecules (which would have a vibrational mode), white dwarfs with pure helium atmospheres do not suffer from CIA. Their atmospheres are thus less opaque to infrared radiation and they cool rapidly. Hence, both massive and helium-rich white dwarfs may have cooled to below our observational limit.

We examined the details of the CMD further by analyzing the stars whose proper motions match that of the cluster (Fig. 2B and Fig. 3). Preexisting WFPC2 images, which were

used to proper motion–clean the data, overlap only 60% of the area of the ACS field and are much shorter in exposure time (F814W exposure times of 3960, 7440, and 5200 s in each of the 1994, 1997 and 2001 data sets, versus 179.7 ksec with the ACS in 2005) so that their utility, particularly for the very faintest stars, was limited. Distinguishing between cluster and field stars is a serious issue for stars along the main sequence as well as those in the white dwarf region. The main-sequence stars become very red at faint magnitudes, so they may be found on the F814W images but could be unmeasurable on the bluer F606W frames. For the white dwarfs, if they do indeed become bluer as they cool (*5*–*9*), we might expect to lose them on the F814W frames. Nonetheless, the major features are preserved and are much cleaner in Fig. 2B than in Fig. 2A. The main sequence is now seen to continue to F814W ~ 26.0 at (F606W – F814W) ~ 4.0. An F814W magnitude of 26.0 and a F606W magnitude of 30.0 correspond to absolute magnitudes of 13.6 and 17.4, respectively. These absolute magnitudes are more than a full magnitude fainter than the faintest known metal-poor ("population II") field stars (*20*, *21*), which suggests that there remains a population of extremely dim metal-poor stars awaiting discovery in the halo of the galaxy.

The cluster main sequence has two remarkable features: one at F814W ~ 24, where the number counts of stars decline rapidly [noted by (*22*)], and another at F814W ~ 26, where the main sequence appears to terminate. This latter feature is not caused by incompleteness (Fig. 3). Except for a few stars that scatter well away from the main-sequence locus (all these are also outliers in the proper motion distribution, so they are likely interlopers from the field population), there appears to be a complete lack of cluster main-sequence stars fainter than F814W = 26. The presence of an extensive white dwarf population as faint as F814W = 27.8, as well as numerous faint field stars, shows that if a significant population of main-sequence stars fainter than F814W = 26 were present, we would have found it.

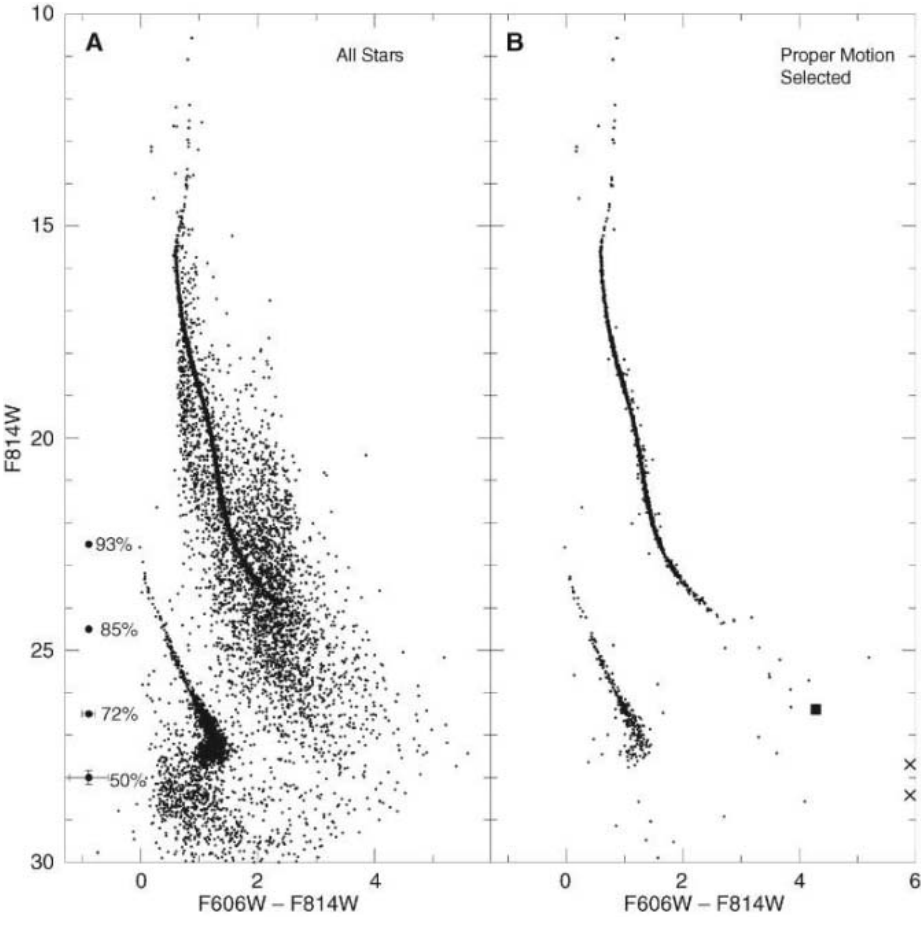

Fig. 2. The CMD of NGC 6397 (**A**) without proper motion selection of cluster members, and (**B**) after cleaning the data with the use of proper motions to exclude noncluster stars in the galactic disk and bulge from the sample (see also Fig. 3). Most of the faint galaxies and artifacts have been removed from (A) by requiring that the found objects pass certain morphological tests. The 1σ photometric errors as a function of magnitude are indicated for white dwarfs by the error bars at F814W = 22.5, 24.5, 26.5, and 28.0, as well as the percentage of stars (either white dwarfs or main sequence) found in the ACS images at each of these magnitudes from artificial star tests. In (B) the cluster main sequence appears to terminate at F814W = 26, (F606W – F814W) = 4. The few scattered objects at lower luminosity are at the extremes of the proper motion selection criteria and are likely interlopers from the large field population. The two X's to the right indicate the F814W magnitudes of the stars that passed the proper motion cuts but whose F606W magnitudes were not measured. The solid square is the location of the hydrogen-burning limit for one particular set of theoretical models (*23*, *24*).

Proper motions. We quantified this result by examining the proper motion distribution for faint red and blue stars (Fig. 3). NGC 6397 is moving relative to the field stars. Over the course of 10 years since the first archival data were taken, the cluster stars have moved by almost 3 ACS pixels with respect to the bulk of those in the field. A displacement this large is trivial to measure, provided we can find the star in the archival data. Figure 3 displays the proper motions for all objects with respect to the cluster as a function of F814W magnitude. The proper motion cuts we made to select cluster stars are shown in Fig. 3A; these stars are all to the left of the red line, which is set by fitting a Gaussian function to the total proper motion distribution in bins one magnitude wide and selecting those stars that lie within two standard deviations from the mean. The remaining plots are proper motions along the detector axes for stars redder than (F606W – F814W) = 1.5 (Fig. 3, B to D) and for blue stars with (F606W – F814W) < 1.5 (Fig. 3E). The circle shown in each plot is the proper motion cut appropriate to that magnitude. The circle has a radius of 0.5 ACS pixels in Fig. 3B and 1.3 pixels in Fig. 3, D and E. By contrast, proper motion errors in x and y range from 0.05 pixels at F814W = 22 to 0.6 pixels at F814W = 26. It is clear that clumps corresponding to cluster stars are seen in Fig. 3, B and C, but that no concentration is seen for red main-sequence stars with F814W > 26 (Fig. 3D). This coincides with the impression in Fig. 2B that there are no obvious cluster stars fainter than this limit. Figure 3E illustrates the displacements for stars with (F606W – F814W) < 1.5 and F814W > 26, which includes cluster white dwarfs, blue field stars, and unresolved blue galaxies. Clearly, there is a sizable component of stars moving with the cluster at these faint magnitudes (the white dwarfs), so that the deficiency seen for the main-sequence stars is real and not due to incompleteness.

Hydrogen-burning limit. The apparent termination of our observed main sequence lies close to the predicted hydrogen-burning limit (Fig. 2B, solid square); the lowest mass star capable of stable nuclear fusion of hydrogen in its core is 0.083 solar masses at the low heavy element abundance of NGC 6397 (*23*, *24*). We caution, however, that different models may yield different results. At masses just above the hydrogen-burning limit, the relation between the mass and luminosity of a star is very steep; an extremely small change in mass results in a large

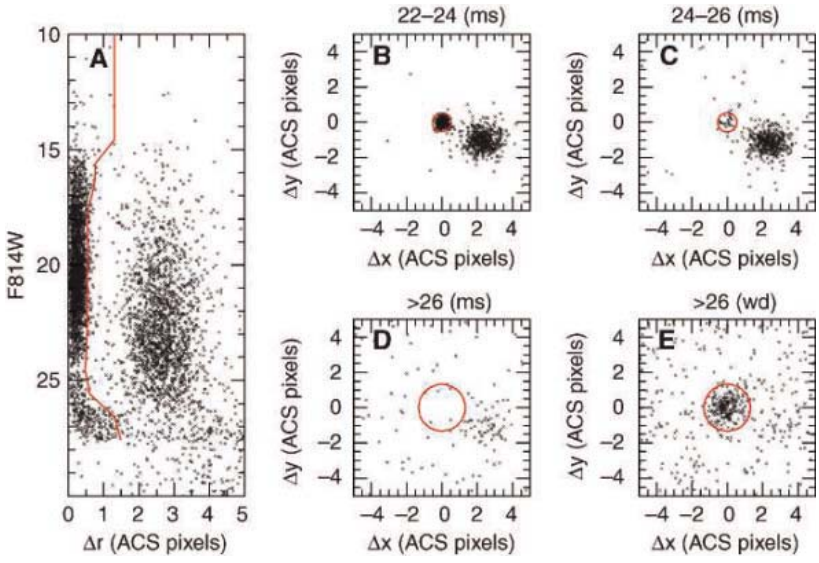

Fig. 3. (**A**) The F814W magnitude plotted against total stellar proper motion displacement Δr (scaled to 10 years) with respect to the cluster. The units are ACS pixels that project to 0.05 arc sec on the sky. The red line shows the selection criterion; all stars to the left of the line are considered to be cluster members. (**B** to **E**) Displacements in the x and y directions on the detector ($-x$ is approximately north; ms, main sequence; wd, white dwarf). The NGC 6397 stars are those in the tight clump at (0,0); the bulk of the field stars are located in the diffuse clump about 3 pixels away.

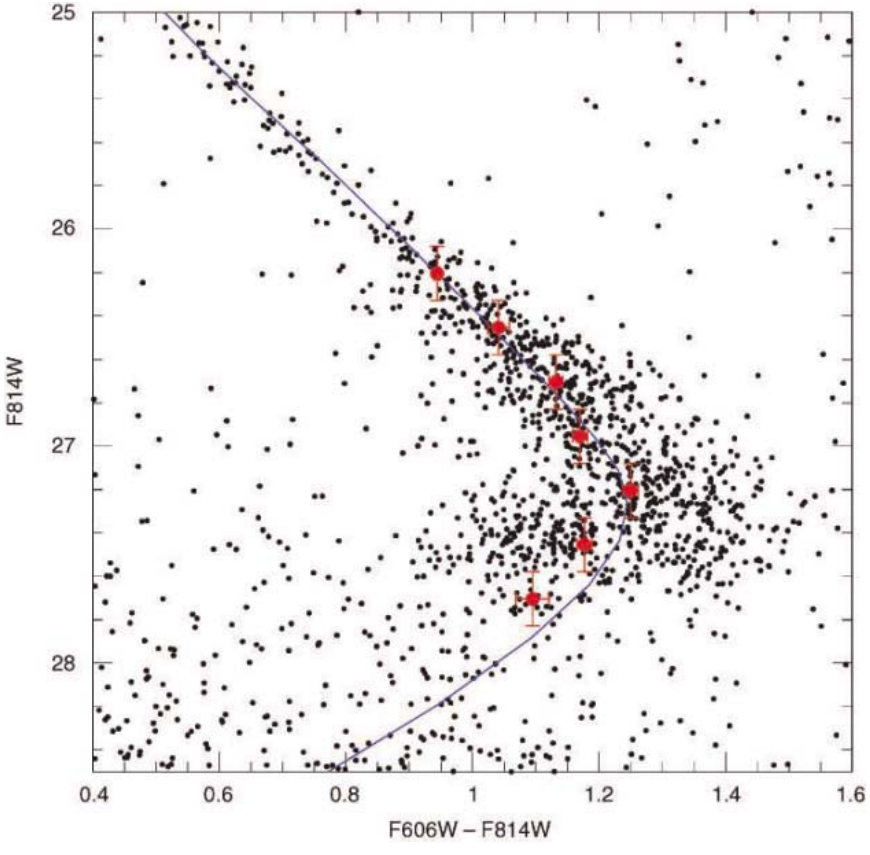

Fig. 4. The white dwarf region of the full CMD (i.e., not proper motion–cleaned) overlaid with the empirical cooling sequence (red dots with 1σ error bars) derived as described in the text. We use the full CMD here in lieu of the proper motion–cleaned one to avoid artificial truncation of the cooling sequence from losses of stars from the shorter exposure, earlier epoch data. The solid blue curve is a theoretical cooling sequence using the atmospheric models of Bergeron *et al.* (*7*) and a cooling model for 0.5 solar mass white dwarfs of Hansen (*6*).

change in luminosity. This is because at low masses, electron degeneracy pressure becomes important in supporting the star. The temperature no longer increases with increasing pressure as it does for a classical gas. This has the effect of decreasing the central temperature and hence the nuclear energy generation rate (*25*). As stars approach the hydrogen-burning limit in mass, we thus expect to see a steep decline in their number counts as a function of luminosity. This makes it highly improbable that any stars will be found at the hydrogen-burning limit.

Blue hook. The blue hook feature in the white dwarf cooling sequence remains after proper motion cleaning, leading us to conclude that we are indeed seeing the predicted CIA signature (*5*–*9*). We quantified the nature of the hook by deriving an empirical cooling sequence. We fit the observed color distribution in F814W magnitude bins of width 0.25 with a model of the dispersion in color determined from artificial star tests. This resulted in a relation between color and magnitude that is purely empirical and can be compared to any theoretical models of the cooling. In Fig. 4, we show the comparison between this relation and one particular theoretical cooling sequence. Note that there is indeed a blue hook in the empirical relation and that we see excellent agreement between this and the model curve. This concordance suggests that further detailed modeling of these cool white dwarfs will provide a strong constraint on the white dwarf cooling age of NGC 6397.

Final remarks. In 1984, the late Vittorio Castellani and Vittoria Caloi suggested to the European Space Agency that HST be used to locate the end of the hydrogen-burning main sequence in the nearest globular star clusters. We believe that we have met this challenge. In addition, the blue hook and a truncation in the white dwarf cooling region have also been located. These features can now be exploited to learn more about the structure of low-mass stars, brown dwarfs, the original massive stellar component in globular clusters, white dwarf atmospheres and cooling, and ultimately the ages of these oldest known stellar populations.

References and Notes

1. A. Burrows, W. B. Hubbard, D. Saumon, J. I. Lunine, *Astrophys. J.* **406**, 158 (1993).
2. D. N. Spergel *et al.*, *Astrophys. J. Suppl. Ser.* **148**, 175 (2003).
3. G. Fontaine, P. Brassard, P. Bergeron, *Publ. Astron. Soc. Pac.* **113**, 409 (2001).
4. B. M. S. Hansen *et al.*, *Astrophys. J. Suppl. Ser.* **155**, 551 (2004).
5. B. M. S. Hansen, *Nature* **394**, 860 (1998).
6. B. M. S. Hansen, *Astrophys. J.* **520**, 680 (1999).
7. P. Bergeron, F. Wesemael, A. Beauchamp, *Publ. Astron. Soc. Pac.* **107**, 1047 (1995).
8. G. Chabrier, *Astrophys. J.* **513**, 103 (1999).
9. D. Saumon, S. B. Jacobson, *Astrophys. J.* **511**, L107 (1999).
10. C. Zheng, A. Borysow, *Astrophys. J.* **441**, 960 (1995).
11. A. Borysow, U. G. Jorgensen, Y. Fu, *J. Quant. Spectr. Rad. Trans.* **68**, 235 (2001).

12. M. Gustafsson, L. Frommhold, *Astron. Astrophys.* **400**, 1161 (2003).
13. H. C. Harris *et al.*, *Astrophys. J.* **524**, 1000 (1999).
14. S. T. Hodgkin *et al.*, *Nature* **403**, 57 (2000).
15. B. R. Oppenheimer *et al.*, *Astrophys. J.* **550**, 448 (2001).
16. L. R. Bedin *et al.*, *Astrophys. J.* **624**, L45 (2005).
17. B. M. S. Hansen, *Phys. Rep.* **399**, 1 (2004).
18. I. N. Reid, J. E. Gizis, *Astron. J.* **116**, 2929 (1998).
19. R. G. Gratton *et al.*, *Astron. Astrophys.* **408**, 529 (2003).
20. S. K. Leggett, F. Allard, P. H. Hauschildt, *Astrophys. J.* **509**, 836 (1998).
21. S. Lepine, M. M. Shara, R. M. Rich, *Astrophys. J.* **602**, L125 (2004).
22. I. R. King, J. Anderson, A. M. Cool, G. Piotto, *Astrophys. J.* **492**, L37 (1998).
23. I. Baraffe, G. Chabrier, F. Allard, P. H. Hauschildt, *Astron. Astrophys.* **327**, 1054 (1997).
24. The models in (*23*) have been updated (available at http://perso.ens-lyon.fr/isabelle.baraffe).
25. G. Chabrier, I. Baraffe, *Annu. Rev. Astron. Astrophys.* **38**, 337 (2000).
26. Supported by NASA/HST grant GO-10424 (J.A., B.M.S.H., I.R.K., J.S.K., R.M.R., M.M.S.), a NASA Hubble Fellowship (J.S.K.), the U.S.-Canada Fulbright Fellowship Committee (H.B.R.), the Natural Sciences and Engineering Research Council of Canada (H.B.R.), and the University of British Columbia. H.B.R. thanks I. Ozier for fruitful discussions on CIA, as well as UCLA for support during his extended visit during which most of this paper was written. This research is based on NASA/ESA Hubble Space Telescope observations obtained at the Space Telescope Science Institute, which is operated by the Association of Universities for Research in Astronomy Inc. under NASA contract NAS5-26555. These observations are associated with proposal GO-10424.

31 May 2006; accepted 18 July 2006
10.1126/science.1130691

Warming and Earlier Spring Increase Western U.S. Forest Wildfire Activity

A. L. Westerling,[1,2]* H. G. Hidalgo,[1] D. R. Cayan,[1,3] T. W. Swetnam[4]

Western United States forest wildfire activity is widely thought to have increased in recent decades, yet neither the extent of recent changes nor the degree to which climate may be driving regional changes in wildfire has been systematically documented. Much of the public and scientific discussion of changes in western United States wildfire has focused instead on the effects of 19th- and 20th-century land-use history. We compiled a comprehensive database of large wildfires in western United States forests since 1970 and compared it with hydroclimatic and land-surface data. Here, we show that large wildfire activity increased suddenly and markedly in the mid-1980s, with higher large-wildfire frequency, longer wildfire durations, and longer wildfire seasons. The greatest increases occurred in mid-elevation, Northern Rockies forests, where land-use histories have relatively little effect on fire risks and are strongly associated with increased spring and summer temperatures and an earlier spring snowmelt.

Wildfires have consumed increasing areas of western U.S. forests in recent years, and fire-fighting expenditures by federal land-management agencies now regularly exceed US$1 billion/year (*1*). Hundreds of homes are burned annually by wildfires, and damages to natural resources are sometimes extreme and irreversible. Media reports of recent, very large wildfires (>100,000 ha) burning in western forests have garnered widespread public attention, and a recurrent perception of crisis has galvanized legislative and administrative action (*1*–*3*).

Extensive discussions within the fire-management and scientific communities and the media seek to explain these phenomena, focusing on either land-use history or climate as primary causes. If increased wildfire risks are driven primarily by land-use history, then ecological restoration and fuels management are potential solutions. However, if increased risks are largely due to changes in climate during recent decades, then restoration and fuels treatments may be relatively ineffective in reversing current wildfire trends (*4*, *5*). We investigated 34 years of western U.S. (hereafter, "western") wildfire history together with hydroclimatic data to determine where the largest increases in wildfire have occurred and to evaluate how recent climatic trends may have been important causal factors.

Competing explanations: Climate versus management. Land-use explanations for increased western wildfire note that extensive livestock grazing and increasingly effective fire suppression began in the late 19th and early 20th centuries, reducing the frequency of large surface fires (*6*–*8*). Forest regrowth after extensive logging beginning in the late 19th century, combined with an absence of extensive fires, promoted forest structure changes and biomass accumulation, which now reduce the effectiveness of fire suppression and increase the size of wildfires and total area burned (*3*, *5*, *9*). The effects of land-use history on forest structure and biomass accumulation are, however, highly dependent upon the "natural fire regime" for any particular forest type. For example, the effects of fire exclusion are thought to be profound in forests that previously sustained frequent, low-intensity surface fires [such as Southwestern ponderosa pine and Sierra Nevada mixed conifer (*2*, *3*, *10*, *11*)], but of little or no consequence in forests that previously sustained only very infrequent, high-severity crown fires (such as Northern Rockies lodgepole pine or spruce-fir (*1*, *5*, *12*)].

In contrast, climatic explanations posit that increasing variability in moisture conditions (wet/dry oscillations promoting biomass growth, then burning), and/or a trend of increasing drought frequency, and/or warming temperatures have led to increased wildfire activity (*13*, *14*). Documentary records and proxy reconstructions (primarily from tree rings) of fire history and climate provide evidence that western forest wildfire risks are strongly positively associated with drought concurrent with the summer fire season and (particularly in ponderosa pine–dominant forests) positively associated to a lesser extent with moist conditions in antecedent years (*13*–*18*). Variability in western climate related to the Pacific Decadal Oscillation and intense El Niño/La Niña events in recent decades along with severe droughts in 2000 and 2002 may have promoted greater forest wildfire risks in areas such as the Southwest, where precipitation anomalies are significantly influenced by patterns in Pacific sea surface temperature (*19*–*22*). Although corresponding decadal-scale variations and trends in climate and wildfire have been identified in paleo studies, there is a paucity of evidence for such associations in the 20th century.

We describe land-use history versus climate as competing explanations, but they may be complementary in some ways. In some forest types, past land uses have probably increased the sensitivity of current forest wildfire regimes to climatic variability through effects on the quantity, arrangement, and continuity of fuels. Hence, an increased incidence of large, high-severity fires may be due to a combination of extreme droughts and overabundant fuels in some forests. Climate, however, may still be the primary driver of forest wildfire risks on interannual to decadal scales. On decadal scales, climatic means and variability shape the character of the vegetation [e.g., species populations and their drought tolerance (*23*) and biomass (fuel) continuity (*24*), thus also affecting fire regime responses to shorter term climate variability]. On interannual and shorter time scales, climate variability affects the flammability of live and dead forest vegetation (*13*–*19*, *25*).

High-quality time series are essential for evaluating wildfire risks, but for various reasons (*26*), previous works have not rigorously documented changes in large-wildfire frequency for

[1]Scripps Institution of Oceanography, La Jolla, CA 92093, USA. [2]University of California, Merced, CA 95344, USA. [3]U.S. Geological Survey, La Jolla, CA 92093, USA. [4]Laboratory of Tree-Ring Research, University of Arizona, Tucson, AZ 85721, USA.

*To whom correspondence should be addressed. E-mail: awesterling@ucmerced.edu

western forests. Likewise, detailed fire-climate analyses for the region have not been conducted to evaluate what hydroclimatic variations may be associated with recent increased wildfire activity, and the spatial variations in these patterns.

We compiled a comprehensive time series of 1166 large (>400 ha) forest wildfires for 1970 to 2003 from federal land-management units containing 61% of western forested areas (and 80% above 1370 m) (*26*) (fig. S1). We compared these data with corresponding hydroclimatic and land surface variables (*26–34*) to address where and why the frequency of large forest wildfire has changed.

Increased forest wildfire activity. We found that the incidence of large wildfires in western forests increased in the mid-1980s (Fig. 1) [hereafter, "wildfires" refers to large-fire events (>400 ha) within forested areas only (*26*)]. Subsequently, wildfire frequency was nearly four times the average of 1970 to 1986, and the total area burned by these fires was more than six and a half times its previous level. Interannual variability in wildfire frequency is strongly associated with regional spring and summer temperature (Spearman's correlation of 0.76, $P < 0.001$, $n = 34$). A second-order polynomial fit to the regional temperature signal alone explains 66% of the variance in the annual incidence of these fires, with many more wildfires burning in hotter than in cooler years.

The length of the wildfire season also increased in the 1980s (Fig. 1). The average season length (the time between the reported first wildfire discovery date and the last wildfire control date) increased by 78 days (64%), comparing 1970 to 1986 with 1987 to 2003. Roughly half of that increase was due to earlier ignitions, and half to later control (48% versus 52%, respectively). Later control dates were no doubt partly due to later ignition dates, given that the date of the last reported wildfire ignition increased by 15 days, but a substantial increase in the length of time the average wildfire burned also played a role. The average time between discovery and control for a wildfire increased from 7.5 days from 1970 to 1986 to 37.1 days from 1987 to 2003. The annual length of the fire season and the average time each fire burned were also moderately correlated with the regional spring and summer temperature (Spearman's correlations of 0.61 ($P < 0.001$) and 0.55 ($P < 0.001$), respectively.

The greatest increase in wildfire frequency has been in the Northern Rockies, which account for 60% of the increase in large fires. Much of the remaining increase (18%) occurred in the Sierra Nevada, southern Cascades, and Coast Ranges of northern California and southern Oregon ("Northern California," in fig. S2). The Pacific Southwest; the Southern Rockies; the Northwest; coastal, central, and southern California; and the Black Hills each account for 11%, 5%, 5%, <1%, and <1%, respectively. Interestingly, the Northern Rockies and the Southwest show the same trend in wildfire frequency relative to their respective forested areas. However, the Southwest's absolute contribution to the western regional total is limited by its smaller forested area relative to higher latitudes.

Increased wildfire frequency since the mid-1980s has been concentrated between 1680 and 2590 m in elevation, with the greatest increase centered around 2130 m. Wildfire activity at these elevations has been episodic, coming in pulses during warm years, with relatively little activity in cool years, and is strongly associated with changes in spring snowmelt timing, which in turn is sensitive to changes in temperature.

Fire activity and the timing of the spring snowmelt. As a proxy for the timing of the spring snowmelt, we used Stewart and colleagues' dates of the center of mass of annual flow (CT) for snowmelt-dominated streamflow gauge records in western North America (*32–34*). The annual wildfire frequency for the region is highly correlated (inversely) with CT at gauges across the U.S. Pacific Northwest and interior West, indicating a coherent regional signal of wildfire sensitivity to snowmelt timing (Fig. 2).

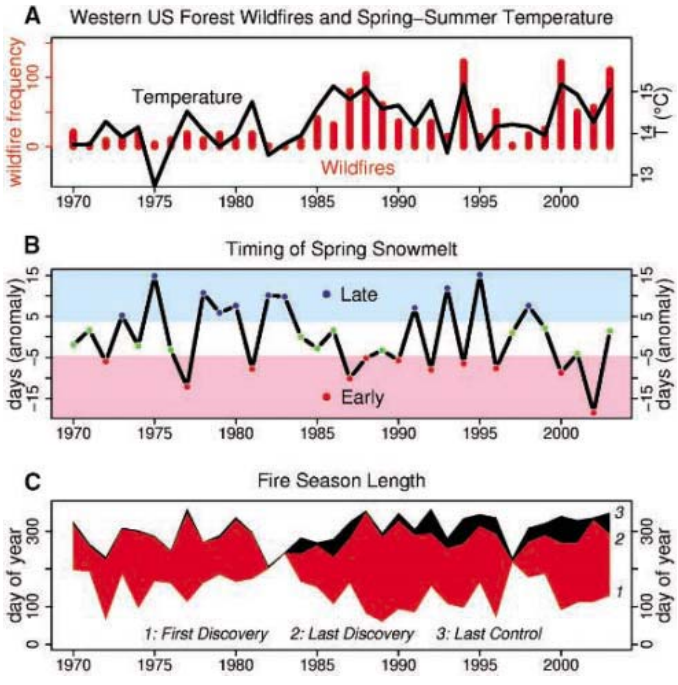

Fig. 1. (**A**) Annual frequency of large (>400 ha) western U.S. forest wildfires (bars) and mean March through August temperature for the western United States (line) (*26*, *30*). Spearman's rank correlation between the two series is 0.76 ($P < 0.001$). Wilcoxon test for change in mean large–forest fire frequency after 1987 was significant ($W = 42$; $P < 0.001$). (**B**) First principle component of center timing of streamflow in snowmelt dominated streams (line). Low (pink shading), middle (no shading), and high (light blue shading) tercile values indicate early, mid-, and late timing of spring snowmelt, respectively. (**C**) Annual time between first and last large-fire ignition, and last large-fire control.

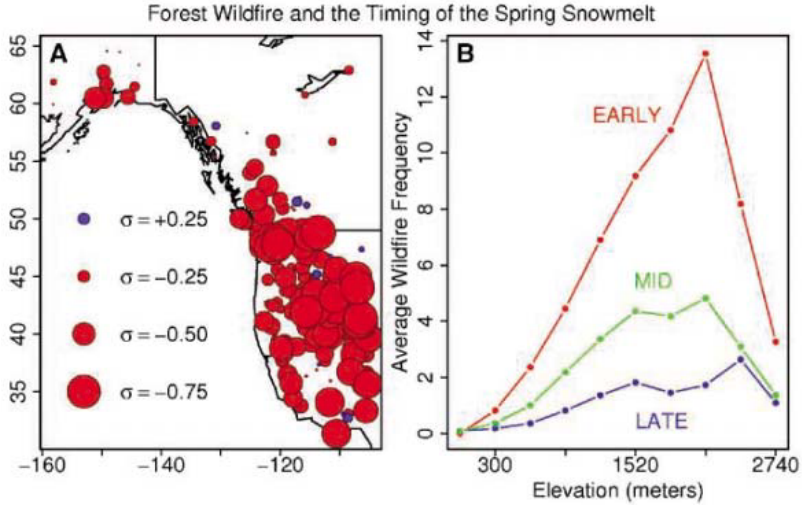

Fig. 2. (**A**) Pearson's rank correlation between annual western U.S. large (>400 ha) forest wildfire frequency and streamflow center timing. *x* axis, longitude; *y* axis, latitude. (**B**) Average frequency of western U.S. forest wildfire by elevation and early, mid-, and late snowmelt years from 1970 to 2002. See Fig. 1B for a definition of early, mid-, and late snowmelt years.

The negative sign of these correlations indicates that earlier snowmelt dates correspond to increased wildfire frequency. Following Stewart *et al*., we used the first principal component (CT1) of CT at western U.S. streamflow gauges as a regional proxy for interannual variability in the arrival of the spring snowmelt (Fig. 1) (*26*, *32*). This signal had its greatest impact on wildfire frequency between elevations of 1680 and 2590 m (Fig. 2), with a nonlinear response at these elevations to variability in snowmelt timing. Overall, 56% of wildfires and 72% of area burned in wildfires occurred in early (i.e., lower tercile CT1) snowmelt years, whereas only 11% of wildfires and 4% of area burned occurred in late (i.e., upper tercile CT1) snowmelt years.

Temperature affects summer drought, and thus flammability of live and dead fuels in forests through its effect on evapotranspiration and, at higher elevations, on snow. Additionally, warm spring and summer temperatures were strongly associated with reduced winter precipitation over much of the western United States (Fig. 3). The arrival of spring snowmelt in the mountains of the western United States, represented here by CT1, is strongly associated with spring temperature (*26*). Average spring and summer temperatures throughout the entire region are significantly higher in early than in late years (Fig. 3), peaking in April. The average difference between early and late April mean monthly temperatures in forested areas was just over 2°C, and it increased with elevation.

Snow carries over a substantial portion of the winter precipitation that falls in western mountains, releasing it more gradually in late spring and early summer, providing an important contribution to spring and summer soil moisture (*35*). An earlier snowmelt can lead to an earlier, longer dry season, providing greater opportunities for large fires due both to the longer period in which ignitions could potentially occur and to the greater drying of soils and vegetation. Consequently, it is not surprising that the incidence of wildfires is strongly associated with snowmelt timing.

Changes in spring and summer temperatures associated with an early spring snowmelt come in the context of a marked trend over the period of analysis. Regionally averaged spring and summer temperatures for 1987 to 2003 were 0.87°C higher than those for 1970 to 1986. Spring and summer temperatures for 1987 to 2003 were the warmest since the start of the record in 1895, with 6 years in the 90th percentile—the most for any 17-year period since the start of the record in 1895 through 2003—whereas only 1 year in the preceding 17 years ranked in the 90th percentile. Likewise, 73% of early years since 1970 occurred in 1987 to 2003 (Fig. 1).

Spatial variability in the wildfire response to an earlier spring. Vulnerability of western U.S. forests to more frequent wildfires due to warmer temperatures is a function of the spatial distribution of forest area and the sensitivity of the local water balance to changes in the timing of spring. We measured this sensitivity using the October-to-September moisture deficit—the cumulative difference between the potential evapotranspiration due to temperature and the actual evapotranspiration constrained by available moisture—which is an important indicator of drought stress in plants (*24*). We used the percentage difference in the moisture deficit for early versus late snowmelt years scaled by the fraction of forest cover in each grid cell to map forests' vulnerability to changes in the timing of spring (Fig. 4) (*26*). The Northern Rockies and Northern California display the greatest vulnerability by this measure—the same forests accounting for more than three-quarters of increased wildfire frequency since the mid-1980s. Although the trend in temperature over the Northern Rockies increases with elevation, vulnerability in the Northern Rockies is highest around 2130 m, where the greatest increase in fires has occurred. At lower elevations, the moisture deficit in early years is increasing from a high average value (i.e., summer drought tends to be longer and more intense at lower elevations), whereas at higher elevations the longer dry season in early years is still relatively short, and vegetation is somewhat buffered from the effects of higher temperatures by the available moisture.

Discussion. Robust statistical associations between wildfire and hydroclimate in western forests indicate that increased wildfire activity over recent decades reflects sub-regional responses to changes in climate. Historical wildfire observations exhibit an abrupt transition in the mid-1980s from a regime of infrequent large wildfires of short (average of 1 week) duration to one with much more frequent and longer burning (5 weeks) fires. This transition was

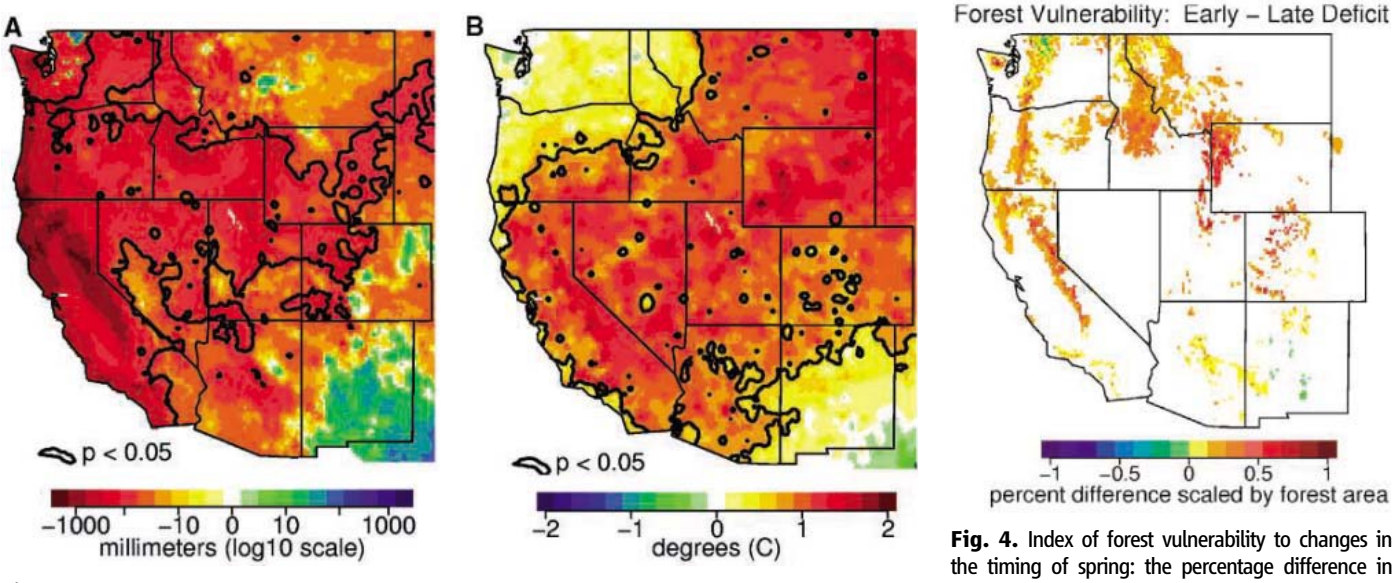

Fig. 3. Average difference between early and late snowmelt years in average precipitation from October through May (**A**) and average temperature from March through August (**B**). Contours enclose regions in which a *t* test for the difference in mean between 11 early and 11 late years was significant ($P < 0.05$). The null hypothesis that precipitation from October through May is normally distributed could not be rejected using the Shapiro-Wilk test for normality ($P > 0.05$ for more than 95% of 24,170 grid cells, $n = 49$ for precipitation; $P > 0.05$ for more than 95% of 24,170 grid cells, $n = 50$ for temperature). See Fig. 1B for a definition of early, mid-, and late snowmelt years.

Fig. 4. Index of forest vulnerability to changes in the timing of spring: the percentage difference in cumulative moisture deficit from October to August at each grid point in early versus late snowmelt years, scaled by the forest-type vegetation fraction at each grid point, for 1970 to 1999 (*26*). See fig. S3 for a map of forest vulnerability for 1970 to 2003 over a smaller spatial domain. See Fig. 1B for a definition of early, mid-, and late snowmelt years.

marked by a shift toward unusually warm springs, longer summer dry seasons, drier vegetation (which provoked more and longer burning large wildfires), and longer fire seasons. Reduced winter precipitation and an early spring snowmelt played a role in this shift. Increases in wildfire were particularly strong in mid-elevation forests.

The greatest absolute increase in large wildfires occurred in Northern Rockies forests. This sub-region harbors a relatively large area of mesic, middle and high elevation forest types (such as lodgepole pine and spruce-fir) where fire exclusion has had little impact on natural fire regimes (*1*, *5*), but where we found that an advance in spring produces a relatively large percentage increase in cumulative moisture deficit by midsummer. In contrast, changes in Northern California forests may involve both climate and land-use effects. In these forests, large percentage changes in moisture deficits were strongly associated with advances in the timing of spring, and this area also includes substantial forested area where fire exclusion, timber harvesting, and succession after mining activities have led to increased forest densities and fire risks (*10*, *11*). Northern California forests have had substantially increased wildfire activity, with most wildfires occurring in early years. Southwest forests, where fire exclusion has had the greatest effect on fire risks (*2*, *3*), have also experienced increased numbers of large wildfires, but the relatively small forest area there limits the impact on the regional total, and the trend appears to be less affected by changes in the timing of spring. Most wildfires in the Southern Rockies and Southern California have also occurred in early snowmelt years, but again forest area there is small relative to the Northern Rockies and Northern California. Thus, although land-use history is an important factor for wildfire risks in specific forest types (such as some ponderosa pine and mixed conifer forests), the broad-scale increase in wildfire frequency across the western United States has been driven primarily by sensitivity of fire regimes to recent changes in climate over a relatively large area.

The overall importance of climate in wildfire activity underscores the urgency of ecological restoration and fuels management to reduce wildfire hazards to human communities and to mitigate ecological impacts of climate change in forests that have undergone substantial alterations due to past land uses. At the same time, however, large increases in wildfire driven by increased temperatures and earlier spring snowmelts in forests where land-use history had little impact on fire risks indicates that ecological restoration and fuels management alone will not be sufficient to reverse current wildfire trends.

These results have important regional and global implications. Whether the changes observed in western hydroclimate and wildfire are the result of greenhouse gas–induced global warming or only an unusual natural fluctuation is beyond the scope of this work. Regardless of past trends, virtually all climate-model projections indicate that warmer springs and summers will occur over the region in coming decades. These trends will reinforce the tendency toward early spring snowmelt (*36*, *37*) and longer fire seasons. This will accentuate conditions favorable to the occurrence of large wildfires, amplifying the vulnerability the region has experienced since the mid-1980s. The Intergovernmental Panel on Climate Change's consensus range of 1.5° to 5.8°C projected global surface temperature warming by the end of the 21st century is considerably larger than the recent warming of less than 0.9°C observed in spring and summer during recent decades over the western region (*37*).

If the average length and intensity of summer drought increases in the Northern Rockies and mountains elsewhere in the western United States, an increased frequency of large wildfires will lead to changes in forest composition and reduced tree densities, thus affecting carbon pools. Current estimates indicate that western U.S. forests are responsible for 20 to 40% of total U.S. carbon sequestration (*38*, *39*). If wildfire trends continue, at least initially, this biomass burning will result in carbon release, suggesting that the forests of the western United States may become a source of increased atmospheric carbon dioxide rather than a sink, even under a relatively modest temperature-increase scenario (*38*, *39*). Moreover, a recent study has shown that warmer, longer growing seasons lead to reduced CO_2 uptake in high-elevation forests, particularly during droughts (*40*). Hence, the projected regional warming and consequent increase in wildfire activity in the western United States is likely to magnify the threats to human communities and ecosystems, and substantially increase the management challenges in restoring forests and reducing greenhouse gas emissions.

References and Notes

1. C. Whitlock, *Nature* **432**, 28 (2004).
2. W. W. Covington, *Nature* **408**, 135 (2000).
3. C. D. Allen *et al.*, *Ecol. Appl.* **12**, 1418 (2002).
4. J. L. Pierce, G. A. Meyer, A. J. T. Jull, *Nature* **432**, 87 (2004).
5. T. Schoennagel, T. T. Veblen, W. H. Romme, *BioScience* **54**, 661 (2004).
6. M. Savage, T. W. Swetnam, *Ecology* **71**, 2374 (1990).
7. A. J. Belsky, D. M. Blumenthal, *Conserv. Biol.* **11**, 315 (1997).
8. S. J. Pyne, P. L. Andrews, R. D. Laven, *Introduction to Wildland Fire* (Wiley, New York, 1996).
9. W. W. Covington, M. M. Moore, *J. For.* **92**, 39 (1994).
10. K. S. McKelvey *et al.*, in *Sierra Nevada Ecosystems Project: Final Report to Congress* (Univ. of California, Davis, CA, 1996), vol. 2, chap. 37.
11. G. E. Gruell, *Fire in Sierra Nevada Forests: A Photographic Interpretation of Ecological Change Since 1849* (Mountain Press, Missoula, MT, 2001).
12. T. Schoennagel, T. T. Veblen, W. H. Romme, J. S. Sibold, E. R. Cook, *Ecol. Appl.* **15**, 2000 (2005).
13. R. C. Balling, G. A. Meyer, S. G. Wells, *Agric. For. Meteorol.* **60**, 285 (1992).
14. E. K. Heyerdahl, L. B. Brubaker, J. K. Agee, *Holocene* **12**, 597 (2002).
15. K. F. Kipfmueller, T. W. Swetnam, in *Wilderness Ecosystems, Threats, and Management*, D. N. Cole, S. F. McCool, W. T. Borrie, J. O'Loughlin, Eds. (U.S. Forest Service, RMRS-P-15, Fort Collins, CO, 2000), vol. 5, pp. 270–275.
16. T. W. Swetnam, J. L. Betancourt, *J. Clim.* **11**, 3128 (1998).
17. T. T. Veblen, T. Kitzberger, J. Donnegan, *Ecol. Appl.* **10**, 1178 (2000).
18. A. L. Westerling, T. J. Brown, A. Gershunov, D. R. Cayan, M. D. Dettinger, *Bull. Am. Meteorol. Soc.* **84**, 595 (2003).
19. T. W. Swetnam, J. L. Betancourt, *Science* **249**, 1017 (1990).
20. A. Gershunov, T. P. Barnett, *J. Clim.* **11**, 1575 (1998).
21. A. Gershunov, T. P. Barnett, D. R. Cayan, *Eos* **80**, 25 (1999).
22. A. L. Westerling, T. W. Swetnam, *Eos* **84**, 545 (2003).
23. N. L. Stephenson, *Am. Nat.* **135**, 649 (1990).
24. N. L. Stephenson, *J. Biogeogr.* **25**, 855 (1998).
25. T. W. Swetnam, *Science* **262**, 885 (1993).
26. Materials and methods are available as supporting material on *Science* Online.
27. K. E. Mitchell *et al.*, *J. Geophys. Res.* **109**, D07S90 (2004).
28. E. P. Maurer, A. W. Wood, J. C. Adam, D. P. Lettenmaier, B. Nijssen, *J. Clim.* **15**, 3237 (2002).
29. A. F. Hamlet, D. P. Lettenmaier, *J. Hydrometeor.* **6**, 330 (2005).
30. NCDC, "Time bias corrected divisional temperature-precipitation-drought index," documentation for data set TD-9640 (DBMB, NCDC, NOAA, Asheville, NC, 1994); available online (www.ncdc.noaa.gov/oa/climate/onlineprod/drought/readme.html).
31. X. Liang, D. P. Lettenmaier, E. F. Wood, S. J. Burges, *J. Geophys. Res.* **99**, 14415 (1994).
32. I. T. Stewart, D. R. Cayan, M. D. Dettinger, *J. Clim.* **18**, 1136 (2005).
33. D. R. Cayan, S. A. Kammerdiener, M. D. Dettinger, J. M. Caprio, D. H. Peterson, *Bull. Am. Meteorol. Soc.* **82**, 399 (2001).
34. J. R. Slack, J. M. Landwehr, *U.S. Geol. Surv. Open-File Rep. 92–129* (1992).
35. J. Sheffield, G. Goteti, F. H. Wen, E. F. Wood, *J. Geophys. Res.* **109**, D24108 (2004).
36. National Assessment Synthesis Team, *Climate Change Impacts on the United States: The Potential Consequences of Climate Variability and Change* (U.S. Global Change Research Program, Washington, DC, 2000).
37. J. T. Houghton *et al.*, Eds., *IPCC Climate Change 2001: The Scientific Basis* (Cambridge Univ. Press, Cambridge and New York, 2001).
38. S. W. Pacala *et al.*, *Science* **292**, 2316 (2001).
39. D. Schimel, B. H. Braswell, in *Global Change and Mountain Regions: An Overview of Current Knowledge*, U. M. Huber, H. K. M. Bugmann, M. A. Reasoner, Eds., vol. 23 of *Advances in Global Change Research* (Springer, Dordrecht, Netherlands, 2005), pp. 449–456.
40. W. Sacks, D. Schimel, R. Monson, *Oecologia,* in press.

41. We thank M. Dettinger and D. Schimel for help. This work was supported by grants from the National Oceanographic and Atmospheric Administration's Office of Global Programs, the National Fire Plan by means of the U.S. Forest Service's Southern Research Station, and the California Energy Commission.

Supporting Online Material

www.sciencemag.org/cgi/content/full/1128834/DC1
Materials and Methods
Figs. S1 to S3
References

17 April 2006; accepted 28 June 2006
Published online 6 July 2006;
10.1126/science.1128834
Include this information when citing this paper.

The Molecular Architecture of Axonemes Revealed by Cryoelectron Tomography

Daniela Nicastro,[1]*† Cindi Schwartz,[1] Jason Pierson,[1] Richard Gaudette,[1] Mary E. Porter,[2] J. Richard McIntosh[1]

Eukaryotic flagella and cilia are built on a 9 + 2 array of microtubules plus >250 accessory proteins, forming a biological machine called the axoneme. Here we describe the three-dimensional structure of rapidly frozen axonemes from *Chlamydomonas* and sea urchin sperm, using cryoelectron tomography and image processing to focus on the motor enzyme dynein. Our images suggest a model for the way dynein generates force to slide microtubules. They also reveal two dynein linkers that may provide "hard-wiring" to coordinate motor enzyme action, both circumferentially and along the axoneme. Periodic densities were also observed inside doublet microtubules; these may contribute to doublet stability.

Eukaryotic cilia and flagella are built on the axoneme, a cylindrical array of nine doublet microtubules (MTs) that surround two singlet MTs called the central pair (*1*, *2*) (Fig. 1, A and B). Understanding axoneme structure, function, and regulation is important because defects in this organelle are associated with diverse medical problems (*3*). The motors that transduce chemical energy into the mechanical force for MT sliding are dyneins, large motor enzymes that are organized in two rows along each doublet MT (Figs. 1 and 5, C and D). Other structures in the axoneme resist sliding, causing the axoneme to bend (*4*). Because cytoplasmic isoforms of dynein contribute to several forms of MT-based motility (*5*), and because dynein's mechanics are distinct from those of the other molecular motors, learning how this enzyme works would be useful.

All dyneins include one or more heavy chains (DHCs, >500 kD each), one or more intermediate chains (DICs, 45 to 140 kD), and 1 to 10 light chains (DLCs, ~8 to 28 kD) (*5*). The dynein motor domain (~350 kD at the C terminus of the DHC) is related to the AAA family of adenosine triphosphatases. It connects two potential levers: a cargo-binding tail, which is also the binding site of several DICs and DLCs, and an MT-binding stalk (*6*). Because flagella generate periodic waves of bending whose speed and form can vary, dynein's activity probably switches from one side of the axoneme to the other and propagates in a controlled manner (*7*). Flagellar waveforms seem to result from regulatory and mechanical interactions between projections from the central MTs and the radial spokes (Fig. 1, F and G; Fig. 5, C and D). These structures contain components that modulate kinases and phosphatases on doublet MTs (*2*). They appear to act through a doublet-associated structure called the dynein regulatory complex (DRC) (*1*). Given that isolated axonemes are motile (*7*), it seems likely that all essential regulatory machinery is built into this structure.

Axonemes from many organisms have been studied by conventional electron microscopy (EM), using thin sections, negative staining, or metal replicas of quickly frozen, deep-etched samples (*1*, *6*, *8*). These studies demonstrated the 24-nm axial periodicity of the outer dynein

[1]Laboratory for 3D Electron Microscopy of Cells, Department of Molecular, Cellular, and Developmental Biology, CB 347, University of Colorado, Boulder, CO 80309–0347, USA. [2]Department of Genetics, Cell Biology, and Development, 6–160 Jackson Hall, 321 Church Street SE, University of Minnesota, Minneapolis, MN 55455, USA.

*Present address: Brandeis University, Rosenstiel, 415 South Street, Waltham, MA 02454, USA.
†To whom correspondence should be addressed. E-mail: nicastro@colorado.edu

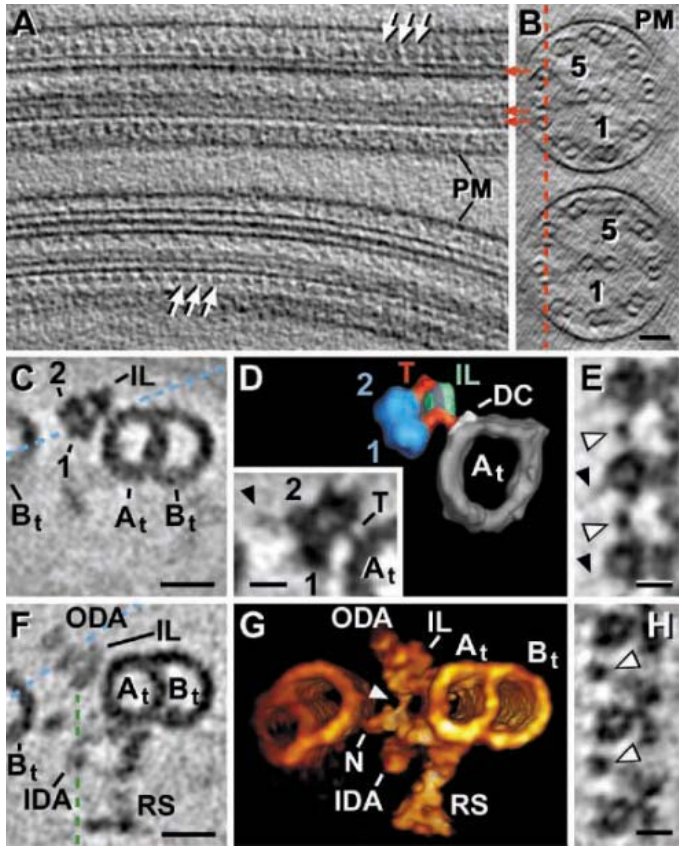

Fig. 1. Cryo-ET of sea urchin sperm [(A) to (E)] and *Chlamydomonas* flagella [(F) to (H)]. Longitudinal (A) and transverse (B) tomographic slices through flagella are shown; dashed line in (B) indicates the location of (A). (**A**) Dynein motor domains, white arrows. (**B**) Top flagellum is viewed from the proximal end; bottom flagellum is opposite, with doublets labeled 1 and 5; PM, plasma membrane. (C), (D), inset in (D), (F), and (G) are cross sections, viewed from the distal end. (**C**) Slice through an average of 280 repeats; the dashed line defines the orientation of (E). A_t, A tubule; B_t, B tubule; IL, DIC/DLC-tail complex; 1 and 2, motor domains of the ODA. (**D**) Surface rendering of (C) and (D) (inset) with interpretive coloring. The hook-shaped tail (T, red) of the more central DHC connects the dynein head (1, blue area) with A_t; densities near the A_t connection resemble the DC (white area). The tail of the peripheral DHC (2, blue area) is obscured by the IL (green area), but relative positions suggest that it is part of the connection to A_t via the tail of the more central DHC. Note the stalk projecting from 2 toward B_t (inset, arrowhead). (**E**) Slice through three ODA motor domains showing stalks (black arrowheads) on motor rings and parts of OOD linkers (white arrowheads). (**F**) Slice through average of 160 repeats; RS, radial spokes. Dashed blue line, orientation of (H); dashed green line, orientation of Fig. 3, A and B. (**G**) Volume rendering of (F). Note the nexin link (N) and OID linker (white arrowhead). (**H**) Slice through three β-dynein motor domains from the ODA row. Note the asymmetric, ring-shaped dynein motors (the middle head is visibly heptameric) and parts of the OOD linker (white arrowheads). Scale bars, 50 nm in (B), 20 nm in (C) and (F), and 10 nm in (D) (inset), (E), and (H).

arms (ODAs) as well as the complex arrangements of the inner dynein arms (IDAs) and radial spokes within the axoneme's 96-nm longitudinal repeat (*2*, *6*) (Fig. 1, A and B; Fig. 5, C and D). We used electron tomography (ET) to study axonemes in rapidly frozen but otherwise unaltered material. Sea urchin sperm were frozen while in a quiescent state (Fig. 1, A to E); axonemes from the biflagellate alga *Chlamydomonas reinhardtii* were isolated and demembranated in the absence of adenosine triphosphate (ATP) (Fig. 1, F to H) (*9*). Rapid freezing immobilizes samples within milliseconds, raising confidence that the observed structures are accurate representations of physiological states. ET generates three-dimensional (3D) reconstructions with an almost isotropic resolution (*10*) but through images whose signal-to-noise ratio is low because of the low electron dose that must be used with frozen-hydrated material (*11*). To get the resolution and contrast necessary to see individual macromolecules, we used an energy filter to remove inelastically scattered electrons (*11*), correlation-based alignment of equivalent volumes, and 3D volume averaging of repetitive structures, which improves image signal-to-noise ratio [fig. S1, supporting online material (SOM) text, and movie S1] (*12*). With these methods, image resolution was ~4 nm (fig. S1, G and H), which is sufficient to recognize important molecular details.

Mechanistic implications of the positions and shapes of dynein arms. Our images revealed details of dynein's structure in axonemes from both sea urchin (Fig. 1, C to E; Fig. 2, A to D) and *Chlamydomonas* (Fig. 1, F to H; Fig. 2, E and F). A slice through a tomogram that contained the β-dynein heads from three adjacent *Chlamydomonas* ODAs displayed the asymmetry of the dynein motor domain (Fig. 1H): One half of the heptameric ring contained three domains and the other half contained four, which is consistent with images of isolated *Chlamydomonas* IDAs (*13*), *Dictyostelium* cytoplasmic dynein (*14*), and sea urchin ODAs (*12*) (Fig. 1E). The two (sea urchin) or three (*Chlamydomonas*) motor domains in a single ODA formed two or three parallel rings that resembled stacked coins (Fig. 1, C, D, F, and G; Fig. 2, D to F; Fig. 3, A to E; Fig. 5). The plane of each ring ran through the axis of the adjacent B tubule (dashed blue lines in Fig. 1, C and F). Thus, all motor domains were positioned so they could act equivalently on the neighboring MT (Fig. 5C and fig. S4I). The coiled-coil MT-binding stalk probably projects within this plane from the motor domain to the B tubule, although it was often not obvious in our images [but note Fig. 1, D (inset) and E (black arrowheads)]. The ODAs from *Chlamydomonas* [(Fig. 1, F to H) and (*15*)] and sea urchin (Fig. 1, C to E) were similar, suggesting the generality of these relationships and their probable importance for dynein function.

Averages of sea urchin ODAs revealed the tail region of DHCs in situ (Fig. 1, C and D); the tail of the more central DHC was obvious, whereas that of the more peripheral DHC was partially obscured by additional density [Fig. 1, C and D (inset)]. The accessory subunits (the DIC/DLC complex) probably lie near the site where the two tails meet (Fig. 5A). Only the inner α-DHC connected directly to the A tubule; the β-DHC was carried in a piggyback fashion (Fig. 1D) (*12*). The tails of the *Chlamydomonas* outer-arm DHCs were less obvious but still visible (*IL* in Fig. 1, F and G).

ODAs bind the A tubule through the outer-arm docking complex (DC) (*16*). The DC forms a small pointed structure on the A tubule at the base of the ODA (*16*) (Figs. 1D and 2A). Two of the DC subunits are elongated polypeptides, which are thought to join end-to-end at every 24-nm interval and form an extended filament along the A tubule. Tomographic slices through the base of the ODAs (red line in Fig. 2A) revealed a narrow density on the surface of the A tubule (Fig. 2B) that corresponds to the predicted location of the DC.

Orientations of ODA domains in situ modify existing models for dynein's force production. Sea urchin ODA tails appeared hook-shaped (Fig. 1, C and D), like the EM images of the single-headed IDA isoform "c" from *Chlamydomonas* (*13*). Images of dynein c have suggested a rotary motion in dynein's head that shifts the coplanar stalk and/or tail relative to the AAA subdomains (*13*, *14*), indicating that the head acts as a winch (*17*). However, the ODA motor and tail in situ displayed a different 3D orientation, suggesting an alternative interpretation. In axonemes, the ODA tail bent in a plane perpendicular to that of the dynein rings (Fig. 1, C to H). This difference from the planarity seen in vitro (*13*) could result either from isoform differences or from rearrangements during isolation and/or negative staining. Tail and motor domains were both clearly resolved in our averages; moreover, each ODA formed multiple connections, both along and perpendicular to the axoneme axis (Fig. 5, A and B, and movie S2). These structures may provide rigidity, allowing the tail to serve as a fulcrum for dynein's power stroke. In contrast, the ATP-sensitive MT-binding stalks that connect to B tubules were often smeared under our conditions (Fig. 1). Apparently the tails were essentially static relative to the motor ring and A tubule, whereas the stalk's position was variable. Thus, any rotation of the dynein motor that promotes doublet sliding should cause the MT-binding stalk to shift relative to the more rigid tail.

Links between dynein complexes may coordinate dynein activity in axonemes. Tomographic slices that contained a row of ODAs (red and yellow lines in Fig. 2A) showed neighboring arms linked by filamentous structures (Fig. 2, B to F). The orientation and position of these linkers relative to the ODA motor domains showed that they were distinct from the DIC/DLC-tail complex (Fig. 2B; white arrowheads in Fig. 1, E and H). These structures were modeled in 3D as the outer-outer–dynein (OOD) linkers (Fig. 2, D and F; Fig. 5, B and D). In sea urchin sperm, these linkers ran from the ODA motor domain nearest the A tubule,

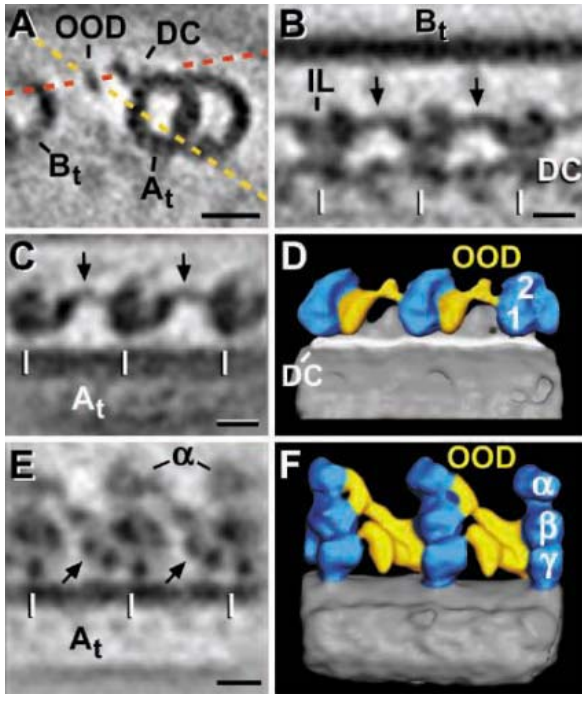

Fig. 2. ODA complexes of sea urchin sperm flagella (**A** to **D**) and *Chlamydomonas* axonemes (**E** and **F**). A cross-sectional view from the distal end (A) and longitudinal views [(B) to (F)] with the proximal end at left are shown. (A) Slice through an average of 280 doublets. The slice orientation is similar to that in Fig. 1C, but the position is between two ODAs, showing a cross section of an OOD linker. Dashed red line, orientation of slice in (B); dashed yellow line, orientation of slice in (C). Slices [(B), (C), and (E)] and surface renderings [(D) and (F)] show three ODAs, connected by OOD linkers (arrows or yellow areas); two-headed sea urchin ODAs [(blue area labeled 1 and 2 in (D)]; or three-headed *Chlamydomonas* ODAs [blue area labeled α, β, and γ in (F)]. White lines in (B), (C), and (E) indicate the 24-nm repeat of ODAs; (D) and (F) correspond to (C) and (E). Both kinds of axonemes have OOD linkers, but sea urchin linkers are almost parallel to the MTs [(B) to (D)], whereas *Chlamydomonas* links are diagonal [(E) and (F)]. Scale bars, 20 nm in (A) and 10 nm in (B), (C), and (E).

up and over to the peripheral motor domain of the neighboring ODA (Fig. 2, C and D; Fig. 5B). In *Chlamydomonas*, the OOD linkers were even larger and more complex (Fig. 2, E and F; Fig. 5D; and fig. S4, D and E). The point of attachment between the OOD linker and the ODAs lay close to the base of the motor domain where the dynein tail begins.

Given the size of these OOD linkers, we reexamined published images, seeking similar densities. Although there are ambiguities in such comparisons (*6*, *8*, *18*) (fig. S4, D and E), similar structures could be seen in previous work. Burgess's intermediate subunit (*18*) resembles our sea urchin OOD linker [compare Fig. 2C with figure 6D in (*18*)]. The diagonal component in *Chlamydomonas* may be our OOD linker [Fig. 2E versus figure 9 in (*19*)]. The presence of linkers in such distantly related species suggests that they are ubiquitous axonemal features. These linkers are ideally positioned to modulate dynein activity along outer doublets during flagellar waveform propagation.

We also found connections between OOD linkers in the outer arms and structures in the IDA region (Fig. 3, A to E; white arrowhead, Fig. 1G). In each 96-nm repeat, two of the four OOD linkers connected to the IDA region, forming part of a triskelion; one connection was proximal to the first radial spoke, whereas the other was distal to the second spoke (black arrows, Fig. 3, A to C, and movie S3). These connections are outer-inner–dynein (OID) linkers (Fig. 5D). The proximal OID linker connected with the base of an IDA called I1 (Fig. 3, A and C), whereas the second OID linker connected with the DRC, a crescent-shaped structure above the second radial spoke (*20*, *21*) (Figs. 1G and 3, A to E). The OID linkers suggest a mechanism for coordinating inner and outer dynein arm activities: Signals from the central pair and radial spokes are transmitted first to the I1 dynein and DRC to generate flagellar waveforms. From there, the signals may go through OID linkers to the ODAs to modulate flagellar beat frequency. This model is consistent with observations from flagellar mutants and indicates that ODAs are downstream on the signaling pathway (*22*).

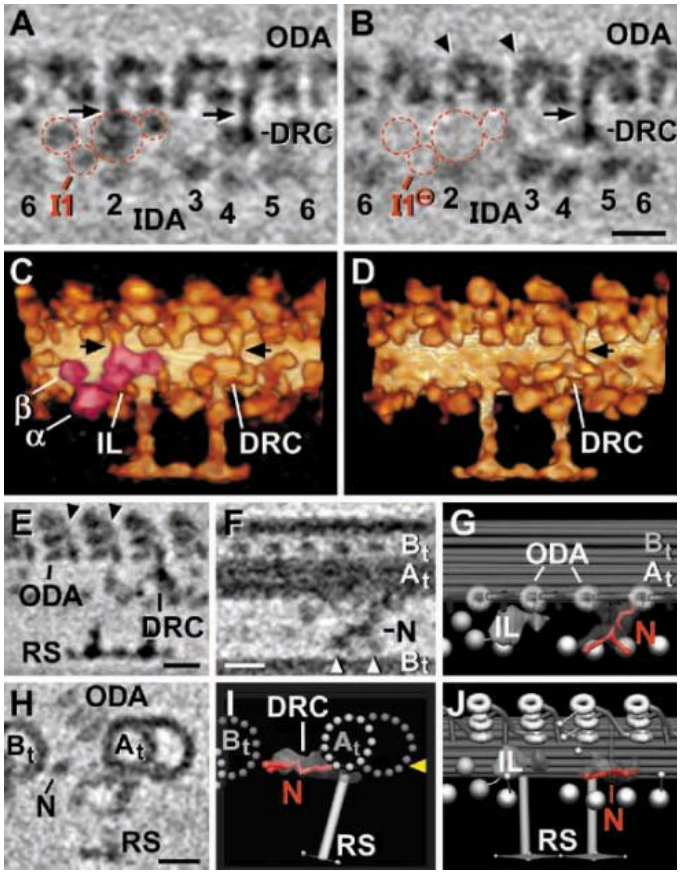

Fig. 3. Organization of IDAs (**A** to **E**) and nexin link (**F** to **J**) in *Chlamydomonas* axonemes. Wild-type [(A) and (C)] and *pf9* mutant [(B), (D), and (E)] axonemes show clear differences. Longitudinal slices [(A), (B), and (E)] and volume renderings [(C) and (D)] are viewed from the B tubule of the adjacent doublet, with the proximal end on the left; the orientation of (A) and (B) is indicated by the dashed green line in Fig. 1F; (C) and (D) correspond to (A) and (B). The I1 complex (dashed red circles or red areas) is missing in the mutant (*I1*$^-$). Note the OID linkers (arrows) between the ODA and IDA rows. Arrowheads, OOD linkers; α and β, 1-alpha and 1-beta motor domains of the I1 complex; 2 to 6, single-headed IDAs. (E) Similar to (B) but oriented to include all three ODA motor domains and radial spoke heads (RS); OOD linkers (arrowheads) connect to α- and perhaps β-DHCs on their proximal sides, whereas in (B) the OOD linkers connect to β- and γ-DHCs on their distal sides. Slices [(F) and (H)] through an average of 160 nexin links (N) and graphic models [(G), (I), and (J)] of the same structure; the orientations of (G) and (I) correspond to (F) and (H). Nexin spans the distance between A and B tubules of adjacent doublets; it is connected to the DRC. It terminates on the A tubule close to RS2, but branches near the B tubule [arrowheads in (F) at tips of the branches]. Nexin zigzags between the A tubule and the bifurcation point. (F) is a longitudinal slice at the position of the yellow arrowhead in (I). Scale bars, 20 nm [(B), (E), (F), and (H)].

IDA organization in *Chlamydomonas* axonemes. IDAs are structurally and functionally more complex than ODAs, and they are both necessary and sufficient for generating the diversity of flagellar waveforms (*22*). In *Chlamydomonas*, at least eight different inner-arm DHCs are organized with various DICs and DLCs into seven distinct complexes: one two-headed dynein (I1) and six single-headed isoforms (*22*). We observed the IDAs in 3D within the 96-nm axoneme repeat (Fig. 3, A to E) (*6*, *20*, *21*). The reproducibility and sensitivity of our methods were revealed by comparisons between wild-type axonemes and a previously characterized *IDA* mutant (*pf9-3*) (*23*) that fails to assemble the I1 dynein (fig. S2). Tomographic slices through this region in wild-type axonemes revealed at least three densities: the two I1 motor domains and the DIC/DLC complex (Fig. 3, A and C; Fig. 5D; fig. S2, B to F; movies S3 and S5) missing in the *pf9-3* mutant (Fig. 3, B and D; fig. S2, G to K; movies S4 and S5). The DIC/DLC complex of I1 (*6*, *20*, *21*) made contact with neighboring structures in both ODA and IDA regions (Fig. 3, A and C; Fig. 5D). One of these contacts corresponded to the proximal OID linker, which is consistent with known interactions between ODA components and the I1 subunits DIC138 and DLC7b (*24*).

ET of the IDAs identified five additional globular domains per 96-nm repeat; these domains lay in the same row as one of the I1 motor domains and were of comparable size (Fig. 1G; Fig. 3, A to E; Fig. 5, C and D; fig. S4, E, H, and I; movie S6). We interpret such densities as the motor domains of five single-headed IDAs (Fig. 3, A to D; Fig. 5D]. The IDAs appeared attached to the A tubule by long tails (fig. S4, F to H); several of these inserted close to the base of both radial spokes and/or below the DRC, which is consistent with the failure of certain IDAs to assemble in *DRC* mutants (*21*, *25*).

Each of the IDA and ODA motor domains was situated with its surface ~12 nm from the adjacent B tubule (Fig. 5C and fig. S4I). This distance is consistent with the length of the MT-binding stalk that projects from isolated dynein motor domains (*17*), suggesting that all of these dyneins could interact with the B tubule and contribute to force production. MT-binding stalks were visible in only a few averages [Fig. 1, D and E; movie S2), suggesting that their positions were variable, as one would expect for structures that adopt various conformations.

The nexin link associates with the dynein regulatory complex. Nexin was identified in early EM of axonemes (*4*) as a flexible protein that connects neighboring doublet MTs (Fig. 1G; Fig. 3, F to J; fig. S3) (*6*, *26*, *27*). Nexin is thought to contribute elastic resistance that converts doublet sliding into axoneme bending (*4*, *26*). In our images, one end of the *Chlam-*

ydomonas nexin formed a bifurcated attachment to the B tubule (Fig. 3, F, G, and J; fig. S3, A and B); the other was attached to the A tubule close to the base of the second radial spoke, adjacent to the DRC (Fig. 3, F, G, I, and J; fig. S3, D to G).

The crescent-shaped density of the DRC made contact with both ODAs and IDAs, as well as with radial spoke 2 (Figs. 3 and 5, C and D). A considerable fraction of the mass connected with the DRC extended some nanometers from the surface of the A tubule (Figs. 3I and 5C; movies S3 to S6). Indeed, nexin appeared to form a major part of the DRC (*20*, *26*). These images support a model in which the DRC and nexin interact with and mediate regulatory signals between the radial spokes and both inner and outer dynein arms (*20*, *21*, *26*).

The axonemes we studied were more or less straight, but even so nexin was longer (~40 nm) than the shortest distance between adjacent doublets (~30 nm) (Fig. 3F and fig. S3, A to E). Moreover, the part of the link that connected the A-MT anchor and B-MT bifurcation point appeared as a zigzag structure (Fig. 3, F, G, and I; fig. S3, A to E). This configuration may provide a reservoir of folded protein that could contribute to both the overall length extension and to the elastic restoring force that nexin is thought to provide for doublet MT sliding.

Structures on the inner surfaces of doublet microtubules might increase their stability. Doublet MTs are notable for both their unusual architecture and their stability as compared with cytoplasmic MTs. The A tubule was a complete cylinder of 13 protofilaments (A1 to A13), but the B tubule contained only 11 filaments (B1 to B11), one of which (B11) looked thinner than the others (Fig. 1, C and F; Fig. 4, D, E, H, and I) (*28*). The A tubule appeared slightly oval in cross sections (Fig. 1, C and F; Figs. 2A and 4D). Many proteins associate with the outer surfaces of doublet MTs, but we did not expect to find periodic densities on the inner surfaces of A and B tubules in both sea urchin (Fig. 4, G to I) and *Chlamydomonas* axonemes (Fig. 4, A to F; fig. S2, D to F and I to K). Averages of 96-nm repeats revealed three MT inner proteins (MIPs) that differed in location, size, and periodicity. MIP1 was the smallest. It lay next to protofilament A5 and showed 8-nm periodicity along the MT axis [Fig. 4, A, D, G, and H; purple dot in Fig. 4, E and F, and Fig. 5C]. MIP2 was larger, was positioned between protofilaments

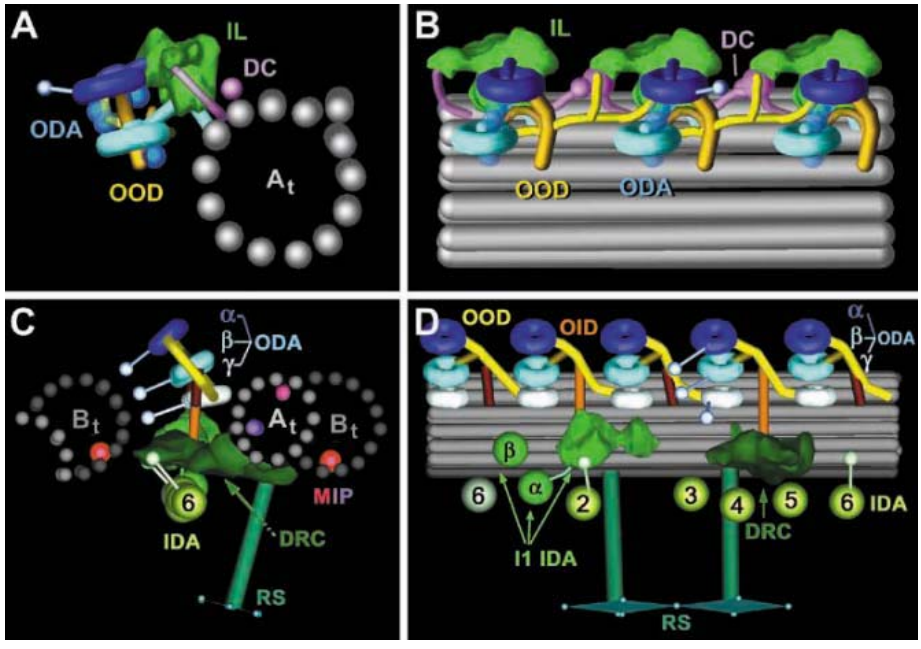

Fig. 5. Summarizing models of the ODA row in the sea urchin sperm flagellum (**A** and **B**) and the 96-nm repeat in *Chlamydomonas* axonemes (**C** and **D**). (A) and (C) are viewed from the distal end; in (B) and (D), the proximal end is at left. (A) and (B) show the ODA row, the OOD linker (yellow), IL (green), DC (pink), and additional densities surrounding the dynein motor domains (blue). These seem to form supporting structures around the ODA complexes. [(C) and (D)] MT-associated structures in *Chlamydomonas* axonemes. α and β, 1-alpha and 1-beta DHC of the I1 complex; 2 to 6, single-headed IDAs; alpha (α), beta (β), and gamma (γ)–ODA, DHCs of the ODAs; OID linker (orange area); OOD linker (yellow area).

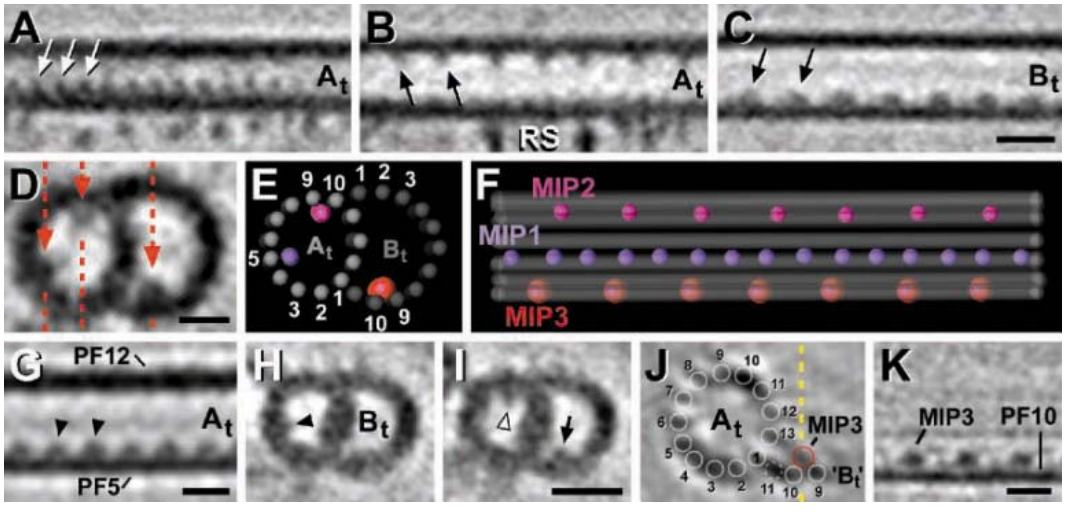

Fig. 4. MIPs in sea urchin sperm [(G) and (I)] and *Chlamydomonas* axonemes [(A) to (F), (J), and (K)]. In longitudinal views [(A) to (C), (F), (G), and (K)], the proximal end is at left; in cross sections [(D), (E), and (H) to (J)], the view is from the distal end. (**A** to **D**) Slices of MT doublets showing periodic densities attached to the inner MT wall (arrows). Dashed lines in (D) indicate the positions of the slices depicted in [(A), MIP1], [(B), MIP2], and [(C), MIP3]. The MIPs show 8-nm [white arrows in (A)] or 16-nm [black arrows in (B) and (C)] periodicities, respectively. (**E** and **F**) Graphic model of a 96-nm repeat showing MIPs (purple, MIP1; pink, MIP2; red, MIP3) relative to the protofilaments (numbered) of A_t and B_t. (**G** to **I**) MIP1 [black arrowheads in (G) and (H)], MIP2 [white arrowhead in (I)], and MIP3 [black arrow in (I)] in outer doublets of sea urchin sperm flagella. (**J** and **K**) MT doublet with protofilaments 1 to 13 of A_t, but only protofilaments 9 to 11 of the B_t tubule. MIP3 is still present, suggesting that it may enhance the stability of protofilaments 9 to 11 of this tubule. The dotted yellow line in (J) indicates the orientation of the slice in (K). The image quality of the partial doublet is lower than that of other averages because there were no other doublets with similar protofilament losses at other orientations relative to the missing wedge to help compensate for the missing information; the anisotropy of the resolution is obvious, especially along the *z* axis [horizontal in (J)]. Scale bars, 20 nm in (C) and (I) and 10 nm in (D), (G), and (K).

A9 and A10, and showed 16-nm periodicity [Fig. 4, B, D, and I; pink dot in Fig. 4 (E and F) and Fig. 5C]. MIP3 was the largest and lay between protofilaments B9 and B10 with 16 nm-periodicity [Fig. 4, C, D, and I; red dot in Fig. 4, E and F, and Fig. 5C]. The MIPs were present in all outer doublets and in both sea urchin (Fig. 4, G to I) and *Chlamydomonas* (Fig. 4, A to F), suggesting that they are universal features of axonemes. Although material has previously been seen in the lumen of doublets from insect and human sperm (*29*), MIPs have not been recognized as a consistent, periodic feature of outer doublets. Images of homogenized, high salt–extracted sea urchin sperm flagella also revealed features inside doublet MTs (*30*), but this study was limited by nonphysiological conditions and by the anisotropic resolution that is characteristic of single-axis tomography (fig. S1).

Doublet MTs treated with increasing concentrations of ionic detergents dissolve in a defined sequence: first the outer portion of the B tubule, then the rest of the B tubule, followed by the outer portion of the A tubule and then the remainder of the A tubule, leaving a ribbon of three protofilaments (*31*). Our axonemes were incubated in physiological buffers, but occasionally they contained a few partially dissolved doublets that were consistent with this pattern of disintegration. In one example, the A tubule was intact, but only protofilaments B9 to B11 remained; these still bound MIP3 (Fig. 4, J and K), suggesting that MIPs give structural stability to MTs protofilaments. Several small ligands, such as Taxol, interact with the luminal side of the MT wall and affect polymer stability (*32*). Perhaps MIPs alter doublet stability in a similar way. Doublet stability may also be affected by the especially robust ribbon of three protofilaments that include tubulin, tektin, and several tightly associated proteins (*28*). Tektin may also associate with the DRC and IDAs (*33*). Notably, MIP1 was in the A tubule close to the DRC, and MIP3 was in the B tubule near the attachment of nexin (Fig. 5C). Perhaps the MIPs provide structural reinforcement at sites of mechanical stress and information transfer. The further characterization of these proteins may provide valuable physiological and therapeutic insights.

Future comparisons between wild-type and mutant axonemes should help to define the function of additional components in the axoneme. Work on mutant axonemes from human patients may also help to clarify the underlying causes of diseases related to flagellar and ciliary dysfunction. Given the complexity of axoneme structure and the biological importance of its many functions, cryo-ET is likely to play a major role in clarifying both the normal and abnormal mechanisms of this conserved biological machine.

References and Notes

1. M. E. Porter, W. S. Sale, *J. Cell Biol.* **151**, F37 (2000).
2. E. F. Smith, P. Yang, *Cell Motil. Cytoskeleton* **57**, 8 (2004).
3. J. Pan, Q. Wang, W. J. Snell, *Lab. Invest.* **85**, 452 (2005).
4. G. B. Witman, J. Plummer, G. Sander, *J. Cell Biol.* **76**, 729 (1978).
5. M. Sakato, S. M. King, *J. Struct. Biol.* **146**, 58 (2004).
6. U. W. Goodenough, J. E. Heuser, *Structure of the Soluble and in Situ Ciliary Dyneins Visualized by Quick-Freeze Deep-Etch Microscopy,* vol. 1 of *Cell Movement*, F. P. Warner, Ed. (Liss, New York, 1989).
7. I. R. Gibbons, *J. Cell Biol.* **91**, 107s (1981).
8. P. Lupetti *et al.*, *Cell Motil. Cytoskeleton* **62**, 69 (2005).
9. Materials and methods are available as supporting material on *Science* Online.
10. J. Frank, *Electron Tomography: Three-Dimensional Imaging with the Transmission Electron Microscope* (Plenum, New York, 1992).
11. A. J. Koster *et al.*, *J. Struct. Biol.* **120**, 276 (1997).
12. D. Nicastro, J. R. McIntosh, W. Baumeister, *Proc. Natl. Acad. Sci. U.S.A.* **102**, 15889 (2005).
13. S. A. Burgess, M. L. Walker, H. Sakakibara, P. J. Knight, K. Oiwa, *Nature* **421**, 715 (2003).
14. M. P. Koonce, M. Samso, *Trends Cell Biol.* **14**, 612 (2004).
15. H. Sakakibara, S. Takada, S. M. King, G. B. Witman, R. Kamiya, *J. Cell Biol.* **122**, 653 (1993).
16. S. Takada, R. Kamiya, *J. Cell Biol.* **126**, 737 (1994).
17. S. A. Burgess, P. J. Knight, *Curr. Opin. Struct. Biol.* **14**, 138 (2004).
18. S. A. Burgess, S. D. Dover, D. M. Woolley, *J. Cell Sci.* **98**, 17 (1991).
19. G. B. Witman, N. Minervini, *Symp. Soc. Exp. Biol.* **35**, 203 (1982).
20. D. N. Mastronarde, E. T. O'Toole, K. L. McDonald, J. R. McIntosh, M. E. Porter, *J. Cell Biol.* **118**, 1145 (1992).
21. L. C. Gardner, E. O'Toole, C. A. Perrone, T. Giddings, M. E. Porter, *J. Cell Biol.* **127**, 1311 (1994).
22. R. Kamiya, *Int. Rev. Cytol.* **219**, 115 (2002).
23. S. H. Myster, J. A. Knott, E. O'Toole, M. E. Porter, *Mol. Biol. Cell* **8**, 607 (1997).
24. L. M. DiBella *et al.*, *Mol. Biol. Cell* **15**, 4633 (2004).
25. G. Piperno, K. Mead, M. LeDizet, A. Moscatelli, *J. Cell Biol.* **125**, 1109 (1994).
26. D. M. Woolley, *J. Cell Sci.* **110**, 85 (1997).
27. C. B. Lindemann, L. J. Macauley, K. A. Lesich, *Biophys. J.* **89**, 1165 (2005).
28. D. Nojima, R. W. Linck, E. H. Egelman, *Curr. Biol.* **5**, 158 (1995).
29. B. A. Afzelius, R. Dallai, S. Lanzavecchia, P. L. Bellon, *Tissue Cell* **27**, 241 (1995).
30. H. Sui, K. H. Downing, *Nature*, **442**, 475 (2006).
31. G. B. Witman, K. Carlson, J. Berliner, J. L. Rosenbaum, *J. Cell Biol.* **54**, 507 (1972).
32. K. H. Downing, *Annu. Rev. Cell Dev. Biol.* **16**, 89 (2000).
33. H. A. Yanagisawa, R. Kamiya, *Mol. Biol. Cell* **15**, 2105 (2004).

34. We thank R. Linck for helpful discussions, D. Mastronarde for help with image processing, and the National Center for Research Resources (grant RR 000592 to J.R.M.) and NIH (grant 2R37-GM55667 to M.E.P.) for financial support.

Supporting Online Material

www.sciencemag.org/cgi/content/full/313/5789/944/DC1
Materials and Methods
SOM Text
Figs. S1 to S4
References
Movies S1 to S6

11 April 2006; accepted 5 July 2006
10.1126/science.1128618

REPORTS

Electronically Induced Atom Motion in Engineered $CoCu_n$ Nanostructures

Joseph A. Stroscio,[1]* Francesca Tavazza,[2] Jason N. Crain,[1] Robert J. Celotta,[1] Anne M. Chaka[2]

We have measured the quantum yield for exciting the motion of a single Co atom in $CoCu_n$ linear molecules constructed on a Cu(111) surface. The Co atom switched between two lattice positions during electron excitation from the tip of a scanning tunneling microscope. The tip location with highest probability for inducing motion was consistent with the position of an active state identified through electronic structure calculations. Atom motion within the molecule decreased with increased molecular length and reflected the corresponding variation in electronic structure.

Atom manipulation with the scanning tunneling microscope (STM) is accomplished by using a tunable chemical bond between the adatom and the scanning tip and/or local electronic excitations via the tunneling electrons (*1*–*3*). The dynamics of atomic motion during such processes can be followed by analyzing the noise in the tunneling signal (*4*, *5*). Such atomic motion is ultimately controlled by both the energy landscape and the type of excitation and relaxation pathways the atoms encounter, as revealed by recent tunneling noise spectroscopy studies for single atoms and small molecules (*6*–*11*). Through clever design of molecular configurations, energy barriers can be engineered to facilitate long-range motion in larger molecular nanostructures (*12*).

In this report, we demonstrate that motion of a single atom within a larger nanostructure can be induced by using electron excitation mechanisms in the STM. The use of tunneling noise spectroscopy measurements, together with den-

[1]Center for Nanoscale Science and Technology, [2]Chemical Science and Technology Laboratory, National Institute of Standards and Technology, Gaithersburg, MD 20899–8412, USA.

*To whom correspondence should be addressed. E-mail: joseph.stroscio@nist.gov

sity functional calculations, allows us to study molecular stability and the energy barriers hindering atom motion, each as a function of nanostructure size. In the $CoCu_n$ linear structures we studied, we mapped the probability for inducing motion and found it is localized on the atomic scale but is not centered over the adatom whose movement is induced. These probability maps are found to be consistent with the location of a resonant state that overlaps the Fermi edge (chemically active "frontier" molecular orbitals). We also show how to use the quantum electronic structure of the linear nanostructure to "tune" the atom dynamics by changing the energy barriers for motion.

We built $CoCu_n$ linear chain nanostructures by using STM atom manipulation techniques (*1*–*3*, *13*). The construction began by bringing together two Cu atoms to form a Cu_2 dimer and then attaching a single Co atom to the dimer (fig. S1, A to C). The Co atom resides in the same face-centered cubic (fcc) site as the Cu atoms, resulting in a linear configuration (Fig. 1A). The Co atom can be induced to switch to the nearby hexagonal close-packed (hcp) site to create a canted molecular configuration (Fig. 1B). This switching occurred when inelastic electron tunneling injected energy into the Co-Cu bonds and caused vibrational excitation (fig. S1C and Fig. 1C). Noise features in the STM topograph are seen on the left side of the Co atom, corresponding to imaging the Co atom in the linear configuration (Fig. 1A) part of the time and in the canted configuration (Fig. 1B) at other times as the image is acquired. Noise features were not observed at very low tunneling biases, which produced an image of a stationary linear molecule. Low-frequency (~1 Hz) noise, on the time scale of the STM scan, was observed to begin at ~10 mV bias (Fig. 1C) and suggested an energy threshold for atom motion.

The tunneling noise associated with the Co atom in the $CoCu_2$ molecule switching between the fcc and hcp sites exhibits two-state random telegraph noise characteristics (Fig. 1D inset). Random telegraph noise is associated with an exponentially distributed residence time distribution (Fig. 1D), which is fit to yield the average residence time, τ, for the atom in a particular state. Insight into the mechanisms and energy barriers for the atom motion can be obtained from determining the atom transfer rate, $R = \tau^{-1}$, and quantum yield (probability of switching per tunneling electron), $(I\tau/e)^{-1}$, as a function of tunneling current, I, and voltage, V (*4*–*11*). For the $CoCu_2$ molecule and a tunneling bias voltage of 40 mV, the transfer rate for the Co atom from the fcc site is observed to vary as a power law in the tunneling current, I^N, where $N = 1.3 \pm 0.1$ (Fig. 2B). The near-unity value of N implies a predominantly single-electron process for switching the Co atom in the $CoCu_2$ molecule.

A clear, single voltage threshold of ~15 mV, largely independent of the initial current setpoint, was observed in the quantum yield measurements (Fig. 2A). The nearly constant quantum yield above threshold is consistent with the near-unity power-law dependence of transfer rate versus current, because the tunneling current is linear in bias voltage in this voltage range. We interpret these results by using a model where the Co atom overcomes the po-

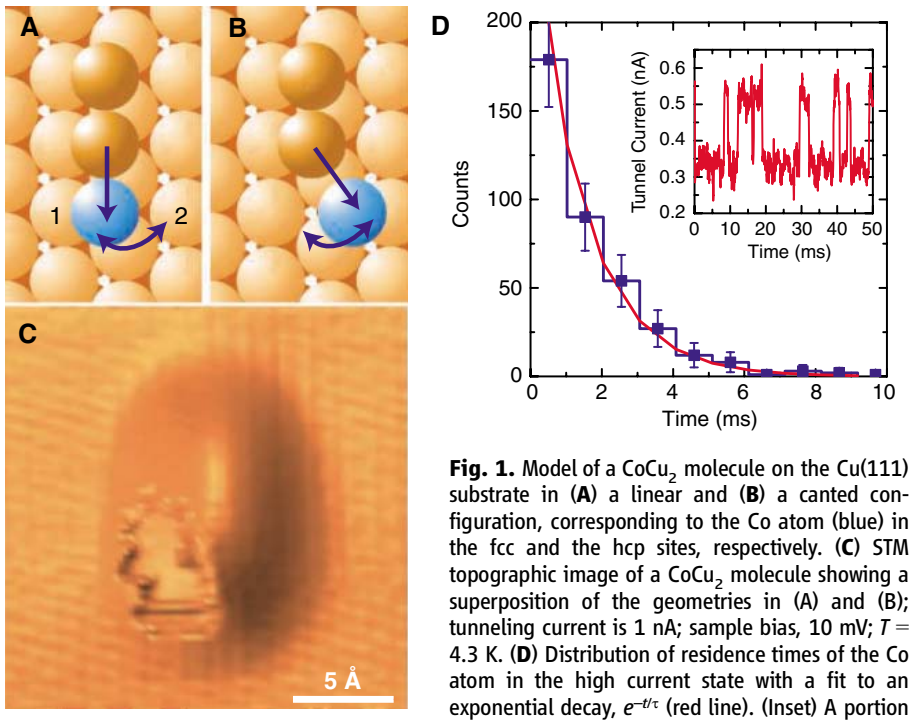

Fig. 1. Model of a $CoCu_2$ molecule on the Cu(111) substrate in (**A**) a linear and (**B**) a canted configuration, corresponding to the Co atom (blue) in the fcc and the hcp sites, respectively. (**C**) STM topographic image of a $CoCu_2$ molecule showing a superposition of the geometries in (A) and (B); tunneling current is 1 nA; sample bias, 10 mV; T = 4.3 K. (**D**) Distribution of residence times of the Co atom in the high current state with a fit to an exponential decay, $e^{-t/\tau}$ (red line). (Inset) A portion of the tunneling current–versus–time trace obtained in the left vicinity of the Co atom in the $CoCu_2$ molecule at 15.4 mV sample bias.

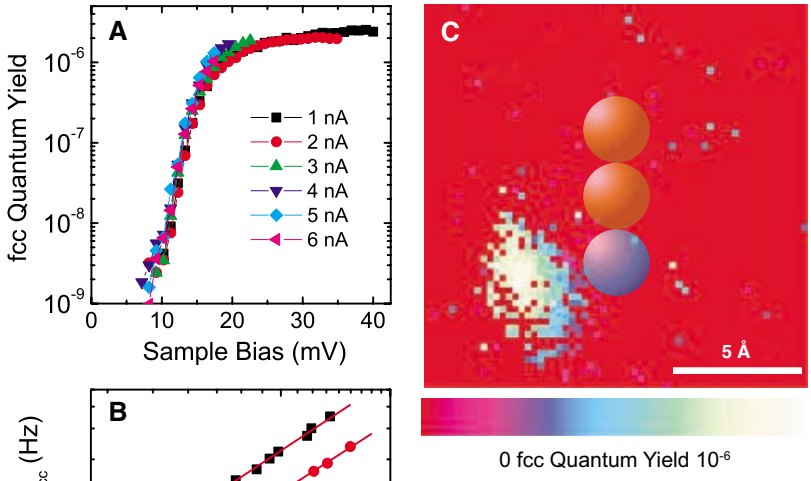

Fig. 2. (**A**) Fcc quantum yield as a function of sample bias at fixed tip-sample separation. Symbols correspond to different set-point currents for each measurement. The tip-sample separation varied by 0.75 Å when changing the current set point from 1 to 6 nA at 40 mV sample bias. (**B**) Transfer rate for the Co atom out of the fcc site as a function of tunneling current obtained at a fixed sample bias of 40 mV for the $CoCu_2$ molecule. The three curves were obtained at different locations near the Co atom and are fit to I^N (red lines). The average of the three data sets yields $N = 1.3 \pm 0.1$ (red lines). (**C**) Simultaneous spatial images of the quantum yield and STM topography (not shown) for the $CoCu_2$ molecule; sample bias, 40 mV; tunnel current, 1 nA; T = 4.3 K. Positions of the Co (blue) and Cu (gold) atoms are schematically superimposed on the quantum yield image.

tential barrier between fcc and hcp sites via an inelastic electron tunneling excitation. In the resonance tunneling model (*14*–*17*), a small fraction of electrons tunnels inelastically into a $CoCu_2$ state to create a positive- or negative-ion resonance state. While an electron is temporarily trapped in this state, the $CoCu_2$ molecular ion resides on an excited-state potential until the resonance decays on the time scale of femtoseconds and leaves the molecule in an excited vibrational state. If the electron energy is sufficient to place this excited vibrational state near the top of the potential barrier, bond breaking can occur. When the energy relaxation rate is much faster than the tunneling rate, a single-step or few-steps excitation is favored; bond breaking occurs after a minimum number of inelastic scattering events contributes a total energy sufficient to overcome the potential barrier. In this resonance tunneling model, the voltage threshold of ~15 mV corresponds to the potential barrier height for the Co atom in the $CoCu_2$ molecule to transfer between fcc and hcp sites.

We also examined the spatial distribution of the excitation probability for inducing motion. Naïvely, we might expect the probability to be centered over the atom of interest. The STM topographic image in Fig. 1C, however, shows that Co atom switching is only observed when the STM probe tip is in a certain location. More detailed measurements were made by recording the tunneling noise spectrum at each pixel along with the STM topography to obtain simultaneous atom dynamics and STM topographic data. The noise spectra at each lateral position were analyzed to obtain a spatial map of transfer rates and quantum yields for leaving the fcc and the hcp sites. The spatial map of the quantum yield (Fig. 2C) for Co atom motion for the $CoCu_2$ molecule shows that the probability for inducing motion is localized on the atomic scale and is positioned to the left of the Co atom. Density functional theory (DFT) calculations link the vibrational coupling excitation to a resonant *d* state localized on the Co atom (Fig. 3, A and C). The localized position of the quantum yield (Fig. 2C) is consistent with the calculated density of states at the Fermi level (E_F), which shows a maximum to the left of the Co atom, and demonstrates the need to inject energy into the appropriate Co-Cu substrate bond (Cu atom labeled no. 1 in Fig. 1A) to move the Co atom from the favored fcc site. This insight raises the possibility that molecular orbital analysis may be used to guide the design and the control of single-atom manipulation by STM in nanostructures.

Varying the Cu chain length affects the quantum electronic states of the molecule (*18*), in turn influencing the atom dynamics. We systematically varied the $CoCu_n$ molecular structure by building longer Cu segments. Topographic images of $CoCu_n$ molecules with *n* values from 2 to 5 display a varying degree of tunneling noise near the Co atom (Fig. 3B). The noise feature is seen to diminish with longer molecular length and is almost absent when *n* reaches 5, indicating increased stability of the Co atom in the fcc site. DFT calculations elucidate the electronic origins for this trend, focusing on a state (Fig. 3A) that is both localized near the Co atom and important at low tunneling bias voltages. Analysis of the calculated density of states shows a depletion of active Co *d* states at E_F as the molecular chain length increases. This depletion of active states at E_F is consistent with the observed lower quantum yield for motion (Fig. 4A).

In addition to the overall reduction in quantum yield, the threshold voltage for excitation appears to shift to higher energy with longer molecular length (Fig. 4A). This shift indicates that the Co atom at the fcc site experiences a higher potential barrier to transfer from the fcc to the hcp site. By directly comparing the energies of the linear and canted configurations (Fig. 1, A and B), DFT calculations once more provide an understanding of the atom motion. Figure 4B shows the variation in energy as the

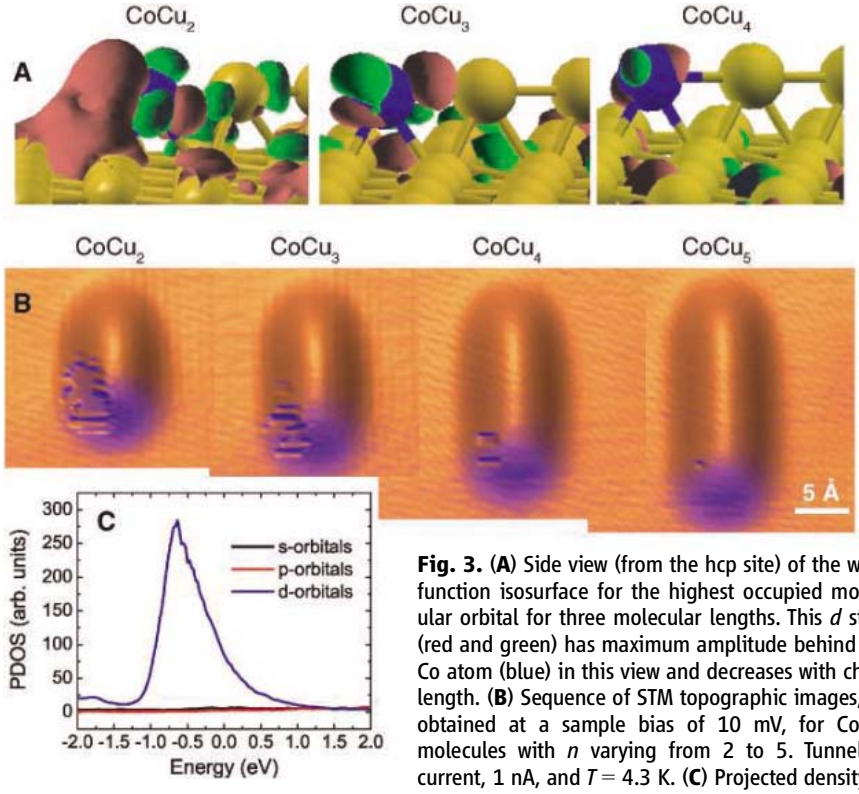

Fig. 3. (**A**) Side view (from the hcp site) of the wave function isosurface for the highest occupied molecular orbital for three molecular lengths. This *d* state (red and green) has maximum amplitude behind the Co atom (blue) in this view and decreases with chain length. (**B**) Sequence of STM topographic images, all obtained at a sample bias of 10 mV, for $CoCu_n$ molecules with *n* varying from 2 to 5. Tunneling current, 1 nA, and $T = 4.3$ K. (**C**) Projected density of states (PDOS, in arbitrary units) of Co in the $CoCu_2$ molecule on the Cu(111) surface.

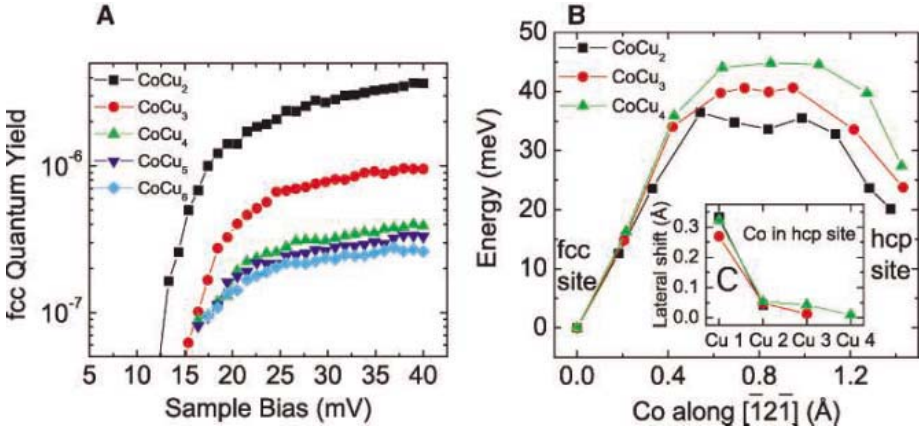

Fig. 4. (**A**) Fcc quantum yield for the Co atom for the various $CoCu_n$ molecules. (**B**) DFT calculations of the energy path for the Co moving from the fcc site (linear configuration) to the hcp site (canted configuration) for three molecular lengths. (**C**) The absolute value of the displacement of the Cu chain atoms with respect to their fcc position for the canted configuration.

Co atom moves from the fcc site to the hcp site for three molecular lengths. As the Cu chain increases, so does the energy difference between fcc and hcp sites and the energy barrier dividing them (Fig. 4B). These trends correspond to a stabilization of the linear configuration of the molecule and explain the experimental observation of increased stability of the fcc site as n increases (Figs. 3B and 4A). The motion of the Co atom becomes progressively hindered as the Cu chain length increases, because more atoms in the Cu chain must bend away from their energetically favored fcc positions, as is illustrated in Fig. 4C, where the resulting lateral shifts of the Cu chain atoms from their ideal positions are plotted for different chain lengths.

Because the smallest atomic-scale switch will likely involve modulating the electrical conductivity through the control of a single atom, the extension of studies such as this to semiconductor and insulating thin films could point the way to new classes of atomic-scale electronic and magnetic devices.

References and Notes

1. D. M. Eigler, E. K. Schweizer, *Nature* **344**, 524 (1990).
2. J. A. Stroscio, D. M. Eigler, *Science* **254**, 1319 (1991).
3. L. Bartels, G. Meyer, K.-H. Rieder, *Phys. Rev. Lett.* **79**, 697 (1997).
4. D. M. Eigler, C. P. Lutz, W. E. Rudge, *Nature* **352**, 600 (1991).
5. B. C. Stipe, M. A. Rezaei, W. Ho, *Science* **279**, 1907 (1998).
6. T. Komeda, Y. Kim, M. Kawai, B. N. J. Persson, H. Ueba, *Science* **295**, 2055 (2002).
7. A. J. Heinrich, C. P. Lutz, J. A. Gupta, D. M. Eigler, *Science* **298**, 1381 (2002); published online 24 October 2002 (10.1126/science.1076768).
8. W. Ho, *J. Chem. Phys.* **117**, 11033 (2002).
9. J. I. Pascual *et al.*, *Nature* **423**, 525 (2003).
10. J. A. Stroscio, R. J. Celotta, *Science* **306**, 242 (2004); published online 9 September 2004 (10.1126/science.1102370).
11. M. Lastapis *et al.*, *Science* **308**, 1000 (2005).
12. K.-Y. Kwon *et al.*, *Phys. Rev. Lett.* **95**, 166101 (2005).
13. Measurements were made in a cryogenic ultrahigh-vacuum STM instrument of our own design. We deposited Co and Cu atoms onto a Cu(111) surface, which was initially cleaned by ion sputtering and annealing. Co and Cu atoms can be chemically distinguished on the Cu(111) surface on the basis of STM spectroscopy measurements of the Co Kondo resonance. STM measurements were made by using Ir probe tips and a substrate temperature of 4.3 K.
14. B. N. J. Persson, A. Baratoff, *Phys. Rev. Lett.* **59**, 339 (1987).
15. J. W. Gadzuk, *Phys. Rev. B* **44**, 13466 (1991).
16. G. P. Salam, M. Persson, R. E. Palmer, *Phys. Rev. B* **49**, 10655 (1994).
17. S. Gao, M. Persson, B. I. Lundqvist, *Phys. Rev. B* **55**, 4825 (1997).
18. S. Fölsch, P. Hyldgaard, R. Koch, K. H. Ploog, *Phys. Rev. Lett.* **92**, 056803 (2004).

19. We thank S. Blankenship for technical assistance and are grateful for several fruitful discussions with J. W. Gadzuk, D. Penn, and M. Stiles. This work was supported in part by the Office of Naval Research.

Supporting Online Material

www.sciencemag.org/cgi/content/full/313/5789/948/DC1
Fig. S1

10 May 2006; accepted 11 July 2006
10.1126/science.1129788

Controlling the Electronic Structure of Bilayer Graphene

Taisuke Ohta,[1,2]* Aaron Bostwick,[1]* Thomas Seyller,[3] Karsten Horn,[2] Eli Rotenberg[1]†

We describe the synthesis of bilayer graphene thin films deposited on insulating silicon carbide and report the characterization of their electronic band structure using angle-resolved photoemission. By selectively adjusting the carrier concentration in each layer, changes in the Coulomb potential led to control of the gap between valence and conduction bands. This control over the band structure suggests the potential application of bilayer graphene to switching functions in atomic-scale electronic devices.

Carbon-based materials such as carbon nanotubes (CNTs), graphite intercalation compounds, fullerenes, and ultrathin graphite films exhibit many exotic phenomena such as superconductivity (*1*–*3*) and an anomalous quantum Hall effect (*4*–*6*). These findings have caused renewed interest in the electronic structure of ultrathin layers of graphite, such as graphene: a single hexagonal carbon layer that is the building block for these materials. There is a strong motivation to incorporate graphene multilayers into atomic-scale devices, spurred on by rapid progress in their fabrication and manipulation.

We studied the valence band (VB) structure of a bilayer of graphene and demonstrated that through selective control of the carrier concentration in the graphene layers, one can easily tune the band structure near the Dirac crossing. Similar control can be achieved in principle by varying the electric field across the bilayer film in an atomic-scale switching device.

The electronic states of graphene can be well described within basic calculational schemes (*7*–*9*). Graphene is a flat layer of carbon atoms arranged in a hexagonal lattice with two carbon atoms per unit cell. Of the four valence states, three sp^2 orbitals form a σ state with three neighboring carbon atoms, and one p orbital develops into delocalized π and π* states that form the highest occupied VB and the lowest unoccupied conduction band (CB). The π and π* states of graphene are degenerate at the corner (K point) of the hexagonal Brillouin zone (BZ) (Fig. 1A). This degeneracy occurs at the so-called Dirac crossing energy E_D, which at the normal half-filling condition coincides with the Fermi level (E_F), resulting in a pointlike metallic Fermi surface (Fig. 2E).

Strictly speaking, undoped graphene is a semimetal because although there is a state crossing at $E_D = E_F$, the density of states there is zero and conduction is possible only with thermally excited electrons at finite temperature. In applying an effective mass description for the VB and CB (*7*), one arrives at a formal equivalence between the resulting differential equation and the Dirac equation, hence charge carriers in the vicinity of E_F may be termed "Dirac fermions" (with the crossing point at K being named the Dirac point). Moreover, the particular band structure at the BZ boundary (that is, a linear dispersion) leads to an effective mass $m^* = 0$ at the point where the VB and CB meet. The peculiar band structure in ultrathin graphite layers results in a number of unusual electronic transport properties, such as an anomalous quantum Hall effect (*4*–*6*, *10*).

The graphene band structure is sensitive to the lattice symmetry. If the hexagonal layer structure is composed of nonequivalent elements, such as in boron nitride, the lateral, in-plane symmetry is broken, resulting in the formation of a large gap between π and π* states (*11*). The symmetry can also be broken with respect to the c axis by stacking two graphene layers in Bernal stacking (the stacking fashion of graphite) as suggested by McCann and Fal'ko (*12*) (Fig. 1B). Because the unit cell of a bilayer contains four atoms, its band structure acquires two additional bands, π and π* states, in each valley split by interlayer (A-B) coupling, and two lower energy bands. If the individual graphene layers in a bilayer are rendered inequivalent (Fig. 1C), then an energy gap between low-energy bands forms at the former Dirac crossing point (*12*). Provided that the charge state is such that E_F lies within the gap, a semimetal-to-insulator transition occurs. If this symmetry breaking could be controlled externally, the electronic conductivity would change through this transition, suggesting that a switch with a thickness of two atomic layers could be constructed.

To see whether this gedanken experiment can be realized, we synthesized bilayer graphene

[1]Advanced Light Source, Lawrence Berkeley National Laboratory, One Cyclotron Road, Berkeley, CA 94720, USA. [2]Department of Molecular Physics, Fritz-Haber-Institut, der Max-Planck-Gesellschaft, Faradayweg 4-6, D-14195 Berlin, Germany. [3]Institut für Physik der Kondensierten Materie, Universität Erlangen-Nürnberg, Erwin-Rommel-Strasse 1, D-91058 Erlangen, Germany.

*These authors contributed equally to this work.
†To whom correspondence should be addressed.

films on a silicon carbide (SiC) substrate [6H polytype with (0001) orientation], following the recipe in (*13*), and measured their electronic properties using angle-resolved photoemission spectroscopy (ARPES) (*14*). As initially grown, our films had a slight *n*-type doping, acquired by depletion of the substrate's dopant carriers. Because we measured at low temperature, the dopant electrons in the SiC were frozen out and the substrate was a nearly perfect insulator, whereas the excess carriers left in the film, having been separated from their dopant atoms, had high mobility. Because the SiC states are well separated from both E_F and E_D [the SiC VB lies ~2.6 eV below E_F and the CB ~0.4 eV above E_F (*15*)], we can regard the bilayer graphene states as practically decoupled from the substrate and therefore as representing a true two-dimensional semimetal.

These films can sustain high current densities. At a temperature of 30 K, which is cold enough to preclude any conduction through the substrate, we can pass 400 mA through a macroscopic sample (5 by 15 mm), corresponding to a current of ~1 nA (10^{10} to ~10^{11} electrons/s) per graphene C atom, which is the same order of magnitude reported for single-walled CNTs (*16*) and graphene multilayers (*10*).

The symmetry of the bilayers is broken by the dipole field created between the depletion layer of the SiC and the accumulation of charge on the graphene layer next to the interface, rendering the two graphene layers inequivalent with respect to charge and electrostatic potential in the as-prepared films. We can induce further *n*-type doping by the deposition of potassium atoms onto the vacuum side, which donate their lone valence electrons to the surface layer, forming another dipole (*17*, *18*). These surface and interface dipole fields together act as the symmetry-breaking factor, which controls the presence or absence of the gap at the crossing energy E_D (Fig. 1, B and C). The net dipole field between the two graphene layers results from the short screening length (~4 Å) along the *c* axis (*7*), which is comparable to the layer thickness (~3.4 Å). A similar charge localization has been observed at the surface of graphite and graphene multilayers in an externally applied field (*19*, *20*).

Figure 2, A to C, shows the binding energy–momentum dispersion relation of π, π*, and σ states along high-symmetry directions measured by ARPES. The ~0.4-eV splitting of the π state (as in Fig. 1B) confirms that the sample is composed predominantly of two graphene layers (*14*). In Fig. 2, A and B, the crossing point E_D can be clearly observed because this bilayer is *n*-type–doped through carrier depletion from the SiC substrate. In the constant-energy contours in the momentum space of π and π* states near E_F (Fig. 2, D to F), we can clearly see the electron and hole pockets above and below E_D, respectively. Besides the primary bilayer graphene states, we can identify six weak replicas of the π and π* states surrounding the primary states, especially in Fig. 2F. Low-energy electron diffraction shows that graphene layers grown on the SiC substrate display a nearly commensurate superstructure with relative lattice constant ($6\sqrt{3} \times 6\sqrt{3}$) rotated 30° with respect to the substrate because of the difference between the graphene lattice constant of ~2.46 Å and that of SiC, 3.07 Å (*21*). The replicas of the π and π* states are presumably brought about by scattering off of this superstructure in a fashion similar to those in other nearly incommensurate systems (*22*, *23*).

The effects of doping the bilayers are shown in Fig. 3, which compares the as-prepared film (Fig. 3A) to two coverages of potassium. Our samples consisted predominantly of bilayer graphene, but depending on preparation conditions, we found minority regions of single- or triple-layer graphene within our probe area; the contribution of these minority domains has been subtracted from the data in Fig. 3. Beside the more or less rigid shift of the π and π* states toward higher binding energy because of an increased carrier concentration, the upper unoccupied π* state drops below E_F at n = 0.0125 electron per unit cell (Fig. 3B) and continues dropping down with higher potassium coverage. The electron carrier densities of each stage are determined from the relative sizes of the Fermi surfaces with respect to the surface BZ of graphite.

Plotted next to the intensity maps are calculated tight-binding bands (solid lines) (*12*), where the low-lying electronic states near the K point of the BZ are described by the solution of a simple 4 × 4 Hamiltonian as

$$\varepsilon_\alpha(k) = \pm\left[\frac{\gamma_1^2}{2} + \frac{U^2}{4} + \left(v^2 + \frac{v_3^2}{2}\right)k^2 + (-1)^\alpha\sqrt{\Gamma}\right]^{1/2}$$

where the band index α = 1,2 and

$$\Gamma = \frac{1}{4}(\gamma_1^2 - v_3^2k^2)^2 + v^2k^3(\gamma_1^2 + U^2 + v_3^2k^2) + 2\gamma_1 v_3 v^2 k^3 \cos 3\phi$$

and $v_3 = \sqrt{3}\, a\gamma_3/2\hbar$.

Here k is the momentum in Å^{-1}, ϕ is the azimuthal angle, v is the band velocity (m/s × $\hbar$ ×

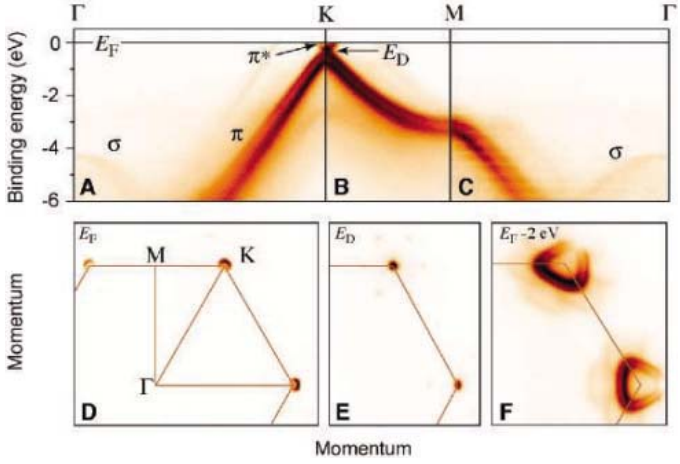

Fig. 2. Energy-momentum dispersion relation of π, π*, and σ states of bilayer graphene. (**A** to **C**) Energy-momentum dispersion along high-symmetry directions. (**D** to **F**) Constant energy contours at E_F, E_F –0.4 eV = E_D, and E_F –2 eV. The high-symmetry points, directions, and BZ zone boundaries are indicated in (D).

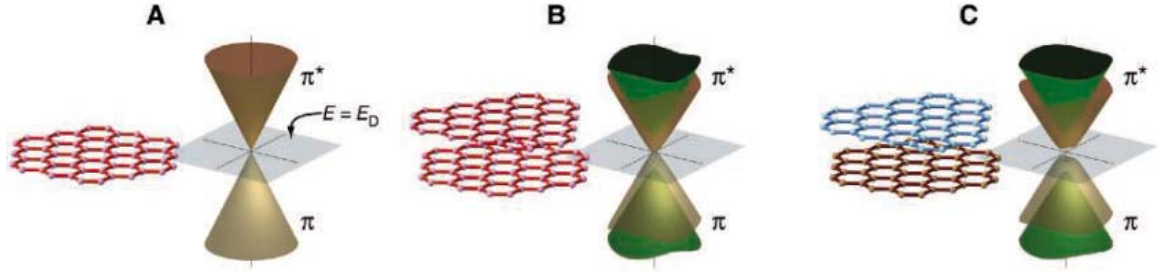

Fig. 1. Electronic structure of a single (**A**), symmetric double layer (**B**), and asymmetric double layer (**C**) of graphene. The energy bands depend only on in-plane momentum because the electrons are restricted to motion in a two-dimensional plane. The Dirac crossing points are at energy E_D.

10^{10}), U is the difference in the onsite Coulomb potentials of the two layers, γ_1 (eV) and γ_3 (eV) are out-of-plane nearest-neighbor and next–nearest-neighbor interaction parameters, and a (Å) is the graphite lattice constant (*24*, *25*). These parameters are adjusted to reproduce the measured band structures over a large energy range (*14*). U is chosen to match the gap at the K point.

The most important feature in Fig. 3 is the variation in the apparent gap at the K point: first open in Fig. 3A, then closed in Fig. 3B, and finally open again in Fig. 3C. This gap variation is reproduced by our tight-binding calculation and is attributed to the variation in the relative potentials of the two layers as discussed above. Away from the K point, the gap is generally smaller than the prediction because the cusps extending into the gap between the π and π* bands are much sharper than in the model. As a result, the gap for the uncovered film (Fig. 3A) is not clearly resolved, although a shift of the bands is readily apparent from the flattening of the π* band edge and the lack of spectral weight at E_D. Sufficient asymmetry was developed for higher doping that the gap is unambiguously open in Fig. 3C.

The measured π* state of bilayer graphene (Fig. 3C) does not agree with the tight-binding band, particularly around 200 meV below E_F, where a slight kink is observed in the bands. This is presumably due to electron mass renormalization by electron-phonon coupling.

In order to systematically follow the evolution of the gap between π and π* states, photoemission spectra at the K point (the center cut of the bands in Fig. 3) as a function of doping are shown in Fig. 4A. The blue markers are the positions of the tight-binding π and π* bands. The data and calculated energies of the π and π* states clearly display the closing and reopening of the gap. The yellow line is the energy difference $E_F - E_D$, which increases by about 0.32 eV with respect to the as-grown sample, reflecting the overall doping level of the film.

The variation of carrier concentration has a marked influence on the band structure as derived from a comparison of the experimental results with the tight-binding calculation (Fig. 4). The Coulomb potential difference U displays a sign change at the electron concentration where the gap closes. It is expected that U increases with an increase of the charge difference in either graphene layer, induced by the fields at the respective interfaces. We have estimated the potential of each graphene layer from Poisson's equation, based on the Schottky barrier height of 0.4 eV (*15*), assuming infinitely thick graphene multilayers, and find that for the as-prepared sample, the potential difference between the first and second layers shows reasonable agreement with the Coulomb potential difference U estimated from the size of the gap evaluated in the tight-binding model. The resulting electric field in the graphene layers is similar in magnitude to that induced in a device structure (*26*). Moreover, a monotonic increase is seen in γ_1, which measures the interlayer interaction as a function of electron concentration in both layers. This suggests that at higher electron density, the overlap between π orbitals of adjacent graphene layers increases. This may be due to the smaller interlayer distance caused by a shorter screening length.

Our results demonstrate that by controlling the carrier density in a bilayer of graphene, the occupation of electronic states near E_F and the magnitude of the gap between the VB and CB can be manipulated. We have chosen potassium doping as a means of achieving this, but the switching functionality may be readily induced by an electric field across the bilayer in a device structure, in such a way that the potentials on either layer have opposite sign (*10*). The deposition of alkali atoms on epitaxially grown multilayer graphene films thus provides, beyond an opportunity to obtain their wave vector–resolved electronic structure as reported here, a path to studying their physical properties in a devicelike context.

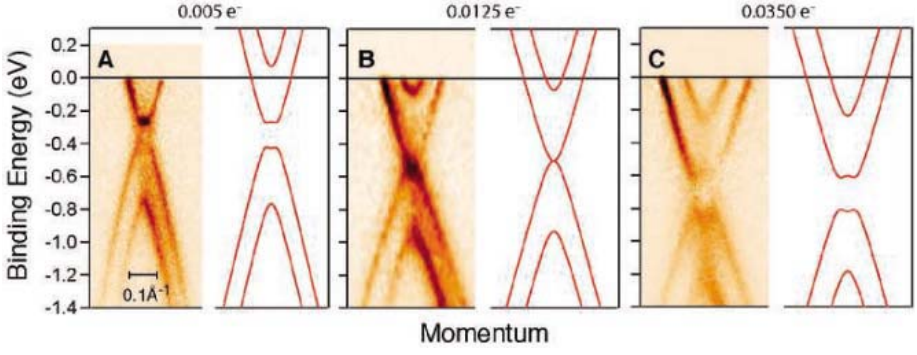

Fig. 3. Evolution of gap closing and reopening by changing the doping level by potassium adsorption. Experimental and theoretical bands (solid lines) (**A**) for an as-prepared graphene bilayer and (**B** and **C**) with progressive adsorption of potassium are shown. The number of doping electrons per unit cell, estimated from the relative size of the Fermi surface, is indicated at the top of each panel.

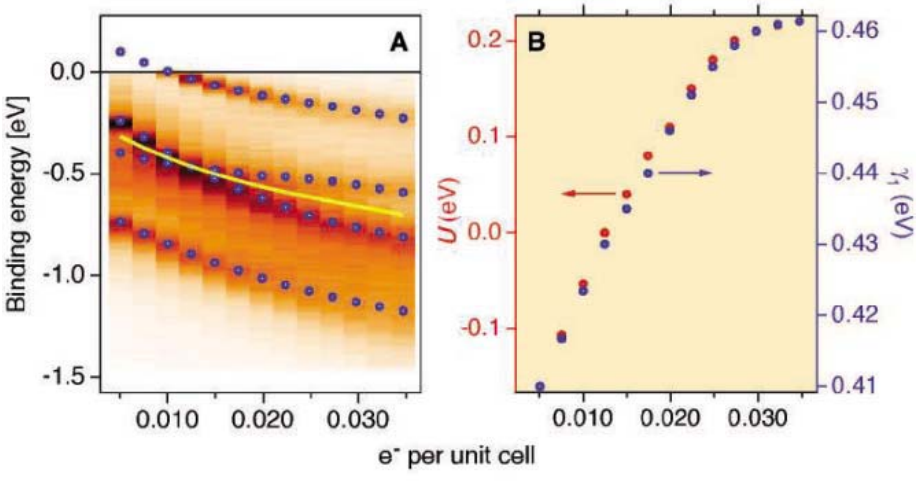

Fig. 4. Variation of states at the K point with increasing potassium coverage. (**A**) The image map shows the energy distribution curve at K as a function of potassium coverage. The blue markers are the fitted positions of the tight-binding π and π* bands, and the yellow line indicates E_D. The closing and reopening of the gap between π and π* states are clearly shown. (**B**) The influence of doping concentration on the band parameters U and γ_1.

References and Notes

1. Z. K. Tang *et al.*, *Science* **292**, 2462 (2001).
2. N. B. Hannay *et al.*, *Phys. Rev. Lett.* **14**, 225 (1965).
3. T. E. Weller, M. Ellerby, S. S. Saxena, R. P. Smith, N. T. Skipper, *Nat. Phys.* **1**, 39 (2005).
4. K. S. Novoselov *et al.*, *Nature* **438**, 197 (2005).
5. Y. Zhang, Y.-W. Tan, H. L. Stormer, P. Kim, *Nature* **438**, 201 (2005).
6. K. S. Novoselov *et al.*, *Nat. Phys.* **2**, 177 (2006).
7. D. P. DiVincenzo, E. J. Mele, *Phys. Rev. B* **29**, 1685 (1984).
8. P. R. Wallace, *Phys. Rev.* **71**, 622 (1947).
9. S. Reich, J. Maultzsch, C. Thomsen, P. Ordejón, *Phys. Rev. B* **66**, 035412 (2002).
10. K. S. Novoselov *et al.*, *Science* **306**, 666 (2004).
11. X. Blase, A. Rubio, S. G. Louie, M. L. Cohen, *Phys. Rev. B* **51**, 6868 (1995).
12. E. McCann, V. I. Fal'ko, *Phys. Rev. Lett.* **96**, 086805 (2006).
13. I. Forbeaux, J.-M. Themlin, J.-M. Debever, *Phys. Rev. B* **58**, 16396 (1998).
14. Information on materials and methods is available as supporting material on *Science* Online.
15. Th. Seyller, K.V. Emtsev, F. Speck, K.-Y. Gao, L. Ley, *Appl. Phys. Lett.* **88**, 242103 (2006).

16. Z. Yao, C. L. Kane, C. Dekker, *Phys. Rev. Lett.* **84**, 2941 (2000).
17. At 30 K, the mobility of the potassium atoms is substantially reduced as compared to that at 90 K, where the condensed phase of potassium atoms is found (*18*). It is thus reasonable to assume that the potassium atoms mainly adsorb onto and interact with the surface of the graphene layer in the low-temperature deposition we used (around 30 K).
18. K. M. Hock, R. E. Palmer, *Surf. Sci.* **284**, 349 (1993).
19. Y. Zhang, J. P. Small, W. V. Pontius, P. Kim, *Appl. Phys. Lett.* **86**, 073104 (2005).
20. K. S. Novoselov, F. Schedin, D. Jiang, A. A. Firsov, A. K. Geim, *Phys. Rev. B* **72**, 201401 (2005).
21. I. Forbeaux, J.-M. Themlin, J.-M. Debever, *Phys. Rev. B* **58**, 16396 (1998).
22. J. N. Crain, K. N. Altmann, C. Bromberger, F. J. Himpsel, *Phys. Rev. B* **66**, 205302 (2002).
23. Eli Rotenberg *et al.*, *Phys. Rev. Lett.* **91**, 246404 (2003).
24. J. C. Slonczewski, P. R. Weiss, *Phys. Rev.* **109**, 272 (1958).
25. J. W. McClure, *Phys. Rev.* **108**, 612 (1957).
26. S. V. Morozov *et al.*, *Phys. Rev. B* **72**, 201401 (2005).
27. This work and the Advanced Light Source were supported by the U.S. Department of Energy, Office of Basic Sciences. K.H. and T.O. were supported by the Max Planck Society and the European Science Foundation under the EUROCORES SONS program.

Supporting Online Material
www.sciencemag.org/cgi/content/full/313/5789/952/DC1
Materials and Methods
Figs. S1 to S3
References

31 May 2006; accepted 12 July 2006
10.1126/science.1130681

Two-Dimensional Nematic Colloidal Crystals Self-Assembled by Topological Defects

Igor Muševič,[1,2]* Miha Škarabot,[1] Uroš Tkalec,[1] Miha Ravnik,[2] Slobodan Žumer[2,1]

The ability to generate regular spatial arrangements of particles is an important technological and fundamental aspect of colloidal science. We showed that colloidal particles confined to a few-micrometer-thick layer of a nematic liquid crystal form two-dimensional crystal structures that are bound by topological defects. Two basic crystalline structures were observed, depending on the ordering of the liquid crystal around the particle. Colloids inducing quadrupolar order crystallize into weakly bound two-dimensional ordered structure, where the particle interaction is mediated by the sharing of localized topological defects. Colloids inducing dipolar order are strongly bound into antiferroelectric-like two-dimensional crystallites of dipolar colloidal chains. Self-assembly by topological defects could be applied to other systems with similar symmetry.

Dispersions of colloids or liquid droplets in a nematic liquid crystal show a diversity of self-assembled structures, such as linear chains (*1*, *2*), anisotropic clusters (*3*), two-dimensional (2D) hexagonal lattices at interfaces (*4*, *5*), arrays of defects (*6*), particle-stabilized gels (*7*), and cellular soft-solid structures (*8*). The ability of liquid crystals to spontaneously arrange foreign particles into regular geometric patterns is therefore highly interesting for developing new approaches to building artificial colloidal structures, such as 3D photonic band-gap devices (*9*). Current approaches to fabrication rely on the controlled sedimentation of colloids from solutions (*10*), growth on patterned and prefabricated templates on surfaces (*11*), external-field–assisted manipulation (*12*), and precision lithography combined with mechanical micromanipulation (*13*).

In isotropic solvents, the spatial aggregation of colloids is controlled by a fine balance between the attractive dispersion forces and the Coulomb, steric, and other repulsive forces. The nature of colloidal interactions in nematic liquid crystals is quite different. Nematic liquid crystals are orientationally ordered complex fluids, in which rodlike molecules are spontaneously and collectively aligned into a certain direction, called the director. Because of their anisotropy, the orientation of nematic liquid crystals can be manipulated by external electric or magnetic fields, or even by anisotropic surfaces, which is an important issue in liquid crystal display technology. When foreign particles are introduced into the nematic liquid crystal, the orientation of nematic molecules is locally disturbed because of their interaction with the surfaces of the inclusions. The disturbance spreads on a long (micrometer) scale and can be considered as an elastic deformation of the nematic liquid crystal. Because the elastic energy of deformation depends on the separation between inclusions, structural forces between inclusions are generated. The structural forces in liquid crystals are long-range (on the order of micrometers) and spatially highly anisotropic, thus reflecting the nature of the order in liquid crystals (*14*–*17*).

In our experiments, a dispersion of micrometer-sized silica spheres in the nematic liquid crystal pentylcyanobiphenyl (5CB) was introduced into a rubbed thin glass cell with thickness varying along the direction of rubbing from

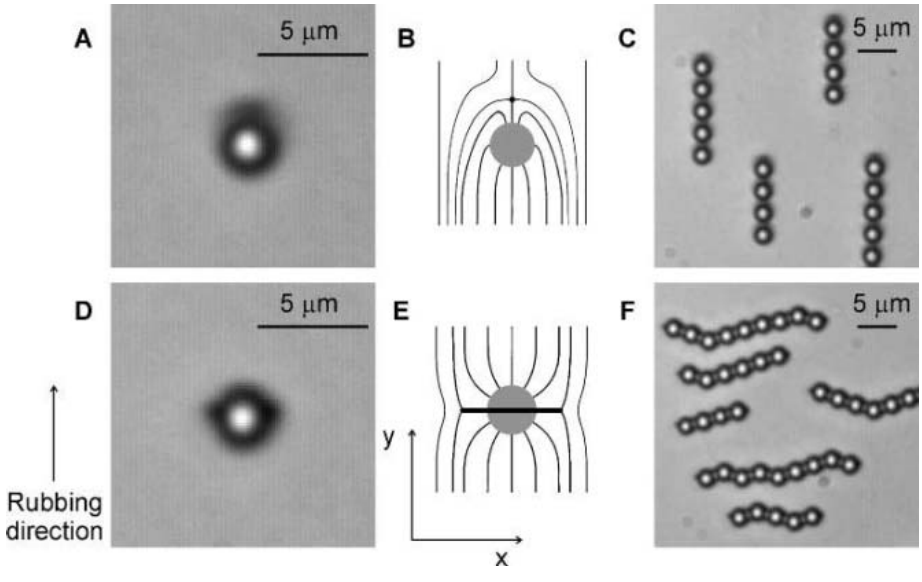

Fig. 1. Dipolar and quadrupolar colloids in a thin layer of a nematic liquid crystal. (**A**) Micrograph of a $d = 2.32$ μm silica sphere in an $h = 5$ μm layer of 5CB with a hyperbolic hedgehog defect (black spot on top). (**B**) The nematic order around the colloid has the symmetry of an electric dipole. (**C**) Dipoles spontaneously form dipolar (ferroelectric) chains along the rubbing direction. (**D**) The same type of colloid in a thin ($h = 2.5$ μm) 5CB layer. The two black spots on the right and left side of the colloid represent the Saturn ring. (**E**) The nematic order has in this case the symmetry of an electric quadrupole. (**F**) Quadrupoles spontaneously form kinked chains perpendicular to the direction of rubbing.

[1]J. Stefan Institute, Jamova 39, 1000 Ljubljana, Slovenia. [2]Faculty of Mathematics and Physics, University of Ljubljana, Jadranska 19, 1000 Ljubljana, Slovenia.

*To whom correspondence should be addressed. E-mail: igor.musevic@ijs.si

one to several colloidal diameters [supporting online material (SOM), section 1]. The colloidal surfaces were treated chemically to induce perpendicular surface orientation of the 5CB, whereas the surfaces of the confining cell were treated to induce parallel orientation. The resulting elastic distortion of the 5CB around the colloids generated repulsive forces between the colloids and the walls of the cell, thus elastically stabilizing the colloids in the middle of the nematic layer. In thinner parts of the cell, the colloids were surrounded by a distorted nematic liquid crystal that had a director field with a symmetry reminiscent of that of an electric quadrupole (*18*–*21*). In thicker parts, the nematic liquid crystal around the colloids had a symmetry like that of an electric dipole (*1*, *2*, *18*, *19*).

Figure 1A shows a micrograph of a silica sphere with diameter $d = 2.32 \pm 0.02$ μm in a nematic layer with a thickness (h) of 5 μm. The structure of the director field around the colloid is shown in Fig. 1B. It is distorted dipolarly, with a hyperbolic hedgehog defect (*18*, *19*) that appears as a dark spot on the top of the colloid in Fig. 1A. The colloid and the hedgehog are oriented along the rubbing direction (the y axis in Fig. 1), thus forming an analog of an electric dipole (*22*, *23*). Dipoles spontaneously assemble into dipolar (ferroelectric-like) chains oriented along the rubbing direction (Fig. 1C). For thickness smaller than the critical one $h_c = 3.5 \pm 0.1$ μm, the dipolar field around the colloid is strongly influenced by the confining surfaces. The symmetry of the director field around the colloid is now quadrupolar (Fig. 1E), with a closed disclination line (Saturn ring) surrounding the colloid (*24*). The two black spots on the right and left side of the colloid in Fig. 1D represent the top view of the Saturn ring, encircling the colloid. Quadrupolar colloids spontaneously self-assemble into kinked chains oriented perpendicular to the rubbing direction (Fig. 1F).

In the experiments, laser tweezers were used to position colloids (*25*) and assist their assembly into stable 2D structures. The temporal position of the colloids was video-monitored by means of an optical microscope and image capture. Analysis of the colloidal trajectories (*25*) allowed us to determine the separation dependence of the structural forces between colloids and the binding energy of colloids in colloidal assemblies.

Figure 2 shows time sequences of the self-assembly of quadrupolar colloids in a thin cell. A single pair of quadrupolar colloids is attracted at an angle of ~73°, measured from the rubbing direction (Fig. 2A), which promotes the growth of kinked quadrupolar chains in a direction perpendicular to rubbing (Fig. 2, B and C). Comparison of Fig. 2, B and C, shows that an additional colloid can either be added to a position that creates an additional kink or promote the growth of straight chains that are tilted with respect to the rubbing direction. Figure 2D shows that the additional colloid is also attracted laterally to an already-formed chain and promotes the growth of truly 2D quadrupolar colloidal crystals. The colloids are in all cases attracted to a specific position, already at a separation of several micrometers, which demonstrates the long-range and anisotropic nature of structural nematic forces. The measured binding energy of an additional quadrupole, attracted along the kinked quadrupolar chain, is $\sim 3.4 \times 10^{-18}$ J ($\sim 800\ k_B T$). The measured lateral attraction of an isolated quadrupole toward the side of a quadrupolar chain is much weaker ($\sim 120\ k_B T$) than the binding energy of a colloid in a quadrupolar chain. A stack of quadrupolar chains can rearrange in an almost hexagonal structure with a more symmetric distribution of Saturn ring defects.

An example of directed 2D assembly of quadrupolar colloidal crystal is shown in Fig. 2E. A single colloid was positioned with laser tweezers close to a crystallite and released from the optical trap. The sequence of images demonstrates the attraction of an isolated colloid into the unoccupied corner of a small crystallite. The structural force between an isolated colloid and an already formed quadrupolar 2D nematic crystallite was attractive when the colloid approached the chain at its ends. When the colloid approached the chain or an already-formed crystallite in a lateral direction, the force was at first repulsive, but when the colloid was forced closer to the chain, it formed nematic bonds with the chain. The measured elastic attractive potential for the sequence in Fig. 2E is presented in Fig. 2F, demonstrating strong attraction over large separations of more than 5 μm. As a result, stable 2D crystals with oblique 2D lattices were assembled (Fig. 2G), which were stable over a time period of several days. The shape of the unit cell was that of a general parallelogram with $a = 2.69 \pm 0.04$ μm, $b = 3.01 \pm 0.05$ μm, and $\gamma = 56° \pm 1°$. We also observed that such 2D quadrupolar nematic colloidal crystals were quite susceptible to external perturbations, such

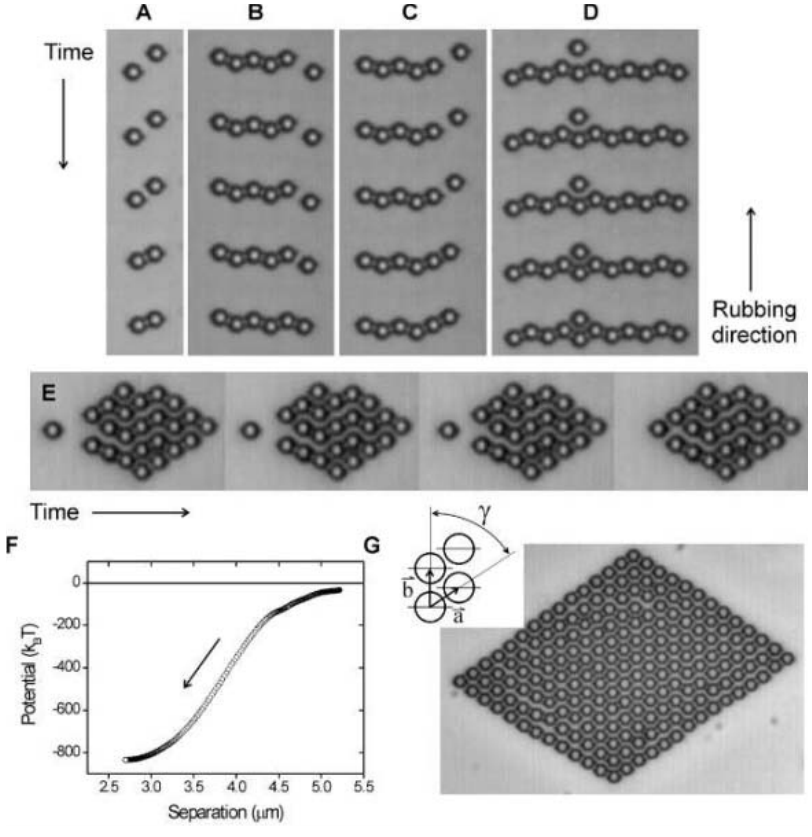

Fig. 2. Growth of 2D quadrupolar nematic colloidal crystals. (**A**) Time sequence showing the spontaneous assembly of a quadrupolar pair of colloids. An additional colloid is attracted to the chain: (**B**) into a position that creates a kink, (**C**) in a straight and tilted line, or (**D**) laterally. The time between individual frames in (A) to (C) was 0.8 s and 2.2 s in (D). The cell thickness was $h = 2.7$ μm. (**E**) Directed assembly of quadrupolar colloids in a 2D crystal. The colloid was positioned close to the corner of an already formed crystallite and released. Directed attraction into a unoccupied corner due to the structural force is clearly shown. The time difference between individual frames was 5 s. (**F**) Measured elastic energy of the colloid as a function of its separation from the unoccupied corner position (*25*). The arrow indicates the direction of movement of the colloid. (**G**) Large quadrupolar crystal formed by directed assembly by means of laser tweezers.

as flow of the nematic liquid crystal due to external pressure, change of temperature, etc. This indicates the existence of a huge variety of metastable structures within an ensemble of ordered quadrupolar nematic colloids in thin nematic layers.

At large cell thickness, colloids are dipolar and tend to spontaneously form linear chains along the rubbing direction (*1*, *2*). We have measured the binding energy of a single dipolar colloid in a dipolar chain, which is ~4500 k_BT and is much stronger than the binding energy of a single quadrupole in a quadrupolar chain. We visualize these dipolar chains as 1D "ferroelectric" objects, polarized along the direction of their dipoles.

The structural force between an isolated dipolar colloid and the ferroelectric colloidal chain depends on the orientation of the dipolar colloid, as shown in two time sequences in Fig. 3, A and B. For the parallel orientation of the dipoles (Fig. 3A), the colloid is repelled from the ferroelectric chain, whereas for the antiparallel orientation of the dipoles (Fig. 3B), the colloid is strongly attracted toward the chain. The measured elastic dipolar potentials are shown in Fig. 3C for parallel and antiparallel orientation. The measured elastic potential of lateral attraction is extremely strong at micrometer separation (~3000 k_BT) and is much stronger than the lateral attraction in quadrupolar chains. At close proximity, the separation between the colloids is stabilized by the hyperbolic hedgehog defect, generating short-range repulsive structural force (*18*, *19*). The combination of a long-range attraction and short-range elastic repulsion thus allows us to grow stable 2D dipolar nematic crystals, as shown in Fig. 3D. The crystal is easily formed by pairs of antiparallel ferroelectric colloidal chains that form a parallelogram unit cell with lattice constants $a = 2.95 \pm 0.03$ μm, $b = 2.84 \pm 0.02$ μm, and $\gamma = 61° \pm 1°$. This corresponds to a 520-nm surface-surface separation between colloids along the chains and a 640-nm separation between the nearest colloids in sequent ferroelectric chains. The crystal structure is extremely robust against external perturbations and remains stable for several weeks. As an illustration of its robustness, the crystal can be grabbed by laser tweezers and moved to a new position as a single unit (fig. S1).

In order to identify the binding mechanism and to prove that it is indeed liquid crystal that stabilizes our colloidal crystals, we examined the system with numerical modeling. When dealing with small colloidal particles and defects in liquid crystals, a Landau–de Gennes description based on the nematic order parameter tensor $Q_{ij} = S/2(3n_in_j - \delta_{ij})$ is most appropriate, as it takes into account not only Frank elasticity due to deformation (*18*, *19*) but also local variations of the degree of order. The order parameter tensor is a 3 × 3 symmetric traceless matrix, whose invariants are used to phenomenologically construct the free energy F of the nematic, constrained by colloidal particles and surfaces of the cell (*26*)

$$F = +\frac{1}{2}L\int_{LC}\left(\frac{\partial Q_{ij}}{\partial x_k}\right)\left(\frac{\partial Q_{ij}}{\partial x_k}\right)dV + \int_{LC}\left(\frac{1}{2}AQ_{ij}Q_{ji} + \frac{1}{3}BQ_{ij}Q_{jk}Q_{ki} + \frac{1}{4}C(Q_{ij}Q_{ji})^2\right)dV + \frac{1}{2}W\int_{Surf.Col.}(Q_{ij} - Q^0_{ij})(Q_{ji} - Q^0_{ji})dS. \quad (1)$$

The first term in Eq. 1 represents the increase of the free energy due to spatial variations of the nematic order, whereas the second term represents the contribution to the free energy due to the nematic order. The interaction of the nematic liquid crystal with the surfaces of the colloids is represented by the third term. We chose a single elastic constant approximation (L); A, B, and C are conventional nematic material constants; W is the strength of surface anchoring; and Q^0_{ij} is the order parameter preferred by the surface (SOM, section 3). We set the orientation of the nematic molecules parallel to the surfaces of the cell with the bulk value of the order parameter. The free energy therefore covers all three fundamental liquid crystal phenomena relevant to our experiments: elasticity, the possible formation of defects, and the finite interaction of a liquid crystal with the surfaces of the colloids.

The minimum of the free energy is found by solving a system of coupled nonlinear partial differential equations with relevant boundary conditions (SOM, section 4). We did this numerically by an explicit Euler finite difference relaxation algorithm on a cubic mesh (*27*). Colloids with both quadrupolar and dipolar symmetry appear as possible solutions. Results for a particular choice of parameter values (*28*) are presented in Fig. 4.

In the case of 2D nematic quadrupoles, numerical calculations reproduce the experiments very well. Figure 4, A and B, show one of the stable solutions for the 2D nematic quadrupolar colloidal crystals, where the director field with local quadrupolar symmetry is periodic in two dimensions. In this case, the orientational defects (Saturn rings) are localized around nearly hexagonally packed colloids. The binding force between colloids comes from sharing of the elastically distorted region around individual colloids. At equilibrium, the lattice constants of an oblique 2D lattice are $a = 1.15d$ and $b = 1.32d$,

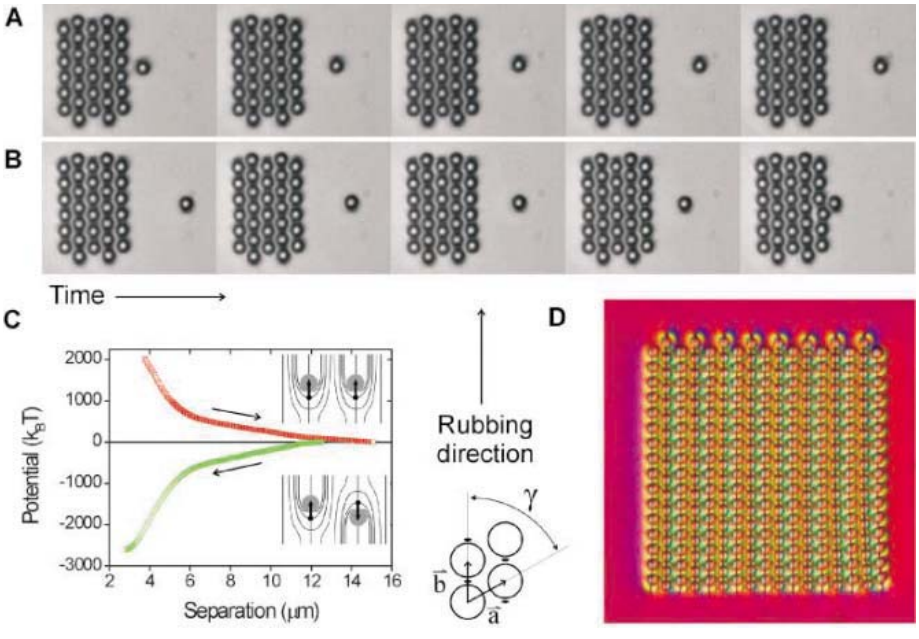

Fig. 3. Assembly of dipolar colloids into 2D nematic colloidal crystals. (**A**) A dipolar nematic colloid is repelled from the neighboring ferroelectric chain if its dipole is parallel to the dipoles in the chain. The time difference between images was 4 s. (**B**) The colloid is attracted to the chain if its dipole is antiparallel to the dipoles in the chain. The time difference between images was 4 s. (**C**) Measured attractive and repulsive elastic potential for two different orientations of the colloidal dipole. Arrows indicate the direction of movement of the colloid (*25*). Like dipoles are repelled from and unlike dipoles are attracted to the chain. (**D**) A 2D dipolar colloidal crystal formed by pairs of antiparallel dipolar chains. Different colors represent different orientations of the nematic molecules.

with $\gamma = 55°$, which is in perfect agreement with the experimental values $a = 1.16d$, $b = 1.3d$, $\gamma = 56°$. We have also calculated the free energy of such a 2D quadrupolar crystal after "stretching" it in x and y directions, which is shown in Fig. 4C. The minimum of the free energy (green area) indeed proves that colloids are bound collectively in two dimensions by liquid crystal Frank elasticity. In addition we have estimated the effective binding force $\mathcal{F} = -\partial F/\partial x$ per colloid bond. At a colloid separation increase of $0.1d$, one finds $\mathcal{F} = -13$ pN, which is roughly comparable to the experimental value of –3 pN. The material constants were not optimized to fit the experiment.

A stable 2D colloidal structure with local dipolar symmetry of the director field is presented in Fig. 4, D and E. Because of the strong confinement set by the nematic orientation at the surface of the thin cell (*28*), the hyperbolic hedgehog defect has "opened" and appears in a form of a small defect ring with the same topological properties. This reduces the separation along the dipolar chains and enhances the anisotropy of the lattice. The lattice constants of the oblique 2D lattice are $a = 1.26d$ and $b = 1.01d$, with $\gamma = 66°$, which is in agreement with the experimental values $a = 1.27d$, $b = 1.23d$, $\gamma = 61°$. The free energy landscape F for 2D dipolar colloids is presented in Fig. 4F. Compared to the quadrupolar case (Fig. 4C), the potential well is much steeper, indicating much stronger and anisotropic binding. In particular, bonds between dipolar colloids are extremely strong along the direction of dipolar chains and relatively weaker between the chains. As a result of strong confinement, imposed in our calculations (and consequent opening of the hyperbolic hedgehog defect), the dipoles are so strongly attracted along the chain that their surfaces actually touch. This is evidenced by the green area in the energy landscape in Fig. 4F, which indicates that at equilibrium, the colloids are touching each other along the chain. Nevertheless, the numerical analysis clearly proves the existence of collectively bound dipolar colloids in two dimensions.

The main result of our work is that stable and long-range–ordered nematic colloidal crystals exist in thin nematic layers. Unlike forces that are responsible for the long-range order of colloids in isotropic host liquids, the forces that bind nematic colloids together are of structural origin and therefore much richer in the sense of their anisotropy. We have found two different types of 2D nematic colloidal crystals in our experiments: those with quadrupolar and dipolar symmetry. In both cases, the binding mechanism is the same and represents a fine balance between two basic mechanisms: (i) the colloids minimize the total free energy of elastically distorted nematic crystals by approaching each other and thus sharing topological defects (regions of distortion) with each other; and (ii) when colloids are in close proximity, repulsive structural forces are generated because of strong spatial variation of the nematic order. A delicate balance between these two effects governs the positional and orientational ordering of nematic colloidal crystals.

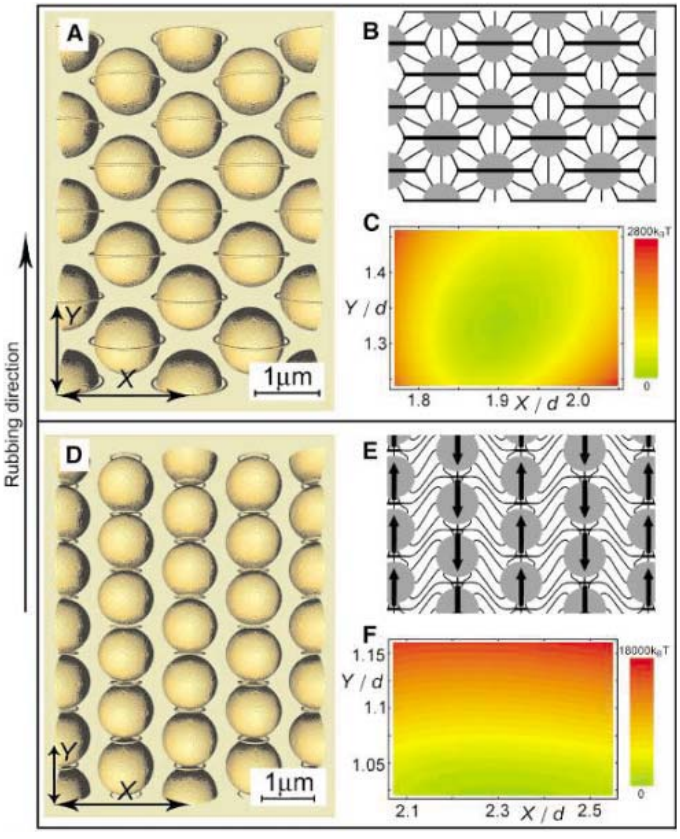

Fig. 4. Stable quadrupolar and dipolar nematic colloidal crystals in two dimensions. (**A**) Crystal with quadrupolar symmetry. The Saturn defects are localized and surround the colloids. The image represents isosurfaces, where the magnitude of the order parameter is $S = 0.45$. (**B**) Schematic view of the quadrupolar director field, with the heavy line representing the Saturn defect. (**C**) Free energy landscape F, calculated for a unit cell with a total of two quadrupolar colloids bound by Saturn defects. (**D**) Stable 2D crystal with dipolar symmetry. The hyperbolic hedgehog defects have opened because of the strong confinement. Again, a surface with $S = 0.45$ is shown. (**E**) Schematic view of a 2D stable crystal of dipolar nematic colloids. The arrows indicate the direction of the topological dipole; note the antiferroelectric arrangement of dipoles. Thin lines represent the local direction of nematic molecules. (**F**) Calculated F for a unit cell with a total of two dipolar colloids.

References

1. P. Poulin, H. Stark, T. C. Lubensky, D. A. Weitz, *Science* **275**, 1770 (1997).
2. J. C. Loudet, P. Barois, P. Poulin, *Nature* **407**, 611 (2000).
3. P. Poulin, D. A. Weitz, *Phys. Rev. E* **57**, 626 (1998).
4. V. G. Nazarenko, A. B. Nych, B. I. Lev, *Phys. Rev. Lett.* **87**, 075504 (2001).
5. I. I. Smalyukh *et al.*, *Phys. Rev. Lett.* **93**, 117801 (2004).
6. M. Yada, J. Yamamoto, H. Yokoyama, *Langmuir* **18**, 7436 (2002).
7. M. Zapotocky, L. Ramos, P. Poulin, T. C. Lubensky, D. A. Weitz, *Science* **283**, 209 (1999).
8. S. P. Meeker, W. C. K. Poon, J. Crain, E. M. Terentjev, *Phys. Rev. E* **61**, R6083 (2000).
9. S. Noda, T. Baba, Eds., *Roadmap on Photonic Crystals* (Kluwer Academic, Dordrecht, Netherlands, 2003).
10. V. W. A. de Villeneuve *et al.*, *Science* **309**, 1231 (2005).
11. A. van Blaaderen, R. Ruel, P. Wiltzius, *Nature* **385**, 321 (1997).
12. P. Y. Chiou, A. T. Ohta, M. C. Wu, *Nature* **436**, 370 (2005).
13. K. Aoki *et al.*, *Nat. Mater.* **2**, 117 (2003).
14. J. C. Loudet, P. Poulin, *Phys. Rev. Lett.* **87**, 165503 (2001).
15. M. Yada, J. Yamamoto, H. Yokoyama, *Phys. Rev. Lett.* **92**, 185501 (2004).
16. I. I. Smalyukh, O. D. Lavrentovich, A. N. Kuzmin, A. V. Kachynski, P. N. Prasad, *Phys. Rev. Lett.* **95**, 157801 (2005).
17. T. Araki, H. Tanaka, *J. Phys. Condens. Matter* **18**, L193 (2006).
18. T. C. Lubensky, D. Pettey, N. Currier, H. Stark, *Phys. Rev. E* **57**, 610 (1998).
19. H. Stark, *Phys. Rep.* **351**, 387 (2001).
20. N. Yuedong Gu Abbott, *Phys. Rev. Lett.* **85**, 4719 (2000).
21. H. Stark, *Phys. Rev. E* **66**, 032701 (2002).
22. O. D. Lavrentovich, *Liquid Crystals* **24**, 117 (1998).
23. Similar to charges in electrostatics, topological defects in nematics are sources (and sinks) of the director field. Defects, such as hedgehogs, are characterized by integer topological charge, specifying the number of times that the unit sphere is wrapped by all the directors around the defect core. A point defect (hedgehog) with charge 1 can open into a line defect (Saturn ring) with the same charge.
24. A similar transformation was predicted for dipolar colloids in an external magnetic field (*19*).
25. M. Škarabot *et al.*, *Phys. Rev. E* **73**, 021705 (2006).
26. P. G. de Gennes, J. Prost, *The Physics of Liquid Crystals* (Oxford Science Publications, Oxford, ed. 2, 1993).
27. W. H. Press, B. P. Flannery, S. A. Teukolsky, W. T. Vetterling, *Numerical Recipes* (Cambridge Univ. Press, Cambridge, 1986).
28. In both quadrupolar and dipolar calculations, the following numerical values for parameters were used: $A = -0.172 \times 10^6$ J/m^3, $B = -2.12 \times 10^6$ J/m^3, $C = 1.73 \times 10^6$ J/m^3,

$L = 4.0 \times 10^{-11}$ N, $W = 1.0 \times 10^{-2}$ J/m^2. The diameter of the colloids was 1.0 μm and the cell thickness was 2.0 μm. For this particular choice of parameter values, both configurations are stable. The quadrupole is metastable with respect to the dipole, and therefore by only changing the initial conditions for the relaxation algorithm, either dipolar or quadrupolar defect structures were generated. Periodic boundary conditions in x and y directions were used.

Supporting Online Material
www.sciencemag.org/cgi/content/full/313/5789/954/DC1
Materials and Methods
Fig. S1
References

8 May 2006; accepted 6 July 2006
10.1126/science.1129660

Switchable Surfactants

Yingxin Liu,[1] Philip G. Jessop,[1]* Michael Cunningham,[1] Charles A. Eckert,[2] Charles L. Liotta[2]

Many industrial applications that rely on emulsions would benefit from an efficient, rapid method of breaking these emulsions at a specific desired stage. We report that long-chain alkyl amidine compounds can be reversibly transformed into charged surfactants by exposure to an atmosphere of carbon dioxide, thereby stabilizing water/alkane emulsions or, for the purpose of microsuspension polymerization, styrene-in-water emulsions. Bubbling nitrogen, argon, or air through the amidinium bicarbonate solutions at 65°C reverses the reaction, releasing carbon dioxide and breaking the emulsion. We also find that the neutral amidines function as switchable demulsifiers of an aqueous crude oil emulsion, enhancing their practical potential.

Surfactants are designed to stabilize emulsions during certain stages in cleaning, manufacturing, oil recovery, and other processes. Temporary emulsions (emulsions that are desired only during one stage of a process) are of practical interest in many areas, including (i) emulsion and microsuspension polymerizations, because of the low viscosity and efficient heat transfer compared with bulk polymerization; (ii) cleaning and metal degreasing of equipment; (iii) viscous oil transportation through pipelines, because the emulsion is far less viscous than the oil itself (*1*, *2*); (iv) enhanced oil-recovery (EOR), because surfactants help labilize oil by lowering the oil/water interfacial tension (*3*, *4*); (v) separation of oil from oil sands (*5*); and (vi) even some cosmetic emulsions which are intended to separate upon use (*6*). In these applications, an emulsion is only useful during one stage of a process, after which the surfactant becomes a liability that hinders separation of the components. The problem of how to break surfactant-stabilized temporary emulsions has not been resolved satisfactorily in the literature.

Cleavable or switchable surfactants could be used to address this problem, but they still have several drawbacks. A cleavable surfactant can be irreversibly converted, typically by application of a chemical or photochemical trigger, into one or more molecules with greatly reduced surface activity. This ability is usually conferred on the surfactant by incorporating a cleavable functional group such as an ester between the hydrophilic headgroup and the hydrophobic tail (*7*). A switchable surfactant, by contrast, can undergo fully reversible interconversions between active and inactive forms. Emulsions stabilized by either type of surfactant can thus be broken by application of the appropriate trigger. Solid materials such as particles that are temporarily protected by surfactants during synthesis can be deprotected and purified. Switchable surfactants have the additional advantages that their activity can be delayed until needed, they can be recovered and reused afterward, and their removal from the product stream can be facilitated by switching the surfactant to the form least soluble in the relevant medium.

At the same time, the nature of the trigger can limit the practical viability of cleavable and switchable surfactants. Triggers based on the addition of acids, bases, oxidants, or reductants suffer from economic and environmental costs, as well as the potential for product contamination or modification by these reagents. Mild and inexpensive triggers are therefore preferable. Photochemical approaches are hindered by the opacity of many emulsions. Surfactants in which the head-group functionality or the polarity of the tail can be switched electrochemically have been reported (*8*–*14*), but they contain expensive ferrocenyl groups, highly toxic viologen groups, or groups sensitive to O_2.

Here, we report switchable surfactants that use benign gases (CO_2 and air) as the triggers to switch them "on" and "off". The chemistry behind the transformation was uncovered during our earlier studies of amidine reactivity: On exposure to 1 atmosphere of gaseous CO_2, amidines mixed with water (*15*) or an alcohol (*16*) react exothermically to form the bicarbonate or alkylcarbonate salts. The reaction can be reversed by bubbling N_2 or Ar through the neat liquid salt, or else through a solution if the salt is a solid. We reasoned that an amidine with a long alkyl chain should be a poor surfactant but would become an effective surfactant on conversion to the charged amidinium bicarbonate by exposure to water and CO_2. A further benefit of the amidine systems is that the product generated by switching off the surfactant has negligible surface activity and water solubity—a substantial environmental advantage.

To evaluate this hypothesis, two such amidines, **1a** and **1b**, were prepared and characterized. Their reaction with CO_2 and water to produce amidinium bicarbonate salts (**2a** and **2b**) was confirmed by bubbling CO_2 through wet ether or wet acetonitrile solutions of **1a,b** and collecting and characterizing the precipitate (Reaction 1). The bicarbonate salts can be reconverted to the amidines by bubbling argon through solutions of **2a,b** in tetrahydrofuran; the products were isolated and their structures confirmed by ^{1}H nuclear magnetic resonance (NMR) and infrared (IR) spectroscopy. Thermogravimetric analysis of solid **2a** (fig. S1) showed that the CO_2 and water are driven off between 50 and 63°C (*17*).

The reversibility and repeatability of the process were confirmed by monitoring the conductivity of a solution of **1a** in wet dimethyl sulfoxide (DMSO) while CO_2 and then argon were bubbled through the solution over three cycles (Fig. 1). The conductivity rose when CO_2 was bubbled through the

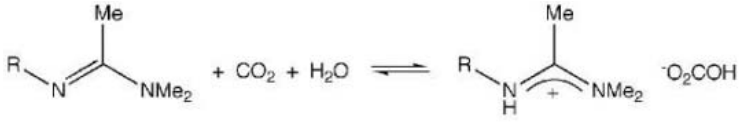

1a R = $C_{16}H_{33}$ **2a**
1b R = $C_{12}H_{25}$ **2b**

(1)

[1]Departments of Chemistry and Chemical Engineering, Queen's University, Kingston, Ontario K7L 3N6, Canada,. [2]Schools of Chemistry and Chemical Engineering, Georgia Institute of Technology, Atlanta, GA 30332–0100, USA.

*To whom correspondence should be addressed. E-mail: jessop@chem.queensu.ca

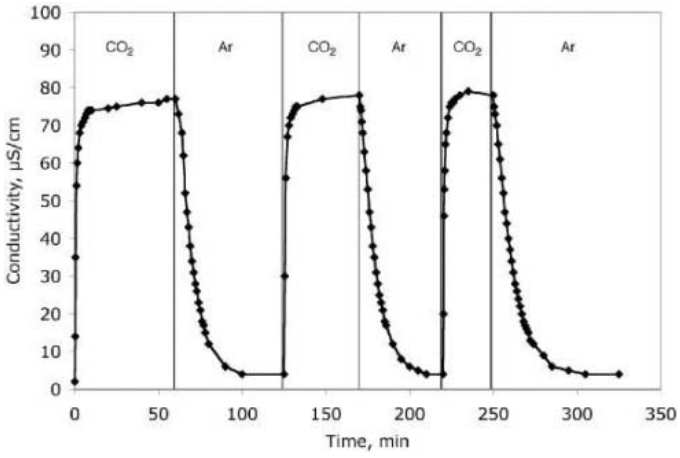

Fig. 1. The conductivity of a DMSO solution of **1a** at 23°C as a function of time during three cycles of treatment with CO_2 followed by argon.

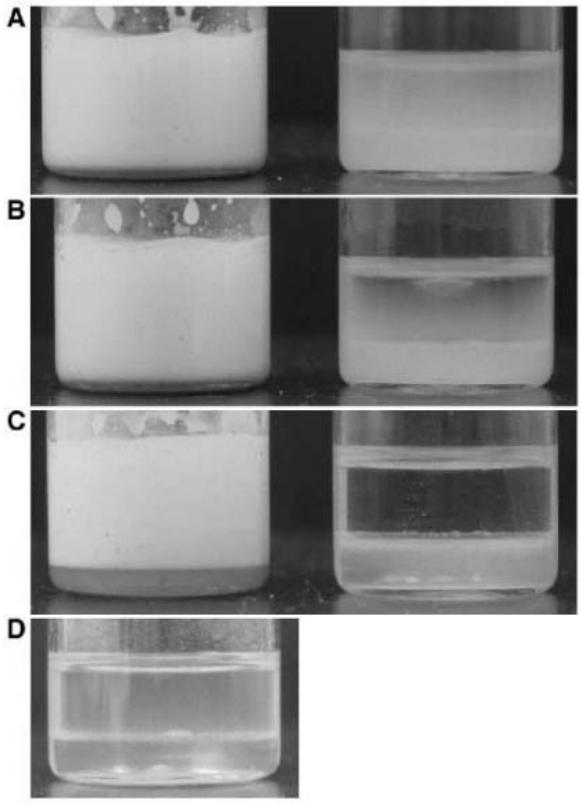

Fig. 2. Photographs of 2:1 (v/v) hexadecane/water mixtures containing **1a** and either CO_2 (left) or argon (right) after 10 min of shaking followed by a waiting period of (**A**) 5 min, (**B**) 30 min, and (**C**) 24 hours. (**D**) Photograph of the CO_2-induced emulsion after treatment with argon at 65 to 70°C for 2 hours (*26*).

solution, and it dropped upon argon addition. Air was found to have the same effect as argon.

The capacity of the amidines for stabilizing an emulsion was evaluated by automated shaking of mixtures of hexadecane and water containing **1a** (90 mg). Although an emulsion formed, it clearly separated into two layers within 5 min after the cessation of shaking (Fig. 2). However, if the solution was treated with CO_2 for an hour before the shaking, the emulsion was much more stable. It showed no evidence of separation for 3 hours, at which point a very thin layer of cloudy liquid began to appear at the bottom of the flask. After one day, the emulsion still occupied 82% of the liquid volume (Fig. 2C). Bubbling argon through the emulsion at 65°C resulted in a complete separation of the hexadecane and water into two clear layers.

Similar experiments were performed with crude oil, but with notably different results (Fig. 3). Light crude oil, when shaken with water but without any additive, was able to form a fairly stable emulsion, presumably as a result of naturally occurring surfactants in the oil (*18*, *19*). A stable emulsion also resulted from treatment of the same oil/water mixture with compound **1a** and CO_2. However, addition of compound **1a** under argon does not lead to a stable emulsion; the mixture separates into two layers within 30 min, revealing that the uncharged amidine functions as a demulsifier (*20*). This demulsifying effect suggests that variations of these switchable surfactants may be useful in oil production for such applications as the breaking emulsions after EOR, oil-sands separations, and even cleaning of equipment. Although demulsifiers are known, including some that contain closely related head groups such as cyclic amidines (*21*), reversible switching between surfactant and demulsifier is, to our knowledge, unprecedented. Application of this technology to oil industry operations may depend on modifying the structure of the switchable demulsifier so that it will demulsify emulsions of heavy crudes.

Surfactants are also used to protect the surfaces of nanoparticles, colloids, latexes, and other particulates during their synthesis; in the absence of a coating of surfactant, these particles tend to agglomerate into undesirably large particles. In many cases, once the synthesis is complete, protection by the surfactant is no longer needed. For some applications, such as the preparation of supported metal catalysts, the complete removal of the surfactant is desired but difficult because the surfactant binds too strongly to the surface. For other applications, mere deactivation of the surfactant is desired and not necessarily removal. In either case, a switchable surfactant would be advantageous. As a preliminary demonstration that the amidine-based switchable surfactants can be used to protect growing particles during synthesis and then can be switched off, we tested their use in a microsuspension polymerization (Reaction 2) (*22*, *23*). Microsuspension and emulsion polymerizations, techniques very commonly used for polymerizations involving radical mechanisms, require surfactants to protect the growing polymer particles during the synthesis. The product is a latex, meaning a surfactant-stabilized dispersion of polymeric particles in water. Isolation of the polymer from the suspension is facilitated if the surfactant can be switched off. The current industrial method to isolate the polymeric product is the addition of salts to coagulate the dispersion, followed by filtration and removal of the surfactant and added salts by washing (*24*). The washing step is often ineffective in removing the surfactants, resulting in polymers that are unnecessarily hydrophilic, which can be undesirable in many applications. An alternative route is to perform the polymerization in an organic solvent, but this approach is undesirable for two reasons. First, the removal of the solvent from the product is hindered by the high viscosity of the product mixture. More important, the use of the solvent increases emissions of volatile organic compounds (*25*). Although many polymers are made by surfactant-stabilized

methods, styrene polymerization was chosen as a test example. The radical polymerization of styrene, initiated by thermal decomposition of an azo-based free radical initiator, was performed in a styrene-in-water emulsion stabilized by **2b** under CO_2. Switching the surfactant off by bubbling argon or nitrogen through the system at 65°C and then cooling to room temperature and adding more water allows the polymer to settle. The settling is accelerated if the sample is centrifuged. However, without the argon/nitrogen treatment, the polymer failed to settle within an observation period of 3 days or with centrifuging (Fig. 4).

Future work in this area will include quantitative measurement and improvement of the rate of surfactant switching and optimization of the surfactant designs for specific applications, especially in nanoparticle synthesis, polymerization, and the oil industry applications that we have described.

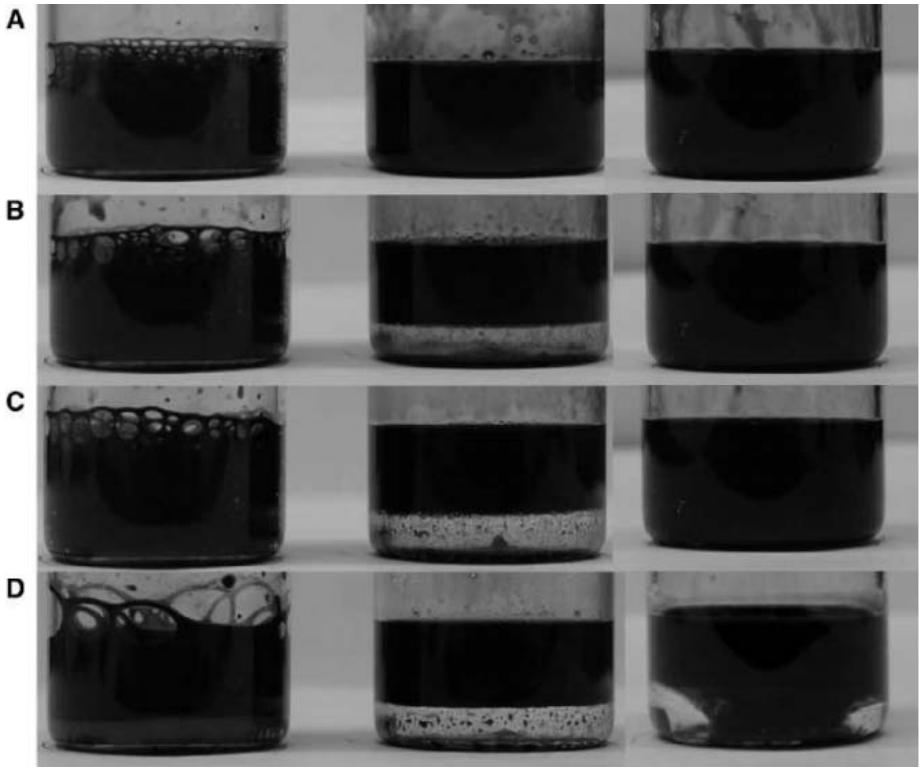

Fig. 3. Photographs of 2:1 (v/v) crude oil/water mixtures containing either **1a** and CO_2 (left), **1a** and argon (center), or only argon (right) after 10 min of shaking followed by a waiting period of (**A**) 5 min, (**B**) 30 min, (**C**) 60 min, and (**D**) 15.5 hours.

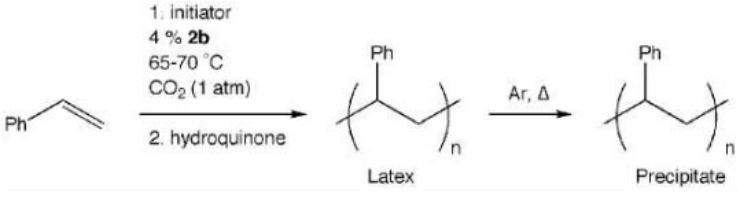

(2)

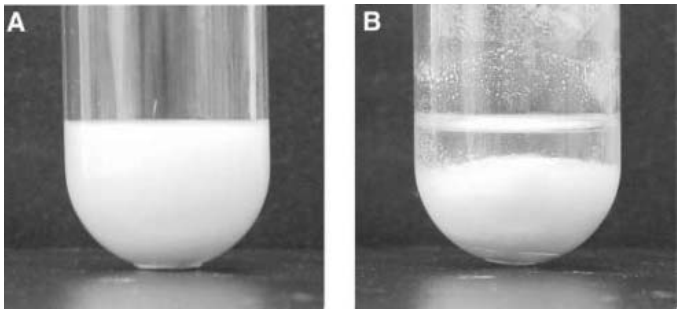

Fig. 4. Photographs of a latex suspension of polystyrene particles after polymerization in the presence of **2b** and (**A**) after centrifugation or (**B**) after argon treatment followed by centrifugation.

References and Notes

1. B. M. Yaghi, A. Al-Bemani, *Energy Sources* **24**, 93 (2002).
2. D. Langevin, S. Poteau, I. Henaut, J. F. Argillier, *Oil Gas Sci. Technol.* **59**, 511 (2004).
3. T. Austad, J. Milter, in *Surfactants: Fundamentals and Applications in the Petroleum Industry*, L. L. Schramm, Ed. (Cambridge Univ. Press, Cambridge, 2000), pp. 203–249.
4. L. L. Schramm, S. M. Kutay, in *Surfactants: Fundamentals and Applications in the Petroleum Industry*, L. L. Schramm, Ed. (Cambridge Univ. Press, Cambridge, 2000), pp. 79–120.
5. J. Masliyah, Z. Zhou, Z. Xu, J. Czarnecki, H. Hamza, *Can. J. Chem. Eng.* **82**, 628 (2004).
6. R. Y. Lochhead, W. J. Hemker, J. Y. Castaneda, *Soap, Cosmet., Chem. Spec.* **63**, 28 (1987).
7. K. Holmberg, in *Reactions and Synthesis in Surfactant Systems*, J. Texter, Ed. (Dekker, New York, 2001), pp. 45–58.
8. T. Saji, K. Hoshino, S. Aoyagui, *J. Am. Chem. Soc.* **107**, 6865 (1985).
9. P. Anton, P. Koeberle, A. Laschewsky, *Prog. Colloid Polym. Sci.* **89**, 56 (1992).
10. P. Anton, A. Laschewsky, M. D. Ward, *Polym. Bull. (Berlin)* **34**, 331 (1995).
11. H. Sakai, M. Abe, in *Mixed Surfactant Systems*, M. Abe, J. F. Scamehorn, Eds. (Dekker, New York, 2005), pp. 507–543.
12. M. M. Schmittel *et al.*, *Chem. Commun.* **2005**, 5650 (2005).
13. S. S. Datwani, V. N. Truskett, C. A. Rosslee, N. L. Abbott, K. J. Stebe, *Langmuir* **19**, 8292 (2003).
14. N. Aydogan, N. L. Abbott, *Langmuir* **17**, 5703 (2001).
15. D. J. Heldebrant, P. G. Jessop, C. A. Thomas, C. A. Eckert, C. L. Liotta, *J. Org. Chem.* **70**, 5335 (2005).
16. P. G. Jessop, D. J. Heldebrant, L. Xiaowang, C. A. Eckert, C. L. Liotta, *Nature* **436**, 1102 (2005).
17. Materials and methods are available as supporting material on *Science* Online.
18. S. Poteau, J.-F. Argillier, D. Langevin, F. Pincet, E. Perez, *Energy Fuels* **19**, 1337 (2005).
19. S. Acevedo, B. Borges, F. Quintero, V. Piscitelly, L. B. Gutierrez, *Energy Fuels* **19**, 1948 (2005).
20. Similar experiments with heavy crude gave much more stable emulsions, with no separation after 1 day for the experiments without amidine or with amidine under CO_2, and only partial separation after 1 day for the experiment with amidine under argon. Amidine **1b** was less effective than **1a** as a demulsifier; the light crude oil/water mixture separated only after 3.5 hours.
21. M. De Groote, B. Keiser, Surface-active compounds containing imidazoline rings, U.S. Patent 2,574,537, 1951.
22. M. F. Cunningham, H. K. Mahabadi, H. M. Wright, *J. Polym. Sci. Polym. Chem.* **38**, 345 (2000).
23. M. F. Cunningham, *Polym. React. Eng.* **7**, 231 (1999).
24. R. M. Fitch, *Polymer Colloids* (Academic Press, San Diego, 1997), pp. 173–225.
25. D. Urban, B. Schuler, J. Schmidt-Thümmes, in *Chemistry and Technology of Emulsion Polymerisation*, A. M. v. Herk, Ed. (Blackwell, Oxford, 2005), pp. 226–256.
26. The rates of, and minimum times required for, the conversion of **1** to **2**, the conversion of **2** to **1**, and the transport of the surfactant to the liquid-liquid interface have not yet been quantified.

27. We thank Shell and Imperial Oil for gifts of crude oil, and the Canada Research Chair program and the Natural Sciences and Engineering Research Council of Canada for funding the work.

Supporting Online Material

www.sciencemag.org/cgi/content/full/313/5789/958/DC1
Materials and Methods
SOM Text
Figs. S1 to S3
Table S1
References

30 March 2006; accepted 6 July 2006
10.1126/science.1128142

A Homomolecular Porous Network at a Cu(111) Surface

Greg Pawin, Kin L. Wong, Ki-Young Kwon, Ludwig Bartels*

Anthraquinone molecules self-assemble on a Cu(111) surface into a large two-dimensional honeycomb network ($\sqrt{304} \times \sqrt{304}$)$R23^\circ$ with pore diameters of ≈50 Å. The spontaneous formation of a pattern containing pores roughly five times larger than the size of the constituent molecules is unprecedented. The network originates from a delicate balance between substrate-mediated repulsion and intermolecular attraction involving an unusual chemical motif: hydrogen bonding between a carbonyl oxygen and an aromatic hydrogen atom. Substrate-mediated long-range adsorbate-adsorbate repulsion has been observed on anisotropic surfaces and in the context of the absence of pattern formation. Its applicability for the design of tailored molecular films is explored here.

The arrangement of molecules on surfaces is governed by a combination of interactions with the substrate and with neighboring molecules. For most organic molecules, simple patterns result, in which each adsorbate occupies the same kind of adsorption site and surrounds itself with neighbors just beyond its van der Waals surface. Phenomena such as dipolar (*1*) and quadrupolar (*2*) interactions can lead to more complex surface patterns, such as aggregates of a fixed number of molecules (*1*). Hydrogen bonding can cause the formation of molecular rows (*3*, *4*) and well-ordered binary phases of quite appealing pattern (*5*). Yokoyama *et al*. (*6*) reported that similar interactions can also be found for the interaction of cyano groups with H atoms of benzene rings, where formally no hydrogen bonding is expected.

We report a chemical motif that leads to the formation of a honeycomb pattern of anthraquinone molecules on a Cu(111) surface. The pattern has an unprecedented pore diameter of ≈50 Å, which is several times the size of its constituent molecules. We attribute the formation of such a large-scale supramolecular assembly to a delicate balance between local intermolecular attraction and long-distance substrate-mediated repulsion.

We used two customized scanning tunneling microscopy (STM) systems operated under ultrahigh vacuum (UHV) conditions (base pressure $<10^{-10}$ torr) to study submonolayer coverages of anthraquinone on Cu(111) samples. Sample preparation involved cycles of argon sputtering and annealing, followed by an inspection of the sample cleanliness by STM at 80 K. Anthraquinone was deposited thermally from a glass tube attached to the UHV chamber in a line-of-sight fashion onto the cold sample. A subsequent increase of the sample temperature beyond 180 K (typically to room temperature) facilitated the rapid formation of the patterns discussed in this report. During deposition (<20 s), the background pressure remained below 2×10^{-9} torr, and low temperature measurements (10 K) confirmed the absence of co-adsorbates.

Individual anthraquinone molecules appear as almost rectangular features with slightly rounded edges. They exhibit a central "waist" generated by opposing lateral indentations. The molecules are aligned with one of the high-symmetry directions of the substrate, similar to 9,10-dithioanthracene (*7*) and acenes in general (*8*). Work by Chiang's group (*9*) shows that oxygen can cause an apparent indentation of an organic molecule, which provides a consistent interpretation of the central waist.

In STM images of anthraquinone coverages of one molecule per several tens of substrate unit cells, we find an extended regular honeycomb pattern (Fig. 1). The sides of each hexagon consist of three parallel molecules, whose adsorption configuration resembles that of isolated molecules. The vertices consist of three anthraquinone molecules (one from each row) that form a triangle. The diameter of the hexagons is >50 Å and each hexagon encloses >200 uncovered Cu atoms. A model of this film ($\sqrt{304} \times \sqrt{304}$)$R23^\circ$ pattern is shown (Fig. 1, right). The formation of a superstructure and of empty pore space of this magnitude (which is ≈5 times the size of the constituent molecules) is unprecedented in both homogeneous and heterogeneous molecular films.

A detailed analysis of the anthraquinone pattern reveals that the oxygen atoms reside very close to hydrogen atoms of neighboring molecules, both along the sides and at the vertices of the hexagons (Fig. 2). To quantify this observation, we performed density functional theory calculations of the molecule on a 6 by 4 unit cell of substrate atoms, similar to (*7*). Based on the resultant anthraquinone adsite and bond length, we found that the oxygen atoms approached the hydrogen atom in the number 1 (row) or 2 (vertex) positions of the adjacent molecule at an O-H-C distance of ≈2.8 Å, which is comparable to hydrogen bonds in water and to the bond length reported in the cyano-arene system (*6*). Hydrogen bonding between a carbonyl and an arene has not been described previously, yet it appears sufficiently strong to govern the relative placement of anthraquinone molecules on Cu(111).

Although hydrogen bonding can explain the geometric motifs underlying the honeycomb pattern, it does not indicate why each trimer is separated from its neighbor by a row of exactly three anthraquinone molecules. For further understanding of this phenomenon, we turn to coverages in which the density of molecules is insufficient to produce a regular honeycomb pattern. Here we find very few trimers. Rather, the anthraquinone molecules arrange themselves in rows. The setup of the

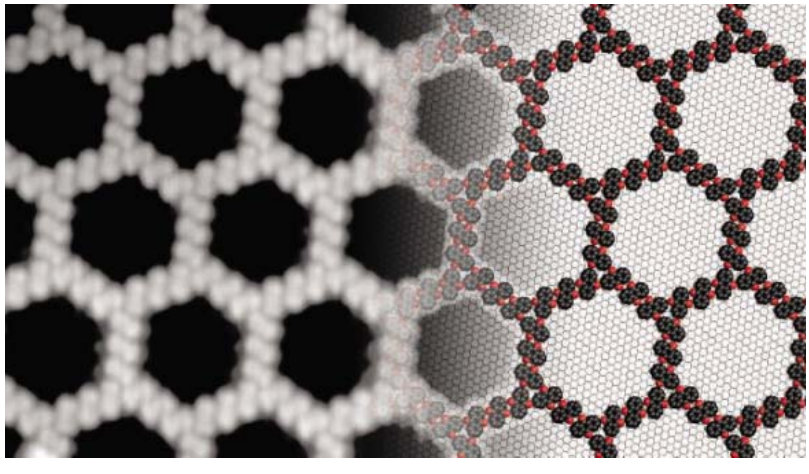

Fig. 1. (**Left**) STM image of the honeycomb network of anthraquinone molecules on a Cu(111) surface. Bias, 1.3 V; current, 73 pA; size, 260 Å by 150 Å. (**Right**) A model of the ($\sqrt{304} \times \sqrt{304}$)$R23^\circ$ unit cell. Red spheres, oxygen atoms; black spheres, carbon atoms; background, copper surface.

Pierce Hall, University of California, Riverside, CA 92521, USA.

*To whom correspondence should be addressed. E-mail: ludwig.bartels@ucr.edu

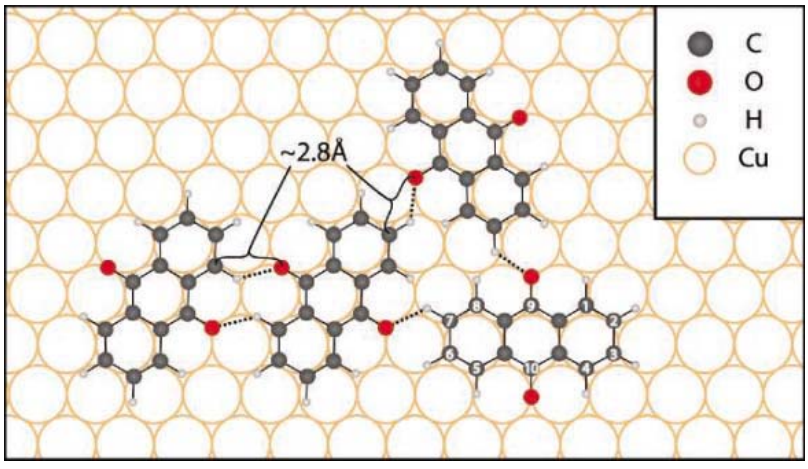

Fig. 2. Model of the anthraquinone molecules forming a row (**left**) and a vertex (**right**). C-H-O distances are indicated. The standard numbering of carbon atoms in anthracene is also indicated.

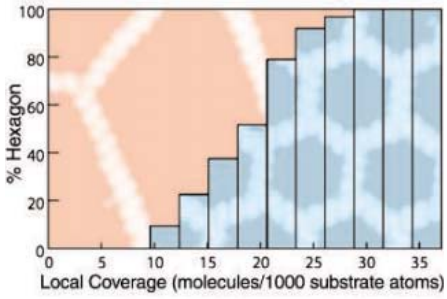

Fig. 3. Percentage of anthraquinone molecules forming trimers or being directly attached to a trimer (as necessary to form the hexagon pattern) at different local coverage values (defined as the number of neighbors within a 50 Å radius).

rows is identical to the sides of the hexagons described above, yet they are often several tens of molecules long. Occasionally, bends of 120° occur (resembling the vertices of the honeycombs) or adjacent molecules are shifted by one adsite along their neighbor's side. A statistical analysis of >1000 molecules shows that only at local coverages above ≈15 molecules per 1000 substrate atoms does the hexagon pattern start to emerge (Fig. 3). Also, we observed that parallel molecular rows almost never run in close proximity (<50 Å) to one another.

We observed the honeycomb pattern at temperatures between 10 and 200 K. If the anthraquinone coverage is increased beyond the nominal coverage of an ideal honeycomb pattern, islands of closely packed anthraquinone rows emerge that are surrounded by the honeycomb pattern. Thus, the honeycomb pattern appears to be favorable only at a very specific coverage regime. The honeycomb pattern is not affected by coadsorption of molecules, such as CO and water.

The honeycomb pattern maximizes the net intermolecular separation while preserving molecular rows. The adoption of this pattern by anthraquinone suggests that, despite attractive interactions between adjacent molecules, long-range repulsive interactions are present in this system. At very low coverage, these interactions prevent the formation of trimers and higher multimers in favor of molecular rows, whereas at higher coverages they prevent the proximity of parallel lines in favor of more even distribution of adsorbates that is afforded by the honeycomb pattern. Substrate-mediated long-range repulsion has been described as the origin of the spacing of pentacene molecules along the trenches of a Cu(110) surface, as well as for a variety of simple adsorption systems (*10*–*13*); however, such repulsion was generally associated with the absence of ordered patterns rather than the formation of regular two-dimensional patterns as shown here.

High-level theoretical modeling of this system appears to be impossible at this point because of the large size of the $(\sqrt{304} \times \sqrt{304})R23^\circ$ unit cell. Thus, we can only speculate about the nature of the repulsive interactions whose effect is observed here; potential candidates include (i) charging of the molecules by interaction of the carbonyl groups with the substrate, (ii) confinement and/or scattering of the Cu(111) surface state (*13*) [which is known to favor adsorbate separations of ≈54 Å in approximate agreement with the $(\sqrt{304} \times \sqrt{304})R23^\circ$ cell] (*14*), and (iii) compressive strain of the substrate lattice induced by the presence of the carbonyl oxygen atoms in the substrate hollow site. Notably, the sulfur analog of anthraquinone, 9,10-dithioanthracene, does not form a honeycomb structure (*7*).

In the simplest possible mathematical model of a system governed by short-range attraction and long-range repulsion, the total interaction energy (U_{tot}) is given by

$$U_{tot} = \sum_{i,j}^{i \neq j} \left[U_{attr}(\vec{r}_i, \vec{r}_j) + U_{rep}(\vec{r}_i, \vec{r}_j) \right] \quad (1)$$

If we assume that the long-range repulsive potential is of the type $a_r/|r_i - r_j|^\alpha$ [$\alpha = 1$ representing a compressive force (*15*), $\alpha = 2$ representing the interactions of screened charges] and the short-range attractive potential is of the type $-a_a/|r_i - r_j|^\beta$ ($\beta = 3$ representing dipole-dipole attraction, $\beta = 6$ representing the attractive portion of a Lennard-Jones potential) (where a is the prefactor and r is the distance), then, in each case, a range of ratios a_r/a_a exists, in which a honeycomb pattern is energetically favorable over both a hexagonal pattern of individual molecules (which fails to maximize attractive interactions between closely adjacent molecules) and a pattern of parallel adsorbate rows (which fails to minimize long-range repulsion).

Numerical simulations show that this observation is quite generally valid. Different power laws of the attractive and repulsive potential cause the honeycomb pattern of various numbers of molecules per hexagon side to be favorable for different a_r/a_a ratios. Consequently, judicious engineering of the relation between the strength of the short-range attraction and the long-range repulsion allows tailoring of film patterns and pore sizes almost at will. Adsorbate films with tailored pores could serve as templates for the growth of nanoparticles at surfaces, providing homogeneous spatial and size distributions for catalytic, electronic, or mechanic applications, as well as for biocompatibility and the reduction of friction (*16*–*18*).

References and Notes

1. M. Bohringer *et al.*, *Surf. Sci.* **444**, 199 (2000).
2. K. Wong, K. Kwon, B. Rao, A. Liu, L. Bartels, *J. Am. Chem. Soc.* **126**, 7762 (2004).
3. S. Clair *et al.*, *J. Phys. Chem. B* **108**, 14585 (2004).
4. J. V. Barth *et al.*, *Angew. Chem. Int. Ed.* **39**, 1230 (2000).
5. J. A. Theobald, N. S. Oxtoby, M. A. Phillips, N. R. Champness, P. H. Beton, *Nature* **424**, 1029 (2003).
6. T. Yokoyama, S. Yokoyama, T. Kamikado, Y. Okuno, S. Mashiko, *Nature* **413**, 619 (2001).
7. K. Y. Kwon *et al.*, *Phys. Rev. Lett.* **95**, 166101 (2005).
8. L. Wan, K. Itaya, *Langmuir* **13**, 7173 (1997).
9. A. Loui, S. Chiang, *Appl. Surf. Sci.* **237**, 559 (2004).
10. J. Repp *et al.*, *Phys. Rev. Lett.* **85**, 2981 (2000).
11. T. Mitsui, M. K. Rose, E. Fomin, D. F. Ogletree, M. Salmeron, *Phys. Rev. Lett.* **94**, 036101 (2005).
12. K. L. Wong, B. V. Rao, G. Pawin, E. Ulin-Avila, L. Bartels, *J. Chem. Phys.* **123**, 201102 (2005).
13. S. J. Stranick, M. M. Kamna, P. S. Weiss, *Science* **266**, 99 (1994).
14. P. Hyldgaard, T. L. Einstein, *J. Cryst. Growth* **275**, e1637 (2005).
15. J. M. Rickman, D. J. Srolovitz, *Surf. Sci.* **284**, 211 (1993).
16. A. Kuhnle *et al.*, *Langmuir* **18**, 5558 (2002).
17. J. V. Barth, G. Costantini, K. Kern, *Nature* **437**, 671 (2005).
18. J. A. Theobald, N. S. Oxtoby, N. R. Champness, P. H. Beton, T. J. S. Dennis, *Langmuir* **21**, 2038 (2005).
19. Support by NSF (grant CHE 0132996) is gratefully acknowledged.

28 April 2006; accepted 7 July 2006
10.1126/science.1129309

Evolutionary Paths Underlying Flower Color Variation in *Antirrhinum*

Annabel C. Whibley,[1]* Nicolas B. Langlade,[1]* Christophe Andalo,[2] Andrew I. Hanna,[3] Andrew Bangham,[3] Christophe Thébaud,[2] Enrico Coen[1]†

To understand evolutionary paths connecting diverse biological forms, we defined a three-dimensional genotypic space separating two flower color morphs of *Antirrhinum*. A hybrid zone between morphs showed a steep cline specifically at genes controlling flower color differences, indicating that these loci are under selection. *Antirrhinum* species with diverse floral phenotypes formed a U-shaped cloud within the genotypic space. We propose that this cloud defines an evolutionary path that allows flower color to evolve while circumventing less-adaptive regions. Hybridization between morphs located in different arms of the U-shaped path yields low-fitness genotypes, accounting for the observed steep clines at hybrid zones.

A prevalent metaphor for describing evolutionary processes is the adaptive landscape, commonly visualized in three dimensions as an undulating surface of fitness values over a two-dimensional (2D) space representing various genotypes (*1*, *2*). Different species may be considered to be at separate peaks on the landscape or to lie along ridges of high fitness. The notion of peaks is favored by the incompatible adaptive features of species, whereas ridges are favored as a way of accounting for underlying adaptive continuity. More recently, it has been argued that the issue of peaks versus ridges is an artifact of low-dimensional visualizations of fitness spaces as landscapes (*3*). What seem like separate peaks in 3D landscapes may be connected by paths in higher dimensions: the higher the dimensionality, the more likely such connections exist. However, it has proved difficult to demonstrate these paths in nature because of the challenge of dealing with higher dimensional genotypic and phenotypic spaces. We address this issue by combining molecular, genetic, and computational approaches to analyze flower color variation in natural populations and species of *Antirrhinum*.

Southern Europe contains 17 to 28 *Antirrhinum* species and subspecies, the number depending on taxonomic criteria (*4*–*7*). Although the species display diverse morphologies and flower colors, they can be crossed with each other and with the model species *A. majus* to give fertile progeny, reflecting their recent evolutionary origin (*8*–*10*). In most cases, the species occupy nonoverlapping geographical regions, precluding natural hybridization. Hybrid zones arise where species or morphs come into contact, as happens in a region of the Pyrenees for the yellow-flowered *A. m. striatum* and the magenta-flowered *A. m. pseudomajus* (Fig. 1A).

Previous studies on nine species from the *Antirrhinum* group identified several major loci involved in natural flower color variation (*11*–*13*). These include the linked *ROSEA* (*ROS*) and *ELUTA* (*EL*) loci, affecting the intensity and pattern of magenta anthocyanin pigment, and *SULFUREA* (*SULF*), affecting the distribution of yellow aurone pigment. To test whether these loci were important for color differences between *A. m. striatum* and *A. m. pseudomajus*, we crossed the two morphs to *A. majus* lines of known genotype (Fig. 2A). The F1s derived from the magenta morph were all magenta. By contrast, the yellow morph failed to complement mutations in *ROS* and *SULF* (Fig. 2A). The yellow morph also gave progeny with reduced magenta pigmentation when crossed to wild type, with a pattern similar to that conferred by the dominant *EL* allele. Like *EL*, the dominant allele from the yellow morph was tightly linked to *ROS* (*14*) (two recombinants were recovered out of 1300 test-cross progeny). Thus, *A. m. pseudomajus* is likely *ROS el*/*ROS el; SULF*/*SULF*, whereas *A. m. striatum* is *ros EL*/*ros EL; sulf*/*sulf*.

To assess further the contribution of *ROS EL* and *SULF* alleles to flower color differences, we intercrossed the two morphs. F2 individuals had a range of flower colors that were scored for magenta and yellow on the basis of overall visual appearance (Fig. 2B). The distributions for color were consistent, with a single segregating locus of major effect controlling each component of flower color (Fig. 2C). Individuals with a high yellow score were

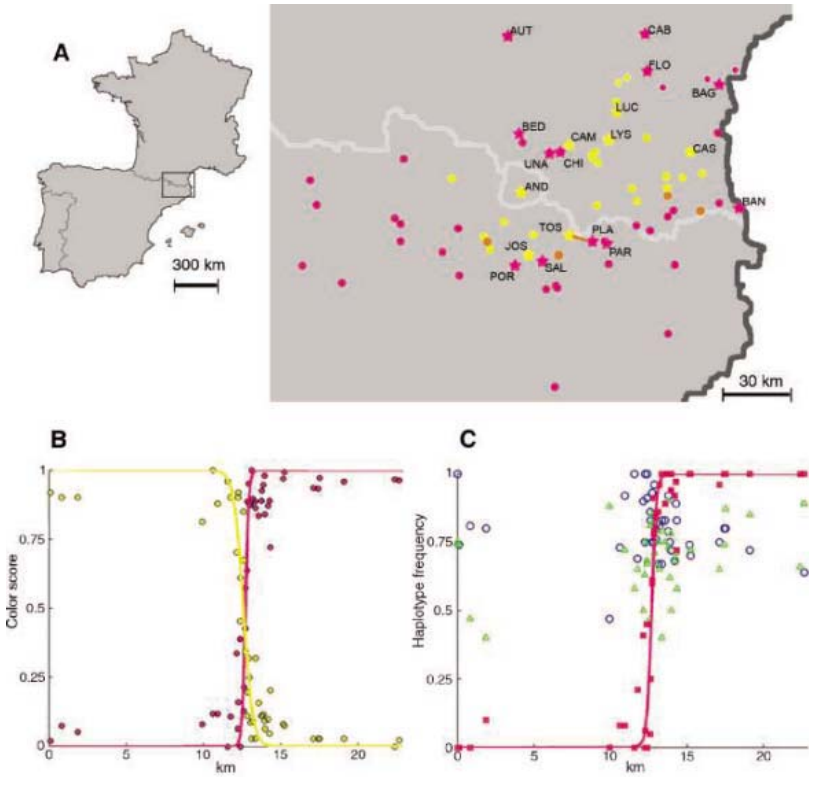

Fig. 1. Populations, phenotypes, and allele frequencies. (**A**) Location of the studied hybrid zone (orange line), other hybrid zones (orange circles), and sampled *A. m. pseudomajus* (magenta) and *A. m. striatum* (yellow) populations. Genetically studied populations are starred. (**B**) Clines in magenta and yellow color scores in subpopulations along a transect through the hybrid zone. (**C**) Frequencies of *ROS1* (magenta squares) and *PAL* (blue circles) haplogroups and a 6–base pair polymorphism at *DICH* (green triangles) in subpopulations along the hybrid zone transect. For *ROS1*, all markers were collapsed to a two-allele system.

[1]Department of Cell and Developmental Biology, John Innes Centre, Colney Lane, Norwich NR4 7UH, UK. [2]Laboratoire Evolution et Diversité Biologique, UMR 5174 CNRS–Université Paul Sabatier, 31062 Toulouse Cédex 9, France. [3]School of Computing Sciences, University of East Anglia, Earlham Road, Norwich NR4 7TJ, UK.

*These authors contributed equally to this work.
†To whom correspondence should be addressed. E-mail: enrico.coen@bbsrc.ac.uk

sulf/*sulf*, whereas those with a low yellow score were either *SULF*/*SULF* or *SULF*/*sulf*, indicating that *SULF* genotype was the major determinant of variation in yellow. Individuals with a low magenta score were *ros EL*/*ros EL*, those with an intermediate score were *ROS el*/*ros EL*, and those with a high magenta score were *ROS el*/*ROS el*. Therefore, variation in magenta was largely accounted for by the *ROS EL* loci. These results allowed us to create an appropriate genotypic space for the F2. Digital images of representative flowers of four genotypes were warped to the same average flower shape. Principal component analysis on variation in pixel color at each position in the flower then allowed us to define a 3D genotypic space controlling flower color (*15*–*17*) (Fig. 2D).

The role of flower color variation in natural populations was assessed by analyzing a hybrid zone between *A. m. pseudomajus* and *A. m. striatum*. Scoring 493 plants across the hybrid zone revealed a steep cline for flower color (Fig. 1B). Allelism tests on 14 plants from the contact zone with a range of phenotypes confirmed that flower color was largely determined by *ROS*, *EL*, and *SULF* genotypes. For *ROS*, more extensive genotyping could be carried out by using molecular markers. The *ROS* locus comprises a tandem duplication of two MYB-related transcription factors, ROS1 and ROS2, with ROS1 having a greater role in flower color variation (*13*). We sequenced a 1.2-kb region of *ROS1*, from the promoter to the start of the second exon. Sequences from 13 yellow and 15 magenta morphs from locations distant from the contact zone showed that *ROS1* alleles fell into three major groups (haplogroups) (Fig. 3A). One haplogroup was specific to yellow morphs and was identical to the *ros*^{dor} allele of *A. majus*, hypothesized to have been derived from the wild (*13*). The other two haplogroups were found only in magenta morphs. *ROS1* sequences were used to design primers that allowed haplogroups to be distinguished by polymerase chain reaction. Genotyping 528 plants from the hybrid zone showed that the cline in *ROS1* haplogroup frequency coincided with magenta flower color (Fig. 1C).

Assuming that the hybrid zone arose from contact between previously separate yellow and magenta populations, the observed clines in flower color and genotype might have two explanations (*18*, *19*). One is that *A. m. striatum* and *A. m. pseudomajus* came into recent contact and the clines reflect a neutral mixing of alleles between the populations. Alternatively, there has been a longer history of contact, and clines reflect selection maintaining morph differences. To evaluate these possibilities, we analyzed molecular variation at loci not involved in magenta and yellow morph differences. According to the neutral model, these loci should have a cline similar to that of *ROS1*. The *PALLIDA* (*PAL*) and *DICHOTOMA* (*DICH*) loci were chosen because they are linked to *ROS* [16 centimorgan (cM) and 9 cM from *ROS*, respectively], and sequences are available for primer design (*20*, *21*). Alleles were sequenced from 18 individuals on either side of the hybrid zone. Most *PAL* alleles fell into two major haplogroups (Fig. 3B). *DICH* alleles showed little haplogroup structure, although several DNA polymorphisms were detected. We genotyped 496 plants across the hybrid zone for the two *PAL* haplogroups and a polymorphism at *DICH*. No cline was observed for *PAL* or *DICH*, indicating that these genes were subject

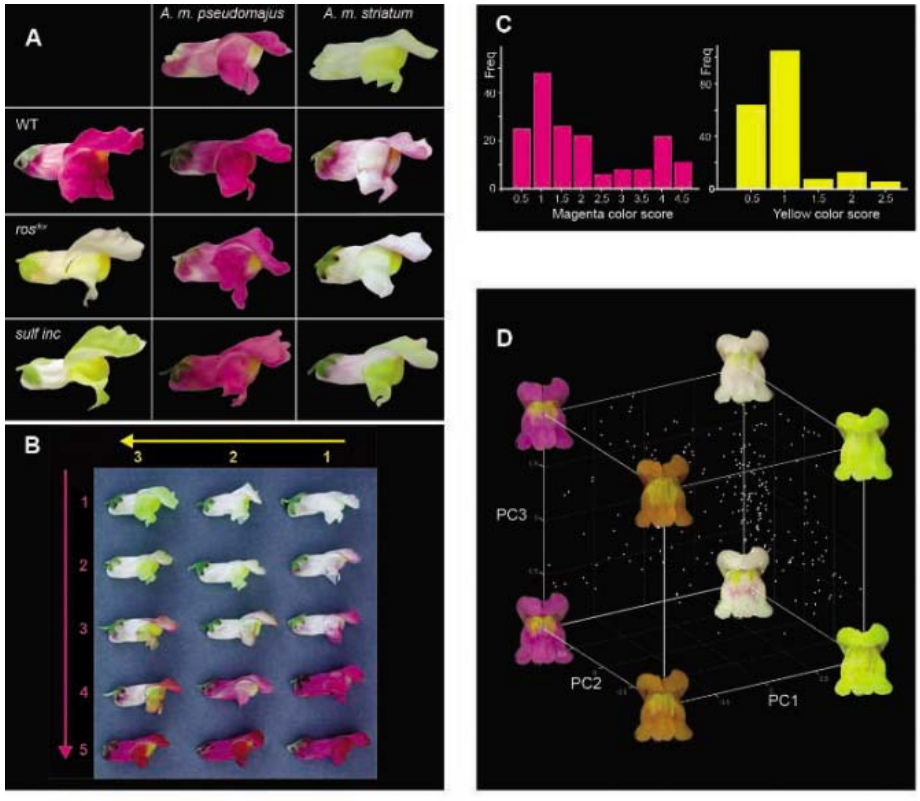

Fig. 2. Phenotypes and complementation tests. (**A**) F1 flowers from crosses between *A. m. pseudomajus* and *A. m. striatum* (top row) and cultivated *A. majus* genotypes (left column). *A. majus* homozygous lines are wild type (*ROS el; SULF*), *rosea*^{dorsea} (*ros*^{dor} *el; SULF*), and *sulfurea incolorata* (*ROS el; sulf; inc*). (**B**) Numerical scoring system for ranking magenta and yellow flower color. (**C**) Frequency of magenta (left) and yellow (right) scores in an F2 population from *A. m. striatum* × *A. m. pseudomajus*. (**D**) Genotypic space capturing flower color variation with three principal components (PCs). The four genotypes used for PC analysis were *ROS el/ROS el; SULF/–*, *ros EL/ros EL; sulf/sulf*, *ROS el/ros EL; SULF/–*, and *ros EL/ros EL; SULF/–* (dash indicates unknown allele). Positions for 174 F2 and 110 F3 plants are shown as white points.

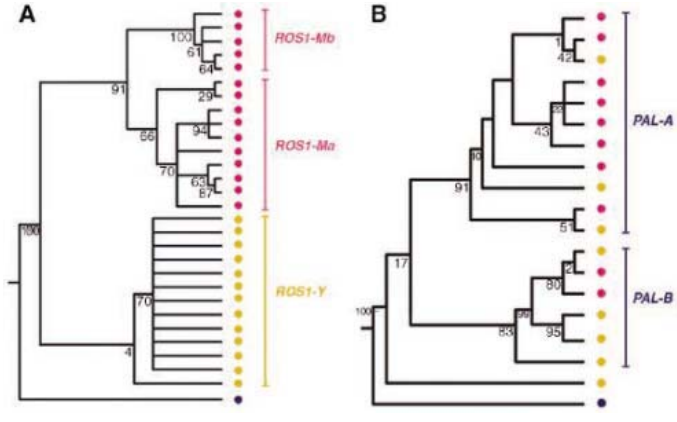

Fig. 3. Molecular variation at *ROS1* and *PAL*. Sequences for *A. m. striatum* (yellow) and *A. m. pseudomajus* (magenta) from individuals collected outside the contact zone. Phylogenies and bootstrap values were generated by using maximum parsimony analysis, with *A. latifolium* (blue) as the outgroup. (**A**) *ROS1* molecular phylogeny. Yellow morphs contained one haplogroup (*ROS1-Y*), whereas magenta morphs contained a mixture of two haplogroups (*ROS1-Ma* and *ROS1-Mb*). (**B**) *PAL* molecular phylogeny. Most sequences belong to one of two haplogroups (*PAL-A* and *PAL-B*), but there is no clear association between haplogroup and flower color.

to different evolutionary factors than *ROS1* (Fig. 1C). This was also supported by genotyping 16 *A. m. striatum* and *A. m. pseudomajus* populations distant from the hybrid zone (Fig. 1A and table S1). In all cases, the *ROS1* haplogroup correlated with flower color, whereas *PAL* and *DICH* loci showed no such association.

The simplest interpretation of these results is that spatial variation in *PAL* and *DICH* allele frequencies reflects historical gene flow between populations, whereas the *ROS1* cline has been maintained by selection on flower color. The cline could be maintained, for example, if intermediate genotypes have lower fitness than the parental morphs (*22*). Thus, magenta and yellow morphs might represent distinct peaks on an adaptive landscape, whereas intermediate forms represent an intervening low fitness valley. However, this raises the problem of how the low fitness valley was traversed when the two morphs diverged from a common ancestor.

To address this issue, we mapped the range of phenotypes exhibited by *Antirrhinum* species within the defined genotypic space (Fig. 2D). This was achieved by photographing several flowers from each species (Fig. 4A) and warping the images to the same flower shape (Fig. 4B). We then determined the position in the genotypic space that best approximated the color for each flower (Fig. 4C). The approximation was evaluated by warping the resulting image back to the initial flower shape and comparing it to the original image (Fig. 4D). Much of the variation in flower color was captured within the 3D genotypic space, consistent with previous studies showing that the *ROS*, *EL*, and *SULF* loci play important roles in color variation in the species group as a whole (*11*–*13*) (Fig. 4E).

When flowers from 19 species were mapped into the genotypic space, they collectively formed a broad U-shaped cloud of points (Fig. 4, F to H). Flowers from each species formed smaller clusters within this broader cloud. Magenta *A. m. pseudomajus* flowers localized near one end of the cloud, whereas yellow *A. m. striatum* flowers were near the other end. Intermediate positions within the cloud corresponded to various other patterns and intensities of color. However, certain color combinations were excluded from the cloud, even though they were observed in F2 and hybrid zone populations. For example, orange flowers, having a broad spread of both yellow and magenta (*ROS el*/*ROS el; sulf*/*sulf*), were not within the cloud (Fig. 4F). The absence of this genotype in wild species could be explained if individuals with orange flowers have lower fitness, perhaps because they are less attractive to pollinators (*23*–*25*). The role of pollinators in propagating *A. m. pseudomajus* and *A. m. striatum* is likely to be of central importance because the species are self-incompatible, seed dispersal is limited (involving gravity or water runoff), and individuals typically survive for only 1 to 3 years.

Taken together, our results suggest that magenta and yellow morphs did not evolve through intermediate genotypes giving orange flowers, but that instead evolution followed the route defined by the U-shaped cloud. According to this view, the cloud represents a region of high fitness, allowing flower color to evolve without incurring major fitness costs. However, when genotypes, such as magenta and yellow morphs, from distant parts of the cloud meet, they can generate progeny that lie outside the high fitness cloud, creating a barrier to exchange of flower color alleles. This would account for the observed steep cline at loci controlling color differences in the hybrid zone. A 2D slice through the U-shaped cloud, passing perpendicularly through its two arms, would yield an adaptive landscape with two separate peaks. The cloud therefore represents a high fitness path between what might otherwise seem like distinct peaks, showing how higher dimensional representations allow adaptive continuity and incompatibility to be more easily reconciled (*2*).

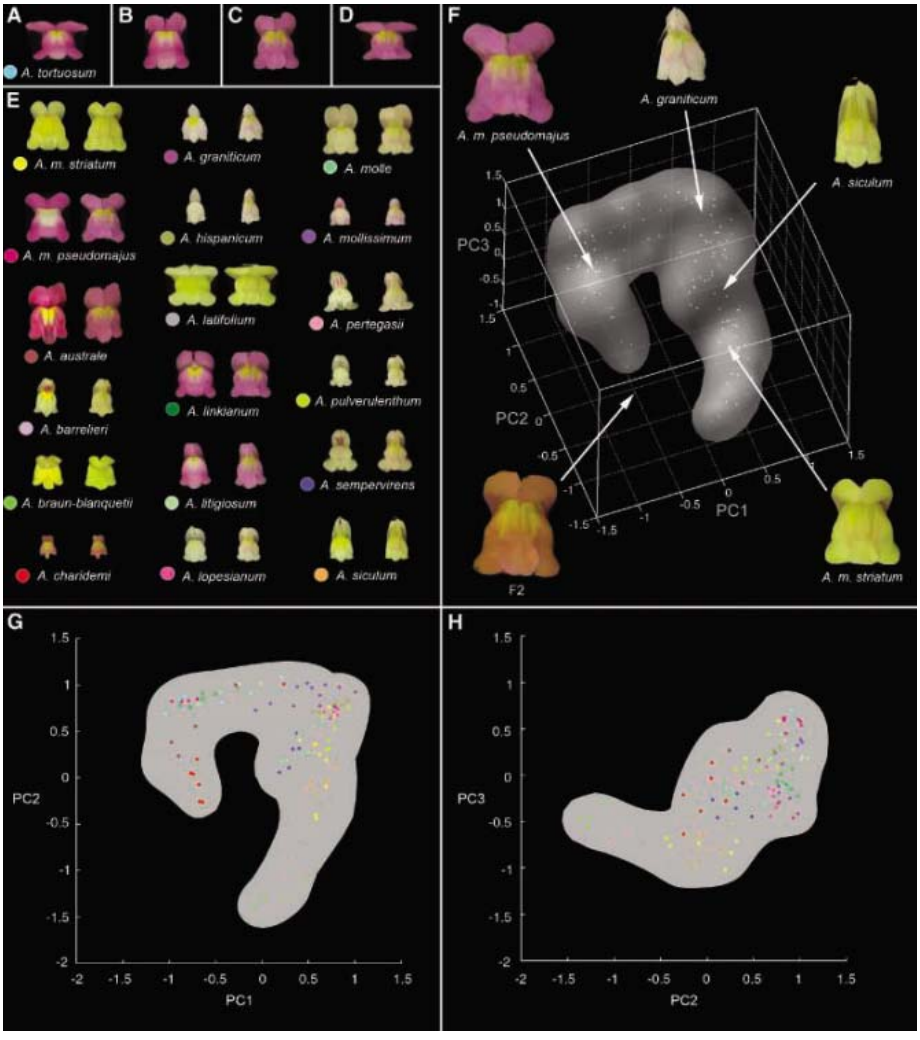

Fig. 4. *Antirrhinum* species placed in 3D genotypic space. (**A**) Mean *A. tortuosum* flower. (**B**) *A. tortuosum* flower warped to mean shape used to generate genotypic space (Fig. 1C). (**C**) Projection of (B) into genotypic space. (**D**) Image obtained when (C) is warped back to the mean *A. tortuosum* flower shape. (**E**) Projection of 19 *Antirrhinum* species into genotypic space. In each case, flower on the left shows the mean appearance, whereas flower on the right shows the appearance after projection into genotypic space [equivalent to (A) and (D) for each species]. (**F**) Cloud obtained for flowers from 19 species represented in genotypic space. Each point shows the position of a single flower projected into genotypic space. Examples of flowers from different positions in the genotypic space are illustrated. (**G** and **H**) Two different 2D projections of the cloud, with each species color-coded as in (E).

References and Notes

1. S. Wright, in Vol. 1 of *Proceedings of the Sixth Annual Congress of Genetics*, D. F. Jones, Ed. (Genetics Society of America, Austin, TX, 1932), p. 356–366.
2. S. Gavrilets, *Fitness Landscapes and the Origin of Species*, S. Levin, H. Horn, Eds., no. 41 of *Monographs in Population Biology* (Princeton Univ. Press, Princeton, NJ, 2004).
3. S. Gavrilets, *Trends Ecol. Evol.* **12**, 307 (1997).
4. W. Rothmaler, *Taxonomische Monographie der Gattung Antirrhinum* (Akademie-Verlag, Berlin, 1956).
5. D. A. Webb, in *Flora Europaea*, T. Tutin *et al.*, Eds. (Cambridge Univ. Press, Cambridge, 1972), vol. 3.

6. D. Sutton, *A Revision of the Tribe Antirrhineae* (Oxford Univ. Press, Oxford, 1988).
7. I. Mateu-Andres, J. G. Segarra-Moragues, *Ann. Bot. (Lond.)* **92**, 647 (2003).
8. P. Vargas, J. A. Rosselló, R. Oyama, J. Güemes, *Plant Syst. Evol.* **249**, 151 (2004).
9. Z. Schwarz-Sommer, B. Davies, A. Hudson, *Nat. Rev. Genet.* **4**, 657 (2003).
10. T. Gubitz, A. Caldwell, A. Hudson, *Mol. Biol. Evol.* **20**, 1537 (2003).
11. J. Hackbarth, P. Michaelis, G. Scheller, *Z. Indukt. Abstammungs- Vererbungslehre* **80**, 1 (1942).
12. H. Stubbe, *Genetik und Zytologie von Antirrhinum L. sect. Antirrhinum* (Veb Gustav Fischer Verlag, Jena, Germany, 1966).
13. K. Schwinn *et al.*, *Plant Cell* **18**, 831 (2006).
14. E. Baur, *Bibl. Genet.* **4**, 1 (1924).
15. G. W. Horgan, *Comput. Electron. Agric.* **31**, 169 (2001).
16. T. F. Cootes, G. J. Edwards, C. J. Taylor, *IEEE Trans. Pattern Anal. Mach. Intell.* **23**, 681 (2001).
17. N. B. Langlade *et al.*, *Proc. Natl. Acad. Sci. U.S.A.* **102**, 10221 (2005).
18. N. H. Barton, G. M. Hewitt, *Annu. Rev. Ecol. Syst.* **16**, 113 (1985).
19. N. H. Barton, B. O. Bengtsson, *Heredity* **57**, 357 (1986).
20. D. Luo *et al.*, *Cell* **99**, 367 (1999).
21. E. S. Coen, R. Carpenter, C. Martin, *Cell* **47**, 285 (1986).
22. W. S. Moore, J. T. Price, in *Hybrid Zones and the Evolutionary Process*, R. G. Harrison, Ed. (Oxford Univ. Press, Oxford, 1993), pp. 196–225.
23. D. W. Schemske, H. D. Bradshaw Jr., *Proc. Natl. Acad. Sci. U.S.A.* **96**, 11910 (1999).
24. L. Chittka, J. D. Thomson, Eds., *Cognitive Ecology of Pollination* (Cambridge Univ. Press, Cambridge, 2001).
25. H. D. Bradshaw Jr., D. W. Schemske, *Nature* **426**, 176 (2003).

26. We thank C. Martin and J. Venail for providing the *ROS* sequence before publication; M. Burrus, L. Copsey, J. Bowers, C. Cazettes-Vicedo, and Z.-L. Liu for their help with carrying out genotyping and genetics; M. Bernardet, M. Cruzan, and J. Leneveu for their help in the field; and G. Hewitt for helping to initiate this project. This research was funded by grants from the Biotechnology and Biological Sciences Research Council, UK. Sequences are deposited in GenBank; accession numbers DQ866629 to DQ866657 for *ROSEA1*, DQ866658 to DQ866676 for *PALLIDA*, and DQ866677 to DQ866701 for *DICHOTOMA*.

Supporting Online Material

www.sciencemag.org/cgi/content/full/313/5789/963/DC1
Materials and Methods
Figs. S1 to S3
Tables S1 and S2
References

25 April 2006; accepted 21 July 2006
10.1126/science.1129161

Plant Genotypic Diversity Predicts Community Structure and Governs an Ecosystem Process

Gregory M. Crutsinger,[1]* Michael D. Collins,[1] James A. Fordyce,[1] Zachariah Gompert,[2] Chris C. Nice,[2] Nathan J. Sanders[1]

Theory predicts, and recent empirical studies have shown, that the diversity of plant species determines the diversity of associated herbivores and mediates ecosystem processes, such as aboveground net primary productivity (ANPP). However, an often-overlooked component of plant diversity, namely population genotypic diversity, may also have wide-ranging effects on community structure and ecosystem processes. We showed experimentally that increasing population genotypic diversity in a dominant old-field plant species, *Solidago altissima*, determined arthropod diversity and community structure and increased ANPP. The effects of genotypic diversity on arthropod diversity and ANPP were comparable to the effects of plant species diversity measured in other studies.

Ecological theory (*1*, *2*) and field experiments (*3*, *4*) have revealed a positive relationship between the diversity of plant species and the diversity of associated consumers. At least two mechanisms might explain this pattern. First, because approximately 90% of herbivorous insects exhibit some degree of host specialization (*5*), as plant species richness increases, so should the number of associated herbivore species. This resource specialization hypothesis has some theoretical support (*1*, *2*, *6*). Second, if aboveground net primary productivity (ANPP) increases as plant species richness increases (*7*), then more herbivore individuals, and therefore more species, will be supported by increases in available energy (this has been called the more individuals hypothesis) (*8*). An increase in the number of herbivore species by either of these mechanisms should support more predator species (*9*). Recent studies have shown that population genotypic diversity, like plant species diversity, can have extended consequences for communities and ecosystems (*10*–*14*). However, no studies to date have explicitly linked intraspecific genotypic diversity, the structure of associated communities, and the potential mechanisms driving these patterns, such as energy availability. This paucity of studies exists despite numerous calls for such research within the literature regarding biodiversity-ecosystem function (*7*, *15*). We tested whether host-plant genotypic diversity determines the structure of associated arthropod communities and governs an ecosystem process, ANPP, that influences arthropod species richness.

We manipulated the plot-level genotypic diversity (the number of genotypes per plot) of *Solidago altissima*, tall goldenrod, a common perennial plant throughout eastern North America. Twenty-one *S. altissima* ramets were collected from local *S. altissima* patches growing in fields near the study site, and each ramet was identified as a unique genotype by means of amplified fragment length polymorphism. From these 21 genotypes, we established 63 1-m^2 experimental plots, each containing 12 individuals and 1, 3, 6, or 12 randomly selected genotypes, mimicking the densities and levels of genotypic diversity found in natural patches of similar size. We censused arthropods on every ramet in each plot five times over the course of the growing season. In total, we counted 36,997 individuals of ~136 species. We estimated ANPP at the peak of the growing season using nondestructive allometric techniques (*16*).

Total cumulative arthropod species richness increased with plant genotypic diversity. The number of arthropod species was, on average, 27% greater in 12-genotype plots than in single-genotype plots (Fig. 1), indicating that plant genotypic diversity was an important determinant of arthropod diversity. When we examined the effects of genotypic diversity on community structure, we found that herbivore species richness (Fig. 2B) and predator richness (Fig. 2A) also increased with increasing genotypic diversity. The effects of genotypic diversity on arthropod communities were nonadditive (Fig. 1). That is, total arthropod richness and herbivore and predator richness were all greater in the 6- and 12-genotype plots than would be predicted by summing the number of arthropod species associated with the corresponding genotypes grown in monoculture ($P < 0.01$).

ANPP also increased with plant genotypic diversity and was 36% greater in 12-genotype plots than in single-genotype plots (Fig. 2C). The effect of genotypic diversity on ANPP could be due to increased niche complementarity (mixed genotypes used available resources more completely or mixed genotypes facilitated one another, thereby increasing ANPP in mixtures) (*7*, *15*) or to sampling or selection effects (increased ANPP caused by randomly assembled mixtures having a higher probability of containing highly productive genotypes) (*17*). Using standard techniques (*18*) we found that selection effects were highly variable and were not significantly different from zero ($P > 0.60$ for all treatments), indicating that highly productive genotypes do not dominate in mixtures and drive observed increases in ANPP. Selection

[1]Department of Ecology and Evolutionary Biology, University of Tennessee, Knoxville, TN 37996, USA. [2]Department of Biology, Texas State University, San Marcos, TX 78666, USA.

*To whom correspondence should be addressed. E-mail: gcrutsin@utk.edu

effects were not related to genotypic diversity (fig. S1A). We also found complementarity effects to be highly variable, generally positive, but not significantly different from zero ($P > 0.20$ for all treatments). We found a marginally significant increase in complementarity with increasing genotypic diversity (fig. S1B), indicating that positive interactions among genotypes in mixtures may lead to increases in ANPP with increasing genotypic diversity.

Arthropod richness might respond to genotypic diversity either because of increased productivity in plots with higher genotypic diversity, as the more individuals hypothesis predicts (*8*), or because genotypes vary in susceptibility to particular herbivores, as the resource specialization hypothesis predicts (*6*). Like species richness, arthropod abundances increased with plant genotypic diversity (*19*). In addition, there was a positive relationship between ANPP and both arthropod richness and abundance (*19*). Arthropod richness and abundance were positively correlated with one another (*19*). To test whether the effects of ANPP and genotypic diversity on arthropod species richness resulted from species-rich plots having more arthropod individuals, as the more individuals hypothesis predicts (*8*), we used rarefaction to examine the response of rarefied arthropod species richness to plant genotypic diversity. Rarefaction corrects for differences in the number of individuals among plots (*20*). There was no relationship between rarefied total arthropod richness and ANPP, or between rarefied herbivore and predator richness and ANPP ($P > 0.10$ in all cases), indicating that ANPP controls richness by affecting the number of individual arthropods. Rarefied total richness and rarefied herbivore richness instead increased as plot-level plant genotypic diversity increased, but rarefied predator richness did not (fig. S2). However, rarefied predator richness did depend on rarefied herbivore richness, suggesting an indirect effect of host-plant genotypic diversity on predator diversity mediated by herbivore diversity (fig. S2). These results indicate that increasing genotypic diversity increases the amount of resources (ANPP) available to herbivores. As ANPP increased, so did arthropod abundance, resulting in increases in the number of species, as the more individuals hypothesis predicts (*8*). When we controlled for variation in arthropod abundance using rarefaction, genotypic diversity explained an additional 12% of the variation in rarefied total and rarefied herbivore richness, indicating a second mechanism by which genotypic diversity affects arthropod communities: by increasing the diversity of resources available, as predicted by the resource specialization hypothesis (*6*). Moreover, the abundance and composition of herbivore assemblages were more similar within *Solidago* genotypes than among genotypes, and particular genotypes were more susceptible to herbivory than were others (supporting online text and figs. S3 to S5). Taken together, these results suggest that particular herbivores are associated with particular host-plant genotypes.

To compare our results to studies that have examined how plant species diversity affects arthropod diversity and ANPP, we calculated the standardized effect sizes (SESs) (*21*) of genotypic diversity using our data and the SESs of plant species diversity using data from the Cedar Creek Long Term Ecological Research Biodiversity II experiment (*3*). A SES measures the number of standard deviations that the most diverse plots (12 genotypes in our case, 16 species from Cedar Creek) is above or below the single-genotype or single-species plots. The SES of plant genotypic diversity on arthropod diversity in our study (SES = 1.80) was nearly two times the SES of plant species diversity on arthropod diversity from Cedar Creek (SES = 0.93). The SES of plant genotypic diversity (SES = 1.33) on ANPP in our study was similar to the SES of plant species diversity on ANPP at Cedar Creek (SES = 1.35). Our results indicate that the effect of genotypic diversity within a host-plant population on associated arthropod communities and ANPP is directly comparable to the effect of species diversity within a plant community (*3*, *4*). A field experiment that orthogonally manipulates genotypic diversity and species diversity in concert could

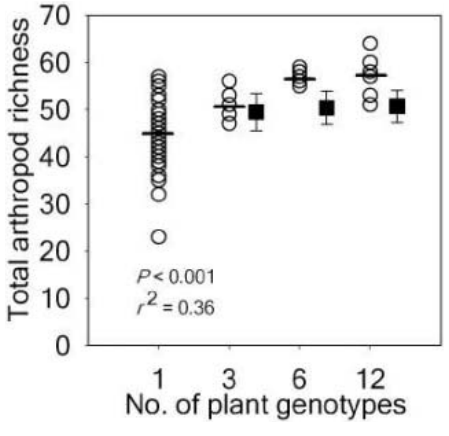

Fig. 1. Relationship between population-level genotypic diversity of *S. altissima* and total arthropod species richness. Circles indicate plot-level observations, and horizontal lines indicate treatment means. Squares indicate the number of arthropod species predicted by simple additive models. Error bars indicate 95% confidence interval.

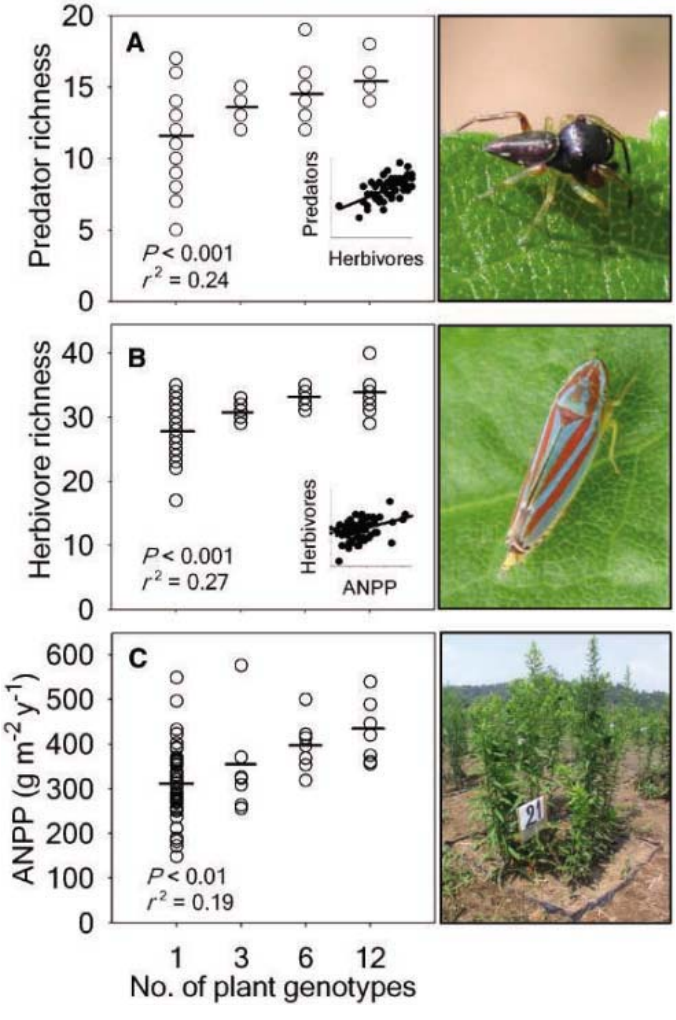

Fig. 2. Relationship between population-level plant genotypic diversity and predator species richness (**A**), herbivore species richness (**B**), and ANPP of *S. altissima* (**C**). Open circles indicate plot-level observations, and horizontal lines indicate treatment means. The inset in (A) shows the relationship between herbivore species richness and predator species richness ($r^2 = 0.36$, $P < 0.001$), and the inset in (B) shows the relationship between ANPP and herbivore richness ($r^2 = 0.17$, $P < 0.001$).

further elucidate the relative contributions of intra- and interspecific diversity on community- and ecosystem-level processes.

Our work indicates two mechanisms underlying the relationships among intraspecific genotypic diversity, the diversity of associated consumers, and ecosystem processes. We explicitly showed that the effect of genotypic diversity on arthropods does not occur simply because of increased ANPP in diverse plots. It also arises because of an increase in the diversity of resources available to herbivores. These effects are nonadditive and cascade across trophic levels to structure associated communities. Our results demonstrate the need to incorporate intraspecific variation into current ecological theory that has emphasized the importance of interspecific variation (*3*, *4*, *7*, *15*, *17*, *18*) or theory that ignores differences among species (*22*). Given the focus of conservation efforts on how the loss of species from communities affects ecosystem processes, our work suggests that the loss of genotypes from populations can no longer be overlooked (*14*, *23*–*25*).

References and Notes

1. G. E. Hutchinson, *Am. Nat.* **93**, 145 (1959).
2. R. H. MacArthur, *Geographical Ecology* (Harper & Row, New York, 1972), pp. 169–194.
3. E. Siemann, D. Tilman, J. Haarstad, M. Ritchie, *Am. Nat.* **152**, 738 (1998).
4. N. M. Haddad, D. Tilman, J. Haarstad, M. Ritchie, J. M. H. Knops, *Am. Nat.* **158**, 17 (2001).
5. E. Bernays, M. Graham, *Ecology* **69**, 886 (1988).
6. P. W. Price, in *Variable Plants and Herbivores in Natural and Managed Systems*, R. F. Denno, M. S. McClure, Eds. (Academic Press, New York, 1983), pp. 559–596.
7. D. U. Hooper *et al.*, *Ecol. Monogr.* **75**, 3 (2005).
8. D. S. Srivastava, J. H. Lawton, *Am. Nat.* **152**, 510 (1998).
9. M. D. Hunter, P. W. Price, *Ecology* **73**, 724 (1992).
10. Y. Y. Zhu *et al.*, *Nature* **406**, 718 (2000).
11. A. R. Hughes, J. J. Stachowicz, *Proc. Natl. Acad. Sci. U.S.A.* **101**, 8998 (2004).
12. J. A. Schweitzer, J. K. Bailey, S. C. Hart, T. G. Whitham, *Ecology* **86**, 2834 (2005).
13. T. B .H. Reusch, A. Ehlers, A. Hämmerli, B. Worm, *Proc. Natl. Acad. Sci. U.S.A.* **102**, 2831 (2005).
14. M. T. J. Johnson, M. J. Lajeunesse, A. A. Agrawal, *Ecol. Lett.* **9**, 24 (2006).
15. M. Loreau, S. Naeem, P. Inchausti, Eds., *Biodiversity and Ecosystem Functioning: Synthesis and Perspectives* (Oxford Univ. Press, Oxford, 2002), pp. 237–242.
16. See supporting material on *Science* Online.
17. M. A. Huston, *Oecologia* **110**, 449 (1997).
18. M. Loreau, A. Hector, *Nature* **413**, 548 (2001).
19. Abundances were positively related to genotypic diversity (total: $r^2 = 0.27$, $P < 0.001$; herbivores: $r^2 = 0.29$, $P < 0.001$; predators: $r^2 = 0.07$, $P = 0.03$). There was a positive relationship between ANPP and arthropod richness (total: $r^2 = 0.24$, $P < 0.001$; herbivores: $r^2 = 0.17$, $P < 0.001$; predators: $r^2 = 0.15$, $P = 0.001$) and total abundance ($r^2 = 0.19$, $P < 0.001$) and herbivore abundance ($r^2 = 0.23$, $P < 0.001$). Arthropod richness and abundance were correlated ($r = 0.74$, $P < 0.001$; herbivores: $r = 0.70$, $P < 0.001$; predators: $r = 0.29$, $P = 0.02$).
20. N. J. Gotelli, G. R. Graves, *Null Models in Ecology* (Smithsonian Institution, Washington, DC, 1996), pp. 21–46.
21. S. M. Scheiner, J. Gurevitch, Eds., *The Design and Analysis of Ecological Experiments* (Chapman & Hall, New York, 1993), pp. 347–369.
22. S. P. Hubbell, *A Unified Neutral Theory of Biodiversity and Biogeography* (Princeton Univ. Press, Princeton, NJ, 2001).
23. T. G. Whitham *et al.*, *Ecology* **84**, 559 (2003).
24. G. W. Luck, G. C. Daily, P. R. Ehrlich, *Trends Ecol. Evol.* **18**, 331 (2003).
25. G. M. Wimp *et al.*, *Ecol. Lett.* **7**, 776 (2004).

26. We thank K. Crawford, C. Engel, J. Hite, J. Ledford, and K. McFarland for help in the field and lab and W. Abrahamson, J. Bailey, M. Cadotte, A. Classen, R. Dunn, V. Eviner, N. Gotelli, M. Johnson, J. Schweitzer, D. Simberloff, J. Weltzin, J. Williams, and three anonymous reviewers for helpful comments. This research was funded by an Environmental Protection Agency Science to Achieve Results graduate fellowship, a Hilton Smith Graduate Fellowship, and the University of Tennessee.

Supporting Online Material

www.sciencemag.org/cgi/content/full/313/5789/966/DC1
Materials and Methods
SOM Text
Figs. S1 to S8
Table S1
References

4 April 2006; accepted 12 June 2006
10.1126/science.1128326

p53-Mediated Inhibition of Angiogenesis Through Up-Regulation of a Collagen Prolyl Hydroxylase

Jose G. Teodoro, Albert E. Parker, Xiaochun Zhu, Michael R. Green*

Recent evidence suggests that antiangiogenic therapy is sensitive to p53 status in tumors, implicating a role for p53 in the regulation of angiogenesis. Here we show that p53 transcriptionally activates the α(II) collagen prolyl-4-hydroxylase [α(II)PH] gene, resulting in the extracellular release of antiangiogenic fragments of collagen type 4 and 18. Conditioned media from cells ectopically expressing either p53 or α(II)PH selectively inhibited growth of primary human endothelial cells. When expressed intracellularly or exogenously delivered, α(II)PH significantly inhibited tumor growth in mice. Our results reveal a genetic and biochemical linkage between the p53 tumor suppressor pathway and the synthesis of antiangiogenic collagen fragments.

The tumor suppressor activity of p53 results from its ability to transcriptionally activate a wide variety of target genes that in turn regulate cell cycle arrest, apoptosis, and suppression of angiogenesis (*1*). Although a number of p53 target genes involved in growth arrest and apoptosis have been identified, the role of p53 in the regulation of angiogenesis is less well understood. Using a polymerase chain reaction (PCR)–based subtractive hybridization strategy (*2*), we identified α(II) collagen prolyl-4-hydroxylase [α(II)PH] as a p53-stimulated gene. In this screen, ecdysone-inducible p53 expression was established in the $p53^{-/-}$ human cell line Saos-2 (Saos-2/Ec-p53 cells). Figure 1A (top) demonstrates that induction of p53 expression in these cells (bottom) stimulated transcription of α(II)PH as well as p21, a known p53 target gene (*3*). Up-regulation of α(II)PH was also observed when endogenous p53 expression was induced in wild-type HCT116 cells by the DNA damage-inducing agent camptothecin, but not in a matched $p53^{-/-}$ cell line (fig. S1). α(II)PH expression was also up-regulated upon expression of p53 from an adenovirus vector in $p53^{-/-}$ H1299 human cancer cells (Fig. 1B). By contrast, expression of p53 had no effect on transcription of another collagen prolyl-4-hydroxylase isoform, α(I)PH, or three other human prolyl hydroxylases, PHD1, 2, and 3.

The α(II)PH promoter region contains three partially overlapping putative p53-binding half sites (see below). We derived reporter constructs by cloning sequences upstream of the α(II)PH transcription start-site or, as a control, the p21 promoter, upstream of the chloramphenicol acetyltransferase (CAT) gene. Ectopic p53 expression increased activity of both p21-CAT and α(II)PH-CAT (Fig. 1C). The chromatin immunoprecipitation (ChIP) experiment of Fig. 1D shows that p53 was recruited to the α(II)PH promoter in vivo. Collectively, the results of Fig. 1 show that α(II)PH is a direct p53 target gene.

Prolyl hydroxylation is a required, rate-limiting step in collagen biosynthesis (*4*), suggesting that p53-mediated stimulation of α(II)PH expression might increase collagen levels. We therefore investigated the effect of p53 expression on endogenous collagen 18 levels. Unexpectedly, the level of full-length collagen 18 was diminished in H1299 cells following expression of wild-type p53 but not a transcriptionally defective p53 mutant (Fig. 2A, left, and fig. S2) (*5*). One explanation for this result is that under these conditions, collagen breakdown was also stimulated. To test this hypothesis,

Howard Hughes Medical Institute, Programs in Gene Function and Expression and Molecular Medicine, University of Massachusetts Medical School, 364 Plantation Street, Worcester, MA 01605, USA.

*To whom correspondence should be addressed. E-mail: michael.green@umassmed.edu

we analyzed conditioned media (CM) from p53-expressing H1299 cells. The results (Fig. 2A, right) indicate that the proteolytically processed ~30- and ~18-kD collagen 18 C-terminal fragments, which corresponded in size to NC1 and the well-characterized antiangiogenic agent endostatin, respectively, were present only in CM from cells expressing wild-type p53.

To verify that p53 expression leads to the production of collagen 18 C-terminal fragments, we derived an H1299 cell line stably expressing full-length collagen 18 bearing a C-terminal V5 epitope tag (H1299/col18-V5 cells). Expression of p53 in these cells resulted in the production of the NC1 fragment and endostatin, which was not observed in control H1299/col18-V5 cells or in cells expressing LacZ (Fig. 2B). Analysis of CM from these cells showed that NC1 and endostatin were present only following expression of p53. Treatment with the caspase inhibitor zVADfmk had no effect on the production of NC1 and endostatin (fig. S3), indicating that processing of collagen 18 is not a nonspecific consequence of p53-mediated apoptosis.

To confirm that α(II)PH activity is necessary for the p53-dependent production of collagen-derived antiangiogenic peptides, we analyzed NC1 and endostatin levels following inhibition of α(II)PH using two strategies. First, in CM from p53-expressing H1299/col18-V5 cells prepared in the presence of the prolyl hydroxylase inhibitor ethyl-3,4-dihydroxy benzoate (EDHB), the levels of NC1 and endostatin were substantially lower (fig. S4). Second, we used an antisense oligonucleotide (AO) to specifically inhibit the production of α(II)PH in p53-expressing H1299/col18-V5 cells. An AO against α(II)PH, but not a control AO, prevented both the induction of α(II)PH observed upon p53

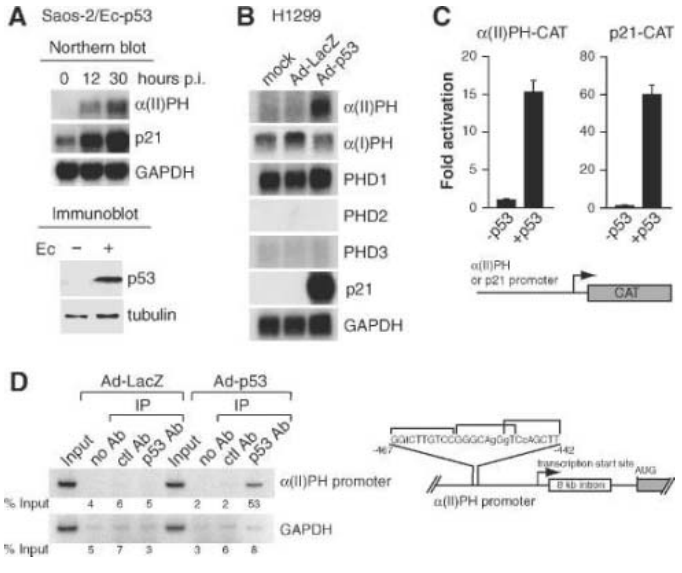

Fig. 1. α(II)PH is a direct p53 target gene. (**A**) (Top) Northern blot monitoring expression of α(II)PH and p21 in Saos-2/Ec-p53 cells at 0, 12, and 30 hours postinduction (p.i.). GAPDH (glyceraldehyde-3-phosphate dehydrogenase) is shown as a loading control. (Bottom) Immunoblot showing p53 protein levels in Saos-2/Ec-p53 cells before and after p53 induction. Tubulin levels were monitored as a loading control. (**B**) Northern blot showing expression of α(II)PH, α(I)PH, and PHD1, 2, and 3 in H1299 cells mock infected or infected with adenovirus expressing LacZ (Ad-LacZ) or p53 (Ad-p53). Expression of p21 and GAPDH were used as positive and loading controls, respectively. (**C**) H1299 cells were cotransfected with the α(II)PH- or p21-CAT reporter construct together with a p53-expression plasmid or vector control, and CAT activity was quantitated. Error bars indicate SEM. (**D**) (Left) ChIP analysis. Input and immunoprecipitated (IP) DNA was amplified by PCR with primer pairs corresponding to the α(II)PH promoter or, as a negative control, the GAPDH coding sequence, and IP DNA was quantitated and presented as the percentage of IP relative to input. (Right) Schematic diagram of the α(II)PH promoter region showing the positions of the putative p53-binding sites.

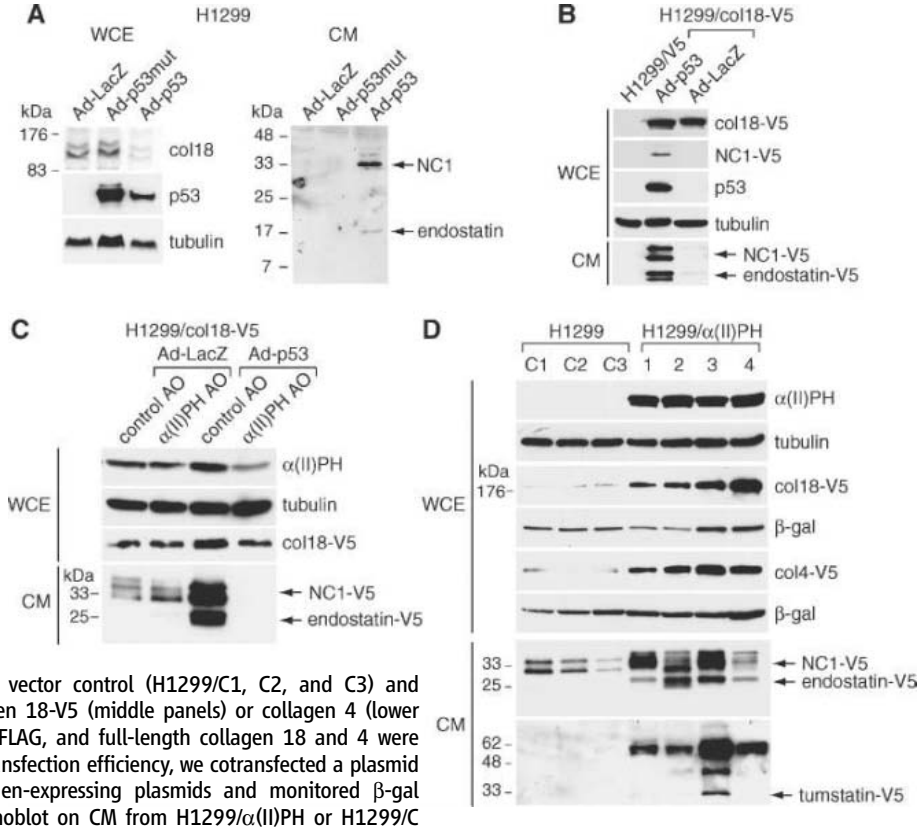

Fig. 2. Expression of p53 stimulates the extracellular release of antiangiogenic collagen 4 and 18 C-terminal fragments. (**A**) (Left) Immunoblot showing expression of endogenous collagen 18 in whole-cell extracts (WCE) from H1299 cells infected with Ad-LacZ, Ad-p53, or Ad-p53mut. Endogenous collagen 18 levels were analyzed by immunoblotting with an antibody against the C terminus; expression of p53 and tubulin were monitored as controls. Molecular size markers are indicated on the left. (Right) Endogenous NC1 and endostatin levels were analyzed by immunoblotting of conditioned media (CM) with an antibody against the C terminus. (**B**) Immunoblot on WCE and CM from H1299/col18-V5 cells infected with Ad-LacZ or Ad-p53. V5-tagged full-length collagen 18 and C-terminal proteolytic fragments were detected with an antibody to V5. Expression of p53 and tubulin were monitored as controls. (**C**) Immunoblot on WCE and CM from H1299/col18-V5 cells infected with Ad-LacZ or Ad-p53 and transfected with either an α(II)PH AO or a control AO. α(II)PH levels were monitored with a polyclonal antibody. (**D**) (Top) Immunoblot on WCE from cell lines stably expressing FLAG-tagged α(II)PH [H1299/α(II)PH1, 2, 3, and 4] or vector control (H1299/C1, C2, and C3) and transfected with a plasmid expressing either collagen 18-V5 (middle panels) or collagen 4 (lower panels). α(II)PH was detected with an antibody to FLAG, and full-length collagen 18 and 4 were detected with an antibody to V5. To normalize for transfection efficiency, we cotransfected a plasmid expressing β-galactosidase (β-gal) with the collagen-expressing plasmids and monitored β-gal protein with an antibody to β-gal. (Bottom) Immunoblot on CM from H1299/α(II)PH or H1299/C cells expressing collagen 18-V5 (upper) or collagen 4-V5 (lower). NC1, endostatin, and tumstatin were detected with an antibody to V5.

expression and the appearance of NC1 and endostatin in the CM (Fig. 2C) (*6*). We conclude that α(II)PH expression is necessary for the p53-mediated production of antiangiogenic collagen fragments.

If the role of p53 in the production of antiangiogenic collagen fragments is to increase α(II)PH expression, then ectopic overexpression of α(II)PH should stimulate production of C-terminal collagen fragments even in the absence of p53. To test this prediction, we derived four independent H1299 cell lines stably expressing α(II)PH [H1299/α(II)PH1, 2, 3, and 4] and transfected into each a plasmid expressing C-terminal V5-tagged collagen 18 or collagen 4, whose C-terminal fragment, tumstatin, has potent antiangiogenic activity (*7*). Ectopic expression of α(II)PH increased production of both full-length collagen 18 and collagen 4 (Fig. 2D, top) as well as endostatin and tumstatin in the CM (Fig. 2D, bottom). Thus, increased α(II)PH expression can stimulate production of full-length collagen and C-terminal antiangiogenic collagen fragments in the absence of p53.

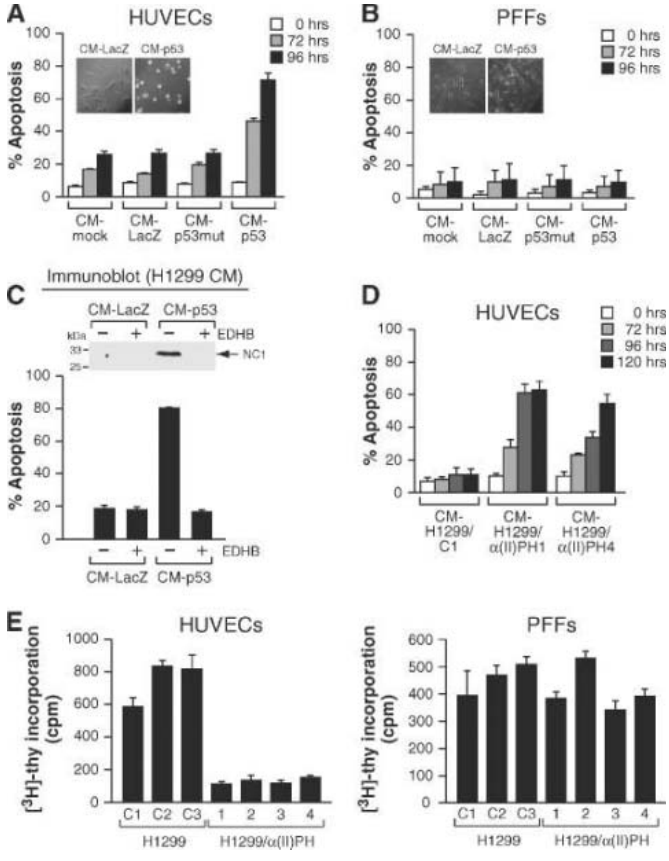

Fig. 3. CM from cells expressing p53 and α(II)PH induces cell death in HUVECs. (**A**) HUVECs were treated with CM from H1299 cells mock infected (CM-mock) or infected with Ad-p53 (CM-p53), Ad-LacZ (CM-LacZ), or Ad-p53mut (CM-p53mut) and assayed for cell viability. (Inset) Micrographs of HUVECs treated with CM. (**B**) PFFs were treated with CM-mock, CM-p53, CM-LacZ, or CM-p53mut and analyzed for cell viability as described in (A). (**C**) (Top) Immunoblot monitoring NC1 levels in CM-p53 or CM-LacZ prepared in the presence or absence of EDHB. (Bottom) HUVECs were treated with the various CMs, and after 96 hours viability was quantitated. (**D**) HUVECs were treated with CM prepared from H1299/α(II)PH or H1299/C lines, and cell viability was assayed. (**E**) [H³]thymidine incorporation proliferation assay for HUVECS (left) and PFFs (right) cocultured with H1299/C or H1299/α(II)PH cell lines. Error bars indicate SEM.

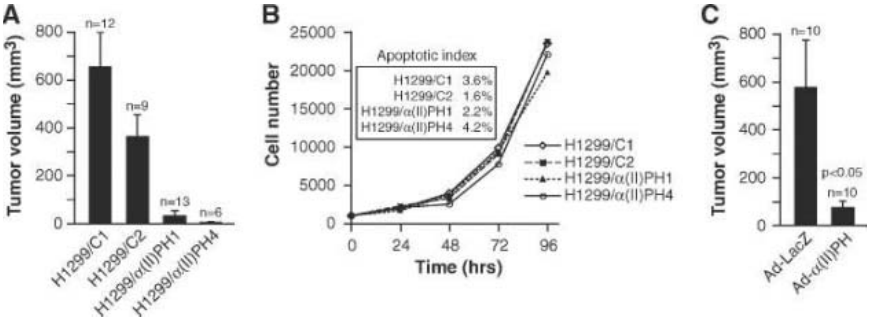

Fig. 4. Expression of α(II)PH inhibits tumor growth in mice. (**A**) Quantitation of tumor volume in xenografted mice. (**B**) Growth rates of α(II)PH-expressing H1299 cell lines and H1299 control cell lines. (Inset) Apoptotic indices, expressed as the percentage of cells undergoing apoptosis. (**C**) Quantitation of B16-derived tumor volume after treatment with either Ad-α(II)PH or Ad-LacZ. Error bars indicate SEM; *P* values were calculated with the Student's *t* test.

The antiangiogenic fragments of several human collagens, including collagen 4 and 18, can inhibit endothelial cell proliferation either by inducing growth arrest or apoptosis (*8*). This suggested that CM from cells ectopically expressing p53, which contains antiangiogenic collagen fragments, could inhibit endothelial cell proliferation. To test this possibility, we conditioned low-serum media in the presence of H1299 cells infected with an adenovirus expressing wild-type p53, mutant p53, or LacZ. CM from H1299 cells expressing p53, but not mutant p53 or LacZ, efficiently induced apoptosis in primary human umbilical vein endothelial cells (HUVECs) (Fig. 3A). By contrast, CM from p53-expressing H1299 cells had no effect on primary foreskin fibroblast (PFF) cells (Fig. 3B), indicating that the death-promoting activity was cell-type specific. To verify that prolyl hydroxylase activity is necessary for the p53-dependent promotion of HUVEC death, we prepared CM from p53-expressing H1299 cells in the presence of EDHB. CM from EDHB-treated, p53-expressing cells lacked the collagen 18 NC1 fragment (Fig. 3C, top) and failed to kill HUVECs (Fig. 3C, bottom) (*9*).

If increased amounts of antiangiogenic collagen fragments is the primary mechanism by which CM from p53-expressing cells inhibits HUVEC growth, then CM from cells expressing α(II)PH should have a similar activity. CM prepared from two of the H1299/α(II)PH cell lines, described above, induced HUVEC death (Fig. 3D). Coculture with all four H1299/α(II)PH cell lines inhibited HUVEC proliferation (Fig. 3E, left), as assessed by ^{3}H-labeled thymidine incorporation, but had no effect on PFFs (Fig. 3E, right). Thus, α(II)PH expression in tumor cells is sufficient to inhibit proliferation of cocultured primary HUVECs.

Inhibition of endothelial cell growth is predicted to inhibit vascularization and limit tumor growth (*10*). To test this possibility, we xenografted two of the α(II)PH-expressing H1299 cell lines into the flanks of nude mice and analyzed tumor growth. Notably, ectopic expression of α(II)PH resulted in near-complete suppression of H1299 tumor growth, as compared with two independently derived control lines, which developed large tumors within a month after injection (Fig. 4A and fig. S5). Because differences in tumor growth rates could be due to clonal variability, we further confirmed these results by injecting into mice a polyclonal population (a pool of ~500 clones) of α(II)PH-expressing [H1299/α(II)PH(p)] or vector control [H1299/C(p)] H1299 cell lines. The tumors derived from mice injected with H1299/α(II)PH(p) cells were significantly reduced in mass (fig. S6A), contained ischemic regions (fig. S6B), and were substantially less vascularized (fig. S6C) than tumors derived from mice injected with H1299/C(p) cells. Compared to control H1299/C(p) tumors, H1299/α(II)PH(p) tumors contained higher levels of tumstatin and

endostatin, as well as regions of intense tumstatin and endostatin accumulation (fig. S6D). These results are consistent with a model in which α(II)PH expression augments production of antiangiogenic collagen fragments. In culture, α(II)PH-expressing H1299 cells and control H1299 cells had comparable growth rates and apoptotic indices (Fig. 4B, inset). Thus, the differences in tumor size in xenografted mice were not because α(II)PH expression reduced the intrinsic growth rate of, or induced apoptosis in, H1299 cells.

Loss of p53 function is a common event in tumor progression (*11*), and our data suggest that p53-negative tumors may lack an important mechanism for limiting tumor vascularization. In support of this idea, xenografted tumors derived from $p53^{-/-}$ HCT116 cells were significantly more vascularized and had large areas lacking tumstatin staining compared with tumors derived from wild-type HCT116 cells (fig. S7).

We next asked whether adenovirus-mediated α(II)PH expression could reduce growth of tumors derived from B16 cells, a highly aggressive mouse melanoma cell line (*12*). Treatment of B16-derived melanomas with α(II)PH-expressing adenovirus significantly reduced tumor volume (Fig. 4C). Thus, α(II)PH can inhibit tumor growth when intracellularly expressed or exogenously delivered.

Although it is well established that C-terminal collagen fragments have an antiangiogenic activity (*13*), their physiological role and connection to cellular growth pathways have not been elucidated. Our results reveal a genetic and biochemical linkage between the p53 tumor suppressor pathway and the production of antiangiogenic collagen fragments. We propose that α(II)PH induction by p53 results in increased synthesis and secretion of full-length collagens, which are then proteolytically processed in the extracellular matrix to produce antiangiogenic peptides. Although this extracellular proteolytic processing occurs, at least to some extent, constitutively in the absence of p53 (Fig. 2D), p53 expression greatly enhances the processing of full-length collagen 18 to endostatin. On the basis of these observations, we propose that p53 activates a transcriptional program that increases synthesis and processing of collagen-derived antiangiogenic peptides. Several alternative mechanisms by which p53 could negatively affect angiogenesis in tumors have also been suggested (*14*–*16*).

In this study, we focused on collagen 18 because its antiangiogenic properties have been extensively characterized. Consistent with our observations, a recent report has demonstrated that a modest increase (~1.6-fold) in the synthesis of endostatin can lead to marked reduction in tumor growth rates in mice (*17*). Our data indicate that p53-dependent up-regulation of α(II)PH also results in increased synthesis of the collagen 4 C-terminal fragment, tumstatin; by analogy, increased synthesis of other collagen 4 C-terminal fragments, such as canstatin and arresten, seems likely. The shedding of multiple collagen-derived antiangiogenic fragments at the tumor-host interface may be part of a general p53-dependent mechanism of inhibiting tumor vascularization and growth.

References and Notes

1. B. Vogelstein, D. Lane, A. J. Levine, *Nature* **408**, 307 (2000).
2. Materials and methods are available as supporting material on *Science* Online.
3. W. S. el-Deiry *et al.*, *Cell* **75**, 817 (1993).
4. K. I. Kivirikko, R. Myllyla, *Methods Enzymol.* **82**, 245 (1982).
5. In H1299 cells, collagen 18 appeared as a doublet, consistent with previous findings that the collagen 18 gene encodes two major splice variants in human cells (*18*).
6. The observed size difference between endogenous and ectopically expressed endostatin is primarily due to the ~4-kD epitope tag present at the C terminus of the ectopically expressed collagen 18. In addition, sequence variation, as well as slight species differences in the site of proteolytic cleavage, may also contribute to small differences in electrophoretic mobility.
7. Y. Maeshima *et al.*, *Science* **295**, 140 (2002).
8. M. S. O'Reilly *et al.*, *Cell* **88**, 277 (1997).
9. Expression of vascular endothelial growth factor (VEGF) was not affected by EDHB treatment (fig. S8) and therefore cannot explain the inability of CM from EDHB-treated, p53-expressing H1299 cells to induce apoptosis in HUVECs.
10. P. Carmeliet, R. K. Jain, *Nature* **407**, 249 (2000).
11. P. Hainaut *et al.*, *Nucleic Acids Res.* **25**, 151 (1997).
12. I. J. Fidler, *Cancer Res.* **35**, 218 (1975).
13. A. G. Marneros, B. R. Olsen, *Matrix Biol.* **20**, 337 (2001).
14. R. Ravi *et al.*, *Genes Dev.* **14**, 34 (2000).
15. L. Zhang *et al.*, *Cancer Res.* **60**, 3655 (2000).
16. K. M. Dameron, O. V. Volpert, M. A. Tainsky, N. Bouck, *Science* **265**, 1582 (1994).
17. M. Sund *et al.*, *Proc. Natl. Acad. Sci. U.S.A.* **102**, 2934 (2005).
18. J. Saarela, R. Ylikarppa, M. Rehn, S. Purmonen, T. Pihlajaniemi, *Matrix Biol.* **16**, 319 (1998).

19. We thank S. Benchimol for providing the plasmid pECH53; B. Vogelstein for the HCT116 cell lines; F. Graham for the adenovirus vectors Ad-LacZ, Ad-p53, and Ad-p53mut; B. Olsen for the collagen 18 cDNAs; and R. Kalluri for the antibody to tumstatin. We also thank members of the Green lab, both past and present, for useful discussions; C. Welch and S. Griggs for technical assistance; and S. Evans for editorial assistance. J.G.T. was supported by postdoctoral fellowships from the National Cancer Institute of Canada and the Medical Foundation Charles A. King Trust. M.R.G. is an investigator of the Howard Hughes Medical Institute.

Supporting Online Material

www.sciencemag.org/cgi/content/full/313/5789/968/DC1
Materials and Methods
Figs. S1 to S9
References

17 February 2006; accepted 27 June 2006
10.1126/science.1126391

Mutations That Increase the Life Span of *C. elegans* Inhibit Tumor Growth

Julie M. Pinkston, Delia Garigan, Malene Hansen, Cynthia Kenyon*

Mutations in *gld-1* cause lethal germline tumors in the nematode *Caenorhabditis elegans*. We find that a wide variety of mutations that extend *C. elegans*' life span confer resistance to these tumors. The long life spans of *daf-2*/insulin-receptor mutants were not shortened at all by *gld-1* mutations; we attribute this finding to decreased cell division and increased DAF-16/p53–dependent apoptosis within the tumors. Mutations that increase life span by restricting food intake or inhibiting respiration did not affect apoptosis but reduced tumor cell division. Unexpectedly, none of these longevity mutations affected mitosis in normal germlines; this finding suggests that cellular changes that lead to longevity preferentially antagonize tumor cell growth.

In nature, there is a strong correlation between physiological aging and tumor susceptibility. Mice, which have short (2-year) mean life spans, frequently acquire tumors after ~1 year, whereas dogs do so after ~10 years and humans only after many decades. Understanding how youthful animals resist tumors may provide new insights into tumor biology, particularly if genes that regulate aging influence tumor susceptibility. Many apoptotic, signaling, and other genes that affect tumors in mammals have orthologs in *C. elegans*. Moreover, mutations affecting insulin/IGF-1 (insulin-like growth factor–1) signaling, mitochondrial activity, and food intake each extend life span in both worms and mammals (*1*–*4*). Thus, *C. elegans* may be a valuable organism in which to investigate links between aging and tumors.

In *C. elegans gld-1* tumor-suppressor mutants, germ cells in the early stages of oogenesis reenter the mitotic cell cycle and overproliferate (*5*). The cells eventually break out of the gonad and fill the body, killing the animal early in life. Like transformed vertebrate cells, these cells proliferate in a growth

Department of Biochemistry and Biophysics, University of California, San Francisco, CA 94158, USA.

*To whom correspondence should be addressed. E-mail: ckenyon@biochem.ucsf.edu

factor–independent manner (*5*), and they do not undergo programmed cell death (*6*). As they do not exhibit an angiogenesis-inducing or clear metastatic phenotype, these cells most likely approximate vertebrate cells in the early stages of tumorigenesis. In this study, we asked whether the lethal effects of this overproliferation could be delayed by longevity mutations that inhibit insulin/IGF-1 signaling [the receptor mutations *daf-2(e1370)* and *daf-2(mu150)*] (*7*, *8*), a mutation that extends life span via caloric restriction [the feeding mutant *eat-2(ad1116)*] (*9*), and mitochondrial mutations that disrupt respiratory chain components [*isp-1(qm150)*] (*10*) or ubiquinone production [*clk-1(qm30)*] (*11*). These mutations affect distinct pathways (*3*, *4*, *9*), although they may converge on common downstream processes. In principle, longevity mutations might not affect the tumor, in which case they would not extend the short *gld-1* mutant life span. Alternatively, as certain p53 mutations that inhibit tumors also accelerate aging and shorten life span (*12*), mutations that lengthen wild-type life span might promote tumor growth and accelerate death. In contrast, all of the longevity mutations tested extended the life spans of *gld-1* mutants (Fig. 1). In fact, the long life spans of the two *daf-2* mutants were not shortened at all by *gld-1* mutations. Thus, we observed a strong correlation between life-span extension and tumor resistance.

How do these longevity mutations affect the tumor? We found that none of the mutations restored oocyte production, but they all reduced germ cell number (Fig. 2). Thus, these mutations were likely to inhibit germ cell proliferation and/or increase germ cell death.

In the wild type, many germ cells undergo apoptosis as they enter oogenesis, but in *gld-1* mutants, this apoptosis is blocked (*6*). Using the dye SYTO12 to label apoptotic cells (*6*), we found that *daf-2* mutations stimulated apoptosis in the *gld-1* germlines (Fig. 3, A and B). *daf-2* mutations also stimulated apoptosis in wild-type germ cells undergoing oogenesis (Fig. 3D). Therefore, *daf-2* mutations appear to trigger a general increase in germline cell death.

How might *daf-2* mutations affect apoptosis? Timed RNA interference (RNAi) experiments showed that *daf-2* acts during adulthood to influence cell death (fig. S1). We found that the transcription factor DAF-16/FOXO, which is required for the longevity of *daf-2* mutants (*8*), was required for *daf-2* mutations to increase germline apoptosis in both the wild type and *gld-1* mutants (Fig. 3D). The *C. elegans* p53 gene *cep-1* (*13*) was required as well (Fig. 3E). p53/*cep-1* does not appear to be a DAF-16 transcriptional target (*14*, *15*). Together, these findings suggest that *daf-2* inhibition during adulthood increases the expression of DAF-16 target genes whose products function, directly or indirectly, along with p53/CEP-1 to stimulate germline apoptosis.

In *C. elegans*, p53 stimulates germline apoptosis in response to genotoxic stress but plays only a minor role in germline apoptosis under normal conditions (*13*). Thus, we hypothesized that *daf-2* mutations might affect apoptosis by shifting cells into a physiological state resembling that induced by genotoxic stress. This idea is attractive because inhibiting *daf-2* activity is known to activate multiple stress resistance processes (*1*, *3*). Consistent with this, we found that DAF-16 was required for the increase in germline apo-

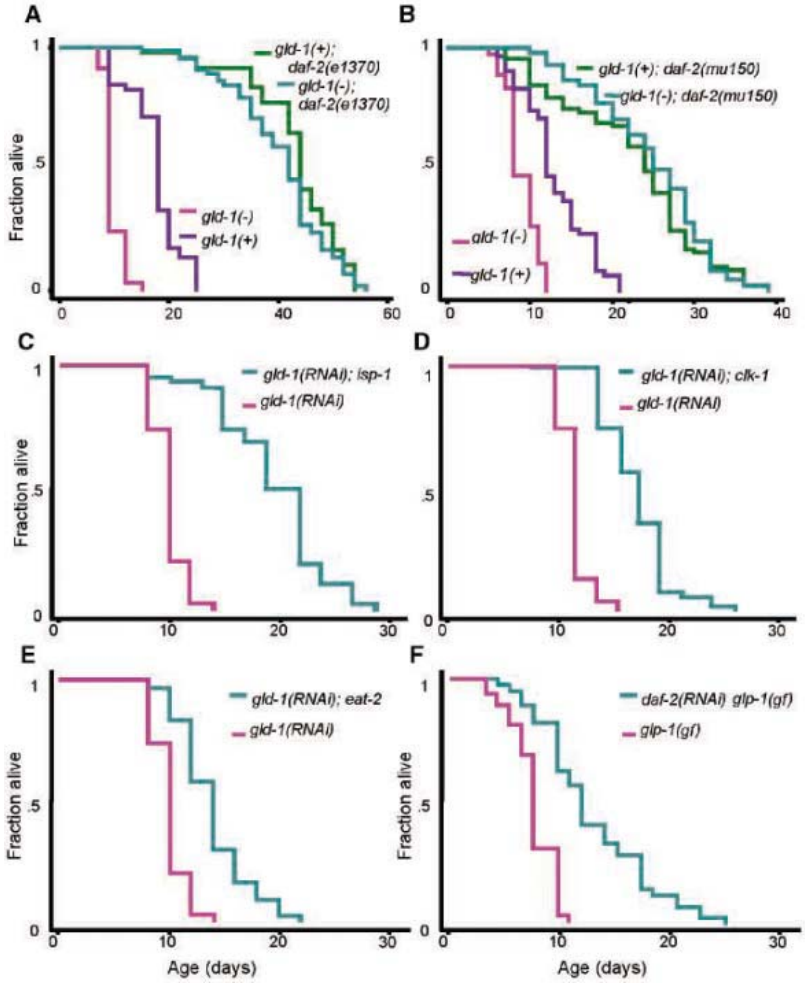

Fig. 1. Mutations that increase longevity delay the death caused by germline-tumor mutations. For each chart, experimental and control animals were grown in parallel. In this and other figures, *gld-1(-)* refers to the null allele *gld-1(q485)*, and all RNAi-treated animals are labeled accordingly. (**A** and **B**) *daf-2(e1370)* (A) and *daf-2(mu150)* mutations (B) suppressed the lethality caused by *gld-1(-)*. Similar results were obtained with *gld-1* RNAi (table S5). In control experiments, a nontumorous *gld-1* mutant (*op236*) (*18*) behaved like the wild type (table S5). (**C** to **E**) *isp-1(qm150)* (C), *clk-1(qm30)* (D), and *eat-2(ad1116)* mutations (E) delayed the death caused by *gld-1* RNAi, although the animals did not live as long as *isp-1*, *clk-1*, or *eat-2* mutants exposed to control RNAi. The magnitude of the life-span extension caused by these mutations was roughly the same in *gld-1(-)* and *gld-1(+)* backgrounds (table S5). (**F**) *daf-2(RNAi)* delayed the death caused by another germline tumor mutant, *glp-1(ar202)*. All experiments were repeated at least twice with similar results (table S5). We considered the possibility that germline tumors shorten life span by down-regulating the life span–extending protein DAF-16, because removing the germ cells in the wild type extends life span in a *daf-16*–dependent manner. However, changes in DAF-16 activity cannot be responsible, because *gld-1* RNAi further shortens the life spans of *daf-16(null)* mutants (table S5). As they near death, the animals become rigid and so packed with germ cells that none of their organs are visible by Nomarski microscopy, a finding consistent with tumors' killing the animal.

ptosis caused by gamma irradiation in wild-type animals (Fig. 3G). In addition, the checkpoint genes *hus-1*, *mrt-2*, and *clk-2*, which act upstream of p53 in the DNA damage–induced apoptotic pathway (*16*), were required for *daf-2* mutations to increase apoptosis in otherwise wild-type animals (Fig. 3G).

The cell death that occurs in wild-type and *gld-1; daf-2(-)* double-mutant germ cells is restricted to cells entering oogenesis. For this reason, we also examined a germline-tumor mutant in which cells do not progress to meiosis. The *glp-1(ar202gf)* mutation renders the GLP-1/Notch receptor, which maintains the germ cells in the stem-cell state, constitutively active (*17*). We found that *daf-2* mutations were unable to stimulate apoptosis in this germline tumor (table S1). Thus, *daf-2* mutations may trigger cell death specifically in cell populations that are already "primed" for apoptosis. Consistent with this interpretation, p53 levels are known to be elevated in *gld-1* mutants (*18*).

The life spans of *gld-1(RNAi); daf-2(-)* animals were shortened when cell death was prevented with either the *ced-3(n1286)* caspase mutation (*19*) or the *cep-1(gk138)* p53 mutation (*20*). [Cell death mutations do not reduce wild-type or *gld-1(+); daf-2(-)* life spans (*7*) (table S2).] Nonetheless, *daf-2* mutations still more than doubled the life spans of both of these apoptosis-defective tumor strains (Fig. 3C). This result suggested that *daf-2* mutations might influence cell proliferation as well as apoptosis.

We assayed cell proliferation using an M phase–specific (phospho–histone H3) antibody (*21*) and found that *daf-2* mutations decreased the number of actively dividing germ cells in *gld-1* mutants (Fig. 4, A and B). We observed a similar decrease when apoptosis was blocked by a *ced-3* mutation (table S3), indicating that the decrease in labeling was not due to increased apoptosis. *daf-2* mutations also inhibited cell division in the *glp1/Notch* germline tumors; consistent with this finding, these animals had a smaller overall germ cell number and increased life spans (Fig. 1F and fig. S2).

daf-16 was required for *daf-2(mu150)* mutations to inhibit *gld-1* germline mitosis. However, a small portion of the effect caused by the stronger allele, *daf-2(e1370)*, was *daf-16* independent (Fig. 4C). Likewise, *daf-2(e1370)* mutations slightly extended the life spans of *gld-1(RNAi) daf-16(null)* mutants (~20%, $P < 0.0001$) (fig. S3).

Unexpectedly, *daf-2(-)* mutations did not affect the number of M-phase germline cells in a wild-type background (although we may not have detected a subtle change with this antibody) (Fig. 4C). Thus, *daf-2(-)*'s antiproliferative effect appeared to be specific to tumor cells. This was particularly intriguing for the *glp-1/Notch* mutant, because its tumors are thought to consist of an overabundance of normal germline stem cells. Perhaps the insulin/IGF-1 pathway, which controls food usage and growth in many species, becomes limiting for cell proliferation in the face of such a large metabolic load.

In *Drosophila*, insulin/IGF-1–pathway mutations were recently reported to prevent normal germ cell growth and maturation (*22*). The discrepancy between this finding and ours may reflect the strength of the mutations examined, because stronger *daf-2* alleles in *C. elegans* inhibit reproduction severely (*23*). In contrast, the *daf-2(mu150)* mutants reproduced normally, in terms of both reproductive timing and brood size, and *daf-2(e1370)* mutants grown at 20°C had only a slight reduction in fecundity (table S4), as reported previously (*7*, *8*).

In humans, PTEN tumor-suppressor mutations stimulate oncogenesis by elevating insulin/IGF-1 signaling (*24*). This inhibits the DAF-16 ortholog FOXO3a, which in turn prevents apoptosis and promotes cell proliferation (*25*). Here, we decreased insulin/IGF-1 signaling (and elevated DAF-16 activity) throughout the animal and obtained a strong tumor-suppressive effect. This may have implications for mammalian tumors, including those that do not carry mutations in the insulin/IGF-1 signaling pathway. Mutations that inhibit growth hormone signaling extend life span and increase tumor resistance in rodents (*26*). Our findings suggest that reduced insulin/IGF-1 signaling, which results from growth hormone deficiency, may be responsible for their cancer resistance, and that this resistance is mediated by FOXO (and possibly p53) activity.

Are these tumor-suppressive mechanisms activated by other longevity pathways? To address this question, we analyzed mutations

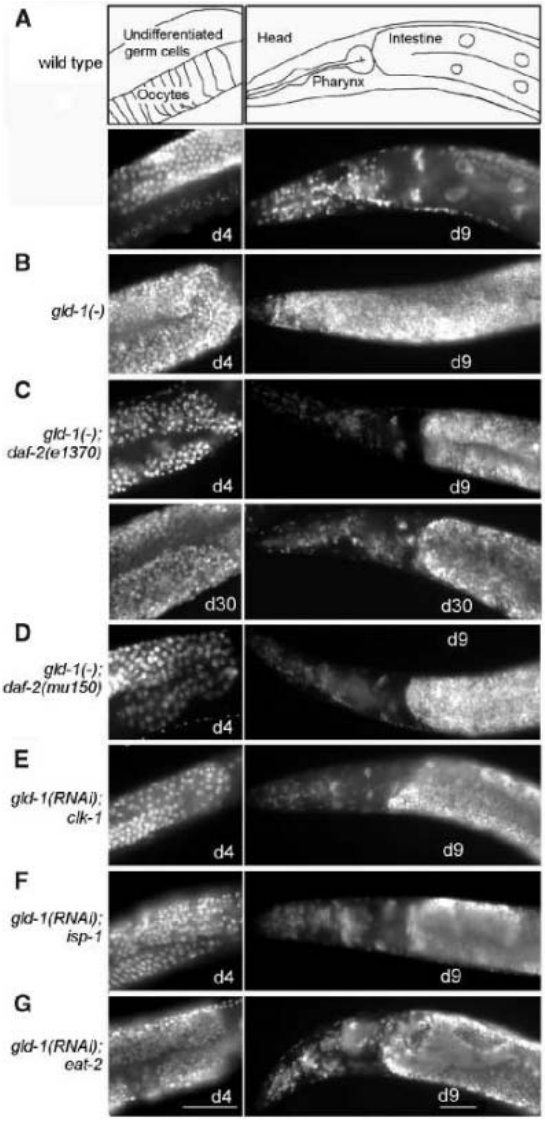

Fig. 2. Mutations that increase longevity reduce germ cell number in *gld-1(-)* mutants. Adult animals were stained with the DNA-intercalating dye DAPI (4′,6′-diamidino-2-phenylindole). Left panels, midpoints of the gonad arms; right panels, heads. In all panels, anterior is to the left; d, day of adulthood. (**A**) Wild type. (**B**) *gld-1(q485)* mutants lack oocytes and have many undifferentiated germ cells in their gonads (left), which later break out of the gonad and fill the head and body (right). (**C**) *gld-1(q485); daf-2(e1370)* and (**D**) *gld-1(q485); daf-2(mu150)* double mutants lack oocytes; however, they have far fewer undifferentiated germ cells (left) and maintain the integrity of their gonads (right), even into old age [(C), lower panel]. The number of germ cells in *gld-1(op236)*, a nontumorous mutant of *gld-1*, is unaffected by *daf-2* RNAi (table S6). (**E** to **G**) *isp-1(qm150)* (E), *clk-1(qm30)* (F), and *eat-2(ad1116)* mutants (G) also have fewer undifferentiated germ cells in the presence of *gld-1* RNAi (left), and the spread of germ cells into the body is delayed (right). Scale bars, 20 μm. For germ cell estimates and statistical analysis, see table S6. We considered the possibility that *daf-2* mutations increased the (low) frequency of transdifferentiation of *gld-1(-)* germ cells into somatic cells. We found, using Nomarski optics, DAPI staining, and neuronal green fluorescent protein markers, that this was not the case (fig. S5).

that cause caloric restriction [*eat-2(ad1116)*] (*9*) or impair mitochondrial activity [*isp-1(qm150)* and *clk-1(qm30)*] (*10*, *11*). None of these mutations affected germline apoptosis in *gld-1* tumor mutants (Fig. 3F and fig. S4). Thus, this effect appears to be specific to the insulin/IGF-1 pathway. However, all of the mutations reduced the number of M-phase germ cells (Fig. 4D). Remarkably, as with *daf-2* mutations, none of these mutations reduced the number of M-phase germ cells in *gld-1(+)* animals (Fig. 4D). Thus, all of the longevity mutations we examined preferentially affected the proliferation of tumor cells. This implies a molecular link between processes that protect or repair cells and processes that disadvantage tumor cell growth.

Caloric restriction inhibits tumorigenesis in mammals, and our findings suggest that inhibiting the mammalian orthologs of *isp-1* and *clk-1* may do so as well. *isp-1* mutations are thought to increase life span by inhibiting respiration (*3*, *4*, *10*). Perhaps tumor cells, which

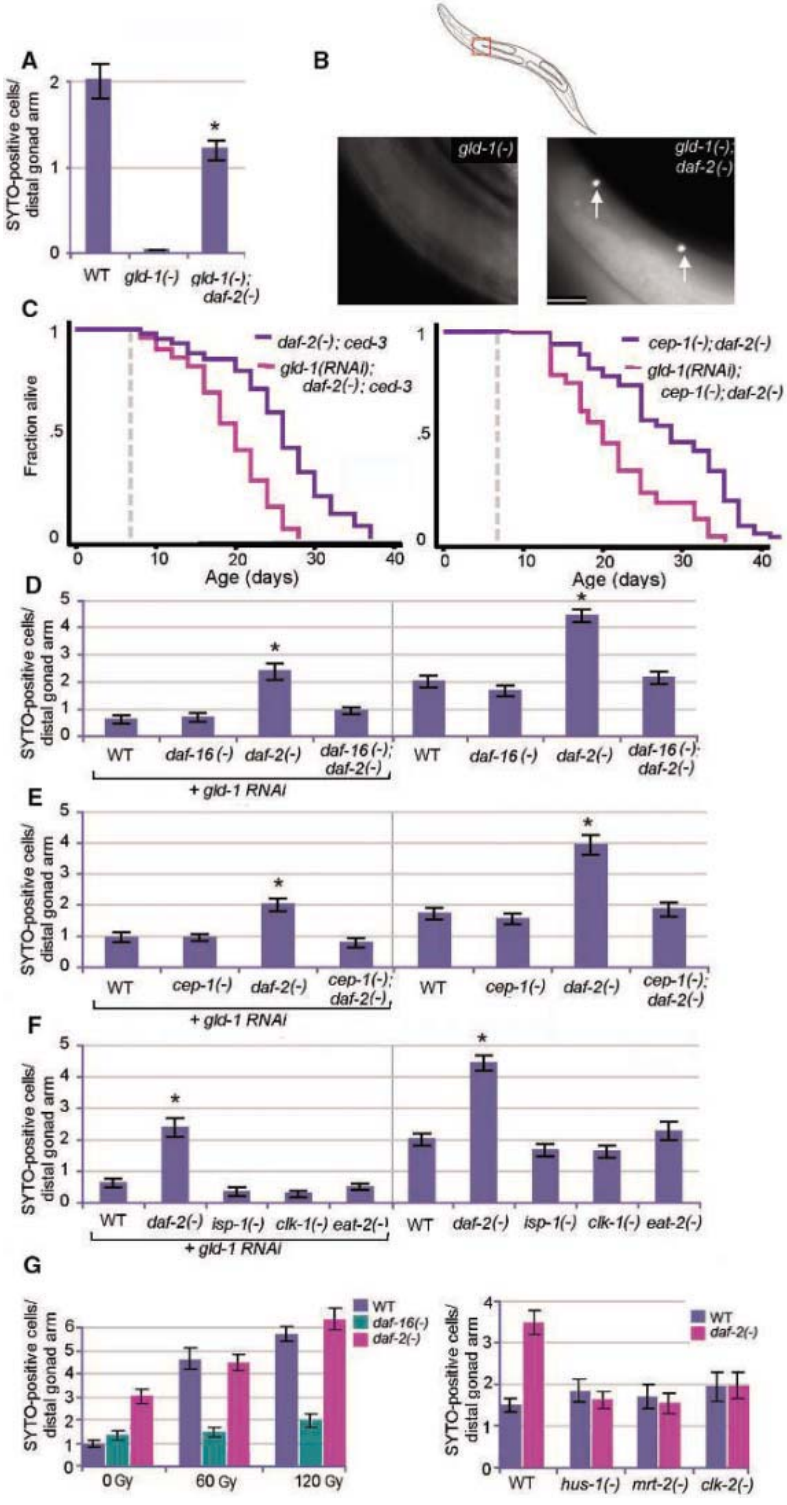

Fig. 3. p53- and DAF-16–dependent germline apoptosis is triggered by insulin/IGF-1 but not by mitochondrial or feeding mutations. Germ cell corpses were identified by SYTO12 labeling of day 2 (48-hour) adults. Each bar represents the mean (±SE) of at least three combined experiments (for details, see table S1); **P* < 0.0001. (**A**) *daf-2(e1370)* mutations partially restored germ cell death in *gld-1(q485)* mutants. This was blocked by a *ced-3(-)* mutation (table S1). (**B**) Representative SYTO12-labeled *gld-1(q485)* mutant (left) and *gld-1(q485); daf-2(e1370)* double mutant (right). Arrows, stained germ cell corpses; scale bar, 20 μm. (**C**) Life spans of *gld-1(RNAi); daf-2(e1370)* animals were reduced ~20% by either *ced-3(n1286)* (left), *cep-1(gk138)* (right), or *ced-4(n1162)* (table S2) mutations. The number of germ cells in a *gld-1(-); daf-2(-)* animal was increased by either a *ced-3(-)* or *cep-1(-)* mutation (table S6). Dashed line, mean life span of animals treated with *gld-1* RNAi. (**D** to **F**) Left panels, *gld-1(RNAi)* animals; right panels, *gld-1(+)* animals; **P* < 0.0001. (D) *daf-2* mutations increased germ cell apoptosis in wild-type as well as *gld-1(-)* animals; this increase was *daf-16* dependent. Residual germ cell apoptosis in *gld-1(RNAi)* animals was likely due to incomplete RNAi knockdown. The requirement of *daf-16* for this apoptosis is consistent with life-span data (fig. S6). (E) The *daf-2*–dependent increase in germ cell apoptosis was reversed by *cep-1(gk138)*. (F) *isp-1(qm150)*, *clk-1(qm30)*, and *eat-2(ad1116)* mutations did not affect germ cell apoptosis in *gld-1(-)* or wild-type animals. (**G**) *daf-16* was necessary for DNA damage–induced apoptosis (left). Germ cell corpses were scored 18 hours after irradiation. The checkpoint genes *hus-1*, *mrt-1*, and *clk-2* were required for *daf-2* RNAi to increase apoptosis in the wild type (right). For details and statistical data, see table S1.

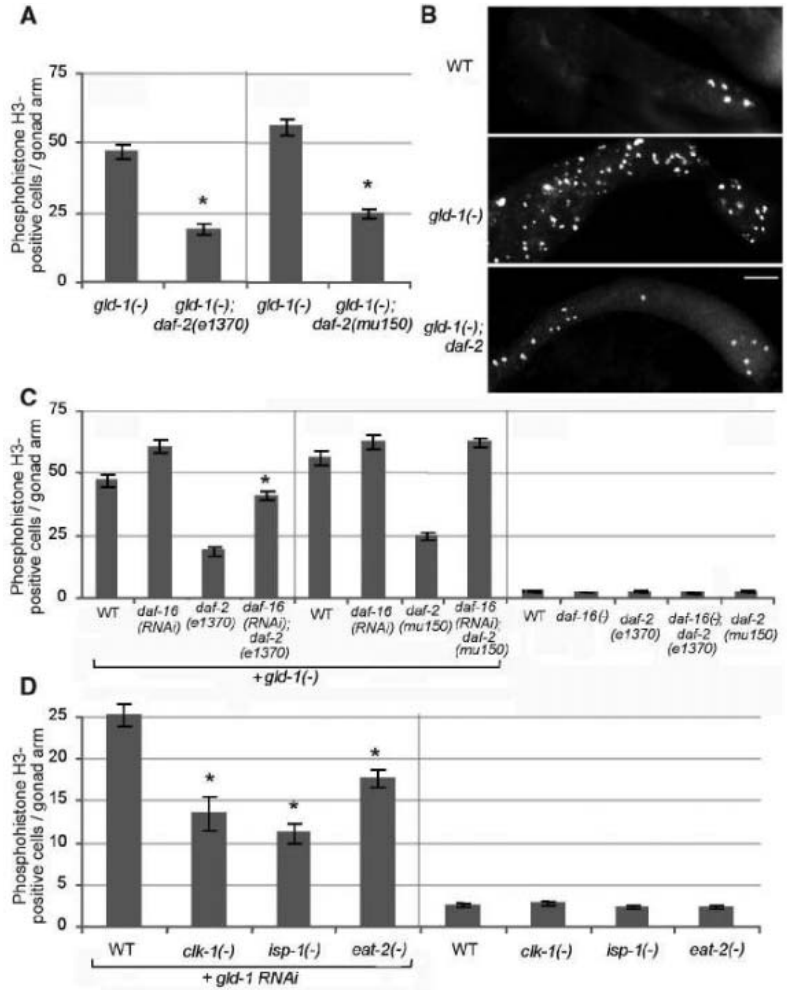

Fig. 4. Longevity mutations reduce the number of M-phase germ cells in *gld-1(-)* but not wild-type animals. Dividing germ cells were scored by antibody labeling to phospho–histone H3 at 36 hours of adulthood. Each bar represents the mean (±SE) of at least three combined experiments; $*P < 0.0001$. (**A**) *daf-2(mu150)* and *daf-2(e1370)* mutations reduced labeled cells in *gld-1(-)* mutants by about 50%. Similar results were obtained with *gld-1(RNAi)* (table S3). (**B**) Representative gonads of wild-type (top), *gld-1(q485)* (middle), and *gld-1(q485); daf-2(e1370)* (bottom) animals labeled with antibody to phospho–histone H3. Scale bar, 20 μm. (**C**) The reduction of mitotic germ cells by *daf-2(e1370)*, but not *daf-2(mu150)*, mutations was incompletely reversed by *daf-16* RNAi. Similar results were obtained in *gld-1(RNAi) daf-16(mu86); daf-2(e1370)* animals (table S3). In contrast, a *cep-1(-)* mutation had no effect on the number of mitotic cells (table S3). In a wild-type background, *daf-2* mutations had no effect on germ cell divisions (right). (**D**) *clk-1(qm30)*, *isp-1(qm150)*, and *eat-2(ad1116)* mutations reduced the number of M-phase cells in *gld-1(RNAi)* animals by about 35%, 50%, and 30%, respectively, but had no effect in a wild-type background. The scale in (D) differs from that in (A) and (C) because *gld-1* RNAi has a less severe effect on proliferation than a *gld-1(q485)* mutation. For details and statistical data, see table S3.

have low rates of respiration, are particularly sensitive to further reductions, or perhaps reducing respiration rates in surrounding cells inhibits tumor growth. The mechanism by which *clk-1* mutations increase life span is not known. *C. elegans clk-1* mutants, which receive essential quinones from the environment (*27*), do not have reduced metabolic output (*28*). The longevity of *clk-1*$^{+/-}$ mice has been associated with increased stress resistance (*2*). It will be interesting to investigate the effects of *clk-1* mutations on mammalian tumors.

Our results show that many *C. elegans* longevity mutations are tumor protective. The generality of our findings, along with the cancer resistance of long-lived calorically restricted and endocrine-mutant rodents, argues that mutations such as the p53 alleles that inhibit tumors but accelerate aging (*12*) may be the exception rather than the rule. It may be that during evolution, longevity and delayed tumorigenesis arose together—for example, from endocrine pathway and mitochondrial mutations that influenced both processes.

References and Notes

1. M. Tatar, A. Bartke, A. Antebi, *Science* **299**, 1346 (2003).
2. X. Liu *et al.*, *Genes Dev.* **19**, 2424 (2005).
3. C. Kenyon, *Cell* **120**, 449 (2005).
4. S. Hekimi, L. Guarente, *Science* **299**, 1351 (2003).
5. R. Francis, E. Maine, T. Schedl, *Genetics* **139**, 607 (1995).
6. T. L. Gumienny, E. Lambie, E. Hartwieg, H. R. Horvitz, M. O. Hengartner, *Development* **126**, 1011 (1999).
7. D. Garigan *et al.*, *Genetics* **161**, 1101 (2002).
8. C. Kenyon, J. Chang, E. Gensch, A. Rudner, R. Tabtiang, *Nature* **366**, 461 (1993).
9. B. Lakowski, S. Hekimi, *Proc. Natl. Acad. Sci. U.S.A.* **95**, 13091 (1998).
10. J. Feng, F. Bussiere, S. Hekimi, *Dev. Cell* **1**, 633 (2001).
11. S. Felkai *et al.*, *EMBO J.* **18**, 1783 (1999).
12. S. D. Tyner *et al.*, *Nature* **415**, 45 (2002).
13. B. Schumacher, K. Hofmann, S. Boulton, A. Gartner, *Curr. Biol.* **11**, 1722 (2001).
14. C. T. Murphy *et al.*, *Nature* **424**, 277 (2003).
15. J. McElwee, K. Bubb, J. H. Thomas, *Aging Cell* **2**, 111 (2003).
16. A. Gartner, S. Milstein, S. Ahmed, J. Hodgkin, M. O. Hengartner, *Mol. Cell* **5**, 435 (2000).
17. A. S. Pepper, D. J. Killian, E. J. Hubbard, *Genetics* **163**, 115 (2003).
18. B. Schumacher *et al.*, *Cell* **120**, 357 (2005).
19. J. Yuan, S. Shaham, S. Ledoux, H. M. Ellis, H. R. Horvitz, *Cell* **75**, 641 (1993).
20. X. Deng *et al.*, *Nat. Genet.* **36**, 906 (2004).
21. K. Ajiro, K. Yoda, K. Utsumi, Y. Nishikawa, *J. Biol. Chem.* **271**, 13197 (1996).
22. L. LaFever, D. Drummond-Barbosa, *Science* **309**, 1071 (2005).
23. D. Gems *et al.*, *Genetics* **150**, 129 (1998).
24. K. Inoki, M. N. Corradetti, K. L. Guan, *Nat. Genet.* **37**, 19 (2005).
25. A. Essafi *et al.*, *Oncogene* **24**, 2317 (2005).
26. M. M. Ramsey *et al.*, *Endocrinology* **143**, 4139 (2002).
27. T. Jonassen, P. L. Larsen, C. F. Clarke, *Proc. Natl. Acad. Sci. U.S.A.* **98**, 421 (2001).
28. B. P. Braeckman *et al.*, *Mech. Ageing Dev.* **123**, 1447 (2002).

29. We thank D. Toczyski, as well as S. Henis-Korenblit and other Kenyon lab members, for helpful discussions and the *Caenorhabditis* Genetics Center for strains. Supported by NIH and the Ellison Foundation for Medical Research (C.K.), NIH training grant AG000278 (J.M.P.), and the Danish Medical and Natural Science Research Councils (M.H.). C.K. is the director of the UCSF Hillblom Center for the Biology of Aging, an ACS Research Professor, and a founder of Elixir Pharmaceuticals.

Supporting Online Material

www.sciencemag.org/cgi/content/full/313/5789/971/DC1
Materials and Methods
Figs. S1 to S6
Tables S1 to S6
References

27 October 2005; accepted 16 June 2006
10.1126/science.1121908

Graded Regulation of the Kv2.1 Potassium Channel by Variable Phosphorylation

Kang-Sik Park,* Durga P. Mohapatra,* Hiroaki Misonou, James S. Trimmer†

Dynamic modulation of ion channels by phosphorylation underlies neuronal plasticity. The Kv2.1 potassium channel is highly phosphorylated in resting mammalian neurons. Activity-dependent Kv2.1 dephosphorylation by calcineurin induces graded hyperpolarizing shifts in voltage-dependent activation, causing suppression of neuronal excitability. Mass spectrometry–SILAC (stable isotope labeling with amino acids in cell culture) identified 16 Kv2.1 phosphorylation sites, of which 7 were dephosphorylated by calcineurin. Mutation of individual calcineurin-regulated sites to alanine produced incremental shifts mimicking dephosphorylation, whereas mutation to aspartate yielded equivalent resistance to calcineurin. Mutations at multiple sites were additive, showing that variable phosphorylation of Kv2.1 at a large number of sites allows graded activity-dependent regulation of channel gating and neuronal firing properties.

Ion channel phosphorylation is crucial to dynamic regulation of neuronal excitability and the integrated function of the brain (*1*). Numerous voltage-gated potassium (Kv) channels with distinct properties are expressed in mammalian neurons, where they exert diverse effects on membrane excitability (*2*). The voltage-gated potassium channel Kv2.1 constitutes the majority of delayed-rectifier potassium currents in most mammalian central neurons (*3*–*5*). However, due to its high threshold for voltage-dependent activation and slow activation kinetics, Kv2.1 does not appear to play a prominent role in the repolarization of single action potentials (*4*, *5*). Rapid calcineurin-dependent dephosphorylation of neuronal Kv2.1 in response to increased intracellular Ca^{2+} concentration upon excitatory synaptic activity, epileptic seizures, neuromodulatory stimuli, and ischemia leads to graded enhancement of Kv2.1 activity by lowering the threshold for voltage-dependent activation and accelerating activation kinetics (*6*–*8*). As such, Kv2.1 acts a rheostat to homeostatically suppress neuronal firing (*9*, *10*), especially during periods of high-frequency firing (*4*, *5*). Recombinant Kv2.1 expressed in cultured human embryonic kidney 293 (HEK293) cells is similarly regulated by calcineurin (*8*). The mechanism whereby such graded changes in Kv2.1 function are achieved requires identification and functional analysis of Kv2.1 phosphorylation sites.

Treatment of native Kv2.1 protein isolated from rat brain (*6*, *11*) or cultured neurons (*6*–*8*), or recombinant rat Kv2.1 from transfected HEK293 cells (*8*), with alkaline phosphatase (AP) results in large (≈30 kD) shifts in electrophoretic mobility, suggesting extensive phosphorylation. More than 20% (132 out of 653) of cytoplasmic amino acids in rat Kv2.1 are serine, threonine, or tyrosine residues, of which up to 60 are predicted as consensus phosphorylation sites. To conduct an unbiased analysis of Kv2.1 phosphorylation sites, we immunopurified recombinant Kv2.1 expressed in HEK293 cells and digested the proteins with trypsin for analysis by liquid chromatography tandem mass spectrometry (LC-MS/MS) (*12*). One representative example of the obtained LC-MS/MS data is shown in Fig. 1A, for a doubly charged, singly phosphorylated Kv2.1 peptide at a mass to charge ratio (*m*/*z*) of 1106.69 that was fragmented to produce a tandem mass spectrum with a nearly complete *y*-ion series and complementary *b*-ion series that described the sequence SGFFVEpSPR (amino acids 645 to 653). The phosphorylation site was unambiguously assigned to serine-651 due to mass assignments from β-eliminated *y*4, *y*5, and *y*6 fragment ions and the transition from *y*2 to *y*3. Similar LC-MS/MS analyses of other Kv2.1 peptides identified 15 serine residues and 1 threonine residue phosphorylated on recombinant Kv2.1 in intact cells (Fig. 1B and Table 1).

To identify Kv2.1 phosphorylation sites dephosphorylated by calcineurin, we compared phosphorylation of Kv2.1 in control cells with Kv2.1 in cells treated with ionomycin, a Ca^{2+} ionophore that activates calcineurin (*8*). Stable

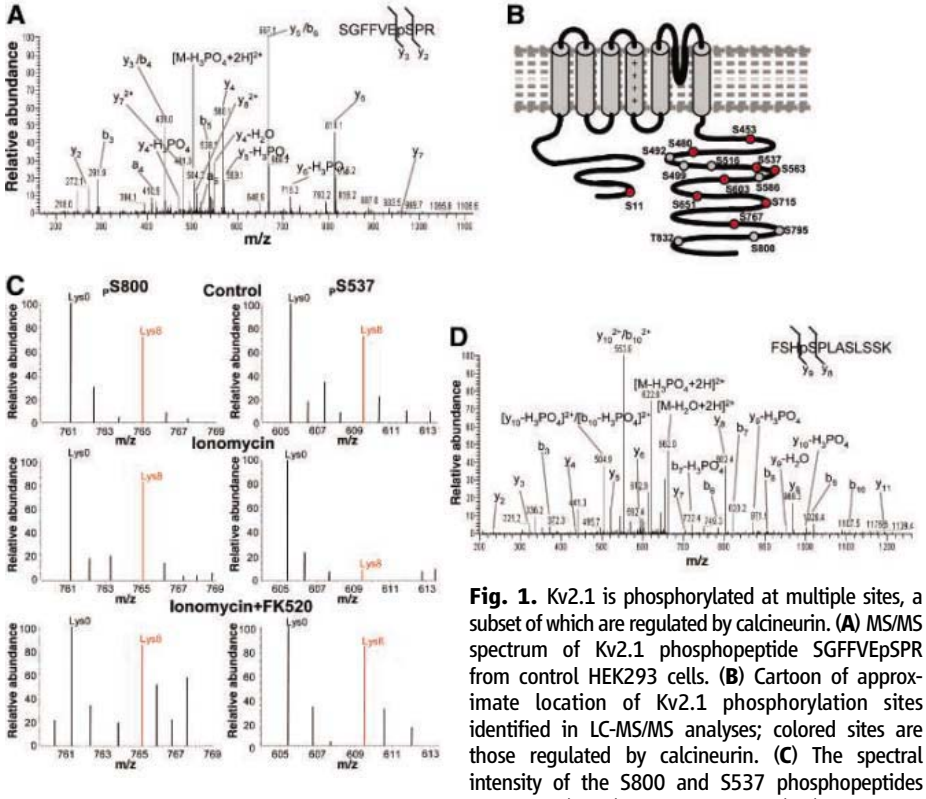

Fig. 1. Kv2.1 is phosphorylated at multiple sites, a subset of which are regulated by calcineurin. (**A**) MS/MS spectrum of Kv2.1 phosphopeptide SGFFVEpSPR from control HEK293 cells. (**B**) Cartoon of approximate location of Kv2.1 phosphorylation sites identified in LC-MS/MS analyses; colored sites are those regulated by calcineurin. (**C**) The spectral intensity of the S800 and S537 phosphopeptides from one set of experiments reflecting the ratio of Arg0,Lys0- (black)– and Arg6,Lys8- (red)–containing peptides. The pS537 but not the pS800 phosphopeptide exhibits Ca^{2+}-dependent dephosphorylation that is inhibited by pretreatment with FK520. (**D**) MS/MS spectrum of rat brain Kv2.1 phosphopeptide FSHpSPLASLSSK. Shown is the product ion spectrum of a doubly charged, singly phosphorylated tryptic peptide at *m*/*z* = 1340.64. Abbreviations for the amino acid residues are as follows: A, Ala; C, Cys; D, Asp; E, Glu; F, Phe; G, Gly; H, His; I, Ile; K, Lys; L, Leu; M, Met; N, Asn; P, Pro; Q, Gln; R, Arg; S, Ser; T, Thr; V, Val; W, Trp; and Y, Tyr.

Department of Pharmacology, School of Medicine, University of California, Davis, CA 95616, USA.

*These authors contributed equally to this work.

†To whom correspondence should be addressed at the Department of Pharmacology, School of Medicine 3502 GBSF, 451 East Health Sciences Drive, University of California, Davis, CA 95616, USA. E-mail: jtrimmer@ucdavis.edu

isotope labeling with amino acids in cell culture (SILAC) (*13*–*15*) was used to metabolically label proteins with mass tags, allowing for subsequent analyses of two chemically identical but isotopically distinct samples in a single LC-MS/MS analysis. Transfected HEK293 cells expressing Kv2.1 were metabolically labeled with either normal $^{12}C_6$-Arg, $^{12}C_6$, $^{14}N^2$-Lys (Arg0,Lys0), or isotopic variant $^{13}C_6$-Arg, $^{13}C_6$,$^{15}N^2$-Lys (Arg6,Lys8) amino acids to ensure mass labeling of every tryptic peptide. Arg0,Lys0-labeled cells were left unstimulated, whereas Arg6,Lys8-labeled cells were stimulated with ionomycin. Equal amounts of cell lysates were mixed, and Kv2.1 was immunopurified from the mixed lysates and subjected to in-gel trypsin digestion and LC-MS/MS. The relative intensities of the two isotopically distinct MS peaks directly reflects the amount of the corresponding phosphopeptide in the two different samples.

Using this assay, we found seven phosphorylation sites in Kv2.1 that were dephosphorylated upon calcineurin activation (Table 1), six in the cytoplasmic C terminus and one in the cytoplasmic N terminus (Fig. 1B). Representative mass spectra for two phosphopeptides, NHFESSPLpTPSPK (pS800) and TQpSQPILNTK (pS537), showed Ca^{2+}-dependent dephosphorylation at S537 but not at S800 (i.e., the Lys8-labeled MS peak height changes relative to the Lys0 peak for pS537 but not pS800; Fig. 1C). None of the seven sites exhibiting Ca^{2+}-dependent dephosphorylation were modified in ionophore-stimulated cells pretreated with the calcineurin inhibitor FK520 (Fig. 1C).

To determine how Ca^{2+}/calcineurin-dependent modulation of phosphorylation at these sites regulates voltage-dependent gating of Kv2.1, we expressed isoforms carrying mutated phosphorylation sites and wild-type Kv2.1 in HEK293 cells. Whole-cell patch-clamp was used to analyze Kv2.1 in untreated cells, and cells treated with ionomycin, or with AP dialyzed through the patch pipette. Maximal ionomycin treatment led to FK520-sensitive hyperpolarizing shifts in voltage-dependent activation (≈26 mV) and steady-state inactivation (≈32 mV) gating of wild-type Kv2.1 (Fig. 2 and Table 1). Maximal Ca^{2+}/calcineurin-dependent dephosphorylation of Kv2.1 did not lead to complete dephosphorylation, because AP treatment induced a further shift in electrophoretic mobility (*8*) and in voltage-dependent gating (by an additional 9 mV; Fig. 2 and Table 1). Serine-to-alanine point mutations in four of the seven calcineurin-regulated Kv2.1 phosphorylation sites resulted in significant hyperpolarizing shifts in both voltage-dependent activation and inactivation in control cells (Fig. 2 and Table 1). Mutations at S11 and S453 affected only inactivation and activation, respectively; the corresponding double mutations exhibited additive effects (Table 1). Mutations at two identified phosphorylation sites (S480, S767) that were not detected in SILAC experiments also yielded shifts in both activation and inactivation gating (Table 1). Treatment with ionomycin or AP resulted in hyperpolarizing shifts in voltage-dependent activation and inactivation of each of these mutants to the same endpoints as wild-type Kv2.1, demonstrating that the effects of the mutations were solely through altered phosphorylation state, and not through secondary effects on overall structure (Table 1). Substitution of phosphoacceptor serine with phosphomimetic and phosphatase-resistant aspartate at these sites yielded mutant channels with wild-type gating characteristics in untreated cells, but with decreased sensitivity to ionomycin- and AP-induced effects (Table 1). The magnitude of the effect of each serine-to-alanine mutation on gating in untreated cells, and of serine-to-aspartate mutations in calcineurin- or AP-treated cells, was similar, suggesting that each phosphorylation site makes a characteristic contribution to gating (Table 1). Point mutations mimicking dephosphorylation (e.g., S563A), as well as calcineurin- and AP-mediated dephosphorylation of wild-type Kv2.1, also led to faster kinetics of channel activation (Fig. 2B, inset) and inactivation (Fig. 2C, inset). Ionomycin treatment of cells expressing S480A caused a hyperpolarizing shift in voltage-dependent gating ≈6 mV greater than that obtained upon ionomycin stimulation of wild-type Kv2.1 and all other mutants, to an endpoint similar to that achieved with AP treatment. This

Table 1. Functional characterization of key Kv2.1 phosphorylation sites. $G_{1/2}$ is the half-maximal conductance calculated from the conductance-voltage (*G-V* curve). $Vi_{1/2}$ is the half-maximal steady-state inactivation potential calculated from the current-voltage (*I-V*) curve. ND, not determined. Values in bold are significantly different ($P < 0.05$) from the respective values for wild-type Kv2.1. Mutation of Ser/Thr to Ala at constitutive phosphorylation sites S492, S499, S516, S586, S795, and T832 did not alter functional phenotype under control, ionomycin-, or AP-treated conditions.

Phosphorylation sites identified by LC-MS/MS	Dephosphorylation by ionomycin (SILAC)	Mutations studied	Voltage-dependent activation and steady-state inactivation parameters of channels					
			Control		Ionomycin-treated		AP-treated	
			$G_{1/2}$	$Vi_{1/2}$	$G_{1/2}$	$Vi_{1/2}$	$G_{1/2}$	$Vi_{1/2}$
Wild type			+16.4 ± 0.6	−26.2 ± 0.4	−10.1 ± 0.6	−58.3 ± 0.5	−19.8 ± 0.7	−60.2 ± 0.8
S563	Yes	S563A	**+0.2 ± 0.5**	**−43.5 ± 0.4**	−9.6 ± 0.4	−59.5 ± 0.7	−18.5 ± 0.8	−56.8 ± 0.8
		S563D	+15.8 ± 0.8	−28.1 ± 0.7	**+5.4 ± 0.3**	**−43.1 ± 0.4**	**−5.7 ± 0.4**	**−48.3 ± 0.5**
S603	Yes	S603A	**+4.3 ± 0.7**	**−34.8 ± 0.4**	−9.3 ± 0.3	**−55.4 ± 0.6**	−18.9 ± 0.5	−58.4 ± 0.4
		S603D	+16.7 ± 0.6	**−32.4 ± 0.4**	**−4.3 ± 0.6**	**−53.3 ± 0.8**	**−15.3 ± 0.7**	**−54.1 ± 0.5**
S537	Yes	S537A	**+5.7 ± 0.4**	**−36.2 ± 0.5**	−9.3 ± 0.6	−58.2 ± 0.6	−19.7 ± 0.3	−59.4 ± 0.7
		S537D	+16.1 ± 0.7	−29.7 ± 1.0	**−3.1 ± 0.5**	**−51.9 ± 0.4**	**−14.1 ± 0.8**	**−53.2 ± 0.4**
S715	Yes	S715A	**+5.9 ± 0.4**	**−35.4 ± 0.5**	−10.1 ± 0.5	−60.3 ± 0.8	−20.1 ± 0.7	−58.8 ± 0.6
		S715D	+15.8 ± 0.4	−26.3 ± 0.3	**−2.7 ± 0.5**	**−54.6 ± 0.7**	**−12.1 ± 0.7**	**−51.7 ± 0.6**
S651	Yes	S651A	+15.9 ± 0.6	−26.2 ± 0.4	−9.7 ± 0.5	−59.3 ± 0.7	−20.4 ± 1.2	−59.7 ± 0.8
S453	Yes	S453A	**+7.2 ± 0.7**	−28.0 ± 0.3	−10.2 ± 0.3	−58.9 ± 0.4	−19.6 ± 0.4	−59.2 ± 0.5
		S453D	+15.9 ± 0.4	−26.2 ± 0.4	**−3.1 ± 0.6**	**−49.6 ± 0.8**	**−9.2 ± 0.6**	**−52.4 ± 0.5**
S11	Yes	S11A	+16.7 ± 0.5	**−42.1 ± 0.7**	−9.7 ± 0.4	−59.1 ± 0.6	−20.3 ± 0.6	−61.1 ± 0.7
		S11D	+16.5 ± 0.6	−27.4 ± 0.5	**−8.7 ± 0.9**	**−47.3 ± 0.4**	−19.2 ± 0.5	**−48.2 ± 0.5**
	S11A + S453A		**+4.6 ± 0.5**	**−39.8 ± 0.7**	−10.4 ± 0.6	−59.3 ± 0.5	−19.8 ± 0.5	−60.1 ± 0.4
	S563A + S603A		**−4.3 ± 0.5**	**−48.2 ± 0.6**	−10.6 ± 0.6	−59.7 ± 0.6	−19.9 ± 0.5	−60.1 ± 0.7
	S453A + S563A + S603A		**−6.9 ± 0.4**	**−47.3 ± 0.4**	−11.3 ± 0.6	−58.9 ± 0.5	−20.7 ± 0.6	−59.5 ± 0.6
S480	ND	S480A	**−0.8 ± 0.5**	**−41.1 ± 0.8**	**−15.7 ± 0.9**	−59.8 ± 0.4	−20.1 ± 0.8	−60.1 ± 0.5
		S480D	+16.2 ± 0.4	−25.9 ± 0.5	**−2.4 ± 1.0**	**−42.7 ± 0.5**	**−4.1 ± 0.7**	**−44.6 ± 0.6**
S767	ND	S767A	**+8.1 ± 0.7**	**−33.1 ± 0.8**	−7.3 ± 1.1	**−54.7 ± 0.8**	−17.6 ± 0.5	−58.9 ± 0.8
		S767D	+15.4 ± 0.8	−26.8 ± 0.4	**+0.7 ± 0.8**	**−48.4 ± 0.6**	**−12.2 ± 0.8**	**−52.1 ± 0.5**
S800	No	S800A	16.7 ± 0.8	−27.4 ± 0.5	−9.8 ± 0.5	−59.1 ± 0.7	−20.1 ± 0.6	−59.9 ± 0.4

suggests that the S480 phosphorylation site singularly distinguishes dephosphorylation catalyzed by endogenous calcineurin and exogenous AP. Serine-to-alanine mutations at the seven phosphorylation sites refractory to Ca^{2+}/calcineurin-dependent modulation yielded, in each case, channels that exhibited wild-type activation and inactivation gating. That mutations at calcineurin-sensitive sites yielded functional effects, whereas those at calcineurin-refractory sites did not, suggests that calcineurin dephosphorylation selectively targets sites affecting voltage-dependent gating of Kv2.1. These data point to complex in vivo modulation of Kv2.1 function by changes in phosphorylation at multiple functionally distinct sites, each with a characteristic contribution to gating. Analyses of one double mutant (S563A/S603A) and one triple mutant (S453A/S563A/S603A) showed a graded response to dephosphorylation at multiple sites, yielding channels that represent a larger shift than obtained with any single point mutant (Table 1), but smaller than predicted from the simple additive effects of the individual mutations.

To determine whether the sites identified as being phosphorylated on Kv2.1 expressed in HEK293 cells were also phosphorylated on native Kv2.1 expressed in rat brain, we generated phosphospecific antibodies against four of the calcineurin-regulated phosphorylation sites (S453, S563, S603, S715) identified above. Phosphospecific antibodies were affinity purified and validated by immunoblot analyses of extracts from HEK293 cells expressing wild-type Kv2.1 and phosphorylation site mutants (Fig. 2D). Each of the phosphospecific antibodies efficiently immunoprecipitated Kv2.1 protein from control rat brain membranes but not AP-treated brain membranes (Fig. 2E), demonstrating that these sites are phosphorylated on rat brain Kv2.1 in vivo. LC-MS/MS analysis (Fig. 1D) of Kv2.1 immunopurified from rat brain revealed an additional seven in vivo sites (S11, S480, S499, S516, S537, S651, S800) originally identified on Kv2.1 expressed in HEK293 cells, and it independently confirmed two of the sites already identified with phosphospecific antibodies (S453, S603).

Kv2.1 is extraordinary in (i) its extensive phosphorylation in untreated HEK293 cells and resting neurons, (ii) its graded modulation through stimulus-induced calcineurin-dependent dephosphorylation, and (iii) the large magnitude (≈35 mV) of the effects of maximal dephosphorylation on voltage-dependent activation. Our unbiased LC-MS/MS analyses, combined with SILAC labeling, reveal that the molecular basis for such regulation is phosphorylation at 16 sites under control conditions and targeted dephosphorylation of at least seven of these sites by calcineurin. Mutagenesis studies reveal that each of the seven calcineurin-modulated sites imparts a unique

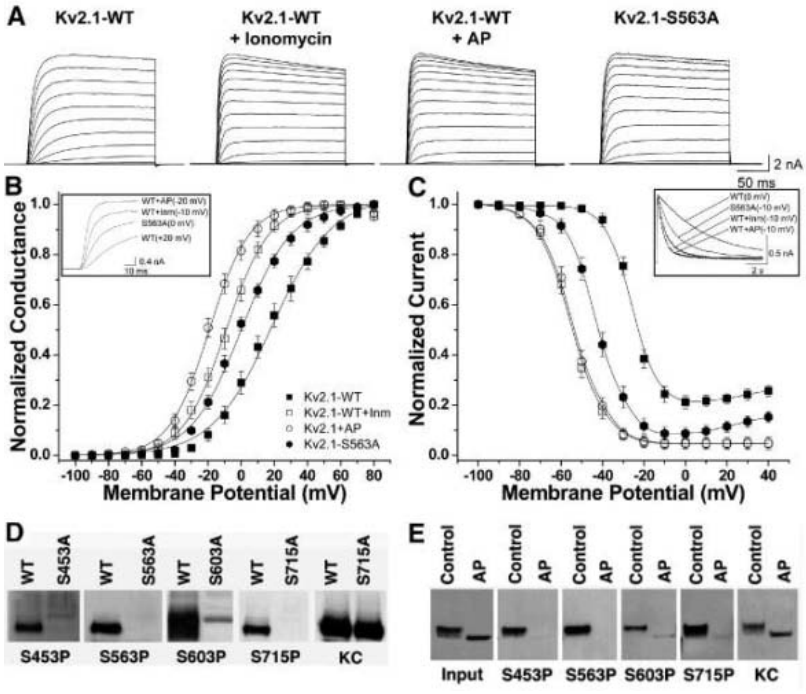

Fig. 2. Analysis of Kv2.1 phosphorylation sites. (**A**) Whole-cell voltage-clamp traces of Kv2.1 currents in HEK293 cells expressing wild-type Kv2.1 (Kv2.1-WT) without or with ionomycin treatment (1 μM for 15 min) or intracellular dialysis of alkaline phosphatase (+AP; 100 U/ml for 30 min), and of the S563A phosphorylation site point mutant under control conditions. From a holding potential of −100 mV, the cells were depolarized for 200 ms in 10-mV increments to +80 mV. (**B**) Conductance-voltage (*G-V*) relationships as a function of voltage-dependent activation and (**C**) voltage-dependent steady-state inactivation relationships of wild-type (WT) and S563A mutant Kv2.1 in HEK cells without or with the drug treatments as described in (A) (*18*). The half-maximal conductance ($G_{1/2}$) and steady-state inactivation ($Vi_{1/2}$) potentials are detailed in Table 1. Current traces for the comparison of activation and steady-state inactivation kinetics, respectively, of WT and S563A mutant Kv2.1 in HEK cells without or with the drug treatments as given in (A) are shown in the insets in (B) and (C). (**D**) Immunoblot analyses performed against extracts from HEK293 cells expressing WT Kv2.1, and the respective phosphorylation-site mutants. We normalized extracts by comparing total Kv2.1 immunoreactivity of the immunoblot samples using the general Kv2.1-specific antibody KC. (**E**) Immunoblot analysis of Kv2.1 levels in input and products of immunoprecipitation reactions performed on control and AP-treated rat brain membranes with the indicated phosphospecific antibodies and the general Kv2.1-specific antibody KC.

and incremental change in voltage-dependent gating. That the overall effect of AP treatment on voltage-dependent activation (≈36 mV) is smaller than that predicted (≈96 mV) from simply summing the incremental shifts obtained with each mutant, that certain sites (e.g., S453, S11) yield changes in only activation or inactivation gating, and that mutation of multiple sites increases the magnitude of the effects together suggest that phosphorylation-dependent regulation of Kv2.1 function is based on both the number and context of sites, analogous to phosphorylation-dependent regulation of Ets-1 DNA binding (*16*). The large number of phosphorylation sites, and the unique individual contribution from sites that can be dephosphorylated in different combinations, provide an effective mechanism for achieving graded regulation of Kv2.1 gating as observed in neurons and HEK293 cells (*6*–*8*). Variable dephosphorylation of Kv2.1 generates a wide array of function that acts as a sensitive rheostat to couple intracellular Ca^{2+} levels to neuronal excitability, analogous to direct Ca^{2+} binding to BK-type potassium channels, and distinct from binary switchlike mechanisms seen in phosphorylation-dependent regulation of other ion channels. That calcineurin is key to this modulation is intriguing given its prominent role in activity-dependent synaptic depression (*17*), such that calcineurin is a homeostatic suppressor of both evoked and intrinsic neuronal activity.

References and Notes

1. S. I. Walaas, P. Greengard, *Pharmacol. Rev.* **43**, 299 (1991).
2. O. Pongs, *FEBS Lett.* **452**, 31 (1999).
3. H. Murakoshi, J. S. Trimmer, *J. Neurosci.* **19**, 1728 (1999).
4. J. Du, L. L. Haak, E. Phillips-Tansey, J. T. Russell, C. J. McBain, *J. Physiol.* **522**, 19 (2000).
5. S. A. Malin, J. M. Nerbonne, *J. Neurosci.* **22**, 10094 (2002).
6. H. Misonou *et al.*, *Nat. Neurosci.* **7**, 711 (2004).
7. H. Misonou, D. P. Mohapatra, M. Menegola, J. S. Trimmer, *J. Neurosci.* **25**, 11184 (2005).
8. D. P. Mohapatra, J. S. Trimmer, *J. Neurosci.* **26**, 685 (2006).
9. D. J. Surmeier, R. Foehring, *Nat. Neurosci.* **7**, 691 (2004).

10. H. Misonou, D. P. Mohapatra, J. S. Trimmer, *Neurotoxicology* **26**, 743 (2005).
11. H. Murakoshi, G. Shi, R. H. Scannevin, J. S. Trimmer, *Mol. Pharmacol.* **52**, 821 (1997).
12. M. Mann *et al.*, *Trends Biotechnol.* **20**, 261 (2002).
13. S. E. Ong *et al.*, *Mol. Cell. Proteomics* **1**, 376 (2002).
14. B. Blagoev *et al.*, *Nat. Biotechnol.* **21**, 315 (2003).
15. I. Kratchmarova, B. Blagoev, M. Haack-Sorensen, M. Kassem, M. Mann, *Science* **308**, 1472 (2005).
16. M. A. Pufall *et al.*, *Science* **309**, 142 (2005).
17. W. Morishita, H. Marie, R. C. Malenka, *Nat. Neurosci.* **8**, 1043 (2005).
18. Materials and methods are available as supporting material on *Science* Online.
19. We thank R. W. Aldrich, J. Engebrecht, W. Li, C. Miller, J. Sack, and M. E. Wright for helpful suggestions and/or critical readings of the manuscript; Y. M. Lee, Y. J. Lee, and M. R. Salemi for initial technical advice in mass spectrometric studies; and L. Guy and D. Siino for technical assistance. Mass spectrometry was performed at the UC Davis Proteomics Facility. This work was supported by NIH grant NS42225 to J.S.T. K.-S.P. was supported in part by the postdoctoral fellowship program of Korea Science and Engineering Foundation, and H.M. by the American Heart Association. D.P.M. acknowledges postdoctoral fellowship support from the Epilepsy Foundation through the support of the American Epilepsy Society and the Milken Family Foundation.

Supporting Online Material
www.sciencemag.org/cgi/content/full/313/5789/976/DC1
Materials and Methods
References

23 December 2005; accepted 16 June 2006
10.1126/science.1124254

The Psychological Risks of Vietnam for U.S. Veterans: A Revisit with New Data and Methods

Bruce P. Dohrenwend,[1,2,3]* J. Blake Turner,[3] Nicholas A. Turse,[3] Ben G. Adams,[4,5] Karestan C. Koenen,[6,7,8] Randall Marshall[1,2]

In 1988, the National Vietnam Veterans Readjustment Study (NVVRS) of a representative sample of 1200 veterans estimated that 30.9% had developed posttraumatic stress disorder (PTSD) during their lifetimes and that 15.2% were currently suffering from PTSD. The study also found a strong dose-response relationship: As retrospective reports of combat exposure increased, PTSD occurrence increased. Skeptics have argued that these results are inflated by recall bias and other flaws. We used military records to construct a new exposure measure and to cross-check exposure reports in diagnoses of 260 NVVRS veterans. We found little evidence of falsification, an even stronger dose-response relationship, and psychological costs that were lower than previously estimated but still substantial. According to our fully adjusted PTSD rates, 18.7% of the veterans had developed war-related PTSD during their lifetimes and 9.1% were currently suffering from PTSD 11 to 12 years after the war; current PTSD was typically associated with moderate impairment.

On 16 December 2004, *The New York Times* reported that, "What was planned as a short and decisive intervention in Iraq has become a grueling counterinsurgency that has put American troops into sustained close-quarters combat on a scale not seen since the Vietnam War" (*1*). These similarities to Vietnam and findings from the congressionally mandated NVVRS (*2*, *3*) that "one in three" Vietnam veterans developed PTSD have led some military and Department of Veterans Affairs' experts to expect a "deluge of troubled soldiers" from the war in Iraq (*1*). A recent report that 35% of Army and Marine veterans of the Iraq war accessed mental health services within a year of returning home seems broadly consistent with this expectation, although it is unclear what proportion of the 35% involved PTSD (*4*).

[1]New York State Psychiatric Institute, New York, NY 10032, USA. [2]Department of Psychiatry, [3]Mailman School of Public Health, Columbia University, New York, NY 10032, USA. [4]Teachers College, Columbia University, New York, NY 10027, USA. [5]Brookdale University Hospital and Medical Center, Brooklyn, NY 11212, USA. [6]Department of Society, Human Development, and Health, [7]Department of Epidemiology, School of Public Health, Harvard University, Boston, MA 02115, USA. [8]Department of Psychiatry, Boston University, Boston, MA 02115, USA.

*To whom correspondence should be addressed. E-mail: dohrenw@pi.cpmc.columbia.edu

The high PTSD rates identified in the NVVRS have been controversial. As measured by rates of combat stress breakdowns, killed in action, or wounded in action, Vietnam has been described as a "low-intensity" war for U.S. forces (*5*). Because rates of combat stress breakdowns, killed in action, and wounded in action have historically predicted the development of PTSD and other psychiatric disorders (*5*, *6*), the psychiatric casualty rates in Vietnam were expected to be low (*7*). Consistent with this, in 1988, the Centers for Disease Control (CDC) reported rates of 14.7% lifetime PTSD and 2.2% current PTSD 11 to 12 years after the Vietnam war ended (*8*). The NVVRS rates of 30.9% lifetime PTSD and 15.2% current PTSD, which were reported at about the same time (*2*, *3*), were inconsistent with expectations.

PTSD diagnoses require antecedent traumatic events, defined at the time of the NVVRS as events that are markedly distressing and "outside the range of usual human experience"—especially events that threaten the life or physical integrity of the individual or someone close to him. The definition also includes witnessing death or serious injury to others (*9*). Critics have argued that the NVVRS 30.9% lifetime rate of PTSD is twice as high as the proportion of veterans (15%) who served in combat roles (*10*–*15*). This anomaly has raised questions about the accuracy of the retrospective reports of PTSD symptoms and war-zone stressors that qualify as traumatic [supporting online material (SOM) text] (*10*–*13*, *16*, *17*) We used military records, historical accounts, diagnostic histories of PTSD by experienced clinicians, Minnesota Multiphasic Personality Inventory validity scales, and data on compensation-seeking to address these concerns about the NVVRS.

The estimated percentage of veterans involved in combat [15%, according to McNally (*12*)] probably includes 10.5% who were infantrymen [(*18*), p. 238] and their combat counterparts in the Marines, Navy, and Air Force. However, the 15% does not include 14% who were regularly exposed to combat hazards while serving in support roles, such as combat engineers and artillery personnel [(*18*), p. 238]. Moreover, estimates of the percentage of veterans exposed to combat dangers increase when Vietnam is recognized as a "war without fronts" rather than a conventional war (*19*). Kolko, for example, reports that 50% of soldiers were considered "combat forces" [(*20*), p. 361], and Baskir and Strauss conclude that about 1.6 million of the 2.15 million men that they estimate were assigned to tours in Vietnam itself "served in combat" [(*21*), p. 53] (SOM text).

We used data from military personnel files (201 files) extracted by the NVVRS investigators (*2*, *3*) together with data that we obtained from military archival sources and historical accounts to develop a record-based military historical measure (MHM) of probable severity of exposure to war-zone stressors that would capture this complexity. We constructed this MHM of exposure for all 1200 veterans in the NVVRS's representative sample of men who served in Vietnam or surrounding areas (Theater veterans) (*22*) (SOM text). The first three components of the MHM are the veteran's military occupational specialty, the monthly killed-in-action rate during his Vietnam service, and the killed-in-action rate in his larger military unit (e.g., division) (*23*). We have combined (*23*), validated (table S1), and refined these three measures with important previously unused data from the military records of the approximately 58,000 U.S. servicemen killed in action in Vietnam (*24*) (SOM text).

Our study revealed a strong positive relationship between our record-based MHM ex-

posure measure and the dichotomous measure of high versus low or moderate war-zone stress constructed by the NVVRS investigators [(*2*), Appendix C] on the basis of the veterans' retrospective reports of their experiences (Fig. 1). For example, 96.5% of the veterans classified as probable low exposure on the MHM were in the combined low or moderate category of the NVVRS self-report measure, and 72.1% of those classified as very high on the MHM were high by self-report.

The NVVRS employed experienced, doctoral level clinicians to give diagnostic examinations to a representative subsample (n = 260) of the veterans who resided in 28 standard metropolitan regions (SMRs) (*22*). These diagnoses were used in the NVVRS to calibrate more economical PTSD symptom scales in the full 1200-member Theater sample [(*2*), Appendix D]. The resulting algorithm was the basis for the NVVRS 15.2% rate of current PTSD in Theater veterans. Although not representative of the entire sample of Theater veterans, the sample from the 28 SMRs had a similar rate of current PTSD (15.4%). Because the NVVRS algorithm for PTSD focused solely on current symptoms, the often quoted but rarely analyzed lifetime rate, 30.9%, was extrapolated from the results of the Structured Clinical Interview for *Diagnostic and Statistical Manual of Mental Disorders* (DSM-III-R) (SCID) diagnoses in the subsample [(*2*), Appendix E].

The subsample diagnostic examinations themselves have received relatively little attention or analysis in the main reports of the NVVRS (*2*, *3*) or in the wider literature, even though the diagnoses contain by far the most detailed data on PTSD and the only data on the history of this disorder. We conducted further analyses of these data because they shed light on the nature of PTSD and its prevalence in Vietnam veterans. Most important, on the basis of information contained in the written records and tape recordings of these diagnoses, we were able to distinguish (i) between war-related first onsets of PTSD and first onsets that occurred before or after service in Vietnam in calculations of lifetime rates and (ii) between past PTSD that remitted and current PTSD that was present in the six months before the diagnostic examinations (*22*). We were also able to identify the types of criterion traumatic events that were reported by the veterans. The majority (86.6%) of the veterans with war-related onsets described events that our raters, blind to diagnostic status, judged to be personally life threatening. Events that involved witnessing death or physical harm to others were also frequently reported.

Unlike the current DSM-IV, the diagnosis of PTSD in DSM-III-R did not require impairment by either disability in social roles or elevated psychological distress. However, because the examiners assessed each veteran's present functioning on the Global Assessment of Functioning (GAF) rating scale as part of the examination with the SCID (*25*), we were able to check whether the high NVVRS rates included substantial numbers of veterans with only mild, unimpairing PTSD.

We found that the majority (84.8%) of the veterans with current war-related PTSD ("current group") were rated as having more than slight impairment at the time of the examination (Table 1). However, only 28.5% had more than moderate difficulty. Moreover, current impairment in veterans with past war-related PTSD ("past group") differed little from impairment in the group with no war-related onsets of PTSD.

The clinicians made ratings of the severity of PTSD at its worst in addition to the severity at the time of the examination. These severity ratings, which are strongly related to the GAF impairment ratings, suggest that the results in Table 1 underestimate impairment when the disorder was at its worst. For example, 36.1% of veterans in the current group were rated mild, 43.1% moderate, and 20.8% severe at the time of diagnosis. When PTSD was at its worst, 3.7% of veterans were rated mild, 31.8% moderate, and 66.5% severe. The results also suggest that at least 85% of veterans in the past group had more than slight impairment when their PTSD was at its most severe (SOM text).

To investigate questions about the possible falsification of symptom reporting, we reasoned that if some NVVRS veterans exaggerated their PTSD symptoms by outright lying or more subtle retrospective distortions (*26*), these veterans should be overrepresented among veterans who reported experiencing high war-zone stress despite having record-based MHMs indicating low or moderate severity of exposure. Using questionnaire measures of dissembling (*27*–*31*)

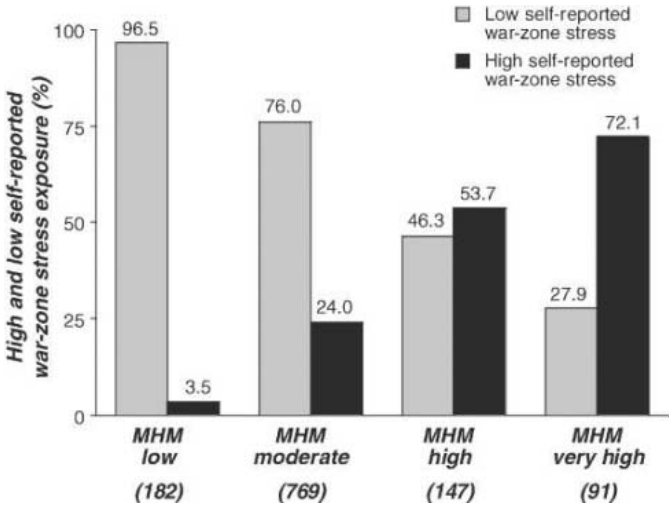

Fig. 1. Self-reports of war-zone stress exposure correlated well with records-based MHM war-zone stress exposure. A high percentage of veterans categorized as low exposure on the basis of records-based MHM evidence had self-reported low exposure. Veterans who self-reported high exposure were the large majority of the MHM very high exposure category. Full sample n = 1189, excluding 11 veterans with missing data on self-reported war-zone exposure. Low and moderate self-reports of exposure were grouped together as "Low self-reported war-zone stress" [(2), Appendix C].

Table 1. Estimated impairment on the GAF scale in the 260-member subsample of veterans diagnosed by experienced clinicians using the SCID (*25*) as having no lifetime war-related first onsets of PTSD (past or current) (n = 158), past war-related first onsets of PTSD (n = 30), and war-related first onsets of PTSD that remained current (n = 59). Percentages are based on data weighted to reflect the complex sampling design (*22*). (Omitted from the analysis are four veterans with prewar onsets, two missing onset information, one missing sampling weight, and six missing impairment scores.) A chi-square test shows that the overall difference in the percentages of male veterans with more than slight impairment is statistically significant at the 0.01 level. Individual tests show that the percentage impaired in veterans with current war-related PTSD is significantly greater at the 0.01 level than the percentage of impaired in veterans with past PTSD and the percentage impaired in veterans with no PTSD.

GAF score	Description of impairment	None (%)	Past (%)	Current (%)
09	Good functioning in all areas	46.6	43.6	0.0
08	No more than slight impairment	29.9	24.0	15.1
07	Some difficulty in social, occupational, or school functioning	18.3	23.9	40.5
06	Moderate difficulty	2.7	8.2	15.6
05	Any serious impairment	1.7	0.3	21.1
04	Major serious impairment in several areas	0.1	0.0	7.0
03	Inability to function	0.0	0.0	0.0
02	Some danger to self or others	0.0	0.0	0.0
01	Persistent danger to self or others	0.0	0.0	0.4

and self-reported symptoms, we found no indication of dissembling and little evidence of exaggeration (SOM text).

The possibility of receiving disability compensation might motivate falsification of symptoms and exposure reports (*16*). Compensation-seeking for psychiatric disability was reported by 9.3% of the veterans. However, there was no elevation of compensation-seeking among veterans discordant on the exposure measures; for example, only 3.0% of those who reported high exposure in the context of low MHM exposure sought compensation compared with 15.6% who were high on both exposure measures.

Veterans' 201 files do not systematically record information about specific war-zone experiences (*32*). However, these files routinely contain, or make it possible to access from historical accounts, other valuable indicators of the likelihood of experiencing traumatic stressors. These indicators include high-exposure military occupational specialty; receipt of a Purple Heart, combat medal, or Combat Infantryman Badge; service in a company with one or more killed in action during the veteran's tour; attachment to a high casualty division; and being in Vietnam during the nationwide Tet offensive of 1968. More than one of these indicators was present for all 30 subsample veterans in our high and very high MHM exposure groups. One or more of these indicators was also present in the 201 files of 47 of the 60 subsample veterans diagnosed with war-related PTSD in the low and moderate MHM exposure groups (SOM text).

To investigate the validity of the reports of the remaining 13 of the 60 veterans with onsets of PTSD but none of the record-based indicators of probable exposure, we compared their narratives of traumatic events with information from military histories (*33*, *34*) and from newspaper accounts of events in Vietnam published contemporaneously in *The New York Times* and the *Los Angeles Times*. These independent sources confirmed the narratives of traumatic events of five veterans: Three veterans reported attacks on air bases, which were reported in detail in a military history of Air Force actions (*33*); one veteran who served in a submarine described a harrowing rescue of U.S. personnel in a downed aircraft, which was corroborated in a newspaper account, as was a typhoon that occurred during a series of attacks on another veteran's base. This left only eight subsample veterans whose accounts were not confirmed by any of our independent checks (SOM text).

Thus, we were able to confirm as plausible the exposure to traumatic stressors of most of the subsample veterans with war-related onsets of PTSD, and most but not all of these war-related PTSD onsets, as we reported earlier, were associated with more than slight impairment. Nevertheless, removing subsample veterans without independent documentation of traumatic exposure and/or with no more than slight impairment somewhat reduces lifetime rates of war-related onsets of PTSD and rates of war-related onsets that remained current (Table 2).

We next investigated whether, as with the NVVRS retrospective measure of exposure and the PTSD algorithm, there is a dose-response relationship between the record-based MHM exposure and clinically diagnosed PTSD (Fig. 2). Our results show that there is. The relationship is especially strong for current PTSD, with less than 1% of the low-exposed veterans receiving this diagnosis, compared with 28.1% of the veterans in the very high exposure category. Omission of the veterans with unconfirmed traumatic exposure and/or those with no more than slight impairment had little effect (SOM text).

The conundrum posed by critics of the NVVRS involves two figures: a 15% rate of combat exposure and a 30.9% lifetime rate of PTSD in Vietnam veterans. Our analyses show that neither figure represents the reality of the psychological risks and their consequences for U.S. forces in Vietnam. First, consistent with estimates from military histories of this war without fronts, at least half of the Theater veterans were involved in combat (*20*, *21*). Second, even the least conservative rates of SCID-diagnosed PTSD from Table 2 (22.5% war-related onsets, 12.2% war-related current) are lower than the previously published NVVRS rates (30.9% lifetime and 15.2% current). These latter rates are based on an algorithm that calibrates self-reports of symptoms to SCID diagnoses in the subsample [(*2*), Appendix E]. This algorithm does not distinguish between war-related PTSD and PTSD with other origins, and scores do not depend crucially on the presence of DSM-III-R traumatic events. These differences probably contribute to the higher rates found with the algorithm.

In contrast, the SCID-based rates, even those fully adjusted for impairment and verification of exposure (18.7% onset and 9.1% current), are higher than the rates in the CDC study (*8*, *35*). The CDC used about half of the items (*36*) from a newly developed module from the Diagnostic Interview Schedule (DIS) (*37*) to diagnose lifetime and current PTSD on the basis of responses to closed questions asked by lay interviewers. This version of the DIS PTSD module has been found to diagnose much lower rates of PTSD in the general population than the other diagnostic instrument that is most widely used by lay interviewers (*38*). Against this background, it is not surprising that the abbreviated CDC adaptation of the DIS PTSD module was found in the NVVRS to miss 78% of veterans who had diagnosable PTSD, according to the SCID clinicians [(*2*), Appendix

Table 2. Percentages of lifetime first onsets (past plus current) (n = 90) and percentages of current first onsets (n = 60) of war-related PTSD in the 260-member SCID-diagnosed subsample of veterans with and without adjustments for the requirements of impairment and/or independent documentation of traumatic exposure. Sample n values are in parentheses and percentages are based on data weighted to reflect the complex sampling design (*22*). (Omitted from the analysis are four veterans with prewar onsets, two missing onset information, and one missing a sampling weight.)

Adjustments	Lifetime (%)	Current (%)
Unadjusted	22.5	12.2
Adjusted for impairment of functioning	21.0	10.4
Adjusted for documentation of exposure	20.3	11.1
Adjusted for both impairment and documentation	18.7	9.1

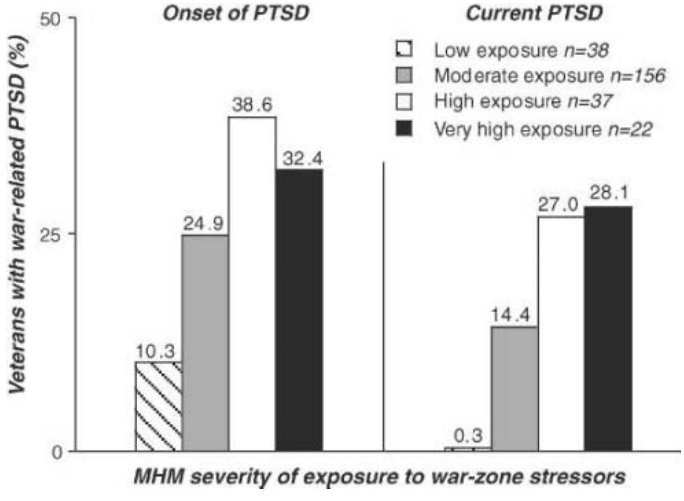

Fig. 2. The percentages of veterans who had suffered from war-related PTSD during their lifetime (Onset of PTSD) and the percentages of those who still suffered from PTSD at the time of the study (Current PTSD) increase with increases in MHM probable severity of exposure to war-zone stressors. Subsample n = 253, omitting four veterans with prewar onset, two missing onset information, and one missing sampling weight.

E]. These results suggest that PTSD is underdiagnosed in both military and civilian samples when this version of DIS PTSD is used.

The SCID diagnostic results in the NVVRS have proved robust to record checks, investigation of compensation-seeking, and measures designed to detect outright falsification. It was sometimes even possible to confirm in contemporary newspaper accounts or military histories the plausibility of the veterans' reports of warzone experiences for which there was no confirmatory evidence in their personnel files. These results suggest that reports of a high rate of unverified trauma in some subgroups of compensation-seeking veterans (*16*) should not be generalized to the population of Vietnam veterans as a whole.

The message from the NVVRS has been that the Vietnam War took a severe psychological toll on U.S. veterans. Our results provide compelling reasons to take this message seriously. The nature of this toll is suggested by the substantial rates of war-related onset and current PTSD and their strong dose-response relationship with severity of exposure—a relationship that cannot be due to biases in self-reports of exposure because it holds for our new prospective, record-based MHM (SOM text). It is especially notable that, conservatively, almost 10% suffered from and were impaired by current PTSD more than a decade after the war. This finding points to the need for further research on the factors that contribute to chronicity (*23*, *39*).

However, the majority of the veterans with high and very high MHM exposure did not develop war-related PTSD (Fig. 2). Even allowing for substantial heterogeneity of individual experiences within these high exposure categories, there appear to be protective factors that reduce vulnerability. Moreover, the trajectory for most veterans with war-related PTSD that causes substantial impairment is toward amelioration or complete remission. This tendency toward improvement is present even for ~10% of veterans who still had impairing current PTSD at follow-up; the impairment most of them showed by this time was not severe. The functioning of the veterans who had developed war-related PTSD but who no longer met criteria for the disorder at follow-up differed little from that of veterans who did not develop war-related PTSD.

These trends toward recovery over time cannot be explained entirely by treatment administered by mental health professionals because less than half the veterans with past war-related PTSD (44.9%) received such treatment. Investigations of other factors that may contribute to initial resilience and psychological readjustment after traumatic war experiences are needed (*23*).

Substantial similarities exist between Vietnam then and Iraq now. Both have been wars without fronts, in which it is often difficult to tell peaceful civilians from enemy combatants. What has been, and can still be, learned about PTSD and Vietnam veterans should be applicable to understanding the psychological risks to U.S. veterans of the war in Iraq.

References and Notes

1. S. Shane, "A deluge of troubled soldiers is in the offing, experts predict," *The New York Times*, 16 December 2004, p. A1.
2. R. A. Kulka *et al.*, *Contractual Report of Findings from the National Vietnam Veterans Readjustment Study, Volume I* (Veterans Administration, Washington, DC, 7 November 1988).
3. R. A. Kulka *et al.*, *Trauma and the Vietnam War Generation* (Brunner/Mazel, New York, 1990).
4. C. Hoge, J. Auchterlonie, C. Milliken, *JAMA* **295**, 1023 (2006).
5. E. Jones, S. Wessely, *Br. J. Psychiatry* **178**, 242 (2001).
6. Z. Solomon, M. Weisenberg, J. Schwarzwald, M. Mikulincer, *Am. J. Psychiatry* **144**, 448 (1987).
7. S. Wessely, *Br. J. Psychiatry* **186**, 459 (2005).
8. Centers for Disease Control, *JAMA* **259**, 2701 (1988).
9. American Psychiatric Association, *Diagnostic and Statistical Manual of Mental Disorders, Third Edition, Revised (DSM-III-R)* (American Psychiatric Association, Washington, DC, 1987).
10. B. G. Burkett, G. Whitely, *Stolen Valor* (Verity, Dallas, TX, 1998).
11. D. Marlowe, *Psychological and Psychosocial Consequences of Combat and Deployment* (Rand Corporation, Santa Monica, CA, 2000).
12. R. J. McNally, *Annu. Rev. Psychol.* **54**, 229 (2003).
13. S. Satel, "Returning from Iraq, still fighting Vietnam," *The New York Times*, 5 March 2004, p. A23.
14. B. Shephard, *A War of Nerves* (Harvard Univ. Press, Cambridge, MA, 2001).
15. S. Wessely, *Br. J. Psychiatry* **186**, 473 (2005).
16. B. C. Frueh, *Br. J. Psychiatry* **186**, 467 (2005).
17. S. M. Southwick, C. A. Morgan III, A. L. Nicholaou, D. S. Charney, *Am. J. Psychiatry* **154**, 173 (1997).
18. M. Clodfelter, *Vietnam in Military Statistics* (McFarland, Jefferson, NC, 1995).
19. T. Thayer, *War Without Fronts* (Westview Press, Boulder, CO, 1985).
20. G. Kolko, *Anatomy of a War* (Pantheon Books, New York, 1985).
21. L. M. Baskir, W. A. Strauss, *Chance and Circumstance* (Knopf, New York, 1978).
22. Materials and methods are available as supporting material on *Science* Online.
23. B. P. Dohrenwend *et al.*, *J. Consult. Clin. Psychol.* **72**, 417 (2004).
24. R. D. Coffelt, R. J. Arnold, D. Argabright, *Electronic Database* (National Archives and Records Administration, Washington, DC, 2002).
25. R. Spitzer, J. Williams, M. Gibbon, *Structured Clinical Interview for DSM-III-R, version NP-V* (New York State Psychiatric Institute, Biometrics Research Department, New York, 1987).
26. A. Young, in *Posttraumatic Stress Disorder*, G. M. Rosen, Ed. (Wiley, West Sussex, England, 2004), pp. 127–146.
27. H. G. Gough, *J. Abnorm. Soc. Psychol.* **42**, 215 (1947).
28. H. G. Gough, *J. Consult. Psychol.* **14**, 408 (1950).
29. H. G. Gough, *California Psychological Inventory Manual* (Consulting Psychologists Press, Palo Alto, CA, 1957).
30. D. N. Weiner, *J. Consult. Psychol.* **12**, 164 (1948).
31. R. L. Greene, Ed., *The MMPI: Use with Specific Populations* (Grune & Stratton, New York, 1988).
32. U.S. National Archives & Records Administration, *Military Service Records and Official Military Personnel Files* (obtained 8 February 2006 through www.archives.gov).
33. R. P. Fox, *Air Base Defense in the Republic of Vietnam, 1961–1973* (Office of Air Force History, Washington, DC, 1979).
34. D. B. Sigler, *Vietnam Battle Chronology* (McFarland, Jefferson, NC, 1992).
35. L. Roberts, *Science* **241**, 788 (1988).
36. W. W. Thompson, I. I. Gottesman, C. Zalewski, *BMC Psychiatry* **6**, 19 (2006).
37. L. N. Robins, J. E. Helzer, J. Croughan, K. S. Ratcliff, *Arch. Gen. Psychiatry* **38**, 381 (1981).
38. R. C. Kessler, A. Sonnega, E. Bromet, M. Hughes, C. Nelson, *Arch. Gen. Psychiatry* **52**, 1048 (1995).
39. R. D. Marshall *et al.*, *J. Nerv. Ment. Dis.* **194**, 275 (2006).

40. We thank C. J. Douglass, D. W. King, L. A. King, Y. Neria, P. E. Shrout, W. E. Schlenger, and three anonymous referees for valuable comments and suggestions. Supported by the National Institute of Mental Health (NIMH) grant R01-MH059309 and grants from The Spunk Fund, Inc. (B.P.D.); also training grant 5T32MH13043 and NIMH K08 MH070627 (K.C.K.).

Supporting Online Material

www.sciencemag.org/cgi/content/full/313/5789/979/DC1
Materials and Methods
SOM Text
Table S1
References

19 April 2006; accepted 12 July 2006
10.1126/science.1128944

Image-Analysis System

The LAS-3000mini is a compact image-analysis system designed for chemiluminescence and bioluminescence analysis, specifically for protein immunoblotting applications. It incorporates Fuji's proprietary Super CCD (charge-coupled device) chip, which allows for resolution of 3.2 to 6.3 million pixels. The LAS-3000mini also features the newly designed F0.85 FUJINON high-sensitivity lens to capture the faintest images, such as expression of calcium binding proteins. The low-noise design captures images at –30°C, allowing for increased exposure times. In addition, the compact body incorporates the modular darkroom and nonparallax tray. Applications include genomics and proteomics imaging and molecular biology.

Fujifilm Life Science For information 630-400-3042
www.fujifilmlifescienceusa.com

Elispot Examinations

For pharmacologists, immunologists, and oncologists who conduct microscopic Elispot examinations in tumor, AIDS, and vaccine research and in the routine lab, Carl Zeiss offers the software KS ELISPOT and KS ELISPOT compact Release 4.9. The software has been optimized for the testing of immunotherapies and the development of vaccines. With the use of the integrating digital color camera AxioCam MRc Rev. 3, the spots in double markings are more distinctly separated due to the enhanced color recognition. In combination with the Zeiss Axio Imager microscope system with fluorescence equipment and the AxioCam camera, fluorescence-marked Elispot specimens can be reliably evaluated.

Zeiss For information +49 3641 64-2770
www.zeiss.de/elispot

Bulk Insulin-Like Growth Factor

IGF-I is an insulin-like growth factor used to supplement serum-free culture media. Bulk IGF-I is available for use in large-scale manufacturing and process development applications. The bulk packaging eliminates the need for multiple vials and reduces the potential risks of compromised product. The product is animal-origin free.

Invitrogen For information 760-268-7438
www.invitrogen.com

Animal-Product Free Products

Two new products, Animal Product Free LB Broth and casein hydrolysate replacement Atholate, are meant to address the safety concerns associated with the use of animal-derived products in the manufacture of pharmaceuticals. Atholate is a proprietary blend of plant protein hydrolysates designed to replace casein-derived hydrolysates while matching their nutritional and performance characteristics. Guaranteed to have no animal derivatives while maintaining quality performance, Atholate is used to prepare bacteriological media for the cultivation of a wide range of microbial species. The line of Animal-Product Free Broth features performance equal or superior to standard LB Broth formulation with casein. The media can be used for cultivation of *Escherichia coli*, *Salmonella*, *Pseudomonas*, *Bacillus*, and other eubacteria species.

Athena Environmental Sciences
For information 410-455-6319 www.athenaes.com

High Definition MS System

The Waters Synapt HDMS system is designed for researchers working at the limits of conventional spectrometry capabilities who need to further characterize and define their samples. The system enables the analysis of samples differentiated by size and shape, as well as mass, to deliver increased specificity and sample definition beyond that achievable by conventional mass spectrometers. The system combines high-efficiency, ion mobility–based measurements and separations with high-performance quadrupole, and time-of-flight mass spectrometry. It features patented Triwave technology, which incorporates three traveling-wave devices with distinct functions: The first traps and releases packets of ions. The second separates ions according to their ion mobility. The third transfers ions for mass analysis.

Waters For information 800-252-4752
www.waters.com

Antigen Retrieval System

The BioGenex EZ-Retriever System is a microwave-based, time- and temperature-controlled system for use in dewax, rehydration, and antigen retrieval of formalin-fixed, paraffin-embedded tissue sections. This programmable benchtop system has the ability to superheat solutions evenly to a temperature of up to 107°C. The system differentiates itself from methods such as the pressure cooker, steamer, water bath, and autoclave by its ease-of-use, high-performance, and high-throughput processing of 96 slides in a single run. It is used in conjunction with the EZ-AR Solutions, a set of unique solutions that enable a one-step dewax, rehydration, and antigen retrieval in formalin-fixed, paraffin-embedded tissue sections. These solutions are nontoxic, aqueous reagents that facilitate highly reproducible and superior staining more rapidly than conventional methods. The EZ-AR Solutions solve many of the problems encountered by traditional tissue pretreatment methods, including result inconsistency, poor stain quality, low efficiency, and high costs.

BioGenex For information 800-421-4149
www.biogenex.com

Newly offered instrumentation, apparatus, and laboratory materials of interest to researchers in all disciplines in academic, industrial, and government organizations are featured in this space. Emphasis is given to purpose, chief characteristics, and availability of products and materials. Endorsement by *Science* or AAAS of any products or materials mentioned is not implied. Additional information may be obtained from the manufacturer or supplier by visiting www.science.labvelocity.com on the Web, where you can request that the information be sent to you by e-mail, fax, mail, or telephone.

POSITIONS OPEN

PLANT PHYSIOLOGICAL ECOLOGIST
Kansas State University

The Division of Biology at Kansas State University invites applications for a tenure-track faculty position in plant physiological ecology at the level of **ASSISTANT** or **ASSOCIATE PROFESSOR,** depending on qualifications and experience, to begin in the 2007 academic year. We seek candidates with interests and expertise in physiological ecology at scales that span individual plants to ecosystems, and that complement well-established and diverse programs in ecology and plant biology, including a highly productive, internationally recognized grassland ecology research program. Ideally, the candidate will conduct research in plant ecophysiology on topics such as whole plant responses to dynamic and changing environmental drivers, soil-plant water and nutrient interactions, the role of ecophysiological processes at the ecosystem and landscape scales, responses of ecosystems to global change phenomena (climate change, elevated CO2, nutrient enrichment, land cover change) or other topics relevant to grassland ecosystems. Opportunities exist to join interdisciplinary research teams where the candidate's knowledge in plant ecophysiology will complement ongoing efforts in plant population and community ecology, ecosystem ecology, climatology, and remote sensing. The successful candidate is expected to develop an independent, extramurally funded research program in his/her area of expertise, to take an active role in the Konza Prairie Long-Term Ecological Research program **(website: http://www.konza.ksu.edu)** and other regional ecological efforts, and to participate in graduate and undergraduate instruction **(website: http://www.ksu.edu/biology).** Minimum requirements for an appointment at the Assistant Professor rank include a Ph.D. degree and postdoctoral experience. Minimum requirements for an appointment at the Associate Professor rank include a Ph.D. degree and postdoctoral experience, plus an independent, nationally recognized research program, demonstrated excellence in teaching, and evidence of participation in interdisciplinary research activities. The successful candidate, at either rank, should demonstrate a strong commitment to excellence in research, teaching, mentoring of students, and to serving a diverse population. Inquiries should be directed to **Dr. David Hartnett (e-mail: dchart@ksu.edu).** Applicants should submit a cover letter, curriculum vitae, and brief description of research and teaching interests, representative reprints, and have three letters of reference sent to: **Chair; Physiological Ecologist Search Committee; Division of Biology; 116 Ackert Hall; Kansas State University; Manhattan, KS 66506-4901.** Review of applications will begin September 15, 2006, and continue until the position is filled. *Kansas State University is an Equal Opportunity/Affirmative Action Employer, and actively seeks diversity among its employees.*

Florida Institute of Technology **(website: http://www.fit.edu),** a premier, independent, technological university located on Florida's East Coast, invites applications for **HEAD** of the Department of Biological Sciences. The University seeks an outstanding individual with skills and resources to advance one of the most productive and well-funded departments on campus. The new Head must be poised to advance the Department's academic reputation and expand the M.S. and Ph.D. programs. Successful applicants must have a doctorate, an international reputation in research with a distinguished publication record, an active research program, and outstanding leadership qualities. Interested candidates are invited to submit detailed curriculum vitae, a letter of application, and contact information for five references. Applications will be treated confidentially and should be submitted electronically to **e-mail: bioheadsearch@fit.edu.** Review of applications will begin October 15, 2006. *Florida Institute of Technology is an Equal Opportunity/Affirmative Action Employer. Women and minorities are encouraged to apply.*

POSITIONS OPEN

BIOCHEMISTRY AND MOLECULAR BIOLOGY FACULTY POSITION
University of California, Los Angeles (UCLA)

The Biochemistry Division of the Department of Chemistry and Biochemistry **(website: http://www.biochemistry.ucla.edu),** in conjunction with the Molecular Biology Institute, is seeking applications for a tenure-track faculty position at the **ASSISTANT PROFESSOR** level. We invite outstanding candidates in any area of biochemistry, chemical biology, or molecular and cellular biology. The new faculty member will be expected to develop a strong and creative research program and contribute to teaching in biochemistry.

Applications should include curriculum vitae, a summary of research accomplishments and future research plans, and two to three reprints of representative publications. Applicants should also arrange to have three letters of reference sent to the address below. To assure consideration, all application materials and letters should be received by October 15, 2006.

All application materials should be sent to: **Chair, Biochemistry Search Committee, c/o Penny Jennings, Department of Chemistry and Biochemistry, University of California, Los Angeles, P.O. Box 951569, Los Angeles CA 90095-1569**

The University of California is an Equal Opportunity/Affirmative Action Employer. Women and minorities are encouraged to apply.

ORGANIC CHEMISTRY
Dartmouth College

Applications are invited for a faculty position at the **ASSISTANT PROFESSOR** level starting July 2007. The Chemistry Department seeks an individual who will establish a nationally recognized research program in organic chemistry at Dartmouth, and who will excel at teaching in our undergraduate and Ph.D. curriculum. Candidates will be expected to be able to teach introductory and advanced courses in organic chemistry, as well as graduate courses in their area of research. Applicants should submit curriculum vitae, a description of their research plans, and a brief statement about their teaching interests. Applicants should also arrange to have three letters of recommendation sent on their behalf. All inquiries and applications will be treated confidentially. Application materials should be sent to: **Chair, Organic Chemist Search Committee, Department of Chemistry, 6128 Burke Laboratory, Dartmouth College, Hanover, NH 03755-3564.** The Committee will begin to consider completed applications on October 15, 2006. *With an even distribution of male and female students and over a quarter of the undergraduate student population members of minority groups, Dartmouth is committed to diversity and encourages applications from women and minorities. Dartmouth College is an Equal Opportunity and Affirmative Action Employer.*

DEVELOPMENTAL BIOLOGIST ASSISTANT PROFESSOR
University of Denver

The Department of Biological Sciences, University of Denver, invites applications for a tenure-track position at the Assistant Professor level to begin September 1, 2007. Candidates using vertebrate or invertebrate model systems relevant to developmental biology are sought. The successful candidate will have a Ph.D. and postdoctoral experience in appropriate fields, will develop an extramurally funded research program, will supervise undergraduate research projects and M.S. and Ph.D. students, and will teach undergraduate and graduate courses in areas of specialty. Submit curriculum vitae, two recent publications, three letters of recommendations, and statements of (a) teaching philosophy and (b) research interests to: **Dr. Jim Platt, Chair, Developmental Biologist Search Committee, Department of Biological Sciences, University of Denver, Denver, CO 80208.** Applications should be received by October 15, 2006. Information about the Department of Biological Sciences can be found at **website: http://www.biology.du.edu.** *The University of Denver is an Equal Opportunity/Affirmative Action Employer.*

Positions @ NIH

The National Institutes of Health

Tenured/Tenure-Track Position
Neuroimmunology (Clinical)
Division of Intramural Research

The Division of Intramural Research of the National Institute of Neurological Disorders and Stroke is recruiting an individual for a tenured or tenure-track position in the area of neuroimmunology with a focus on clinical research. The applicant should have a special interest and experience in translational clinical research relating to multiple sclerosis or other immune mediated disease of the central nervous system. The individual would direct an independent research program on immune mediated diseases of the nervous system and especially multiple sclerosis. The program would conduct its work in conjunction with the Neuroimmunology Branch (NIB) which was established to study the cause and treatment of immunological mediated diseases of the central nervous system. The individual should have a demonstrated background and knowledge in research focused on immune mediated disease of the nervous system and with expertise in human immunology and/or the application of clinical trial methodology to the study of disease mechanisms and testing new therapies. The candidate will have earned a M.D. degree and will have excellent scientific skills in structuring an original and productive research program using outstanding communication and collaborative abilities. The candidate will have a medical license in the United States and preference will be given to a candidate who has completed training in an accredited training program in neurology and is either board eligible or board certified in Neurology. Candidates for a tenured position must have an international reputation and well-documented evidence of ongoing independent accomplishments. An individual selected for a tenure-track position is expected to build a dynamic and productive research group. Laboratory facilities, start-up and sustained research funds and salary will be competitive with premier academic institutions. Applicants should send curriculum vitae, bibliography, statement of research interests, and names of references to: **Dr. Story Landis, Director, National Institute of Neurological Disorders and Stroke, c/o Peggy Rollins, Office of the Scientific Director, Division of Intramural Research, Building 35 Room GA908, NIH, Bethesda, MD 20892**. Applications will be reviewed upon receipt.

Tenured/Tenure-Track Position
Neuroimmunology (Basic/Translational)
Division of Intramural Research

The Division of Intramural Research of the National Institute of Neurological Disorders and Stroke is recruiting an individual for a tenured or tenure-track position in the area of Neuroimmunology. The applicant should have a special interest and experience in translational research relating to multiple sclerosis or other immune mediated disease of the central nervous system. The individual would direct an independent research program on molecular, biological or immunological aspects of immune mediated diseases of the nervous system and especially multiple sclerosis. The program would conduct its work in conjunction with the Neuroimmunology Branch (NIB) which was established to study the cause and treatment of immunological mediated diseases of the central nervous system. The individual should have a demonstrated background and knowledge in research focused on immune mediated disease of the nervous system and with expertise in the use of animal models or in human immunology. The candidate will have a Ph.D. and/or M.D. degree with excellent scientific skills in structuring an original and productive research program using outstanding communication and collaborative abilities. Candidates for a tenured position must have an international reputation and well-documented evidence of ongoing independent accomplishments. An individual selected for a tenure-track position is expected to build a dynamic and productive research group. Laboratory facilities, start-up and sustained research funds and salary will be competitive with premier academic institutions. Applicants should send curriculum vitae, bibliography, statement of research interests, and names of references to: **Dr. Story Landis, Director, National Institute of Neurological Disorders and Stroke, c/o Peggy Rollins, Office of the Scientific Director, Division of Intramural Research, Building 35 Room GA908, NIH, Bethesda, MD 20892 (301-435-2232)**. Applications will be reviewed upon receipt.

National Institutes of Health
Center for Scientific Review

NIH SCIENTIFIC REVIEW ADMINISTRATOR
(Health Scientist Administrator)
Vacancy #'s: CSR-06-140166-DE and CSR-06-140166-MP

We are seeking exceptionally qualified scientists, with doctorate level training and independent research and administrative experience in lung biology and pathology to join a team of Scientific Review Administrators (SRAs) to help shape the future of scientific review. SRAs are responsible for taking a leadership role in providing scientific, administrative, and logistical oversight of the peer review process. The incumbent(s) will be responsible for the initial administrative and scientific review of NIH research grant applications in bioengineering sciences and technology and will possess an M.D. or Ph.D. degree (or have equivalent training and experience), have independent research experience, and strong records of publication or other productivity in academia or industry. These positions are in the Respiratory Sciences Integrated Review Group (IRG). The IRG is responsible for the merit evaluation of grant applications focused on the mechanism(s) of lung injury, repair and remodeling in non-vascular pulmonary tissues or cells including areas such as lung development, pulmonary fibrosis and lung toxicology. A broad knowledge of one or more of these scientific areas is desirable. For additional information on the IRG please see our web site, at: http://cms.csr.nih.gov/PeerReviewMeetings/CSRIRGDescription/RESIRG/

Salary is commensurate with research experience and accomplishments, and a full Civil Service package of benefits (including retirement, health, life and long-term care insurance, Thrift Savings Plan participation, etc.) is available.

For additional information on this position and for instructions on submitting your application, please visit our website at: **http://jobsearch.usajobs.opm.gov/a9nih.asp**

The National Institute of Allergy and Infectious Diseases, a major research component of the NIH and the Department of Health and Human Services, is recruiting for a Staff Scientist. The position will be available in the Respiratory Viruses Section of the Laboratory of Infectious Diseases, and scientists with a M.D. or Ph.D. are eligible. The research activity involves (1) the development of live attenuated flavivirus vaccine candidates and their evaluation in rodents and non-human primates as well as in the clinical trials in humans; (2) the use of novel approaches for construction of chimeric viruses to examine basic questions of viral pathogenesis and the molecular basis of attenuation of highly neurovirulent flaviviruses; (3) the evaluation of the immunologic determinants of resistance to infection and illness caused by these flaviviruses. This full-time research position offers a unique opportunity to work on investigations that range from basic molecular biology to applied vaccinology. Staff Scientist applicants should have at least six years of laboratory work experience in molecular virology and immunology; the salary range is $73,178 - $165,195. Preference will be given to candidates who have experience working with neurotropic viruses. Applicants should submit their curriculum vitae, a letter of research interests, and names and addresses of three references to:

Alexander Pletnev, NIAID, NIH, 12735 Twinbrook Parkway, Twinbrook 3, Room 3W13, MSC 8133, Bethesda, MD 20892-8133, FAX: (301) 480-4873, email: apletnev@niaid.nih.gov. Review of applicants will begin **October 1, 2006** and continue until a successful candidate is identified.

WWW.NIH.GOV

Chief, Laboratory of Bacterial Diseases
National Institute of Allergy and Infectious Diseases
National Institutes of Health

The National Institute of Allergy & Infectious Diseases (NIAID), Division of Intramural Research (DIR) is seeking an outstanding individual to head the newly established Laboratory of Bacterial Diseases (LBD) in Bethesda, Maryland. The laboratory is to be located in the new C.W. Bill Young Center for Biodefense and Emerging Pathogens located on the NIH campus in Bethesda, Maryland.

The mission of the LBD will be to study basic and applied aspects of bacterial diseases related to biodefense or emerging and re-emerging pathogens, focusing on pathogenic bacteria. Exceptional scientists with research interests in basic, translational or clinical aspects of bacterial pathogenesis are encouraged to apply. The long-term goals of the Institute include supporting research that enables the development of new diagnostics, vaccines, and therapeutics.

This position requires an M.D., Ph.D. or equivalent with proven leadership abilities and a strong independent research program. Preference will be given to candidates with a documented record of accomplishment in bacterial disease research, and those whose program(s) are consistent with the mission of the NIAID.

The Laboratory Chief will have independent resources to conduct basic and clinical research and will supervise other Principal Investigators with independent research programs. The successful candidate is expected to lead a strong research program in laboratory and/or clinical research. Committed resources include space, support personnel and an allocated annual budget to cover service, supplies, animals and related resources and salaries. A Laboratory Chief in the DIR is equivalent to a Department Chair in a University or Medical School. Applicants must be U.S. citizens or permanent residents and be eligible for the appropriate security clearance under the CDC Select Agent Program. Salary will be commensurate with experience and qualifications.

Interested candidates may contact **Dr. Karyl Barron, Deputy Director, DIR, NIAID at 301/402-2208 or email (kbarron@niaid.nih.gov)** for additional information about the position and/or infectious diseases research at the NIH.

To apply for the position, candidates must submit curriculum vitae, bibliography, a detailed statement of research interests, and reprints of up to three selected publications, preferably via Email to: Lynn Novelli at novelly@niaid.nih.gov. In addition, the names of three potential references must be sent to **Dr. Steven M. Holland, Chair, NIAID Search Committee, c/o Ms. Lynn Novelli, DIR Committee Manager, 10 Center Drive, MSC 1356, Building 10, Room 4A26, Bethesda, Maryland 20892-1356.** Completed applications **MUST** be received by **Monday, September 25, 2006**. Please refer to **AD#004** on all correspondence. Further information on this position and guidance on submitting your application is available on our website at: **http://healthresearch.niaid.nih.gov**

Chief, Laboratory of Human Bacterial Pathogenesis
National Institute of Allergy and Infectious Diseases
National Institutes of Health

The National Institute of Allergy & Infectious Diseases (NIAID), Division of Intramural Research (DIR) is seeking an outstanding individual to head the Laboratory of Human Bacterial Pathogenesis (LHBP) in Hamilton, Montana.

The mission of the LHBP is to study human bacterial diseases related to emerging and re-emerging pathogens. The research to be conducted in the LHBP is to include; 1) the molecular basis of host-pathogen interactions, 2) the genetic basis of bacterial virulence and pathogenesis, 3) the use of animal modeling to define host defense mechanisms and biology and immunology of host-pathogen interactions, and 4) development of novel and improved intervention strategies to control bacterial infectious diseases. The ultimate goal is to develop diagnostics, vaccines, and therapeutics for emerging and re-emerging infectious diseases.

This position requires a Ph.D. and/or M.D. or equivalent with proven leadership abilities and a strong independent research program. Preference will be given to candidates with a documented record of accomplishment in bacterial disease research, and especially to those whose program(s) are consistent with the mission of the NIAID to study emerging and re-emerging bacterial pathogens.

The Laboratory Chief will have independent resources to lead and conduct laboratory research and translational/clinical research, as appropriate. Mechanisms are available to conduct clinical studies at the Bethesda campus and/or to obtain clinical samples through contract mechanisms at non-NIH institutions. The individual will supervise other Principal Investigators with independent research programs investigating the pathogenicity of Staphylococcus and Streptococcus species. Committed resources include space, support personnel, animal resources and an allocated annual budget to cover service, supplies and salaries. A Laboratory Chief in the DIR is equivalent to a Department Chair in a University or Medical School. Salary is dependent on experience and qualifications.

Interested candidates may contact **Dr. Karyl Barron, Deputy Director, DIR, NIAID at (301) 402-2208 or email (kbarron@niaid.nih.gov)** for additional information about the position. To apply for the position, candidates must submit a curriculum vitae, bibliography, a detailed statement of research interests, and reprints of up to three selected publications preferably via email to: **Felicia Braunstein at braunsteinf@niaid.nih.gov or by US Mail to: Ms. Felicia Braunstein, DIR Committee Manager, 10 Center Drive MSC 1349, Building 10, Rm. 4A-30, Bethesda, Maryland 20892-1349**. In addition, the names of three referees must be sent to **Dr. Tom Schwan, Chairperson, NIAID Search Committee, c/o Ms. Felicia Braunstein, DIR Committee Manager, 10 Center Drive MSC 1349, Building 10, Rm. 4A-30, Bethesda, Maryland 20892-1349**. Please note search **#005** when sending materials. Completed applications **MUST** be received by **October 6, 2006**. Further guidance on submitting your application is available on our website at: **http://healthresearch.niaid.nih.gov**.

WWW.NIH.GOV
Positions @ NIH
THE NATIONAL INSTITUTES OF HEALTH

Postdoctoral Fellowship in Signal Transduction of Innate Immunity

Michael B. Fessler, MD
Environmental Diseases and Medicine Program
Laboratory of Respiratory Biology

Applications are invited for a fellowship in signal transduction of innate immunity. Particular focus will be spent investigating emerging roles for cholesterol, related lipids, and their cellular regulators on the signaling and inflammatory responses triggered by lipopolysaccharide and related stimuli.

Applicants should possess a Ph.D. degree in Molecular Biology, Biochemistry, Immunology, Pharmacology, or a related field, and have no more than five years of previous postdoctoral experience. Expertise in molecular biologic techniques is very strongly preferred; background in lipid sciences is desirable, but not necessary. Salary will be commensurate with experience according to NIH guidelines.

For additional information about this position, contact **Dr. Michael B. Fessler**. For prompt consideration, send or e-mail a cover letter including a summary of relevant experience, CV including list of publications in peer-reviewed journals, and the names/phone numbers of 3 people who could provide letters of reference to: **Michael B. Fessler, M.D., National Institute of Environmental Health Sciences, Division of Intramural Research, Laboratory of Respiratory Biology, P.O. Box 12233, Maildrop D2-01, 111 T.W. Alexander Drive, Room E206, (if express mail), Research Triangle Park, North Carolina 27709. E-mail: fesslerm@niehs.nih.gov**

Postdoctoral Research Opportunity Mechanisms of Glucocorticoid Receptor Signaling in Health and Disease

A postdoctoral fellow position is available in the Molecular Endocrinology Group directed by John A. Cidlowski. Investigations will include molecular and genetic analysis of glucocorticoid receptor signaling mechanisms during inflammation. Examples of our research publications include: Hermoso et al., Mol. Cell. Biol., 24: 4743 – 4756 2004, Schaaf et al., Molecular Endocrinology, 19: 1501 – 1515 2005 and Lu and Cidlowski, Molecular Cell, 18: 331 – 342 2005.

We seek a creative independent scientist with a strong background in molecular biology or knock out animals to contribute towards the understanding of glucocorticoid receptor signaling mechanisms. We have state of the art facilities, core labs and outstanding funding for this research.

Applicants should possess a Ph.D. degree in Biochemistry, Pharmacology, Cell or Molecular biology and have less than three years prior postdoctoral experience. NIH offers excellent salary and health care packages to its trainees.

For consideration please provide a cover letter of interest and curriculum vitae including publications to: **Dr. John A. Cidlowski, Chief, Laboratory of Signal Transduction, NIEHS/NIH, 111 T.W. Alexander Drive, Research Triangle Park, NC 27709, Email: Cidlows1@niehs.nih.gov, Fax: 919-541-1367**

Opportunities in Symptoms Management Research National Institute of Nursing Research, NIH

NINR seeks applications for post-doctoral fellowship positions in its Symptom Management Laboratory. Successful applicants will be expected to conduct innovative clinical or translational research in symptom management in chronic or acute illness. Individuals with documented expertise in biobehavioral approaches to symptom management research are of particular interest. Candidates must have a Ph.D. as well as advanced training and accomplishment in symptom management research. The NINR Symptom Management Laboratory offers unparalleled opportunities for multidisciplinary collaboration throughout NIH.

For additional information, contact **Renee G. Harris at harrisrg@mail.nih.gov.**

To apply, send your CV, cover letter including a summary of relevant experience, and the names and contact information for 3 recent references to: **Renee G. Harris, National Institute of Nursing Research, NIH, 10 Center Drive, CRC-East, Room 2-1339, Bethesda, MD 20892**. Applications will be accepted until the position is filled.

Postdoctoral Research Opportunity Mechanisms of Apoptosis in the Immune System

A postdoctoral fellow position is available in the Molecular Endocrinology Group directed by John A. Cidlowski. Investigations will include molecular and electrophysiological analysis of cellular mechanisms and signaling pathways involved in both suppression and activation of immune cell apoptosis. Examples of our research publications include: Bortner and Cidlowski, J. Biol. Chem., 278: 39176 – 39184 2003, Storey et al., J. Biol. Chem., 278: 33319 – 33326 2003, Heimlich and Cidlowski, 281: 2232 – 2241 2006, Franco and Cidlowski, J. Biol. Chem., in press.

We seek a creative, independent scientist with a strong background in molecular biology, pharmacology, cell biology and/or electrophysiology (patch clamping) to study the roles and regulation of ion channels in apoptosis. We have state of the art facilities, research cores and outstanding funding for this research.

Applicants should possess a Ph.D. degree in Physiology, Molecular biology/Cell biology or Pharmacology and have less than three years prior postdoctoral experience. NIH offers excellent salary and health care packages to its trainees.

For consideration please provide a cover letter of interest and curriculum vitae including publications to: **Dr. John A. Cidlowski, Chief, Laboratory of Signal Transduction, NIEHS/NIH, 111 T.W. Alexander Drive, Research Triangle Park, NC 27709. Email: Cidlows1@niehs.nih.gov, Fax: 919-541-1367**

FACULTY POSITION IN
NEUROPATHOLOGY
THE UNIVERSITY OF CHICAGO

The Department of Pathology at The University of Chicago is seeking an MD or PhD Neuroscientist/Neuropathologist with demonstrated record of independent research in any subspecialty of neuroscience broadly related to disease of the nervous system. Candidate should be BE/BC in Neuropathology, but candidate's primary responsibility will be to establish a strong investigative program for mentoring fellows, residents, medical and graduate students who desire to pursue a research program in Neuropathology.

Amount of clinical responsibility is negotiable on the basis of interest and research program but some participation in the Neuropathology diagnostic service would be expected. Appointment will be at a faculty rank appropriate for level of previous achievement. All levels will be considered for this position. Interested candidates should send CV to:

Vinay Kumar, M.D., FRCPath,
Professor and Chairman
Attn: Neuropathology Search Committee
Department of Pathology
The University of Chicago
5841 South Maryland Ave., MC 3083
Chicago, IL 60637
The University of Chicago is an
Affirmative Action/Equal Opportunity Employer.

THE UNIVERSITY OF CHICAGO

Martin Luther University Halle-Wittenberg
and
Leibniz Institute of Plant Biochemistry Halle
Registration number 6/2006

Independent junior research group leader position

The University of Halle and the Leibniz Institute of Plant Biochemistry will establish a third independent junior research group as part of the Federal State of Sachsen-Anhalt Excellence Initiative "Structures and mechanisms of biological information processing". The group is to work closely with one or more of the local Collaborative Research Centres SFB 610 "Protein states with cell biological and medical relevance", SFB 648 "Molecular mechanisms of information processing in plants" and SFB 604 "Multifunctional signaling proteins: oligomeric protein complexes as mediators of cellular regulatory processes", and the Graduate College GRK1026 "Conformational transitions in macromolecular interactions".

Applications are invited for the following junior group leader position:

Plant protein complexes - structure, function and evolution

The successful candidate should have a research focus in one of the following areas:

- Protein complexes in plant signal transduction and regulation
- Protein complexes in plant microbe interactions
- Plant membrane protein complexes

The group will be located at the Leibniz Institute of Plant Biochemistry (Director Dierk Scheel) on the Weinberg Campus of the University of Halle. The Institute offers

- essential infrastructure from the existing programs in natural product biotechnology (Claus Wasternack), bioorganic chemistry (Ludger Wessjohann), stress and developmental biology (Dierk Scheel), and secondary metabolism (Dieter Strack)
- state of the art technology including platforms for proteomics, metabolic profiling and *in vivo* imaging of protein-protein interactions
- an energetic working environment with a multidisciplinary approach to natural product, molecular interaction, plant microbe interaction and gene function analyses

Appointments will be made at the level of BAT-O Ia for a period of five years. Laboratory space, start up funds and consumables as well as additional salaries for one postdoc, PhD students and a laboratory technician will be made available.

Applicants with a proven publication record in high quality journals should submit their CV and publication list stating registration number 6/2006, together with reprints of the three most important publications, a project sketch of not more than three pages, and the names of three academic referees to

Leibniz Institute of Plant Biochemistry
Managing Director
Prof. Dierk Scheel
Weinberg 3
D-06120 Halle (Saale), Germany

The University of Halle and the Leibniz Institute of Plant Biochemistry are affirmative actions employers. Female Scientists are specifically encouraged to apply for this position. Suitably qualified disabled candidates will be treated preferentially. Further information can be found under http://www.ipb-halle.de and http://www.excellenz-netzwerk-biowissenschaften.uni-halle.de

Closing date for applications is October 31st, 2006.

FACULTY POSITIONS AT THE ROCKEFELLER UNIVERSITY

The Rockefeller University seeks a new generation of exceptional scientists to join its faculty. The focus of the search will be on tenure-track Assistant Professors. We invite applications from outstanding candidates working in the areas of:

- **Biochemistry, Chemistry & Structural Biology**
- **Immunology, Virology & Microbiology**
- **Medical Sciences & Human Genetics**
- **Molecular, Cell & Developmental Biology**
- **Neurosciences & Behavior**
- **Physical Biology, Ecology, Evolution & Bioinformatics**

Applicants are asked to submit:

- A 1-2 page cover letter summarizing their most significant scientific accomplishments and outlining why the research is well suited to The Rockefeller University
- Curriculum Vitae with a publications list
- Statement of Research with a 2 page description of significant research accomplishments and a 2 page description of future research plans (4 pages maximum)
- Relevant publications (optional, a maximum of 3 is allowed)
- Contact information for at least 3 references

Applications are being accepted electronically through our Online Application System at **http://oas.rockefeller.edu.** If you are unable to submit an electronic application, please contact our Faculty Search Administrator at **facultysearch@rockefeller.edu.**

The deadline for receipt of applications is October 1, 2006.

More specific information regarding this search can be found at **http://www.rockefeller.edu/facultysearch/.**

The Rockefeller University is an Affirmative Action/Equal Opportunity/VEVRAA Employer and solicits applications from women and under-represented minorities.

Further information about the research and educational programs at The Rockefeller University can be found at **http://www.rockefeller.edu/**.

U.S. Department of Health and Human Services
National Institutes of Health

The **National Center for Complementary and Alternative Medicine** seeks outstanding candidates for the position of **Director, Division of Extramural Activities**. The Division provides critical infrastructure in support of NCCAM's extramural research and research training programs. Accordingly, the Director, DEA:

- Provides leadership and advice in developing, implementing, and coordinating extramural programs and policies within NCCAM, with other NIH institutes and centers, the NIH Office of the Director, and the extramural community;
- Represents NCCAM on the trans-NIH Extramural Program Management Committee and elsewhere within and beyond NIH;
- Coordinates the receipt, referral, and scientific review of grants, cooperative agreements, and research contracts;
- Oversees the processing of awards by grants management staff;
- Coordinates meetings of the National Advisory Council for Complementary and Alternative Medicine; and
- Manages the Center's committee management activities.

Qualified applicants must have a Ph.D., M.D., or equivalent doctoral degree; extensive knowledge of and experience in directing NIH extramural programs; and broad knowledge and appreciation of complementary and alternative medicine research. Compensation and resources are commensurate with research experience and accomplishments. A full package of benefits is available.

Applicants should email a cover letter, CV/bibliography, and a list of three references to: nccamdirector-r@mail.nih.gov
Subject Line: DEA Director Search
Application Deadline: October 10, 2006
Email receipt of applications and inquiries is preferred; however, candidates needing reasonable accommodation may fax application materials to 301-402-4741.

Information regarding NCCAM is available at nccam.nih.gov.
NIH and DHHS are equal opportunity employers

University of Florida College of Medicine
Department of Medicine
Division of Nephrology, Hypertension and Renal Transplantation

The University of Florida Division of Nephrology, Hypertension & Renal Transplantation seeks nominations and applications for the R. Glenn Davis, M.D., Dialysis Clinic, Inc. Professor of Nephrology Endowed Chair in clinical investigation. This is a full-time, tenure-track faculty appointment at the academic rank of Associate Professor or Professor. The successful candidate will be expected to direct clinical research; serve as an attending physician on inpatient services and an outpatient clinic; and participate in the education of medical students, residents and fellows. Candidates must possess an M.D., be board eligible or board certified in nephrology and have a proven record in clinical investigation in nephrology, hypertension, diabetes or transplantation. Candidates must possess or be eligible for a Florida medical license. Salary and academic rank will be commensurate with the successful candidate's experience. The anticipated start date for this position is January 1, 2007.

Interested parties should forward a curriculum vitae with three letters of recommendation to:

C. Craig Tisher, M.D.
Chair, Search Committee
UF Department of Medicine
Division of Nephrology, Hypertension and Transplantation
PO Box 100224
Gainesville, FL 32610
tisher@dean.med.ufl.edu

The review of applications will begin **September 1, 2006**, and will continue until the position is filled. Please complete the optional Data Applicant Card at **www.hr.ufl.edu/job/datacard.htm**, reference job requisition number **037051**.

The University of Florida is an Equal Opportunity Employer. Women and minorities are encouraged to apply.

ST. LAWRENCE UNIVERSITY

BIOLOGY DEPARTMENT

CELL BIOLOGY

The Biology Department at St. Lawrence University invites applications for a one year position in Cell Biology starting **Fall 2007** at the Visiting Assistant Professor level. A Ph.D. is required and post-doctoral as well as previous teaching experience, especially in a liberal arts and science environment is preferred. We especially welcome applications from candidates who bring diverse cultural and ethnic perspectives to the University.

In support of our majors in biology, biochemistry and neuroscience, the successful candidate will be expected to teach a cell biology course with lab and a team-taught research methods course in biochemistry. Preference will be given to candidates who can also offer an introductory course in immunology and who can help with our general biology courses.

Interested candidates should submit a letter of application, a curriculum vitae, a statement of teaching experience and philosophy that reflects innovative and progressive pedagogies, a statement of research interest, and have three letters of recommendation forwarded to: **Dr. T. Budd, Biology Department, St. Lawrence University, 23 Romoda Drive, Canton, New York 13617**. Applications will be reviewed until the position is filled.

St. Lawrence University, chartered in 1856, is the oldest coeducational university in New York State. Please see the University homepage at **http://www.stlawu.edu** and the Biology Department homepage at **http://it.stlawu.edu/~biology** for more information.

St. Lawrence University is an Affirmative Action/Equal Employment Opportunity employer. Women, members of minority groups, veterans, and persons with disabilities are encouraged to apply.

ST. LAWRENCE UNIVERSITY

BIOLOGY DEPARTMENT

NEUROSCIENCE – HUMAN ANATOMY

The Biology Department at St. Lawrence University invites applications for a one year position in Neuroscience starting **Fall 2007** as a Visiting Assistant Professor. A Ph.D. is required and post-doctoral as well as previous teaching experience, especially in a liberal arts and science environment is preferred. We especially welcome applications from candidates who bring diverse cultural and ethnic perspectives to the University.

In support of our majors in biology and neuroscience, the successful candidate will be expected to teach an introductory neuroscience course with lab, a lab based course in human anatomy, and participate in our spring semester introductory biology course. Candidates will also have the opportunity to offer a course of their own design and interest according to their expertise.

Interested candidates should submit a letter of application, a curriculum vitae, a statement of teaching experience and philosophy that reflects innovative and progressive pedagogies, a statement of research interest, and have three letters of recommendation forwarded to: **Dr. T. Budd, Biology Department, St. Lawrence University, 23 Romoda Drive, Canton, New York 13617**. Applications will be reviewed until the position is filled.

St. Lawrence University, chartered in 1856, is the oldest coeducational university in New York State. Please see the University homepage at **http://www.stlawu.edu** and the Biology Department homepage at **http://it.stlawu.edu/~biology** for more information.

St. Lawrence University is an Affirmative Action/Equal Employment Opportunity Employer. Women, members of minority groups, veterans, and persons with disabilities are encouraged to apply.

ADVANCED MATERIALS PROCESSING AND ANALYSIS CENTER
http://www.ampac.ucf.edu/

University of Central Florida
Director Position

The University of Central Florida, a major metropolitan research university located in Orlando, FL, with over 45,000 students, is searching for a Director of its Advanced Materials Processing and Analysis Center (AMPAC). AMPAC conducts leading-edge interdisciplinary education and research in advanced materials, including miniaturization, nano- materials fabrication, micro- and nano-devices, and acousto-electronics, for applications that include energy, microelectronics, MEMS, nanotechnology and bioengineering. In addition to 9 tenured/tenure-earning faculty and 17 affiliate faculty, AMPAC has five full-time staff who support two major multi-user facilities: the 7,000 ft2 Materials Characterization Facility (MCF) and the 2,600 ft2 class 100/1000 cleanroom Advanced Microfabrication Facility (AMF). These facilities, staff and faculty are foundational elements of the associated interdisciplinary Materials Science and Engineering degree program that has a current enrollment of over 65 graduate students and offers both Ph.D. and M.S. degrees.

UCF seeks candidates with proven track records of research accomplishments in materials science and engineering. The ideal candidate will have a Ph.D. or equivalent from an accredited institution in the field of materials science and engineering or an allied discipline, must be eligible for appointment with tenure at the full professor rank; possess exceptional vision, commitment and leadership skills; and be able to enthusiastically coordinate industry, faculty and administration efforts in growing the research programs of AMPAC.

Review of candidates will begin on **October 16, 2006**, but candidates are welcome to apply after this date. Electronically submit curriculum vitae, a summary of research accomplishments, vision for the Center, and the names and contact information of three references to: **Chair of the Search Committee, AMPAC Director Search, University of Central Florida, 1679 Clearlake Road, Cocoa, FL 32922-5703; ampac_dir@fsec.ucf.edu**.

The University of Central Florida is an Affirmative Action/Equal Opportunity Employer. As a member of the Florida State University System, all application materials and selection procedures are available for public review.

ASSISTANT MEDICAL PROFESSOR (BASIC SCIENCES)

The City College of New York

The CUNY Medical School seeks an Assistant Professor in Neurobiology of Drug Abuse in the Department of Physiology and Pharmacology.

Duties: Candidates must have a demonstrated strong record of scholarly research and publications in neuropharmacology and/or neuroscience that is focused on drug abuse and addiction. Preference will be given to candidates interested in working in a highly collaborative, interdisciplinary environment with interests complementing those of departmental faculty. These include basic cellular, neurochemical, electrophysiological and behavioral approaches to the study of the neurobiology of abused substances. The selected candidates will also participate in teaching activities of the Department.

Qualifications: Ph.D. and/or M.D. with 2 years of post-doctoral work in any area of neuroscience, neurochemistry or neuropharmacology.

Salary: $70,000 - 75,000. Commensurate with qualifications and experience.

Closing Date: Open until filled.

To Apply: Candidates should submit curriculum vitae, cover letter, statement of research plan and at least three professional references to: **Dr. Eitan Friedman - PVN# FY-11540, Department of Physiology & Pharmacology, The Sophie Davis School of Biomedical Education, The City College of New York, 160 Convent Avenue, New York, NY 10031.**

Additional information available at www.ccny.cuny.edu

CUNY/CCNY is an EEO/AA/IRCA/ADA Employer

CITY COLLEGE IS CUNY

nature REVIEWS NEUROSCIENCE

Chief Editor

We are seeking a Chief Editor to guide the development of *Nature Reviews Neuroscience* as an essential resource for the neuroscience community. This is an extremely stimulating role with overall responsibility for the journal's content and coverage of the field, in print and online. Key responsibilities include commissioning and editing reviews, managing the editorial team, planning special projects (such as focus issues and supplements) and coordinating peer-review.

The ideal candidate will have a PhD and post-doctoral experience in a relevant topic combined with a broad interest in neuroscience. Previous publishing experience is not essential, but candidates should have a genuine enthusiasm for communicating scientific ideas. Other important attributes include excellent communication skills, a dynamic, outgoing personality and good team-working skills.

The position is based in Nature Publishing Group's modern London offices, and the terms and conditions are highly competitive, reflecting the critical importance and responsibilities of the role. For further information about *Nature Reviews Neuroscience*, please visit http://www.nature.com/nrn

Applicants should send a CV and a brief cover letter explaining their interest in the post, quoting reference number NPG/LON/399 to: Rebecca Innes, Personnel Assistant, Macmillan Publishers at londonrecruitment@macmillan.co.uk

Closing Date: 1st September 2006

USDA ARS Agricultural Research Service
www.ars.usda.gov

Supervisory Horticulturist/ Agronomist/Geneticist (Plants)/ Botanist
GS-0437/0471/0440/0430-14
Salary Range of $87,533 to $113,791

The Plant Germplasm Introduction and Testing Research Unit in Pullman, WA, is seeking to fill a permanent, full-time highly qualified scientist to lead an Agency research and curation program in plant germplasm. As Research Leader, selectee will provide leadership and direction to a large, multi-site, multi-state program. Provides leadership related to conservation of plant genetic resources throughout the region and nationwide. Collections include primarily landrace and wild types. Formulates policies, plans, and programs necessary for the direction of all service and research activities of three National Plant Germplasm System (NPGS) sites (Pullman, WA, Prosser, WA, and Parlier, CA). Selectee will be responsible for administration of combined budget in excess of $3 million.

For application instructions, please see Vacancy Announcement Number **ARS-X6W-0311**. Applications must be received by **October 16, 2006**. For questions regarding application process, please contact **Barbara Scafone**, **301-501-1416** or **Barbara.Scafone@ars.usda.gov**. U.S. citizenship is required and must be stated on application.

USDA, ARS is an Equal Opportunity Employer and Provider.

Science Director for Weather, National Centre for Atmospheric Science, UK

National Centre for Atmospheric Science
NATURAL ENVIRONMENT RESEARCH COUNCIL

Three year contract in the first instant with the possibility of renewal thereafter, £negotiable

This is an opportunity for an outstanding research scientist to take on the scientific leadership of the UK's National Centre for Atmospheric Science (NCAS) Weather Directorate. NCAS provides the UK with a core strategic research programme in atmospheric science. It has science directorates for Weather, Climate and Atmospheric Composition and also provides airborne, ground-borne, data and computer & modelling facilities and services in support of the UK university atmospheric science research community. This appointment will be made as soon as possible and is initially for 3 years.

In this role, you will lead the NCAS Weather Directorate, developing and managing the NCAS science strategy within the area of weather research. Your personal research programme will contribute directly to this. You will influence and facilitate interaction between the NCAS weather science community and the wider UK science community and stakeholders, including the private sector and government departments. You will also be influential in developing strategy and policy at national and international level.

This is a key role that demands strong leadership, science vision and excellent communication skills. Applicants should have outstanding research records exemplified by an outstanding track record of peer-reviewed publications in international journals and a proven ability to attract and manage research funding.

Employment will be by an institute of your choice (envisaged in the UK), with a suitable remuneration package being agreed between the institute and NCAS.

Further particulars and application forms can be obtained from the NCAS website: **http://www.ncas.ac.uk**

They can also be obtained from Miss Emma Mason (Email: **emma@env.leeds.ac.uk**; Tel: +44 113 343 6408) who can deal with queries that you may have. Informal enquiries may be made to the NCAS Director, Professor Stephen Mobbs (Email: **stephen@env.leeds.ac.uk**; Tel: +44 113 343 5158).

Closing date for applications 17:00 GMT: **16 October 2006**

NCAS supports equal opportunities.

**** Please note the NERC Centres for Atmospheric Science (NCAS) is now renamed to the National Centre for Atmospheric Science.***

MICHIGAN STATE UNIVERSITY

Faculty Positions in Plant Proteomics and Quantitative Biology

As part of an initiative in Systems Biology, the Department of Plant Biology at Michigan State University seeks to fill two faculty positions in Proteomics and in Computational or Theoretical Biology. We are seeking individuals who will address fundamental biological questions in plants and/or in related model systems. Applications from individuals who develop methods to generate and integrate complex or heterogeneous data from metabolomic, proteomic, and genomic studies or build models of metabolic or regulatory networks are especially encouraged. The successful candidates will be expected to develop vigorous independent research programs that are supported by extramural funding. We are particularly interested in recruiting colleagues who will participate in collaborative interdisciplinary research. Each successful candidate may have a joint appointment with another suitable department and will contribute to undergraduate and graduate teaching in their areas of expertise.

These faculty positions are tenure track, academic year appointments at the Assistant Professor level. An appointment at the Associate Professor level will be considered for exceptional candidates. Applicants must have a PhD and postdoctoral research experience is highly desirable. Applications should include a curriculum vitae, a summary of research accomplishments and future research objectives, a brief description of teaching philosophy/goals and three letters of reference. Application materials should be sent electronically to **PLBSYS@msu.edu**. Information about the Department of Plant Biology can be found at **http://www.plantbiology.msu.edu**. The review of applications will begin **October 1, 2006** and will continue until suitable candidates are identified. Questions regarding these positions may be sent to **Robert Last (lastr@msu.edu)**.

Michigan State University is an Equal Opportunity/Affirmative Action Employer. Women and minorities are strongly encouraged to apply. Persons with disabilities have the right to request and receive reasonable accommodation.

Children's Research Institute
A member of Children's Hospital and Health System.

MEDICAL COLLEGE OF WISCONSIN

Section Chief, Developmental Biology

The Department of Pediatrics, Medical College of Wisconsin, is seeking an established scientist to direct a new Section of Developmental Biology. The successful candidate will be an extramurally-funded, nationally-known MD or PhD leader in the field of Developmental Biology with leadership experience in NIH peer-review, and will have the opportunity to develop a translational science program within one of the most rapidly-growing academic Pediatric Departments in the country. The new Children's Research Institute (CRI)/MCW Biomedical Research Building provides a 300,000 square-foot, state-of-the-art home for translational molecular and cell biology. Extramural research support generated by the CRI has increased by 27% over the past two years. Academic accomplishments should be commensurate with an appointment at the level of Professor in the traditional tenure track. Respond by September 15, 2006 with CV and 3 references to:

Ellis D. Avner, MD
Professor of Pediatrics and Associate Dean for Research
Medical College of Wisconsin
Director, Children's Research Institute
PO Box 1997
Milwaukee, WI 53201-1997
eavner@mcw.edu
EEO/AA M/F/D/V

star
Stem Cells and Regenerative Medicine

Stem Cells and Regenerative Medicine Center
Baylor College of Medicine
Houston, Texas

Faculty Position in Stem Cells and Regenerative Medicine Center

This is an opportunity for investigators with experience in stem cell research to develop an independent research program. The Center was established to facilitate basic stem cell research and its clinical translation into cell therapies for human disease. The College is located within the Texas Medical Center, a premier research and clinical environment.

Center investigators interact with basic and clinical colleagues to study diverse topics, including hematopoietic stem cells, vascular regeneration, neural repair, cancer stem cells, and human embryonic stem cells. We and our collaborators have made BCM a top medical school for federal grant funding.

The Center has outstanding core facilities, including Microarray, Microscopy, Flow Cytometry, Proteomics, Biocomputing, Bioimaging, GLP/GMP cell and vector production.

Prospective candidates should provide their CV and a two-page summary of research interests to: **Margaret A. Goodell, Ph.D., One Baylor Plaza, BCM505, Houston, Texas 77030; (713) 798-1246; STAR@bcm.edu; http://www.bcm.edu/star/.**

Baylor College of Medicine is an Equal Opportunity/Affirmative Action/Equal Access Employer.

BCM
Baylor College of Medicine

CHAIR, DEPARTMENT OF BIOCHEMISTRY AND MOLECULAR GENETICS
UNIVERSITY OF COLORADO SCHOOL OF MEDICINE

The University of Colorado School of Medicine seeks applicants for Chair of the Department of Biochemistry and Molecular Genetics. The Department consists of 17 primary faculty as well as more than 20 secondary faculty members. The Department currently occupies over 35,000 square feet of state-of-the-art research and office space, primarily on the 9th and 10th floors of the newly occupied Research Complex at the new UCHSC Fitzsimons campus. Details are available at the departmental web site: **http://www.uchsc.edu/sm/bbgn/**.

Research programs include chromatin structure, gene transcription and translation, RNA structure and enzymatic activity, protein structure, protein degradation, signal transduction, cell cycle regulation, bioinformatics and cell fate determination. Department faculty, currently with over eight million dollars in federal funding, houses both the Molecular Biology and the Biochemistry graduate programs. In addition, department faculty draw graduate students from several other programs including: MSTP, Computational Biosciences, Biomolecular Structure and Biomedical Sciences.

The Chair of the Department of Biochemistry and Molecular Genetics reports to the Dean of the School of Medicine and participates with his staff and other departmental chairs in program development, administration, and budgetary planning and implementation. The position requires excellence in teaching, demonstrated administrative leadership and ability, and, in particular, leadership in research and scholarly activity.

The University of Colorado is committed to the recruitment and employment of a diverse faculty. We encourage applications from women and minorities. Review of applications will continue until the position is filled. Applicants should respond by sending a letter of interest and curriculum vitae to: **John C. Cambier, Ph.D., Ida and Cecil Green Professor and Chairman of the Department of Immunology, Chair, Department of Biochemistry and Molecular Genetics Search Committee, University of Colorado School of Medicine and National Jewish Medical and Research Center, Room K803, 1400 Jackson Street, Denver CO 80206; FAX: [303] 270-2325; Email: Durans@NJC.org.**

The University of Colorado is committed to diversity and equality in education and employment.

USDA ARS Agricultural Research Service
www.ars.usda.gov

The U.S. Department of Agriculture, Agricultural Research Service, Western Integrated Cropping Systems Research Unit, Shafter, California, invites applications for a Supervisory Interdisciplinary position (**Research Agronomist/Research Entomologist/Research Geneticist/Research Plant Pathologist/Research Plant Physiologist**) GS-14/15 ($87,533.00-$133,850.00 per annum). As the Research Leader for this position, you work independently and as a member of a team conducting research to improve and develop cropping systems and improve management of cotton and other crops in the irrigated San Joaquin Valley. Duties also include performance review and evaluation of scientists, communicating with stakeholders, hiring personnel, approving manuscripts for publication and managing human, fiscal and physical resources. (**Announcement ARS-X6W-0315**). The ideal candidate has experience leading a team of productive scientists conducting multidisciplinary research related to improved cotton and other crop management practices. This is a competitive, permanent appointment and U.S. citizenship is required.

Vacancy announcements and where to apply can be found at website **www.usajobs.com**. Closing date for applications is **September 20, 2006**. For more detailed information on this listing, please contact **Edwin Civerolo** at **559-596-2700**.

The USDA is an Equal Opportunity Provider and Employer.

Computational Biologist
Department of Biology
Harvey Mudd College

The Department of Biology at Harvey Mudd College seeks a tenure-track Assistant Professor with teaching and research expertise in computational biology.

We expect that the successful candidate's education and training will be in biology, biophysics, biochemistry, or related disciplines. Teaching will include introductory level biology lecture and laboratory courses, and advanced seminar, lecture, and/or laboratory courses in areas appropriate to the person's expertise. The successful candidate will develop a vigorous independent research program that will involve undergraduate students during the academic year and summer. Harvey Mudd students are well prepared for interdisciplinary research. In their first two years, all Harvey Mudd College students complete a core curriculum comprising courses in Biology, Chemistry, Computer Science, Engineering, Humanities and Social Sciences, Mathematics, and Physics.

The new faculty member's research interests could be in molecular dynamics, protein modeling and protein folding, molecular imaging of biological molecules, or phylogenetic theory. We anticipate that the successful candidate's research will be mainly computational with the opportunity to establish collaborations with experimental scientists, computer scientists, and mathematicians at Harvey Mudd College and the other Claremont Colleges. Depending on the qualifications and interests of the successful candidate, this might be a joint appointment between Biology and another department.

Harvey Mudd College, a member of the Claremont University Consortium, is a small and highly selective private undergraduate college of science, mathematics, and engineering. Claremont is approximately 35 miles east of downtown Los Angeles. A Ph.D. in an appropriate discipline is required, and postdoctoral research experience is highly desirable. Applicants should submit a CV, a statement of teaching experience and interests, a statement of research plans, and arrange for three letters of reference to be mailed directly to the search committee. Send all materials to: **Dr. David Asai, Department Chair, Department of Biology, Harvey Mudd College, 301 Platt Blvd., Claremont, CA 91711 (david_asai@hmc.edu).** Review of applications will begin **October 1, 2006**, and continue until the position is filled. Experience with or demonstrated ability to effectively teach students from diverse backgrounds will be considered among the criteria for appointment.

http://www.biology.hmc.edu/index.html

Harvey Mudd College is an Equal Opportunity Employer and is committed to the recruitment of candidates historically underrepresented on college faculties.

USDA ARS Agricultural Research Service
www.ars.usda.gov

The USDA Agricultural Research Service is seeking three permanent full-time **Research Chemists** (Biochemistry series GS-1320-12/13/14; salary range: GS-12: $71,237.00 to $92,605.00; GS-13: $84,713.00 to $110,122.00; GS-14: $100,104.00 to $130,134.00 per annum) to conduct laboratory research at the Foodborne Contaminants Research Unit located at the Western Regional Research Center in Albany, California. All three assignments include work with Select Agents, requiring experience handling high-consequence pathogens or toxins, and a background suitability check.

Announcement ARS-X6W-0346: Analytical food safety and security for detection of prions in biological samples and toxins in foods. Assay "front-end": sampling, preparation, pre-concentration.

Announcement ARS-X6W-0347: Prion protein conformation conversion in vitro and ex vivo for pathophysiology and identification of surrogate analytes.

Announcement ARS-X6W-0348: Analytical food safety and security for detection of bacterial and plant toxins and surrogates in foods. Assay "back end": cutting-edge technology platforms.

All three vacancies open **August 21, 2006** and close **September 18, 2006**. For complete announcements and application directions, please see **www.afm.ars.usda.gov/divisions/hrd/index.html**. For questions you may contact the hiring supervisor, **John Mark Carter** at **mcarter@pw.usda.gov**. We will fill several additional vacancies this fall, including post-docs and technicians. For further information see **www.ars.usda.gov/pwa/wrrc/fcr**. Must be a US Citizen.

USDA ARS is an Equal Opportunity Employer and Provider.

UNIVERSITY OF BRADFORD
MAKING KNOWLEDGE WORK
INVESTOR IN PEOPLE

Research Council-UK (EPSRC) Fellowship in Medicinal Chemistry

£33,465 - £38,772 per annum **Ref: RCRU2316/S**
INSTITUTE OF CANCER THERAPEUTICS

A five-year fellowship is available to join a team designing and developing novel anti-cancer agents within the new Institute of Cancer Therapeutics in Bradford. The Institute is RAE 5 rated and has an international reputation for translational research leading to the identification of potential drugs and their early clinical evaluation with major funding from CR-UK, Yorkshire Cancer Research, research councils, other cancer charities and industry. It is also designated as the Leeds-Bradford Key Cancer Centre and NTRAC/Experimental Cancer Medicine (ECMC) Centre to provide PKPD support to early phase clinical trials. The research is based in a purpose built new building with floors dedicated to cancer biology, pharmacology, medicinal chemistry and bioscience incubators. You will play a full role in designing and synthesising new chemical entities for biological and pharmacological evaluation within the new Institute and work towards establishing an independent research programme. This position is five years as a RC-UK (EPSRC) Fellow after which it is expected to lead to a permanent lectureship position within the Institute.

Informal enquiries prior to application can be made to Professor Laurence H Patterson, Institute of Cancer Therapeutics on 01274 233226 or by e-mail: l.h.patterson@bradford.ac.uk

Closing date: 8th September 2006

How to apply: jobs@bradford.ac.uk tel: 01274 233091 (minicom: 01274 235807). For more information see www.bradford.ac.uk/jobs

Applications submitted by agencies will not be considered.

Confronting Inequality : Celebrating Diversity

Does your next career step need direction?

There's only one place to go for career advice if you value the expertise of *Science* and the long experience of AAAS in supporting career advancement - ScienceCareers.org. The pages of *Science* and our website ScienceCareers.org offer:

- Thousands of job postings
- Career advice articles and tools
- Funding information
- Networking opportunities

www.sciencecareers.org

POSITIONS OPEN

CELL BIOLOGIST, ASSISTANT PROFESSOR, Tenure Track, Academic Year 100 Percent
PARASITOLOGIST, ASSISTANT PROFESSOR, Tenure Track, Academic Year 100 Percent

The Department of Biology, University of Wisconsin-La Crosse, invites applications for two, academic year, tenure-track positions at the level of Assistant Professor. Applicants must have a strong commitment to undergraduate education. The Cell Biologist will teach radiation biology, a course in an area of expertise, and participate in teaching one or more of the following: cell biology laboratory, genetics laboratory, introductory biology. The Parasitologist will teach parasitology, a course in an area of expertise, and participate in teaching courses in general biology and organismal biology and laboratories in one or more of the following areas: general biology, organismal biology, genetics, anatomy, and physiology. A Ph.D. in a biological science is required. Some previous teaching experience is desirable. Successful candidates are expected to develop an externally funded research program and direct undergraduate and graduate (M.S.) research. Academic year salary competitive and commensurate with experience. Start August 27, 2007. Applicants should submit letter of application, curriculum vitae, statements of teaching philosophy and research interests, graduate and undergraduate transcripts, and three letters of recommendation to: **Dr. Mark Sandheinrich, Department of Biology, University of Wisconsin-La Crosse, La Crosse, WI 54601.** Applications must be received by October 15, 2006, and electronic applications will not be accepted. *As an Affirmative Action Equal Opportunity Employer, the University of Wisconsin-La Crosse is engaged in an effort to be a leader in Wisconsin's movement toward increased diversity and inclusiveness. Women, persons of color, and individuals with a disability are encouraged to apply. If you have a special need/accommodation to aid your participation in our hiring process, please contact* ***Mark Sandheinrich (e-mail:sandhein.mark@uwlax.edu)*** *to make appropriate arrangements.*

FACULTY POSITION
Department of Biological Sciences
University of Alabama in Huntsville

The Department of Biological Sciences invites applications for a tenure-track faculty position as an **ASSISTANT PROFESSOR** to begin August 2007. The successful candidate should be a Ph.D. educated in the biological sciences or related field and have a strong commitment to excellence in undergraduate and graduate education. Ideally, the new hire will pursue an innovative research program that complements existing research strengths in the Department. Applications are especially welcome from candidates in research areas involving proteomics, or systems biology using established model organisms. The selected applicant is expected to maintain a productive, externally funded research program and to teach courses in biochemistry. The University of Alabama, Huntsville (UAH) campus is located in Huntsville, Alabama, which is also home to one of the largest research parks in the country, NASA's Marshall Space Flight Center, and the newly formed Hudson Alpha Institute for Biotechnology. Construction has begun on a new 200,000 square foot Applied Sciences Building that will house the Department of Biological Sciences. The Department offers Bachelor's and Master's of Science degrees as well an interdisciplinary Ph.D. degree in biotechnology. Please send curriculum vitae along with a statement of research interests to: **Search Committee Chair, Department of Biological Sciences, 142 Wilson Hall, University of Alabama in Huntsville, Huntsville, AL 35899,** or e-mail your application to **e-mail: biops@uah.edu.** Include the names, addresses, and telephone/e-mail contact information for three references. Consideration of complete applications will begin on September 1, 2006. For more information about our Department and degree programs offered, please visit **website: http://www.uah.edu/biology/.** *UAH is an Affirmative Action/Equal Opportunity Employer.*

POSITIONS OPEN

Chicago's Jesuit University
LOYOLA UNIVERSITY CHICAGO
Stritch School of Medicine

TENURE-TRACK ASSISTANT/ ASSOCIATE PROFESSORS

The Department of Pharmacology at Loyola University Chicago, Stritch School of Medicine is recruiting tenure-track Assistant/Associate Professors to establish their own independent research as well as interact with existing faculty within the Department and the Cardiovascular, Neuroscience, and Oncology Institutes. Candidates whose research focuses on the dissection of fundamental mechanisms for clinical/therapeutic applications are highly encouraged to apply. Generous startup funds and laboratory space are available. For more information about the Department visit **website: http://www.luhs.org/depts/pharmacology/index.html.** Applicants should have a Ph.D. and/or M.D. degree, and be committed to excellence in research and teaching of pharmacology. Applications should include curriculum vitae and a research interest statement. Three letters of reference to support the candidacy should be sent separately. Address all correspondence to: **Dr. Tarun B. Patel, Chair, Department of Pharmacology, Loyola University Chicago, Stritch School of Medicine, 2160 S. First Avenue, Maywood, IL 60153.** (No electronic applications accepted.) *Equal Employment Opportunity /Affirmative Action Employer.*

TENURE-TRACK ASSISTANT/ASSOCIATE PROFESSOR

The Department of Pathology at the University of California, San Diego (UCSD) **(website: http://medicine.ucsd.edu/Pathology)** announces an open search for outstanding new and midlevel experimental **PATHOLOGISTS.** Applicants should have an M.D. or M.D./Ph.D., significant postdoctoral research experience, and the drive to develop a successful extramurally funded research program. The search is not limited to a specific research field; however, preference will be given to candidates with research plans that complement existing strengths in the Department and in the University as a whole. Board-certified/eligible Pathologists, who are prepared to contribute to our clinical enterprise, in addition to establishing independent research, are particularly encouraged to apply. Successful candidates will occupy newly renovated laboratories and receive startup packages. Opportunities are available to teach in our highly regarded medical school and graduate education programs. Please forward curriculum vitae, names/addresses of at least three references, and a one-page description of your research plan to: **Dr. Steven L. Gonias, Search Committee Chair, c/o Ms. Catherine Schumacher, Search Coordinator, Department of Pathology 0717, University of California San Diego School of Medicine, 9500 Gilman Drive, La Jolla, CA 92093-0717.** Applications by e-mail are acceptable to **e-mail: cdschumacher@ucsd.edu.** Review of applications will begin September 22, 2006, and will continue until positions are filled. *UCSD is an Affirmative Action/Equal Opportunity Employer with a strong institutional commitment to excellence through diversity.*

POSITIONS OPEN

TEXAS A&M UNIVERSITY. The Department of Chemistry at Texas A&M University invites applications for **MULTIPLE TENURE-TRACK FACULTY POSITIONS** in all areas of chemistry, for an anticipated starting date of September 2007. Applications at the Assistant Professor level are particularly sought, but appointments to senior ranks also will be considered for qualified candidates. Successful candidates will be expected to establish and maintain vigorous independent research programs and to teach at both the undergraduate and graduate levels.

Candidates should submit curriculum vitae, a brief description of research plans, including a one-page executive summary, and arrange for three letters of recommendation to be sent to:

Head, Department of Chemistry, Texas A & M University
P.O. Box 30012
College Station, TX 77843-3012

Review of applications will begin on October 15, 2006, and will continue until the positions are filled.

Texas A & M University is an Equal Opportunity/Affirmative Action Employer that is dedicated to the goal of building a culturally diverse and pluralistic faculty and staff who are committed to teaching and working in a multicultural environment. We strongly encourage applications from women, minorities, veterans, and individuals with disabilities. In addition, an aggressive faculty hiring program during the next several years will enable the University to be particularly responsive to the needs of dual-career couples.

SENIOR STAFF ASSOCIATE

Columbia University Division of Nephrology is seeking a Senior Staff Associate, preferably with M.P.H. or M.P.H./J.D., to direct the clinical research effort in the Division of Nephrology and the Division of Clinical Pharmacology and Experimental Therapeutics. Candidate must have experience and expertise in regulations governing the participation of human subjects in research and, in particular, clinical research, including the institutional review boards process, conflicts of interest, Health Insurance Portability and Accountability Act, protocol development, and budgets. Experience managing a clinical/research fellowship program is essential. Appropriate candidate must also be extremely well-organized and have highly developed interpersonal and communication skills and ability to work effectively with individuals at all levels (faculty, staff, committee members, chairpersons, senior academic administrators, and federal oversight agencies).

Please send curriculum vitae and cover letter to: **Mayra Marte-Miraz, Division of Nephrology, Department of Medicine, Columbia University, 630 West 168th Street, Box 30, New York, NY 10032.**

Columbia University is an Affirmative Action/Equal Opportunity Employer.

MICROBIOLOGY
Vassar College

The Department of Biology at Vassar College invites applications for a tenure-track faculty position at the level of **ASSISTANT PROFESSOR** beginning fall 2007. We seek a broadly trained Microbiologist whose research and teaching interests may include but are not limited to the following: pathogenesis, immunology, virology, infectious disease, biomedical microbiology, or environmental microbiology. The successful candidate is expected to develop an upper-level course in his/her specialty as well as teach at the introductory and intermediate levels. Development of a research program with student participation is expected and competitive startup funding is provided. A Ph.D. in biological science is required and postdoctoral experience is preferred. Consideration of applications will begin on 25 September 2006. Applicants should submit curriculum vitae, representative reprints, a statement of research interests and goals, a statement on teaching interests, and three letters of reference to: **Robert Fritz, Chair, Department of Biology, Box 731, Vassar College, Poughkeepsie, NY 12604-0731; e-mail: fritz@vassar.edu. Website: http://biology.vassar.edu/.** *Vassar College is an Equal Opportunity/Affirmative Action Employer and is strongly and actively committed to diversity within its community.*

Science Careers Forum

- How long should it take to get my Ph.D.?
- Academia or industry?
- What will make my resume/cv stand out?
- How do I negotiate a raise?

CONNECT WITH EXPERTS

Moderator Dave Jensen
Industry Recruiter

Dave Jensen has over 20 years of experience in human resource consulting and staffing for the biotechnology and pharmaceuticals industry.

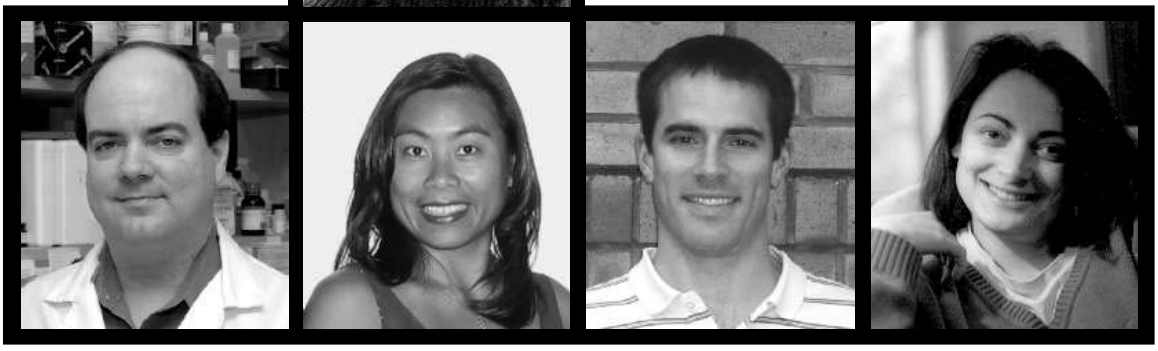

Kevin Foley, Ph.D.
Associate Director of In Vivo Pharmacology Synta Pharmaceuticals

Kevin Foley's research focuses on the discovery and preclinical development of small molecule drugs. He has served as an NIH grant reviewer and as a member of the Scientific Advisory Board for a biotechnology startup company. He has worked in the biotechnology industry since 1998.

Huong Huynh
Program Coordinator, Office of Postdoctoral and Graduate Training Burnham Institute for Medical Research

Huong Huynh is responsible for professional and career development training of postdoctoral scientists and graduate students. She received her Ph.D. in pharmacology from Loma Linda University.

Andrew Spencer, Ph.D.
Scientist PDL Biopharma, Inc.

Andy Spencer has a B.S. in chemistry, and a Ph.D. in biochemistry from Michigan State. As a grad student and postdoctoral fellow, Andy spent over ten years in university research labs before moving to the biotechnology industry in 2003.

Kelly Suter, Ph.D.
Assistant Professor University of Louisville School of Medicine

Kelly Suter has a B.S. in chemistry, a B.A. in biology, a Master's in physiology, and a Ph.D. in physiology. She did a postdoc at Colorado State University and was a postdoctoral fellow and research assistant professor at Emory University.

www.sciencecareers.org
and click on *Science* Careers Forum

ScienceCareers.org
We know science AAAS

CHAIR
Department of Biology
University of Central Florida

The Department of Biology (**http://www.cas.ucf.edu/biology/**) at the University of Central Florida invites applications and nominations for **Department Chair**. Candidates must have a Ph.D. in Biology or a closely related discipline, a commitment to graduate education, strong leadership skills, and credentials meriting Professor rank. Administrative skills, service on key university committees, and faculty experience in a comprehensive Biology Department are preferred. The successful candidate will articulate a vision for continued growth and development of the Department in research, teaching, and service across the biological sciences. Our Department is in a dynamic growth phase, with fifteen new hires in the past seven years, a recent renovation and expansion of facilities, and a recently established Ph.D. in Conservation Biology. Our 22 tenured and tenure-track faculty, two research faculty, and four full-time instructors have diverse teaching and research interests and a strong commitment to the success of our approximately 1000 undergraduate majors, 72 M.S. students, and 26 Ph.D. candidates. Our faculty also supports an interdepartmental Ph.D. in Biomolecular Sciences and actively partners with regional and national research institutes, businesses, and nongovernmental organizations.

The University of Central Florida's 1415-acre main campus is located 13 miles east of downtown Orlando and 40 miles west of Cape Canaveral. We are a major research university with over 45,000 students enrolled in 86 baccalaureate programs and 95 graduate and specialist programs (**http://www.ucf.edu/**). One of the university's main goals is achieving prominence in key research fields and graduate programs, including conservation biology.

Applicants must send a cover letter, curriculum vitae, statements of leadership philosophy, research, and teaching interests, and contact information for three references to: **Dr. Kevin D. Belfield, Biology Search Committee Chair, Department of Biology, University of Central Florida, Orlando FL 32816-2368**. Review of applications will begin **October 15, 2006** and continue until the position is filled.

The University of Central Florida is an Affirmative Action/Equal Opportunity Employer. Minorities and women are encouraged to apply. As an agency of the State of Florida, all application materials and selection procedures are available for public review.

Yale University

Faculty Position in Ecology and Evolutionary Biology

The Department of Ecology and Evolutionary Biology at Yale University invites applications for a faculty position at either the senior or junior level in the field of ecology. We are particularly interested in candidates whose research unites theory and empirical work in ways that shed new light on basic questions. A record of outstanding achievement and a promising research program are more important than the specific research area. Interested candidates should submit their CV, three relevant reprints or manuscripts, brief research and teaching statements, and the names and addresses of four potential evaluators by 30 September 2006. The search will remain open until the position is filled.

Send materials to:

Department of Ecology and Evolutionary Biology
Yale University
P.O. Box 208106
New Haven, CT 06520-8106 USA
Attn: Francine Horowitz

The Department is described at **www.eeb.yale.edu**.

Yale University is an Equal Opportunity/ Affirmative Action Employer. Men and women of diverse racial/ethnic backgrounds and cultures are encouraged to apply.

PENNSTATE University Park 1855

TENURE-TRACK ASSISTANT PROFESSOR OF ECOLOGY DEPARTMENT OF BIOLOGY

The Department of Biology at The Pennsylvania State University (**www.bio.psu.edu**) invites applications for a tenure-track Assistant Professor position in Ecology. We seek candidates who are developing independent research programs that will complement existing research in the department, and are particularly interested in experimental ecologists in the general areas of evolutionary and/or community ecology. The department welcomes applications from scientists working on any taxonomic group or ecological system. The successful candidate is expected to develop an externally funded research program of outstanding quality, and to contribute to teaching at the undergraduate and graduate levels.

Applicants should submit a letter of interest, curriculum vitae, statements of research and teaching interests and have three letters of reference sent to: **Chair of Ecology Search Committee, Box S, Department of Biology, 208 Mueller Laboratory, University Park, PA 16802**. Review of applications will begin on **October 15, 2006** and will continue until the position has been filled.

Women and minorities are encouraged to apply. Penn State is committed to Affirmative Action, Equal Opportunity and the diversity of its workforce.

PRIZES

The Linus Pauling Institute Prize for Health Research Call for Nominations

The Linus Pauling Institute Prize for Health Research is a prize sponsored by the Linus Pauling Institute at Oregon State University (**http://lpi.oregonstate.edu**). The Prize consists of $50,000 and a medal, and is awarded biennially. The LPI functions from the basic premise that an optimum diet and a healthy lifestyle are the keys to optimum health. The mission of the LPI is to determine the function and role of vitamins, essential minerals, and phytochemicals in promoting optimum health and preventing and treating disease; to determine the role of oxidative/nitrative stress and antioxidants in human health and disease; and to help people everywhere achieve a healthy and productive life, full of vitality, with minimal suffering, and free of cancer and other debilitating diseases. The Prize recognizes innovation and excellence in research relating to LPI's mission, with the goal to stimulate innovative research that enhances our knowledge of the role of diet and lifestyle in the primary and secondary prevention of disease and the role of oxidative/nitrative stress in disease pathology. **Procedure:** The nominator should submit a nomination letter, two supporting letters, and the candidate's curriculum vitae. The candidate's research accomplishments in light of the purpose of the Prize should be amply described in the letters. The recipient must be present to accept the Prize and deliver a talk at LPI's "Diet and Optimum Health" conference held in Portland, Oregon, May 16-19, 2007. Nomination packages should be sent to: **Linus Pauling Institute, Attn: Barbara McVicar, Oregon State University, 571 Weniger Hall, Corvallis, OR 97331-6512**. Complete nomination materials must be received by **November 1, 2006**.

POSITIONS OPEN

CURATOR/DIVISION OF FISHES
Field Museum of Natural History

The Department of Zoology of the Field Museum seeks an **ICHTHYOLOGIST** to fill a career-track appointment at the Assistant Curator level. Candidates should have a Ph.D. and a proven record of scientific achievement in collections-based research. Beyond taxonomic focus, we are searching broadly for excellence in evolutionary biology in such areas as phylogenetics, comparative morphology, molecular biology, development, biogeography, coevolution, and conservation.

In addition to research, responsibilities include curation of globally important collections in the Division of Fishes, participation in public exhibit and education programs, and administration. Strong relationships with local universities provide opportunities for participation in graduate and undergraduate training and teaching. Applications should include: (1) curriculum vitae; (2) a statement of research and curatorial interests; (3) names and contact information of three referees; and (4) copies of up to five relevant publications. Review of applications will begin October 1, 2006. Send materials to: **Search Committee, Department of Zoology, Field Museum, 1400 South Lake Shore Drive, Chicago, IL 60605-2496.** Application materials as e-mail attachments preferred (receipt will be acknowledged). **E-mail: zoologysearchfishes@fieldmuseum.org.** The Field Museum's homepage is **website: http://www.fieldmuseum.org.** The Departmental website is **website: http://www.fieldmuseum.org/research_collections/zoology/default.htm.** *The Field Museum is an Equal Opportunity Employer, and encourages applications from women and minorities.*

ANNOUNCEMENT

INDO-U.S. SCIENCE AND TECHNOLOGY FORUM
Fulbright House, 12 Hailey Road, New Delhi-110 001, India
Website: http://www.indousstf.org
THIRD CALL FOR PROPOSAL 2006

The Indo-U.S. Science and Technology Forum (IUSSTF), established under an agreement between the Governments of India and the United States of America, is an autonomous, not-for-profit society that promotes and catalyzes the Indo-U.S. bilateral collaborations in science, technology, engineering, and biomedical research through substantive interaction among government, academia and industry.

The IUSSTF seeks to support innovative programs aimed to stimulate interactions that have a strong potential for generating follow-on activities and building long-term Indo-U.S. S&T relationships. The IUSSTF promotes program that nurtures contacts between the young and midcareer scientists and technologists and fosters active public-private partnership in research and development.

The IUSSTF solicits proposals thrice a year (submission deadline: February, June, October) jointly submitted by the U.S. and Indian Principal Investigators from academia, government funded institutions/laboratories and private R&D entities for: (1.) Knowledge R&D networked and public-private networked Indo-U.S. Centers, (2.) Bilateral workshop, conference, symposium, training schools, et cetera, (3.) Travel grants (i.) To avail already awarded fellowship and sabbatical positions in U.S./ India, (ii.) For selected U.S. participants to attend international conferences / events in India, (iii.) For specific exploratory / planning visits aimed at large-scale collaborations.

Detailed format available at **website: http://www.indousstf.org.**

For further details and electronic submission, contact: **Arabinda Mitra, e-mail: amitra@indousstf.org** and **Michael Cheetham, e-mail: mcheetham@si.edu.**

Submission deadline: 15 October 2006. Award announcement: mid January 2007.

POSITIONS OPEN

POSTDOCTORAL POSITION
Mouse Pancreatic Development

A three-year Postdoctoral position is available in the Department of Surgery at the University of Pittsburgh. The main interest of our laboratory is to study the genetics of pancreatic cancer and diabetes. In particular, we are interested in studying the role of hypoxia during pancreatic development and tumor genesis as well as identifying novel genes involved in pancreatic ductal differentiation. These projects will involve cell specific inactivation of different components of the hypoxic pathway using standard Cre-lox methods, and subsequent analysis of the phenotype(s). Furthermore, the successful candidate will be given the opportunity to manipulate pancreatic differentiation in vitro in our embryonic pancreatic organ culture system.

Qualifications: Individuals with interest in pancreatic development are encouraged to apply. A Ph.D. or equivalent is required, ideally with experience in developmental biology.

Candidates should reply with current curriculum vitae to:

Farzad Esni, Ph.D.
Assistant Professor
University of Pittsburgh
Department of Surgery
Rangos Research Center
3460 Fifth Avenue, Room 8113
Pittsburgh, PA 15213
Telephone: 412-692-5123
Fax: 412-692-3466
E-mail: farzad.esni@chp.edu

The University of Pittsburgh is an Affirmative Action, Equal Opportunity Employer.

UNIVERSITY OF CHICAGO, POSTDOCTORAL POSITIONS available to study (i) 3D molecular structure and structure-function correlations of ion channels and receptors and their physiological role, (ii) nanoscale biomechanics and structural correlates, (iii) bionanosensors and bionanodevices, and (iv) designing/implementing integrated multimodal and multiscale microscopy for biological systems. Techniques include multimodal atomic force/light fluorescence/confocal microscopy/optical tweezers, ion channel electrophysiology, and Bio-Nano microelectromechanical systems (MEMS). Experience in (i) high resolution imaging of membrane proteins with atomic force microscopy, (ii) membrane biochemistry and biophysics of channels and receptors, including their expression, purification, reconstitution and functional characterization, (iii) nanoelectronics and MEMS, and (iv) optoelectronics and nanoscale carriers are required. Highly motivated Postdocs will be part of interdisciplinary teams undertaking basic and translational studies of human diseases and related therapeutics in a new Center for Nanomedicine at the University of Chicago. Send curriculum vitae and names of three references (preferably by e-mail) to: **Professor Ratnesh Lal, Department of Medicine, The University of Chicago, MC6076, Chicago, IL 60620. Fax: 773-702-6500. E-mail: eboyd@medicine.bsd.uchicago.edu.** *The University of Chicago is an Affirmative Action/Equal Opportunity Employer.*

MARKETPLACE

POSITIONS OPEN

TENNESSEE: THEORETICIAN SEARCH REOPENED

The Department of Ecology and Evolutionary Biology at the University of Tennessee, Knoxville, announces a tenure-track position in theoretical evolutionary biology at the **ASSISTANT PROFESSOR** level, to start August 1, 2007. We seek a creative colleague who has an innovative research program utilizing modern analytical and/or computational approaches to address major questions in evolutionary biology. The ability and interest in collaborating with empiricists is a plus. A commitment to excellence in undergraduate and graduate teaching is also expected. The Department has a strong theory group and offers an exciting environment for collaborative research including that with colleagues from other departments and Oak Ridge National Laboratory.

The University welcomes and honors people of all races, genders, creeds, cultures, and sexual orientations, and values intellectual curiosity, pursuit of knowledge, and academic freedom and integrity. For information about the Department visit **website: http:// eeb.bio.utk.edu.** Candidates should apply to: **Theory Search Committee, Department of Ecology and Evolutionary Biology, University of Tennessee, Knoxville, TN 37996.** Applicants should send curriculum vitae, statements of research and teaching goals, up to five reprints, and arrange for three reference letters to be submitted. Electronic applications should be sent to **Ms. Cheryl Lynn** at **e-mail: cjlynn@utk.edu.** Applications will be reviewed beginning 15 September 2006.

The University of Tennessee is an Equal Employment Opportunity/Affirmative Action/Title VI/Title IX/Section 504/ADA/ADEA institution in the provision of its education and employment programs and services.

RESEARCH ASSISTANT PROFESSOR

The Department of Surgery and the McGowan Institute for Regenerative Medicine at the University of Pittsburgh School of Medicine seek qualified applicants to fill a position as Research Assistant Professor in our bioreactor group laboratory. We are looking for researchers interested in advancing basic cell biology findings into research and development on clinical translation for cell-based therapies, stem cell in vitro differentiation, and 3-D perfusion culture technologies. Qualifications: Candidates must have a Ph.D. in biology, bioengineering, or related field. The ideal candidate should have experience working with primary and stem cells, including hepatic cells and embryonal stem cells, and possess technical expertise in cell culture, biochemistry, flow cytometry and immunohistochemistry as well as basic and advanced molecular biology techniques. A background in basic stem cell biology and/or 3-D perfusion culture would be a significant asset.

Closing date is December 31, 2006.

Candidates should reply with current curriculum vitae and the contact information for three references. Please send replies to:

J. Gerlach, M.D., Ph.D.
Professor of Surgery and Bioengineering
University of Pittsburgh
McGowan Institute for Regenerative Medicine
100 Technology Drive, Suite 200
Pittsburgh, PA 15219-3130

The University of Pittsburgh is an Affirmative Action Equal Opportunity Employer.

MARKETPLACE